

INTERNATIONAL AEGEAN CONFERENCES

on Innovation Technologies & Engineering-VI
December 20-22, 2022 / Izmir, Turkey

Proceedings Book

Editors

Assist. Prof. Dr. Adnan AKALIN

Dr. Nihat DEMIRKOL

ISBN: 978-625-6955-63-9

iKSAD Publishing House

INTERNATIONAL AEGEAN CONFERENCES
ON INNOVATION TECHNOLOGIES & ENGINEERING-VI
December 20-22, 2022 / Izmir, Turkey



PROCEEDINGS BOOK

EDITOR

Assist. Prof. Dr. Adnan AKALIN
Dr. Nihat DEMIRKOL

All rights of this book belong to IKSAD Global Publishing House
Authors are responsible both ethically and juridically

IKSAD Global Publications

Issued: 30.12.2022

ISBN: 978-625-6955-63-9

CONFERENCES ID

CONFERENCES TITLE

- **INTERNATIONAL AEGEAN CONFERENCES**
• **on Innovation Technologies & Engineering**

DATE AND PLACE

- December 20-22, 2022 / Izmir, Turkey

ORGANIZATION

- IKSAD- INSTITUTE OF ECONOMIC DEVELOPMENT AND SOCIAL RESEARCHES
- ATLAS INTERNATIONAL JOURNAL ON SOCIAL SCIENCES
ISSN - 2616 - 936X

HEAD OF ORGANIZING COMMITTEE

- Prof. Dr. Natalia LATIGINA

COORDINATOR

- Assist. Prof. Dr. Mehmet Emin KALGI

- Turkey (21), Kyrgyzstan (1), Algeria (2), Pakistan (3), Saudi Arabia (1), Morocco (1), Indonesia (1), Bulgaria (1), Iraq (1), India (4), Iranian (2), Nigeria (1), Egypt (1), Ethiopia (1), Belarus (1), Algeria (1).

- **NUMBER of ACCEPTED PAPERS-43**
- **NUMBER of REJECTED PAPERS-12**

- **Double blinded evaluation process*

SCIENTIFIC COMMITTEE BOARD

- Dr. Maha Hamdan ALANAZI - *Riyad King Abdullah University*
- Dr. Tamalika SULTANA - *Dakka University of Bangladesh*
- Dr. Kenes JUSIPOV - *Kazak Transportation Academy*
- Dr. Nilgün ULUTASDEMİR - *Gumushane University*
- Dr. Murat EYVAZ - *Gebze Technical University*
- Dr. Menekşe ŞAKİR - *Erciyes University*
- Dr. Mehmet GÖKTÜRK - *Gebze Yüksek Teknoloji institute*
- Dr. Sezen TEKİN - *Çankırı Karatekin University*
- Dr. Hakan EYGÜ - *Atatürk University*
- Dr. G. C. Rana - *NSCBM Govt. College Hamirpur*
- Dr. Mohamed EL MALKİ - *Department of Physics*
- Dr. H. Burçin HENDEN ŞOLT - *Zonguldak Bülent Ecevit University*
- Dr. Fatih YILDIRIM - *Atatürk University*
- Dr. F. Gül KOÇSOY - *Firat University*
- Dr. Praveen KUMAR - *HR & OB Division*
- Dr. Norma-Aurea Rangel-Vázquez - *TECNM/Instituto Tecnológico de Aguascalientes*



INTERNATIONAL AEGEAN CONFERENCES Innovation Technologies & Engineering-VI

December 20-22, 2022

IZMIR, TURKEY

CONFERENCES PROGRAM

Online (with ZOOM Conference)

Meeting ID: 829 4677 4684

Passcode: 060606



Turkey (21), Kyrgyzstan (1), Algeria (2), Pakistan (3), Saudi Arabia (1), Morocco (1), Indonesia (1), Bulgaria (1), Iraq (1), India (4), Iranian (1), Nigeria (1), Egypt (1), Ethiopia (1), Belarus (1), Algeria (1), Iranian (1).

IMPORTANT, PLEASE READ CAREFULLY

- ❖ To be able to attend a meeting online, login via <https://zoom.us/join> site, enter ID "Meeting ID or Personal Link Name" and solidify the session.
- ❖ The Zoom application is free and no need to create an account.
- ❖ The Zoom application can be used without registration.
- ❖ The application works on tablets, phones and PCs.
- ❖ The participant must be connected to the session 5 minutes before the presentation time.
- ❖ All congress participants can connect live and listen to all sessions.
- ❖ Moderator is responsible for the presentation and scientific discussion (question-answer) section of the session.

Points to Take into Consideration - TECHNICAL INFORMATION

- ◆ Make sure your computer has a microphone and is working.
- ◆ You should be able to use screen sharing feature in Zoom.
- ◆ Attendance certificates will be sent to you as pdf at the end of the congress.
- ◆ Requests such as change of place and time will not be taken into consideration in the congress program.

Önemli, Dikkatle Okuyunuz Lütfen

- ❖ Kongremizde Yazım Kurallarına uygun gönderilmiş ve bilim kurulundan geçen bildirimler için online (video konferans sistemi üzerinden) sunum imkanı sağlanmıştır.
- ❖ Online sunum yapabilmek için <https://zoom.us/join> sitesi üzerinden giriş yaparak "Meeting ID or Personal Link Name" yerine ID numarasını girerek oturuma katılabilirsiniz.
- ❖ Zoom uygulaması ücretsizdir ve hesap oluşturmaya gerek yoktur.
- ❖ Zoom uygulaması kaydolmadan kullanılabilir.
- ❖ Uygulama tablet, telefon ve PC'lerde çalışıyor.
- ❖ Her oturumdaki sunucular, sunum saatinden 5 dk öncesinde oturuma bağlanmış olmaları gerekmektedir.
- ❖ Tüm kongre katılımcıları canlı bağlanarak tüm oturumları dinleyebilir.
- ❖ Moderatör – oturumdaki sunum ve bilimsel tartışma (soru-cevap) kısmından sorumludur.

Dikkat Edilmesi Gerekenler- TEKNİK BİLGİLER

- ◆ Bilgisayarınızda mikrofon olduğuna ve çalıştığına emin olun.
- ◆ Zoom'da ekran paylaşma özelliğine kullanabilmelisiniz.
- ◆ Kabul edilen bildiri sahiplerinin mail adreslerine Zoom uygulamasında oluşturduğumuz oturuma ait ID numarası gönderilecektir.
- ◆ Katılım belgeleri kongre sonunda tarafınıza pdf olarak gönderilecektir
- ◆ Kongre programında yer ve saat değişikliği gibi talepler dikkate alınmayacaktır

Before you login to Zoom please indicate your name_surname and HALL number:

exp. Hall-1, Name SURNAME



DATE

• 21.12.2022



TIME

• 10⁰⁰–12⁰⁰

SESSION

- HALL-3
- SESSION-1

HEAD OF SESSION: Prof. Dr. Ella ABYLAEVA

Büşra YILDIZ Assoc. Prof. Dr. Ahmet Vefa ORHON	Dokuz Eylul University Dokuz Eylul University	BAMBOO AS A SUSTAINABLE BUILDING MATERIAL
Assist. Prof. Dr. Temel TEMİZ	Yalova University	EVALUATION OF THE CONTACT CONDITIONS OF MARINE STRUCTURES FENDERS WITH SIMPLIFIED METHODS
Assist. Prof. Dr. Hasan SESLİ	Yalova University	EVALUATION OF STRUCTURAL PERFORMANCE OF BUILDINGS BUILT BEFORE AND AFTER 1999 KOCAELİ EARTHQUAKE
Dr. Bahattin GÜLLÜ	Aksaray University	PETROLOGY OF MAFIC DYKES WITHIN THE GÜCÜNKAYA (AKSARAY) GRANITOIDS
Levent AYMAN Osman Taha ŞEN	ASELSAN Inc. Istanbul Technical University	SOUND DETECTION AND CLASSIFICATION IN A NOISY ENVIRONMENT USING PCA AND ICA IN THE TIME DOMAIN AND TIME-FREQUENCY DOMAIN
Rumeysa AKAR Mehmet UÇAR	Kocaeli University Kocaeli University	FUTURE PASSENGER NEEDS IN INTERIORS AND ITS IMPACT ON AUTONOMOUS VEHICLE
Abdullah ERDEMİR Veysel ALVER Prof. Dr. Mete KALYONCU	MPG Machinery Production Group Inc. Co. MPG Machinery Production Group Inc. Co. Konya Technical University	OPTIMIZATION OF THE STEERING LINKAGE OF A FRONT-WHEEL-STEERING VEHICLE BY USING THE BEES ALGORITHM
Kevser İrem DANACI Dr. Erdem AKAGÜNDÜZ	Sivas University of Science And Technology Middle East Technical University	EFFECT OF DATA AUGMENTATION METHOD ON PERFORMANCE IN INFRARED OBJECT DETECTION APPLICATIONS
Prof. Dr. Asan OMURALİEV Prof. Dr. Ella ABYLAEVA	Kyrgyz Turkiye Manas University, Kyrgyz Turkiye Manas University,	ASYMPTOTICS OF A PARABOLIC PROBLEM WITH A NONSMOOTH ANGULAR BOUNDARY LAYER FUNCTION
Hasan YARIM Prof. Dr. Taner BAYSAL	Ege University Ege University	EFFECT OF HIGH INTENSITY PULSED LIGHT TECHNOLOGY ON AFLATOXIN DEGRADATION AND SOME QUALITY PARAMETERS IN DRIED FIGS
Saime Nur KARASU Dr. Yavuz Nuri ERTAŞ Dr. Tuğrul Tolga DEMİRTAŞ	Erciyes University Erciyes University Erciyes University	DEVELOPMENT OF A NOVEL HYDROGEL SYSTEM FOR TISSUE ENGINEERING APPLICATIONS: MICROWAVE ASSISTED METHACRYLATION OF CHIA SEED MUCILAGE



DATE

• 21.12.2022



TIME

• 12³⁰–14³⁰

SESSION

- HALL-3
- SESSION-2

HEAD OF SESSION: Dr. Celaleddin Ensar ŞENGÜL

Dr. Semiha EREN Aliye AKARSU ÖZENÇ Merve ÖZTÜRK	Bursa Uludağ University Bursa Uludağ University Bursa Uludağ University	INVESTIGATION OF PHOTOCATALYTIC COLOR REMOVAL OF REACTIVE BLUE 203 USING H ₂ O ₂ /UV PROCESS
M.A. Sarli E.S. Dalbaşı A.T. Özgüney	Ege University Ege University Ege University	INVESTIGATION OF DYEING POLYESTER WITH DISPERSE DYE IN THE PRESENCE COMB-LIKE POLYCARBOXYLATES DISPERSANT
Merve DÖNMEZ Dr. AYŞE ÖZKAL	Pamukkale University Pamukkale University	HONEY REINFORCED NANOFIBERS
Dr. Celaleddin Ensar ŞENGÜL	14th Regional Directorate of State Hydraulic Works	LOW TEMPERATURE PERFORMANCE ANALYSIS OF POLYPHOSPHORIC ACID AND SBS COMPOSITE POLYMERS IN ASPHALT PAVEMENTS WITH DIFFERENT RATIO AND MIXING TIMES
Dr. Celaleddin Ensar ŞENGÜL	14th Regional Directorate of State Hydraulic Works	PREVENTION OF STRENGTH LOSSES CAUSED BY RAPID COOLING WITH INCREASED WORKABILITY IN ASPHALT PAVEMENTS
Dr. Murat KAVURMACI	Aksaray University	INVESTIGATION OF HYDROGEOCHEMICAL PROPERTIES OF GROUNDWATERS IN ŞEREFLİKOÇHİSAR PLAIN
Assoc. Prof. Dr. Öykü BİLGİN	Sirnak University	DETERMINATION OF SIGNIFICANT CHARACTERIZATION FEATURES OF SIRNAK ASPHALTITE SAMPLE
Fatma DENİZ Mehmet Ali MAZMANCI	Mersin University Mersin University	CALCULATION OF AGRICULTURAL WATER FOOTPRINT OF OLIVES: A CASE STUDY FOR IZMIR



DATE

• 21.12.2022



TIME


• 15⁰⁰–17⁰⁰

SESSION

- HALL-3
- SESSION-3


HEAD OF SESSION: Assist. Prof. Kemal UÇAK

Slimani Sami Zennir Youcef	University of 20 August 1956 Skikda University of 20 August 1956 Skikda	ANALYZE OF OIL AND GAS ACCIDENT ASSOCIATED WITH DRILLING OPERATION USING FISHBONE DIAGRAM
Ibrahim Abdullah Albarakati	King Abdulaziz University	SYNTHESIS, MOLECULAR STRUCTURES AND CATALYTIC ACTIVITIES OF BIS-2,2-BIPYRIDINE PALLADIUM (II) DI CHLORIDE COMPLEXES IN FORMATION OF C-C BOND
Rashid Ali Marjan Uddin Muhammad Taufiq	University of Engineering & Technology Peshawar University of Engineering & Technology Peshawar University of Engineering & Technology Peshawar	TRANSFORM BASED RADIAL BASIS FUNCTION SCHEME FOR SOLVING VARIABLE ORDER DIFFUSION EQUATION
H. BOUHSISS A. En-Naji A. WAHID Abdelkrim Kartouni M. El Ghorba	Hassan II University Hassan II University Hassan II University Hassan II University Hassan II University	STUDY OF THE EVOLUTION OF THE STRESS CONCENTRATION COEFFICIENT AND THE STRESS INTENSITY FACTOR OF ABS SPECIMENS CONTAINING A COMBINED DEFECT
Shinta Dewi	Uin KH Abdurrahman Wahid Pekalongan Indonesia	ANALYSIS OF THE BENEFITS OF PURWACENG AS A MEDICINAL PLANT
Assoc. Prof. M. As. Michailov	SWU "Neofit Rilski"	PECULIARITIES IN DETERMINING THE EFFECTIVENESS OF ENVIRONMENTAL PROTECTION ACTIVITIES
MANKOUR MOHAMED MILOUDI MOHAMED	University of Ahmed Zabana of Relizane University of Ahmed Zabana of Relizane	HVDC LINKS: SOLUTION TO IMPROVE HVAC GRIDS
Nurşah DİK Assist. Prof. Dr. Kemal UÇAK	Muğla Sıtkı Koçman University Muğla Sıtkı Koçman University	ARTIFICIAL NEURAL NETWORK CONTROLLER FOR NONLINEAR DYNAMICAL SYSTEMS
Sima KÜÇÜKÇE Assist. Prof. Kemal UÇAK	Muğla Sıtkı Koçman University Muğla Sıtkı Koçman University	ADAPTIVE SLIDING MODE CONTROLLER FOR INVERTED PENDULUM SYSTEM
Hande DÖNMEZ Assist. Prof. Kemal UÇAK	Muğla Sıtkı Koçman University Muğla Sıtkı Koçman University	SWARM INTELLIGENCE BASED OPTIMAL CONTROL DESIGN METHOD FOR ACTIVE SUSPENSION SYSTEM




DATE

- 22.12.2022



TIME

- 10⁰⁰–12⁰⁰



SESSION

- HALL-3
- SESSION-1

HEAD OF SESSION: Assist. Prof. Dr. Hooman Fatoorehchi

Hamid T. Al-Saad Shahinaz R.A Al-Shawi Hamzah A. Kadhim	University of Basrah University of Basrah University of Basrah	HEAVY METALS IN DISSOLVED AND PARTICULATE WATER OF THE TIGRIS AND EUPHRATES AND SHATT AI-ARAB RIVERS
K. Thamizhmaran	Annamalai University	ACKNOWLEDGEMENTS MODEL FOR DETECTION OF COLLISION USING CRYPTOGRAPHY FOR MANET
K. Thamizhmaran	Annamalai University	EFFICIENT MOBILE AD HOC NETWORK USING DYNAMIC SOURCE ROUTING PROTOCOL
Assist. Prof. Dr. Hooman Fatoorehchi Seyed Amirreza Babaei Niloofar Arabi	University of Tehran University of Tehran University of Tehran	PERFORMANCE ASSESSMENT OF NATURAL GAS DEHYDRATION TECHNOLOGIES
IBRAHIB B. B. USMAN A.	Institute of Applied Sciences Institute of Applied Sciences	ESTIMATION OF GLOBAL SOLAR RADIATION USING FIVE SUNSHINE BASED MODELS FOR ILORIN, NORTH-CENTRAL, NIGERIA
Mostafa M. Hamad	Cairo University	BENTHIC FORAMINIFERA AS BIOSTRATIGRAPHICAL AND PALEOECOLOGICAL INDICATORS: AN EXAMPLE FROM THE MIOCENE DEPOSITS IN GEBEL ABU SHAAR EL QIBLI, GULF OF SUEZ REGION, EGYPT



DATE

• 22.12.2022



TIME

• 12³⁰–14³⁰

SESSION

- HALL-3
- SESSION-2

HEAD OF SESSION: Prof. Mehrdad Karimimoshaver

Shivam Priyadarshi Mainak Pal Lalawmpuia Prof. Dr. Manapuram Muralidhar	Deemed to be University Deemed to be University Deemed to be University Deemed to be University	STUDIES ON ENGINEERING APPLICATION DOMAINS OF INDUSTRY 5.0 IN INDIA
Adane Obsie Bifa Mulugeta Soruma Guta	Wollega University Wollega University	FACTORS AFFECTING PEDESTRIANS' FREE- MOBILITY AND SOCIAL DISTANCING TO COMBAT COVID-19: EVALUATION OF PEDESTRIANS' MOBILITY AND URBAN SPACE IN DOWNTOWN OF NEKEMTE CITY, ETHIOPIA
К.Т.Н. Янкевич Н.С.	Национальная академия наук Беларуси	DEVELOPMENT OF A SYSTEM FOR PREVENTIVE DIAGNOSTICS OF A TECHNICAL OBJECT USING ARTIFICIAL INTELLIGENCE
Mr. Asif Ali	Abdul Wali khan University	ENERGY STORAGE CHARACTERISTICS OF 0.5 BaTiO ₃ –BixNax(Mg0.67Nb0.33)1-xNbx
Bharath Kumar Shanmugam Harsha Vardha Govinda Raj. M Marutiram Kaza2 Rameshwar Sah Harish Hanumanthappa	National Institute of Technology National Institute of Technology National Institute of Technology JSW Steel Limited, Vijayanagar Works JSW Steel Limited, Vijayanagar Works National Institute of Technology	REGRESSION ANALYSIS ON SEPARATION PERFORMANCE OF LINEAR VIBRATING SCREEN
Prof. Mehrdad Karimimoshaver Attiyeh Khorshidi Alireza Gerami	Bu-Ali Sina University Bu-Ali Sina University Bu-Ali Sina University	PEDESTRIANS MOVEMENT PATTERNS IN THE SELF-MADE HABITATS WITH EMPHASIZING ON SECURITY IMPROVEMENT BY COMBINING TWO UAVs AND SPACE SYNTAX
Mourad Nahal Yacine Saharoui Omar Reffas Chaouki Moumeni Naziha Zerari	University of Souk Ahras University of Souk Ahras Badji-Mokhtar University University of Souk Ahras University of Souk Ahras	BAYESIAN NETWORKS EFFECTIVENESS FOR ELECTRICAL SYSTEMS MAINTENANCE PLANNING
Shagufta Noreen Suad Naheed	Jinnah University for Women Jinnah University for Women	BIODEGRADATION OF AZO DYES BY HALOPHILIC BACTERIA









Zoom Toplantı - Hall-3

Kaydediyor

Görüntüle

H-3 dinleyici

Hall-3, Bahattin Güllü

H-3 dinleyici

Hall-3, Rumeysa Akar

Ella Abylaeva

S1 H5 ali nehir

Hall-3, Abdullah ERDEMİR

S1 H5 ali nehir

Hall-3, Busra Yildiz

Hall-3, Session-2, Emin SARLI

H3-TEMEL TEMİZ

H-3 observer

H3-TEMEL TEMİZ

Hasan Sesli

Hall-3 Session-1 Saime Nur Karasu

Hasan YARIM

Keşer İrem DA...

Öznur Süzen

Hasan YARIM

Keşer İrem DANACI

Öznur Süzen

Sesi aç

Videoyu Başlat

Katılımcılar

Sohbet

Ekran Paylaşımı

Kaydet

Yardım İste

Reaksiyonlar

Uygulamalar

Odadan Çık

TR

1°C Bulutlu

TUR

11:09

Zoom Toplantı - Hall-3

Hall-3, Abdullah ERDEMİR ekranını görüntüyorsunuz

Seçenekleri Görüntüle

H-3 dinleyici

Hall-3, Rumeysa...

Hall3, Levent Ay...

Hall 3, Bahattin...

H-3 dinleyici

Hall-3, Abdullah ERDEMİR



Hall-3, Rumeysa Akar

Hall3, Levent Ayman

Ella Abylaeva

Hall 3, Bahattin Güllü

Kaydediyor



MPG

ARI ALGORİTMASI KULLANILARAK ÖNDEN DÜMENLEMELİ BİR ARACIN DÜMENLEME MEKANİZMASININ OPTİMİZASYONU

OPTIMIZATION OF THE STEERING LINKAGE OF A FRONT-WHEEL-STEERING VEHICLE BY USING THE BEES ALGORITHM

Abdullah ERDEMİR¹, Veysel ALVER¹, Prof. Dr. Mete KALYONCU²

1 MPG Makine Prodüksiyon Grubu Makine İml. San. ve Tic. A.Ş., Konya/TÜRKİYE

2 Konya Teknik Ü., Müh. ve Doğa Bil. Fakültesi, Makina Müh. Bölümü, Konya/TÜRKİYE

Sesi aç

Videoyu Başlat

Katılımcılar

Sohbet

Ekran Paylaşımı

Kaydet

Yardım İste

Reaksiyonlar

Uygulamalar

Odadan Çık

TR

0°C Çok bulutlu

TUR

11:50

Zoom Toplantı

Kaydediyor

Katılımcılar (16)

Q Katılımcı bul

HD H-3 dinleyici (Ben)

H-3 ... (Ortak oturum sahibi)

E Ella Abylaeva

HT H3-TEMEL TEMİZ

H3 Hall 3, Bahattin Güllü

HS Hall-3 Session-1 Saime Nur Ka...

Hall-3, Abdullah ERDEMİR

B Hall-3, Busra Yıldız

HL Hall-3, Levent AYMAN

HR Hall-3, Rumeysa Akar

HS Hall-3, Session-2, Emin SARLI

H Hasan Sesli

HY Hasan YARIM

KI Kevser İrem DANACI

Sesimi Aç

Zoom Toplantı - Hall-3

Ella Abylaeva ekranını görüntüyorsunuz

Seçenekleri Görüntüle

Görüntüle

Kaydediyor

Paylaşılan içeriğe geç

Sabitlemeyi Kaldır

Ella Abylaeva

Sesi aç

Videoyu Başlat

Katılımcılar

Sohbet

Ekran Paylaşımı

Kaydet

Yardım İste

Reaksiyonlar

Uygulamalar

Odadan Çık

TR 1°C Bulutlu TUR 11:08

TR 0°C Çok bulutlu TUR 12:16

CONTENT

CONFERENCES ID	I
PROGRAM	II
PHOTO GALLERY	III
CONTENT	IV

Author	Title	No
Büşra YILDIZ Ahmet Vefa ORHON	BAMBOO AS A SUSTAINABLE BUILDING MATERIAL	1
Temel TEMİZ	EVALUATION OF THE CONTACT CONDITIONS OF MARINE STRUCTURES FENDERS WITH SIMPLIFIED METHODS	22
Hasan SESLİ	EVALUATION OF STRUCTURAL PERFORMANCE OF BUILDINGS BUILT BEFORE AND AFTER 1999 KOCAELİ EARTHQUAKE	24
Bahattin GÜLLÜ	PETROLOGY OF MAFIC DYKES WITHIN THE GÜCÜNKAYA (AKSARAY) GRANITOIDS	26
Levent AYMAN Osman Taha ŞEN	SOUND DETECTION AND CLASSIFICATION IN A NOISY ENVIRONMENT USING PCA AND ICA IN THE TIME DOMAIN AND TIME- FREQUENCY DOMAIN	40
Rumeysa AKAR Mehmet UÇAR	FUTURE PASSENGER NEEDS IN INTERIORS AND ITS IMPACT ON AUTONOMOUS VEHICLE	48
Abdullah ERDEMİR Veysel ALVER Mete KALYONCU	OPTIMIZATION OF THE STEERING LINKAGE OF A FRONT-WHEEL- STEERING VEHICLE BY USING THE BEES ALGORITHM	50
Kevser İrem DANACI Erdem AKAGÜNDÜZ	EFFECT OF DATA AUGMENTATION METHOD ON PERFORMANCE IN INFRARED OBJECT DETECTION APPLICATIONS	60
Asan OMURALİEV Ella ABYLAEVA	ASYMPTOTICS OF A PARABOLIC PROBLEM WITH A NONSMOOTH ANGULAR BOUNDARY LAYER FUNCTION	62
Hasan YARIM Taner BAYSAL	EFFECT OF HIGH INTENSITY PULSED LIGHT TECHNOLOGY ON AFLATOXIN	65

	DEGRADATION AND SOME QUALITY PARAMETERS IN DRIED FIGS	
Saime Nur KARASU Yavuz Nuri ERTAŞ Tuğrul Tolga DEMİRTAŞ	DEVELOPMENT OF A NOVEL HYDROGEL SYSTEM FOR TISSUE ENGINEERING APPLICATIONS: MICROWAVE ASSISTED METHACRYLATION OF CHIA SEED MUCILAGE	67
Semiha EREN Aliye AKARSU ÖZENÇ Merve ÖZTÜRK	INVESTIGATION OF PHOTOCATALYTIC COLOR REMOVAL OF REACTIVE BLUE 203 USING H ₂ O ₂ /UV PROCESS	70
M.A. Sarlı E.S. Dalbaş1 A.T. Özgüney	INVESTIGATION OF DYEING POLYESTER WITH DISPERSE DYE IN THE PRESENCE COMB-LIKE POLYCARBOXYLATES DISPERSANT	76
Merve DÖNMEZ AYŞE ÖZKAL	HONEY REINFORCED NANOFIBERS	82
Celaleddin Ensar ŞENGÜL	LOW TEMPERATURE PERFORMANCE ANALYSIS OF POLYPHOSPHORIC ACID AND SBS COMPOSITE POLYMERS IN ASPHALT PAVEMENTS WITH DIFFERENT RATIO AND MIXING TIMES	99
Celaleddin Ensar ŞENGÜL	PREVENTION OF STRENGTH LOSSES CAUSED BY RAPID COOLING WITH INCREASED WORKABILITY IN ASPHALT PAVEMENTS	115
Murat KAVURMACI	INVESTIGATION OF HYDROGEOCHEMICAL PROPERTIES OF GROUNDWATERS IN ŞEREFLİKOÇHİSAR PLAIN	124
Öykü BİLGİN	DETERMINATION OF SIGNIFICANT CHARACTERIZATION FEATURES OF SIRNAK ASPHALTITE SAMPLE	135
Fatma DENİZ Mehmet Ali MAZMANCI	CALCULATION OF AGRICULTURAL WATER FOOTPRINT OF OLIVES: A CASE STUDY FOR	137
Slimani Sami Zennir Youcef	ANALYZE OF OIL AND GAS ACCIDENT ASSOCIATED WITH DRILLING OPERATION USING FISHBONE DIAGRAM	146
Ibrahim Abdullah Albarakati	SYNTHESIS, MOLECULAR STRUCTURES AND CATALYTIC ACTIVITIES OF BIS-2,2-BIPYRIDINE PALLADIUM (II) DI CHLORIDE COMPLEXES IN FORMATION OF C-C BOND	147

Rashid Ali Marjan Uddin Muhammad Taufiq	TRANSFORM BASED RADIAL BASIS FUNCTION SCHEME FOR SOLVING VARIABLE ORDER DIFFUSION EQUATION	141
H. BOUHSISS A. En-Naji A.WAHID Abdelkrim Kartouni M. El Ghorba	STUDY OF THE EVOLUTION OF THE STRESS CONCENTRATION COEFFICIENT AND THE STRESS INTENSITY FACTOR OF ABS SPECIMEN CONTAINING A COMBINED DEFECT	158
Shinta Dewi	ANALYSIS OF THE BENEFITS OF PURWACENG AS A MEDICINAL PLANT	160
M. As. Michailov	PECULIARITIES IN DETERMINING THE EFFECTIVENESS OF ENVIRONMENTAL PROTECTION ACTIVITIES	154
Mankour Mohamed Miloudi Mohamed	HVDC LINKS: SOLUTION TO IMPROVE HVAC GRIDS	171
Nurşah DİK Kemal UÇAK	ARTIFICIAL NEURAL NETWORK CONTROLLER FOR NONLINEAR DYNAMICAL SYSTEMS	172
Sima KÜÇÜKÇE Kemal UÇAK	ADAPTIVE SLIDING MODE CONTROLLER FOR INVERTED PENDULUM SYSTEM	183
Hande DÖNMEZ Kemal UÇAK	SWARM INTELLIGENCE BASED OPTIMAL CONTROL DESIGN METHOD FOR ACTIVE SUSPENSION SYSTEM	197
Hamid T. Al-Saad Shahinaz R.A Al-Shawi Hamzah A. Kadhim	HEAVY METALS IN DISSOLVED AND PARTICULATE WATER OF THE TIGRIS AND EUPHRATES AND SHATT AI- ARAB RIVERS	209
K. Thamizhmaran	ACKNOWLEDGEMENTS MODEL FOR DETECTION OF COLLISION USING CRYPTOGRAPHY FOR MANET	210
K. Thamizhmaran	EFFICIENT MOBILE AD HOC NETWORK USING DYNAMIC SOURCE ROUTING PROTOCOL	219
Hooman Fatoorehchi Seyed Amirreza Babaei Niloofar Arabi	PERFORMANCE ASSESSMENT OF NATURAL GAS DEHYDRATION TECHNOLOGIES	225
IBRAHIB B. B. USMAN A.	ESTIMATION OF GLOBAL SOLAR RADIATION USING FIVE SUNSHINE BASED MODELS FOR ILORIN, NORTH- CENTRAL, NIGERIA	226
Mostafa M. Hamad	BENTHIC FORAMINIFERA AS BIOSTRATIGRAPHICAL AND PALEOECOLOGICAL INDICATORS: AN	227

EXAMPLE FROM THE MIOCENE
DEPOSITS IN GEBEL ABU SHAAR EL
QIBLI, GULF OF SUEZ REGION, EGYPT

Shivam Priyadarshi Mainak Pal Lalawmpuia Manapuram Muralidhar	STUDIES ON ENGINEERING APPLICATION DOMAINS OF INDUSTRY 5.0 IN INDIA	228
Adane Obsie Bifa Mulugeta Soruma Guta	FACTORS AFFECTING PEDESTRIANS' FREE-MOBILITY AND SOCIAL DISTANCING TO COMBAT COVID-19: EVALUATION OF PEDESTRIANS' MOBILITY AND URBAN SPACE IN DOWNTOWN OF NEKEMTE CITY, ETHIOPIA	230
К.Т.Н. Янкевич Н.С.	DEVELOPMENT OF A SYSTEM FOR PREVENTIVE DIAGNOSTICS OF A TECHNICAL OBJECT USING ARTIFICIAL INTELLIGENCE	231
Asif Ali	ENERGY STORAGE CHARACTERISTICS OF 0.5 BaTiO ₃ – BixNax(Mg0.67Nb0.33)1-xNbx	233
Bharath Kumar Shanmugam Harsha Vardha Govinda Raj. M Marutiram Kaza2 Rameshwar Sah Harish Hanumanthappa	REGRESSION ANALYSIS ON SEPARATION PERFORMANCE OF LINEAR VIBRATING SCREEN	234
Mehrddad Karimimoshaver Attiyeh Khorshidi Alireza Gerami	PEDESTRIANS MOVEMENT PATTERNS IN THE SELF-MADE HABITATS WITH EMPHASIZING ON SECURITY IMPROVEMENT BY COMBINING TWO UAVs AND SPACE SYNTAX	235
Mourad Nahal Yacine Saharoui Omar Reffas Chaouki Moumeni Naziha Zerari	BAYESIAN NETWORKS EFFECTIVENESS FOR ELECTRICAL SYSTEMS MAINTENANCE PLANNING	236
Shagufta Noreen Suad Naheed	BIODEGRADATION OF AZO DYES BY HALOPHILIC BACTERIA	237

SÜRDÜRÜLEBİLİR BİR YAPI MALZEMESİ OLARAK BAMBU
BAMBOO AS A SUSTAINABLE BUILDING MATERIAL

Büşra YILDIZ

Mimar, Dokuz Eylül Üniversitesi, Fen Bilimleri Enstitüsü
Architect, Dokuz Eylul University, Graduate School of Natural and Applied Sciences
ORCID ID: 0000-0002-9094-7163

Ahmet Vefa ORHON

Doç. Dr., Dokuz Eylül Üniversitesi, Mimarlık Fakültesi
Assoc.Prof.Dr., Dokuz Eylul University, Faculty of Architecture
ORCID ID: 0000-0003-2465-1951

ÖZET

Bambu, insanlık tarafından kullanılan en eski geleneksel yapı malzemelerinden biridir. Bambunun yapı malzemesi olarak kullanımı uzun bir süreçte gerçekleşmiştir. Özellikle Asya'da geleneksel mimarlıkta bambu yaygın biçimde kullanılmıştır. Ancak endüstriyel çağdan sonra, yapı malzemesi olarak bambu modası geçmiş, ucuz ve kalıcı olmayan ve aynı zamanda düşük sınıf bir malzeme olarak kabul edilmiş, hatta “fakirin kerestesi” olarak adlandırılmıştır. Ancak modern mimarlıkta bambuya bakış sürdürülebilirlik endişeleri ile birlikte büyük ölçüde değişmiştir. Bu makalenin amacı, öncelikle modern bir yapı malzemesi olarak bambuyu tanıtmaktır. Çalışmada geleneksel ve modern mimarlıkta bambu kullanımına dönük sistematik literatür taraması ve içerik analizi yöntemleri kullanılmıştır. İncelenen konu ile ilgili kaynaklar taranıp, elde edilen örnekler sınıflandırılarak sunulmuştur. Araştırmanın sonucuna göre, bambu; ahşap, tuğla veya betondan daha yüksek bir basınç dayanımına ve çeliğe rakip olan bir çekme dayanımına sahiptir. Günümüzde ormanların giderek azalmasıyla birlikte ahşap ihtiyacı artarken, ahşabın yeniden büyümesi ve yapı malzemesi olarak kullanıma hazır hale gelmesi için ihtiyaç duyulan uzun süre bu malzemeye alternatif bir yapı malzemesi ihtiyacını ortaya çıkarmaktadır. Bambu 3-5 yıl gibi kısa bir sürede hasat edilebilen, ahşaba alternatif bir yapı malzemesidir. Bununla birlikte bambu ekim sırasında havaya oksijen de salmaktadır. Bu yetenek çelik, plastik ve beton gibi endüstriyel malzemeler tarafından gerçekleştirilememektedir. Çalışmada değinilen bu ve benzer nedenler bambuyu sürdürülebilir bir doğal kaynak olarak öne çıkartmış ve teknolojik ilerleme ve girişimler, modern inşaat ve yapısal uygulamalarda bambunun geliştirilmesine yardımcı olmuştur.

Anahtar Kelimeler: bambu, sürdürülebilir yapı, sürdürülebilir yapı malzemeleri, alternatif yapı malzemesi

ABSTRACT

Bamboo is one of the oldest traditional building materials used by mankind. The use of bamboo as a building material has taken place over a long period of time. Bamboo has been widely used in traditional architecture, especially in Asia. But after Industrial Revolution, bamboo as a building material was considered obsolete, cheap and low-class material even labelled as "poor man's timber". However, the view of bamboo in modern architecture has changed drastically with sustainability concerns. The purpose of this article is primarily to introduce bamboo as a modern building material. In this study, a systematic literature review on the use of bamboo in traditional and modern architecture was made and content analysis methods were used. The sources related to the subject were scanned and the samples obtained from the sources were presented by classifying them. According to the results of the research, bamboo has a higher compressive strength than wood, brick, and concrete. It also has a tensile strength that rivals steel. Today, while the need for wood increases with the decrease of forests, it takes a long time for wood to grow back and become ready for use as a building material. Therefore, there is a need for a new alternative building material to wood. This material is bamboo. Because bamboo can be harvested in a short period of 3-5 years. In addition, bamboo also releases oxygen into the air during planting. This ability cannot be realized by industrial materials such as steel, plastic, and concrete. These and similar reasons mentioned in this study have highlighted bamboo as a sustainable natural resource. In addition, technological progress and initiatives have helped to develop bamboo in modern construction and structural applications.

Keywords: bamboo, sustainable construction, sustainable building material, alternative building material

1 GİRİŞ

“Eğilen bambu direnen meşeden daha güçlüdür”

Japon Atasözü

Dünya nüfusunun hızlı artışının – bu nüfusun artan yaşam süreleri ve gelişen yaşam refahı beklentileri ile birlikte – dünya kaynakları üzerinde ciddi bir baskı yarattığı bilinen bir gerçektir. Sanayileşmeyle birlikte küresel çevre sorunlarının da sebebi olan bu olgu, dünya kaynaklarının sürdürülebilir kullanımını bir zorunluluk haline getirmiştir. Günümüzde özellikle orman kaynakları, ormanların küresel çevre sorunlarının giderilmesindeki önemli rollerine rağmen, ciddi bir baskı altındadır. Bu noktada, bambu sürdürülebilir bir doğal kaynak olarak öne çıkmaktadır. Birleşmiş Milletler Gıda ve Tarım Örgütü raporuna göre bambu, günümüzde en önemli ahşap-dışı orman ürünüdür. Yine aynı rapora göre bambu, özellikle son 10-15 yılda uygun endüstriyel işlemlerle ahşap yerine kullanılabilecek böylece

dünya ormanlarının korunması ve geliştirilmesi çabalarına katkı sağlayabilecek önemli bir alternatif olarak öne çıkmaya başlamıştır (Bowyer vd., 2014).

Bambu, yapı malzemesi olarak Asya ve Latin Amerika'da uzun zamandır kullanılmaktadır. Küresel çevre sorunlarına karşı sürdürülebilirlik olgusunun zorunlu olarak ön plana çıkmasıyla birlikte bu sağlam, çevre dostu ve sürdürülebilir malzeme sürdürülebilir mimarlık pratiğinde çağdaş uygulamalarla da yerini almaya başlamıştır.

2. DOĞAL BİR KAYNAK OLARAK BAMBU

Türkçe'de Hint Kamışı, Hezaren isimleriyle de bilinen (Türk Dil Kurumu, b.t.) bambu, buğdaygillerden, sıcak ülkelerde yetişen, görece çabuk büyüyen, 75 cins altında 1250 türü kapsayan (Scurlock, Dayton ve Hames, 2000) bir bitki alt familyasının genel adıdır. Bambu türleri Muson Asya'sı ve Güney Amerika'da coğrafi yaygınlık göstermekle birlikte Afrika'nın düzenli yağış alan bölgeleri ve Kuzey Amerika'da da yetişebilmektedir (**Resim 2.1**). Çin, Japonya, Hindistan, Bangladeş, Endonezya, Tayland, Nikaragua, Kolombiya gibi pek çok ülkede doğal bambu ormanları bulunur (**Resim 2.2**). Bambu bitkisi dünyadaki en önemli biyokütle kaynaklarından birisidir; ortalama 10 ton/hektar hesabıyla yapılan bir tahmine göre, orman biyokütlesinin tropik bölgelerde dörtte biri, subtropik bölgelerde beşte biri bambu türlerinden oluşur (Janssen, 2000).



Şekil 2.1 Bambunun coğrafi dağılımı (yeşil renk) (Knighton, 2022)



Şekil 2.2 Sagano Bambu Ormanı (Kyoto, Japonya) (Cripps, 2019)

Cüce bambu türleri 10 cm. boyunda olabilirken diğer türler genellikle 15-20 m.'ye kadar büyür. Tropiklerde bilinen en büyük bambu türü (*Dendrocalamus giganteus*) 30 cm. gövde çapına ve 40 m. (130 ft) yüksekliğe, Avrupa'da ve ABD'de 20-30 m. (65-98 ft) yüksekliğe erişebilir (Scurlock vd., 2000). "En hızlı büyüyen bitki" olarak Guinness rekorlar kitabına

girmiştir. Dünya rekoru olarak, günde 91 cm'ye (35 inç) kadar büyüyen türünün olduğu ve 0.00003 km/sa (0.00002 mph) hızla büyüebildiği tespit edilmiştir. ("Fastest growing plant", b.t.); özellikle Moso (*Phyllostachys edulis*) ve Madake (*Phyllostachys bambusoides*) bambuları hızlı büyümeleriyle bilinir.

Bambu günümüzde, dünya nüfusunun %40'ının (yaklaşık 2.5 milyar insan) günlük hayatlarında çeşitli biçimlerde ve yaygın olarak yer alır (Scurlock vd., 2000). Kullanım alanları en geniş doğal kaynaklardan biridir; elyaf (kâğıt lifi, dokuma elyafı, örgü lifi vb.), gıda maddesi (sürgünlerini haşlayarak yeme, bambu turşusu, bambu birası vb.), yakacak (bambu odunu, bambu kömürü, bambu gazı vb.), endüstriyel ürünler için hammadde (**Resim 2.3**), yapı malzemesi vb. pek çok amaçla kullanılır. 2000 yılında yapılan bir tahmine göre bambu menşeli ürünlerin dünya çapında yıllık ticari cirosu asgari 10 milyar dolardır (Janssen, 2000).



Şekil 2.3 Bambu kullanılan endüstriyel ürünlerden örnekler (a) Masif bambu gözlük çerçevesi (b) Kompozit bambu kask (c) Masif bambu çerçeveli bisiklet (d) Masif bambu gövdeli kol saati (Kişisel arşiv, 2021)

"1945'te Japonya'nın Hiroşima kentindeki atom bombalarının radyasyonundan tekrar kurtulan ve filizlenen ilk bitkidir."

3. YAPI MALZEMESİ OLARAK BAMBU

Bambunun yapı malzemesi olarak kullanımı doğal olarak bolca yetiştiği Güney Amerika, Afrika ve Güneydoğu Asya'da oldukça eski bir uygulamadır. Örneğin, Güney Amerika'da yetişen Guadua cinsi bambunun Ekvator başta olmak üzere bölgede 9500 yıldan bu yana bina yapımında kullanıldığı bilinmektedir (Caffiero, 2006). Bambu yapı geleneği pek çok ülkede kültürel yapıya da işlemiştir. Örneğin Hindistan'da yüksek kastle mensup kişiler taş, orta kastle ahşap ve düşük kastle da bambu yapılarda otururlardı. Hindistan'da bambu yapılar ülkenin kırsal kesimlerinde hala yaygın biçimde kullanılmaktadır. Şiddetli depremlerin görüldüğü Assam ve Kuzeydoğu Hindistan'da bu yapıları kentsel doku içerisinde görmek de

mümkündür. Assam tipi olarak adlandırılan bu yapılar bambu hasır üzerine kireç sıva ile kaplanmıştır (Ghosh, 2008).

Tablo 3.1 Yapı Malzemesi Olarak Bambunun Avantajları

YAPI MALZEMESİ OLARAK BAMBUNUN AVANTAJLARI		
1	Kolay Yetiştirilir	Bambunun gelişme sürecinde gübre, zirai ilaç ve pestisit kullanmaya ihtiyaç yoktur. Sulama gerektirmez.
2	Doğada Bolca Bulunur	Hasat edilen kökten yeni bir sürgün verir, bu nedenle yeniden ekim yapılmasına veya ilave bir yetiştirme alanına gerek kalmadığı için bu durum önemli ölçüde tasarruf sağlamaktadır.
3	Hızlı Büyür	Yaklaşık kırk yılda yetişen iğne yapraklı ve yaprak döken ağaçların aksine, bambu olgunlaştıktan 3-5 yıl sonra hasat edilebilmektedir. Aynı zamanda filizlenmeye başladıktan sonra büyüme hızı oldukça yüksek olan bitki, kısa bir süre içerisinde metrelerce uzunluğa ulaşmaktadır. Bambudan alınan verim, diğer ağaçlardan yaklaşık 25 kat fazladır. Dünya genelinde haftada yaklaşık bin hektar orman kesilmektedir, ağaç yerine bambu kullanarak bu oranı düşürmek ve ormanları korumak mümkündür.
4	Uzun Ömürlü	120 yıla kadar yaşayan türlerine rastlanabilir.
5	Çevre Dostu	Eşdeğer bir ağaçtan %35 daha fazla oksijen üretmektedir. CO2 tutar ve karbon nötrdür. Mükemmel bir toprak erozyonu inhibitörüdür.
6	Düşük Ağırlıklı	Dairesel ve içi boştur. Düşük ağırlıklarından dolayı bambular kolayca kurulur, nakliyesi ve depolanması kolaydır.
7	Yangına Dayanıklı	Yüksek silikat asit içermesi nedeniyle yangına karşı çok dayanıklıdır. İçinden geçen 4000°C'ye kadar kaynar suya dayanabilir.
8	Deprem ve Kasırgalara Dayanıklı (Esnek)	Hafifliği ve esnekliği nedeniyle bambu, özellikle dünyadaki deprem bölgelerinde popüler bir yapı malzemesidir. Bambu, sismik aktivitenin ve şiddetli rüzgarların şoklarını sert beton ve çelik yapılardan çok daha iyi emer.
9	Ekonomik	Çoğu yapı malzemesine kıyasla ekonomiktir.
10	Güvenli	Çimento ve asbest gibi diğer yapı malzemelerinin aksine, bambu sağlık için tehlike oluşturmaz. Bambu, Kun adı verilen doğal bir antibakteriyel biyoajan içerir. İçinde büyümeye çalışan bakterilerin %70'inden fazlasını kendiliğinden yok eder ve dış mikropları da engeller.

11	Geri Dönüştürülebilir	Bambu yapı malzemesi olarak kullanıldığında kullanım ömrü sonunda geri dönüşüm aşamasında da – biyokütle olması nedeniyle –sorunsuz bir malzemedir. Bambu kamışları uygun biçimde parçalanıp toprakta çürümeye bırakıldığında yaklaşık 90 gün içinde çözünüp doğal gübre olarak kullanılabilir (Syeda, Shrujal ve Kumar, 2014).
-----------	------------------------------	---

Tablo 3.2 Yapı Malzemesi Olarak Bambunun Dezavantajları

YAPI MALZEMESİ OLARAK BAMBUNUN DEZAVANTAJLARI		
1	Büzülebilir	Bambu, su kaybettiğinde ahşap ve keresteye kıyasla daha fazla küçülür. Bu nedenle inşaat malzemesi olarak bambu kullanıldığında su kaybını önlemek için uygun önlemlerin alınması çok önemlidir.
2	Koruma Gerekir	Bambu kullanılmadan önce böcek veya mantar saldırısına karşı yeterince korunmalıdır. Bu nedenle, kesildikten sonra bambu hemen özel bir aşılama ve kurutma işleminden geçmelidir. Bambu, ağaç gibi toprakla sürekli temas halinde çürür ve böcekleri çeker. Bu nedenle bambu ve toprak temasını önerilmemektedir.
3	Zor Boyanır	Bambu, mumsu kaplaması nedeniyle boyanmaya elverişli değildir.
4	Zor Birleştirilir	Sürekli düzensiz büyüyen, kıvrımlı bir bitki ile çalışmak oldukça zordur. Ayrıca ağaç veya herhangi başka bir malzemenin birleştirme yöntemleri ile uyumlu değildirler.
5	Yapısı	Silindirik yapısı ve içinin boş olması ise olumsuz özelliklerindedir. Bambu anizotropik bir malzemedir. Boyuna yöndeki özellikler, enine doğrultudakilerden tamamen farklıdır. Boyuna yönde güçlü ve sert olan selüloz lifleri, enine yönde ise yumuşak ve kırılman olan lignin bulunur. Bambu enine ağırlık taşımaz. Yalnızca uzunluğu boyunca (yükseklik açısından) ağırlık taşıyabilir (Syeda, Shrujal ve Kumar, 2014).

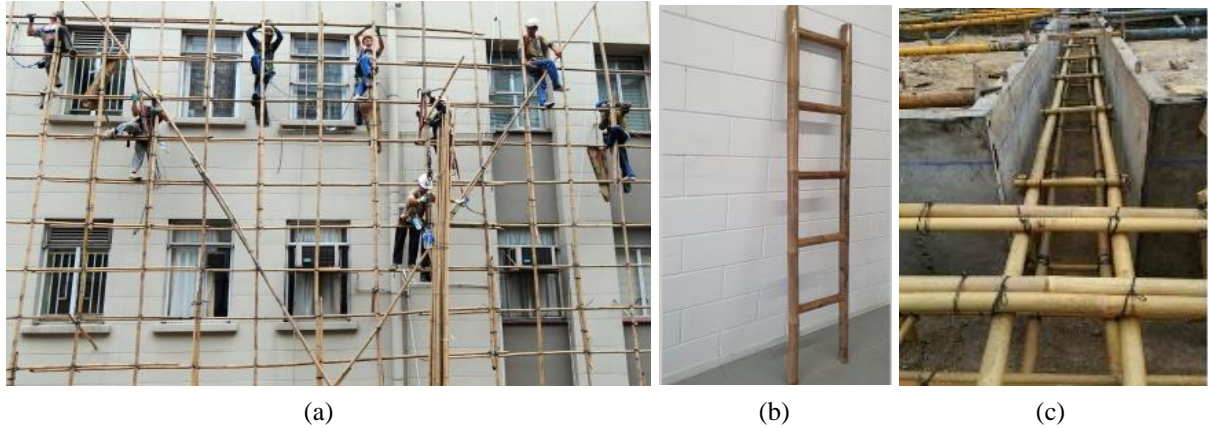
4.YAPI MALZEMESİ OLARAK BAMBUNUN KULLANIM ALANLARI

Bu yazıda bambu yapılarda kullanım **amaçlarına** göre üç ana grupta incelenmektedir. Bu grup başlıkları: 1.) taşıyıcı ürün olarak bambu kullanımı, 2.) bölücü/örtücü ürün olarak bambu kullanımı ve 3.) tamamlayıcı ürün olarak bambu kullanımıdır. Bunlar da daha sonra kendi içlerinde alt başlıklarla **kullanım yerlerine göre** detaylandırılmıştır.

Tablo 4.1 Yapılarda Bambu Kullanım Alanları

YAPILARDA BAMBUNUN KULLANIM ALANLARI		
1. TAŞIYICI ÜRÜNLER	2. BÖLÜCÜ/ÖRTÜCÜ ÜRÜNLER	3. TAMAMLAYICI ÜRÜNLER
a.) Strüktür b.) İskele ve Merdiven c.) Betona Takviye Donatısı	a.) Duvarlar / Bölmeler b.) Çatı Kaplaması c.) Zemin Kaplaması d.) Gölgeleme Elemanları	a.) Doğramalar b.) Bahçe Çitleri ve Korkuluklar c.) Mobilyalar d.) Vitrifiye

4.1. Taşıyıcı Ürünler: Mekanik özellikleri yüksek olan ürünlerdir. Yapıda yük taşıyan bölümlerde (taşıyıcı duvar, kolon, kiriş, döşeme, temel vb.) kullanılır. Yapıdaki kullanım yerlerine göre bu grup kendi içinde üç alt başlıkta incelenmiştir. Bu alt başlıklar: a.) strüktürler b.) iskele ve merdivenler ve c.) betona takviye donatısıdır.



Şekil 4.1 (a) bambu inşaat iskelesi (Yu, 2016)., (b) bambu merdiven ('Bamboo stair (varnish)', b.t.) ve (c) betona donatı elemanı olarak bambu kullanımı ('Bamboo reinforced concrete', 2016)



Şekil 4.2 Çeşitli yapılarda strüktürde farklı yöntemlerle bambu kullanımı ('Bamboo structure', b.t.)

4.2. Bölücü / Örtücü Ürünler: Yapıyı iç ve dış etkenlerden (ısı, ses, su, toz vb.) koruyan, mekanları bölen ve örten/kaplayan ürünlerdir. Yapıdaki kullanım yerlerine göre bu grup kendi içinde dört alt başlıkta incelenmiştir. Bu alt başlıklar: a.) duvarlar ve bölmeler b.) çatı kaplaması c.) zemin kaplaması ve d.) gölgeleme elemanlarıdır.



Şekil 4.3 (a) Bambu duvar kaplaması (John, 2014), (b) Bambu çatı kaplaması (Cortés, 2021), (c) Bambu zemin kaplaması (Admin. b.t.), Bina dış cephe gölgeleme elemanı olarak bambu kullanımı (Treehugger, 2012)

4.3. Tamamlayıcı Ürünler: Bu malzemeler yapılarda taşıma ve koruma özellikleri dışında tali(ikincil) amaçlar (dekorasyon, vitrifiye, tamamlama vb.) için kullanılan malzemelerdir. Aslında yapılarda birçok detayda kullanılabilir ama bu yazıda en çok tercih edilen kullanım yerlerine göre bu grup kendi içinde dört alt başlıkta incelenmiştir. Bu alt başlıklar: a.) doğramalar b.) bahçe çitleri ve korkuluklar c.) mobilyalar ve d.) vitrifiyedir.



Şekil 4.4 (a) Bambu pencere doğraması (Bari, b.t.), (b) Bambu kapı doğraması ve kaplaması (Pridgeon, 2013), (c) Bambu çit (GDMING bamboo fence”, b.t.), (d) bambu mobilyalara birçok örnek (“Sustainable design and”, b.t.), (e)bambu lavabo (“Aria bamboo vessel”, b.t.)

5.YAPI MALZEMESİ OLARAK BAMBUNUN KULLANILDIĞI ÖRNEKLER

Tablo 5.1 Bambu Pavyon Örneği 3: ZERI Pavyonu

YAPININ ADI	ZERI Pavyonu
YERİ	Hannover, Almanya
YAPIM YILI	2000
MİMARİ	Simon Veléz, Marcelo Villegas
BAMBUNUN YAPIDAKİ KULLANIM YERİ	
Taşıyıcı Ürünlerde	Strüktür
Bölücü/Örtücü Ürünlerde	Çatı Kaplaması
AÇIKLAMA	
<p>Öncelikle yapının mimarı Simón Vélez, inşaatta bambu ve Guadua kullanımında uzman olan dünya çapında en ünlü mimardır. Yapı, ZERI (Sıfır Karbon Emisyonu Araştırma İnisyatifi) Galerisi, EXPO 2000 Fuarı'nda Almanya'da sergilenmiştir. Başlangıcı ve sonu olmayan, daire şeklindeki açık tasarımı ile herkesi engelsiz şekilde katılmaya davet etmektedir. Her yerde, herkes tarafından erişilebilir olan kavram ve teknolojileri bünyesinde barındıran evrensel bir organizasyonu sembolize etmektedir (Marshall McLuhan).</p> <p>Yapı, uzunlukları 14-20 metre arasında değişen 20 adet bambu direk üzerine kurulmuştur. Dış sütunlar, ana kirişlerle birbirine bağlanan tek bir taban üzerine oturtulmuştur. İç sütunlar merkez halkaya bağlanmıştır. 40 metre çapındaki çatının yüksekliği mahyada 14,5 metre, oluklarda 7 metredir. Çatı kaplaması olarak on kenarlı çokgen şeklindeki bir yağmurluk (membran), dışta ise bambu ile güçlendirilmiş 3 cm kalınlığındaki çimento kiremitler kullanılmıştır. (Rohrbach ve Gillmann, 2001).</p>	
YAPININ GÖRSELLERİ	
	
Şekil 5.1 ZERI pavyonunun bambu iskeleti detay görüntüleri (Rohrbach ve Gillmann, 2001)	

Tablo 5.2 Bambu Köprü Örneği: Yaya Köprüsü (Footbridge)

YAPININ ADI	Yaya Köprüsü (Footbridge)
YERİ	Santa Fe de Antioquia, Kolombiya
YAPIM YILI	2005
MİMARİ	Jörg Stamm, Juan Carlos Sanz
BAMBUNUN YAPIDAKİ KULLANIM YERİ	
Taşıyıcı Ürünlerde	Strüktür
AÇIKLAMA	
Köprü 30 m açıklığa ve 3 m serbest genişliğe sahiptir. 10 – 14 cm kesitli 600 ‘‘Guadua	

Angustifolia’’ bambusu ile inşa edilmiştir. Bu miktar, 500 kg/m² yük, 15 ton rüzgar kuvveti ve 30 yıllık ömür için hesaplanmıştır. Kemerler için doğal eğriliğe sahip bambular seçilmiştir. Basınç kuvvetleri, büyük bir beton temele aktarılmıştır. Köprünün zemini beton; çatı terracotta kiremitlerle kaplanmıştır. Montajı üç hafta sürmüştür. Kemerli elemanlar, ahşap çivilerle kalıcı bir eğri içinde bir arada tutulan beş bükülmüş bambu kamışından oluşmaktadır. Yapıyı hava koşullarına karşı korumak için bambu elemanların tümünde bir UV engelleyici ile karıştırılmış keten tohumu yağı bazlı bir vernik kullanılmıştır (Minke, 2016).

YAPININ GÖRSELLERİ



Şekil 5.2 Köprünün görünüşleri ve taşıyıcı sistem detay görünüşü (Minke, 2016)

Tablo 5.3 Bambu Konut Örneği 1: Carabanchel’de Bambu Konut

YAPININ ADI	Carabanchel’de Bambu Konut
YERİ	Carabanchel, İspanya
YAPIM YILI	2007
MİMARİ	Foreign Office Architects (FOA)
BAMBUNUN YAPIDAKİ KULLANIM YERİ	
Bölücü/Örtücü Ürünlerde	Gölgeleme Elemanı
AÇIKLAMA	
<p>Avrupa’nın en büyük sosyal konut projelerinden biridir. Bambu saplarıyla kaplı beş katlı bir binadır. Binanın kendisi bambudan inşa edilmemiş olmasına rağmen ilk bakışta bambular göze çarpmaktadır. Proje ile, geniş alanlı ve yüksek kaliteli ucuz konutlar sunmanın yanı sıra, bambu panjurların dikkat çektiği bir dış cephe görüntüsü amaçlanmıştır. Yapının dış yüzeyinin tamamen bambuyla kaplı olmasına karşılık, panjurlar isteğe bağlı olarak açılıp kapatılabilmektedir.</p> <p>Bambu her bakımdan enerji tasarrufu sağlamaktadır. Bu projede bambu; kışın ısı yalıtımı sağlamakta, yazın ise doğal gölgelik özelliğiyle iç mekanı kavurucu sıcak ve güneş ışığından koruyarak serinletmektedir. Aynı zamanda, kalabalık şehirler için önemli bir husus olan ses yalıtımı da sağlayan bir malzemedir (Jewell, 2011).</p>	
YAPININ GÖRSELLERİ	

INTERNATIONAL AEGEAN CONFERENCES
ON INNOVATION TECHNOLOGIES & ENGINEERING-VI
December 20-22, 2022

Şekil 5.3 Binanın tamamen bambularla kaplı dış cephe görünüşü (Jewell, 2011)

Tablo 5.4 Bambu Konut Örneği 4: Colibri Evi

YAPININ ADI	Colibri Evi
YERİ	Cali, Kolombiya
YAPIM YILI	2009
MİMARİ	Juan Carlos Moreno, Mónica Guerrero, Luis Carlos Rios
BAMBUNUN YAPIDAKİ KULLANIM YERİ	
Taşıyıcı Ürünlerde	Strüktür, Merdivenler
Bölücü/Örtücü Ürünlerde	Duvarlar, Zemin Kaplaması
Tamamlayıcı Ürünlerde	Pencere ve Kapı Doğramaları, Korkuluklar
AÇIKLAMA	
<p>Ev, köprülerle birleştirilmiş üç modülden oluşmaktadır. Bambu <i>Guadua angustifolia</i>, bu modüllerin (yapı, duvarlar ve çatı) yapımında kullanılan ana unsurdur. 1. ve 2. modüllerin her biri, nehir taşı temeller üzerinde desteklenen 6 m açıklıklı dört revak ile inşa edilmiştir. Her sütun, birinci katta 13 bambu direktten oluşan bir demet olup, ikinci katta 9 bambu direğe ve üçüncü katta 4 bambu direğe dönüşür. Çatı yapısı, çatının eğrisini oluşturan farklı yükseklikteki payandalara sahip makaslardan oluşmaktadır. Saçaklar ise ana yapıya diyagonal kamışlarla sabitlenmiştir. Bambu kamışlar, palmye ağacı pimleri ve galvanizli tel ankrajlarla birleştirilmiştir. Duvarlar, yaklaşık olarak her 50 cm'de bir meydana gelen ikincil kolonlardan oluşan bir yapıya tutturulmuş <i>guadua</i> kalaslarından yapılmıştır. Yapısal derzler, hava koşullarına maruz kalan bambu kamışların çoğu ve duvarların tümü, kireç, sisal lifleri ve çimento ile stabilize edilmiş bir toprak karışımı ile kaplanmıştır. 3.modül, bir wattle-and-daub sepeti gibi inşa edilmiş oval formu nedeniyle stabildir. Açık salon katının zemini, inşaattan kalan bambularla oluşturulmuştur (Minke, 2016).</p>	
YAPININ GÖRSELLERİ	
	
Şekil 5.4 Konutun iç ve dış cephe görünüşleri ve detayları (Minke, 2016)	

Tablo 5.5 Bambu Konut Örneği 3: Stepped House

YAPININ ADI	Stepped House
YERİ	El Darién, Valle, Kolombiya
YAPIM YILI	2009
MİMARİ	Opción Timagua (Mónica Guerrero and Daniel Benavides)
BAMBUNUN YAPIDAKİ KULLANIM YERİ	
Taşıyıcı Ürünlerde	Strüktür
Bölücü/Örtücü Ürünlerde	Duvarlar, Zemin Kaplaması

INTERNATIONAL AEGEAN CONFERENCES
ON INNOVATION TECHNOLOGIES & ENGINEERING-VI
December 20-22, 2022

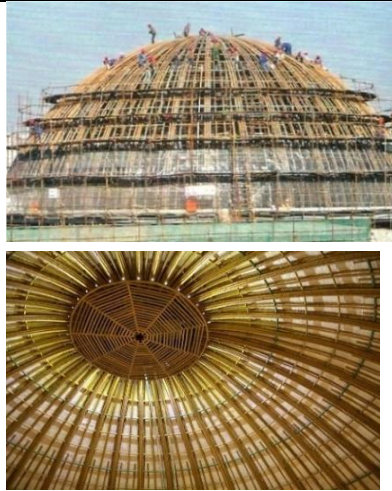
Tamamlayıcı Ürünlerde	Pencere ve Kapı Doğramaları
AÇIKLAMA	
<p>Beş katlı ev, 12 m genişliğinde ve 42 m derinliğinde, 45 derece eğimli bir arsa üzerinde yer almaktadır. Yapı, Guadua Angustifolia'nın piramidal sepet şeklinde üç katlı bir kule yapısını taşıyan beton ve nehir taşı istinat duvarlarından yapılmış iki katlı bir temel üzerine oturmaktadır. Kulede, ana köşe sütunları, her 50 cm'de bir ikincil sütunların bulunduğu üç bambu kamışından oluşur. Bunlar, palmiye ağacı pimleri (<i>Bactris macana</i>) ile birleştirilir. Döşeme plakaları, bir ahşap zemin için bir taban olarak bambu plakalarla kapatılmış, üç kamıştan oluşan ana kirişler, iki kamıştan oluşan ikincil kirişler ve her 40 cm'de bir üçüncül kirişlerden oluşan bir yapıdan oluşur. Duvarların her iki tarafı çamur, kireç, fique lifleri (sisal lifleri) ve bir miktar çimento ile sıvanmış bambu kalaslarla kaplanmıştır. Tonozlu kulenin çatısı, çevresinde eğimli sütunlarla sabitlenir ve bir membran ve boya ile kaplanmış bir kamış örgüsü ve hasırlardan oluşur (Minke, 2016).</p>	
YAPININ GÖRSELLERİ	
	
	
Şekil 5.5 Konutun bambu iskeleti, dış cephe görünüşü ve bambu zemin kaplaması (Minke, 2016)	

Tablo 5.6 Bambu Pavyon Örneği 1: Hint Pavyonu, EXPO 2010

YAPININ ADI	Hint Pavyonu, EXPO 2010
YERİ	Şangay, Çin
YAPIM YILI	2010
MİMARİ	Pradeep Sachdeva, Simón Vélez
BAMBUNUN YAPIDAKİ KULLANIM YERİ	
Taşıyıcı Ürünlerde	Strüktür
AÇIKLAMA	
<p>Pavyon, 35 m çapında ve 17 m yüksekliğinde 980 m² alana sahip kubbeli bir formdadır. Yapı, 36 bambu kemerle tabandan fırlar ve tepede birleşir. Her bir kemer, uç uca</p>	

yerleştirilmiş ve birleştirilmiş 6 bambudan oluşur. Kemerler, yapının sahada doğru geometriye göre inşa edilmesini sağlamak için farklı seviyelerde 10 bambu ve 4 çelik halka ile birleştirilmiştir. Altta bir beton halka ve üstte bir tane daha vardır. Bambuları birleştirirken, derzlerin yakınındaki bambu düğümlerine çimento harcı enjekte edildi. Bambu parçalarının bağlantı noktalarındaki çap farklılıklarını absorbe etmek için en büyük çaptan daha büyük bir çelik levha kullanıldı. Bu plaka ayrıca cıvatanın gömülü olduğu çimento harcı için bir durdurucu görevi görür. Çatı kaplamasına serilen membran nem ve su bariyeri işlevi görür. Bunun üzeri 125.000'den fazla bitki, çok renkli bir desende "Hayat Ağacı" halisinden esinlenerek elle dikildi ve bu bitkilere entegre bakır plakalarla süs tasarımı oluşturmuştur. Kullanılan bambu, yerel olarak "Moso" veya "Mao Zhu" olarak adlandırılan *Phyllostachys heterocycda pube-scens* veya *Phyllostachys edulis*'tir ve Şanghay'ın 200 km batısındaki Anji bölgesinden tedarik edilmiştir.. Bu bambu kamışlar, ılık bir borik asit ve ağartıcı çözeltisi içinde işleme tabi tutuldu ve sıcakken büküldü. Eklemler metalik pimlerle sabitlendi; delinmiş internodlar betonla dolduruldu ("World's largest bamboo", 2010).

YAPININ GÖRSELLERİ



Şekil 5.6 EXPO 2010 Hint pavyonunun bambu iskeleti detay görüntüleri ("World's largest bamboo", 2010)

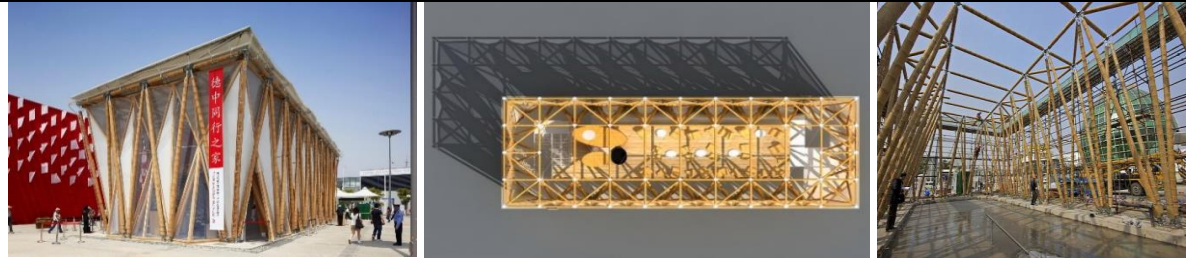
Tablo 5.7 Bambu Pavyon Örneği 2: Alman-Çin Evi, EXPO 2010

YAPININ ADI	Alman-Çin Evi, EXPO 2010
YERİ	Shanghai, Çin
YAPIM YILI	2010
MİMARİ	Markus Heinsdorff
BAMBUNUN YAPIDAKİ KULLANIM YERİ	
Taşıyıcı Ürünlerde	Strüktür
Bölücü/Örtücü Ürünlerde	Zemin Kaplaması
Tamamlayıcı Ürünlerde	Mobilyalar
AÇIKLAMA	

INTERNATIONAL AEGEAN CONFERENCES
ON INNOVATION TECHNOLOGIES & ENGINEERING-VI
December 20-22, 2022

25 × 10 m ölçülerinde, 2 katlı, 8 m yüksekliğinde, 330m² alana sahip binada sergi, oyun ve konferans alanları bulunmaktadır. Çatı konstrüksiyonu, Güney Çin'den tedarik edilen 23 cm'ye kadar kesite sahip 8 m uzunluğundaki Julong bambu direklerinden yapılmıştır. Lamine bambu çerçeveler üst katın zemininde kullanılmıştır. Tüm yapısal bambu elemanlar bir yangın önleyici madde ile işlenmiştir. Paslanmaz çelik bağlantı parçaları özellikle bu köşk için geliştirilmiş olup, kullanımdan sonra yapının kolayca demonte edilebilmesi için tasarlanmıştır. Sütunların dibindeki dişli elemanlar, toleranslara uyum sağlamayı mümkün kılmaktadır. Bambu kamışlarının uç kısımları, iyi bir mekanik bağlantı sağlamak için, önce poliüretan reçine ve ileri seviye poliüretan reçine ile ıslatılmış kum tabakası ile ıslatılmıştır. Bambu kamışlarının uçları daha sonra yüksek oranda uçucu kül ile yapılmış, bambunun iç yüzeyine sıkıca yapışmasını sağlayan beton karışımı ile doldurulmuştur. Betona yerleştirilen çelik bağlantı setleri, bambunun bölümlerinin birbirine bağlanmasını sağlar. Bambu kamışlarının uçları, iyi bir mekanik dayanıklılık sağlamak için önce poliüretan reçinesi ve daha sonra başka bir poliüretan reçinesi ile kum tabakası ile ıslatılmıştır. Uçlar daha sonra yüksek oranda uçucu kül ile yapılmış bir beton karışımı ile doldurulmuş, bu da betonun içi boş bambu bölümünün iç yüzeyine gözenekler veya boşluklar olmadan yapışmasını sağlamıştır. Betona yerleştirilen çelik bağlantı parçaları, bambu bölümlerin birbirine bağlanmasını sağlamaktadır. Pavyonun cephesi ışık geçirgen ETFE membran kaplama, çatısı ise PVC membran kaplanmıştır. Yine Markus Heinsdorff tarafından pavyon için özel olarak tasarlanan mobilyalar, lamine bambu profillerden yapılmıştır (Minke, 2016).

YAPININ GÖRSELLERİ



Şekil 5.7 EXPO 2010 Alman- Çin pavyonunun bambu iskeleti detay görünüşleri (Minke, 2016)

Tablo 5.8 Bambu Konut Örneği 2: Bb Evi (Çiçek Açan Bambu Ev)

YAPININ ADI	Bb Evi (Çiçek Açan Bambu Ev) (Blooming Bamboo Home)
YERİ	Hoan Kiem Bölgesi, Vietnam
YAPIM YILI	2013
MİMARİ	H&P Architects (Doan Thanh Ha, Tran Ngoc Phuong)
BAMBUNUN YAPIDAKİ KULLANIM YERİ	
Taşıyıcı Ürünlerde	Strüktür, Merdiven
Bölücü/Örtücü Ürünlerde	Duvarlar, Çatı Kaplaması, Zemin Kaplaması, Gölgeleme Elemanı
Tamamlayıcı Ürünlerde	Kapı Doğraması, Korkuluk, Mobilya
AÇIKLAMA	
Bu prototip 44 m ² 'lik yapının amacı, Vietnam'da evleri şiddetli sel baskınlarıyla tehdit edilen insanlara bir çözüm sunmaktır. Ayaklıklar üzerinde yükselen ev, 1,5 m yüksekliğindeki bir sele dayanabilmektedir. Bir sel durumunda, entegre geri dönüştürülmüş yağ tankları nedeniyle bina su	

seviyesiyle birlikte yükselir. Her taraftaki ankrajlı çelik kazıklar, yüzer yapıyı yatay olarak yerinde tutar ve sürüklenmesini önler. Bina, ilave modüller ile kolaylıkla büyütülebilir. Sadece bir ev olarak değil, aynı zamanda bir tıp, eğitim veya toplum merkezi olarak da işlev görür. Yapı, 8-10 cm çapında büyük bir bambu türünden ve 4-5 cm çapında daha küçük bir türden yapılmış modüllerden monte edilmiştir. Bambu saplarının her biri 6.60 m veya 3.30 m uzunluğundadır. Kaplama, yerel iklime ve ince bambu, bambu kamyş, sunta veya hindistancevizi yaprakları gibi bölgesel malzemelere göre değişebilir. Kullanıcılar, 25 gün içinde cıvatalayarak, bağlayarak, asarak ve yerleştirerek binayı kendileri monte edebilmektedirler (Minke, 2016).

YAPININ GÖRSELLERİ



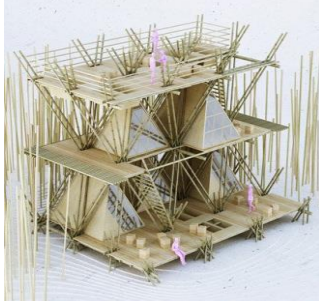
Şekil 5.8 Konutun dış cephe görünüşü ve yapım katmanları diyagramı ve kesiti (Minke, 2016)

Tablo 5.9 Bambu Otel Tasarımı Örneği: Penda'nın Modüler Bambu Oteli

YAPININ ADI	Penda'nın Modüler Bambu Oteli
YERİ	Çin
YAPIM YILI	2014
MİMARİ	Penda
BAMBUNUN YAPIDAKİ KULLANIM YERİ	
Taşıyıcı Ürünlerde	Strüktür
AÇIKLAMA	
<p>Penda'nın ağaç ev eko-oteli, AIM Legend of Tent yarışması için tasarlandı. Yarışma, konukları Çin'in çeşitli kilit noktalarında doğa ile bağlantı kurmaya teşvik eden düşük etkili eko-oteller kurarak büyük Çin bina projelerinin trendini kırmayı amaçlıyor.</p> <p>Ağaç ev Kızılderili Tipi'nden biraz ilham alıyor ve bu göçebe yapı gibi yeniden kullanılabilir, uyarlanabilir ve devam etme zamanı geldiğinde kalıcı hasar bırakmaz. Nitekim Penda'nın tasarım özeti, oteli ömrünün sonuna geldiğinde kolayca sökülebileceğini ve bambunun iskele olarak veya başka bir otel inşa etmek için kullanılabilirliğini belirtiyor.</p> <p>Ağaç ev, iple birbirine bağlanmış bambu çubuklardan yapılmış 4,7 x 4 m (15,4 x 13 ft) ölçülerinde birbirine bağlanan üçgen ızgaralardan oluşur (yapının hiçbir yerinde vida veya çivi kullanılmaz). Iızgaralar yatay veya dikey olarak kolayca genişletilebilir ve çerçeve içine birden fazla modül yerleştirilebilir. Esnek bir ızgara ile ilgili en iyi şey, gerektiğinde yapısal kirişler ekleyebilmenizdir, böylece yapının bir parçası üzerinde daha fazla yük olursa, daha fazla bambu eklenebilir. Penda tarafından önerilen modüllerden bazıları 12 m² (129 sq ft) tek çadır, 20 m² (215 sq ft) tuvalet, 100 m² (1.076 sq ft) lobi ve iki katlı (62 m² /662 sq ft) "başkanlık" çadırıdır (Williams, 2014).</p>	

INTERNATIONAL AEGEAN CONFERENCES
ON INNOVATION TECHNOLOGIES & ENGINEERING-VI
December 20-22, 2022

YAPININ GÖRSELLERİ



Şekil 5.9 Penda'nın Modüler Bambu Oteli bambu iskeleti detay görüntüleri (Williams, 2014)

Tablo 5.10 Bambu Spor Merkezi Örneği: Uluslararası Panyaden Okulu Spor Merkezi

YAPININ ADI	Uluslararası Panyaden Okulu Spor Merkezi
YERİ	Chiang Mai, Tayland
YAPIM YILI	2017
MİMARİ	Markus Roselieb, Tosapon Sittiwong
BAMBUNUN YAPIDAKİ KULLANIM YERİ	
Taşıyıcı Ürünlerde	Strüktür, Merdiven
Bölücü/Örtücü Ürünlerde	Duvarlar, Çatı Kaplaması
Tamamlayıcı Ürünlerde	Kapı, Korkuluk
AÇIKLAMA	
<p>Doğaya saygıyı esas alan Budist değerlerine göre İngiliz sisteminde eğitim veren Uluslararası bir okulun yerleşkesi içinde yapılan bu spor merkezi, doğaya yakın olma felsefesinden hareketle bambu kullanılarak inşa edilmiştir. Yapının taşıyıcı sistemi dışında üst örtü malzemesi de bambudur. Böylece kurumun 'yeşil okul' felsefesine uygun olarak yapının karbon ayak izi de – alternatif yapım sistemlerine göre %90 oranında – azaltılmıştır. Sıcak ve nemli iklimde yer alan yapı, futsal, basketbol, voleybol ve badminton sahaları ile yükseltilebilen bir kulis içeren üstü kapalı, yanları açık bir yapıdır. Sahaların iki yanında yükseltilmiş balkonlar seyir mekânı işlevi görür. 728 m2 alan örten bambu taşıyıcılı ve kaplamalı üst örtünün serbest açıklığı 17.22 m.'dir. Bambu makaslar bu açıklığı çelik takviye veya bağlantı kullanılmaksızın geçecek biçimde tasarlanmıştır. Şantiyede önceden inşa edilen, prefabrik kafes kirişler, bir vinç ile yerine kaldırılmıştır. Yapının ömrünün en az 50 yıl olması beklenmektedir ("Panyaden bamboo sports", b.t.).</p>	
YAPININ GÖRSELLERİ	



Şekil 5.10 Uluslararası Panyaden Okulu Spor Merkezi dış cephe ve iç mekan görüntüleri ("Panyaden bambo sports", b.t.)

Tablo 5.11 Bambu Konferans Merkezi Örneği: Naman Retreat Konferans Salonu

YAPININ ADI	Naman Retreat Konferans Salonu
YERİ	Ngũ HânH Sơn, Vietnam
YAPIM YILI	2015
MİMARİ	VTN (Vo Trong Nghia) Mimarlık
BAMBUNUN YAPIDAKİ KULLANIM YERİ	
Taşıyıcı Ürünlerde	Strüktür
AÇIKLAMA	
<p>3.4 hektarlık bir alanda 80 bungalov, otel, 6 VIP villa ve diğer 20 villanın bulunduğu tatil kompleksi olarak tasarlanmış bölgenin konferans salonu olarak 773 m² alan kaplar. Dikdörtgen planlı, asimetrik eğimli çatılı bir salondur. Tonoz bambu yapısı, binaya ikonik ve etkileyici bir görünüm kazandırıyor. Bina 2 paralel mekandan oluşmaktadır; kapalı salon ve açık koridor. Dış koridor, misafirleri karşılayan bir açık hava lobisi olarak da hizmet veriyor. Ana taşıyıcı yapı, 9,5m çatı yüksekliği ile salonda 13,5 m, koridorda 4 m açıklığı aşan bambu çerçevelerdir. Kemer benzeri izlenim, ana yapının bir parçası olan bükülmüş bambu tarafından yaratılmıştır. Çatı kaplaması olarak saz kullanılmıştır.</p> <p>Bu binada kullanılan 2 çeşit bambu vardır. Düz kolonlar için 8 m'ye kadar ulaşabilen gücü ve uzunluğu nedeniyle "Luong" bambu seçilmiştir. Kemerlerde esneklik özelliğinden dolayı "Tam Vong" bambu kullanılmıştır (Oki, 2015).</p>	
YAPININ GÖRSELLERİ	

Şekil 5.11 Naman Retreat Konferans Salonu bambu iskeleti detay görüntüleri (Oki, 2015)

6.SONUÇ

Sürdürülebilir malzemeler hakkında uzun çalışmalar yapan ve "çevreye zarar vermeden hangi malzemeler kullanılabilir?" sorusuna cevap arayan araştırmacılar; toplu ağaç kesimlerinin,

yapılaşmanın geleceğini iyi bir ekolojik noktaya taşımadığı sonucuna ulaşmışlardır. Bir yapı malzemesi olarak kapsamlı şekilde araştırılan bambunun, çevreye zarar vermeyen en değerli malzemelerden biri olduğu tespit edilmiştir. Bu bitkinin en dikkat çekici tarafı ise, bir günde metrelerce büyüebilmesi ve 3-5 yıl içerisinde hasat edilip yapı malzemesi olarak kullanılabilmesidir. İnsanoğlu bambuyu yüzyıllardır kullanmaktadır. Günümüzde gıdadan inşaata, tekstilden yüksek teknolojilere kadar birçok alanda kullanılmaya devam etmektedir.

Bambu, hafif olmasına karşın, çok esnek ve dayanıklıdır. Silindirik yapısı ve içinin boş olması ise olumsuz özelliklerindedir. Ayrıca, sürekli düzensiz büyüyen, kıvrımlı bir bitki ile çalışmak oldukça zordur. Doğru yaklaşım ve yöntemlerle, sadece bambu kullanarak, temelden çatısına kadar bir evi inşa etmek mümkündür. Bambunun en zorlayıcı kısmı eklemleridir. Eklemlerin standart yapıları yoktur, ayrıca ağaç veya herhangi başka bir malzemenin birleştirme yöntemleri ile uyumlu değildirler. Birçok mimar kendine has teknikler geliştirerek, egzotik binaların tasarımında bambu kullanma konusunda ustalaşmıştır. Klasik konutlar temelin atılması ile başlar, sütunların ve duvarların inşası ile devam eder ve çatı ile bitirilir. Bambu evlerde ise; temel, aynı zamanda duvara da dönüşebilen bir destek kolonunun içine girebilmekte ve yapı kubbeli bir çatı ile tamamlanmaktadır.

Bambunun çok dayanıklı olduğu unutulmamalıdır. Bilim insanları, çimento ile karıştırılan bambunun iki kat daha güçlü olduğunu keşfetmişlerdir. Bu faydaları nedeniyle, bambunun önümüzdeki yıllarda binaların güçlendirilmesinde demir ve çeliğin yerine kullanılabileceği değerlendirilmektedir.

Ekolojik bir ürün olan bambunun özellikleri dikkate alındığında, yeterince etkin kullanılmadığı anlaşılmaktadır. Bambu üretiminde en önemli sorun haşerelere karşı korunmadır. Çevreye ve bambuya zarar vermeyen en iyi çözüm bor çözültisi kullanmaktır. 21. yüzyıl mimarisinde, halihazırda %100 bambudan imal edilen yapılar olduğuna göre, neden daha ileri gidip çevreye zarar vermeyen, ekolojik ve çok fonksiyonlu binalar yapılmasın?

Bambu, CO2 emilimi yapmasının yanı sıra, iğne yapraklı ağaçlara nazaran %35 daha fazla oksijen salgılamaktadır. Bambunun üretimi için enerji harcanmaz, %100 doğal ve kullanıma hazır bir üründür. Hem kaplama malzemesi, hem de temel yapı bileşeni olarak kullanılabilir. Bambu evler, okullar, restoranlar, ibadethaneler ve köprüler inşa edebileceğiniz eşsiz bir malzemedir.

Özellikle gelişmekte olan ülkelerdeki bambu yetiştiriciliği yerel halka istihdam yaratarak; yoksulluğun ortadan kaldırılmasını, yapı malzemesi, tekstil ve yeterli beslenme imkanına sahip olmalarını ve sosyal yaşamlarını güvence altına almalarını sağlamaktadır.

Bambu, halk tarafından yeterince bilinmeyen, mimarların ve yatırımcıların ilgisini yeni yeni çekmeye başlayan bir üründür. Gelecekte sürdürülebilir bir malzeme olarak ön plana çıkarılmalıdır. Özellikle Avrupa ile, tropikal ve subtropikal bölgelere yakın diğer ülkeler bambu hakkında daha fazla bilgiye sahip oldukları ve yeterli yatırım yapıldığı takdirde, kullanım alanları önemli ölçüde artırılabilir.

Gelecekte ahşaba olan talebin yerini bambu ve ikincil işlem görmüş bambu katkı malzemeler alabilirse, özellikle yapı sektöründe artan hammadde ihtiyacı nedeniyle yaşanan ormansızlaşma sorunu da büyük ölçüde ortadan kalkacaktır.

KAYNAKLAR

- Admin. (b.t.). *Visitor anti-robot validation*. Visitor anti-robot validation. 9 Nisan 2022. <https://melbournetopflooring.com.au/bamboo-flooring-melbourne/reasons-install-bamboo-flooring/>
- Aria bamboo vessel sink. (b.t.). *Maykke*. 16 Mayıs 2022. <https://www.maykke.com/aria-bamboo-vessel-sink.html>
- Bamboo reinforced concrete - Mix proportion, design and construction. (12 Aralık 2016). *The Constructor*. <https://theconstructor.org/structural-engg/bamboo-reinforced-concrete-mix-design-construction/15054/>
- Bamboo stair (varnish) – Amennis trading. (b.t.). *Amennis Trading*. 9 Nisan 2022. <https://www.amennis.nl/en/product/bamboo-stair-varnish/>
- Bamboo structure. (b.t.). *BambuBuild*. 9 Nisan 2022. <https://bambubuild.com/vi/ket-cau-tre>
- Bowyer, J., Fernholz, K., Frank, M., Howe, J. E. F. F., Bratkovich, S. T. E. V. E., ve Pepke, E. (2014). *Bamboo products and their environmental impacts: revisited*. Dovetail Partners, Incorporated.
- Caffiero, V. (2006). La madera ecológica del siglo XXI. El bambú como recurso maderable sustentable. *Premio Aquisur de investigación*, 53-64.
- Cortés, C. V. (3 Haziran 2021). *Sistemas de techos para construcciones en bambú*. ArchDaily Perú. <https://www.archdaily.pe/pe/962732/sistemas-de-techos-para-construcciones-en-bambu>
- Cripps, K. (07 Kasım 2019). Kyoto's Sagano bamboo forest, one of the world's prettiest groves. *Edition.cnn*. <https://edition.cnn.com/travel/article/sagano-bamboo-forest/index.html>
- Fastest growing plant. (b.t.). Guinness World Records. *Guinnessworldrecords*. 15.01.2018. <https://www.guinnessworldrecords.com/world-records/fastest-growing-plant>
- GDMING bamboo fence panels balcony privacy screen durable natural sunscreen windbreaker for garden Terrace patio decorative fences with closed and sealed tubes, 18 sizes : Patio, lawn & garden. (b.t.). *Amazon*. 9 Nisan 2022.

- <https://www.amazon.com/Balcony-Privacy-Sunscreen-Windbreaker-Decorative/dp/B08F5B6RVD>
- Ghosh, G. K. (2008). *Bamboo: The wonderful grass*. APH Publishing. New Delhi.
- <https://www.degruyter.com/document/doi/10.1515/9783035608656-fm/html>
- Janssen, J. A. (2000). *Designing and building with bamboo*. *International Network for Bamboo and Rattan* (Vol. 20, s. 1755-1315). Technical Report.
- Jewell, N. (11 Ocak 2011). *Bamboo housing in Carabanchel by foreign office architects (FOA)*. - *Buildipedia*. Buildipedia. <https://buildipedia.com/aec-pros/featured-architecture/bamboo-housing-in-carabanchel-by-foreign-office-architects-foa>
- John. (11 Ağustos 2014). *Kengo Kuma I: Public spaces*. Benedante. <https://benedante.blogspot.com/2014/08/kengo-kuma-1-public-spaces.html>
- Knighton, B. (10 Mart 2022). *From paper to furniture, bamboo almost does it all*. RightAngle. <https://www.raproducts.com/blog/from-paper-to-furniture-bamboo-almost-does-it-all>
- Minke, G. (6 Haziran 2016). *Frontmatter*. De Gruyter.
- Oki, H. (21 Ekim 2015). *Naman retreat conference hall / VTN architects*. ArchDaily. <https://www.archdaily.com/775650/naman-retreat-conference-hall-vo-trong-nghia-architects>
- Panyaden bamboo sports hall / Bamboo architecture. (b.t.). *Bamboo Earth Architecture - Chiangmai Life Construction*. 9 Nisan 2022. <https://www.bamboo-earth-architecture-construction.com/portfolio-item/panyaden-international-school-sports-hall/>
- Pridgeon, B. (31 Ekim 2013). *Bamboo door and potted plant by Bryan Pridgeon*. Fine Art America. <https://fineartamerica.com/featured/bamboo-door-and-potted-plant-bryan-pridgeon.html>
- Rohrbach, D ve Gillmann, S. (2001). *Construction with Bamboo - ZERI Pavillion*. [pdf]. ZERI organisation. <https://bambus.rwth-aachen.de/eng/PDF-Files/ZERI%20Pavillion.pdf>
- Scurlock, J. M. O., Dayton, D. C., ve Hames, B. (2000). *Bamboo: An overlooked biomass resource?*, *Biomass and Bioenergy* 19: 229-244.
- Sustainable design and architecture firm in Bali. (b.t.). *IBUKU*. 9 Nisan 2022. <https://ibuku.com/services/furniture/>
- Syeda, A., Shrujal, B., ve Kumar, J. (2014). *A case study on bamboo as green building material*. *International Journal of Engineering and Advanced Technology*, 4, 78-82.
- Treehugger. (1 Aralık 2012). *Green design | Bamboo architecture, architecture, passive house*. Pinterest. <https://tr.pinterest.com/pin/129056345543470724/>
- Türk Dil Kurumu. (b.t.). *Bambu*. *TDK Güncel Türkçe Sözlük*. 10 Ocak 2018. <http://www.tdk.gov.tr>

- Williams, A. (16 Temmuz 2014). *Bamboo treehouse eco-hotel concept is at one with the birds*. New Atlas. <https://newatlas.com/bamboo-hotel-penda/32969/>
- World's largest bamboo dome adorns Indian pavilion at Shanghai expo. (21 Temmuz 2010). *Designcurial*. <https://www.designcurial.com/news/world-s-largest-bamboo-dome-adorns-indian-pavilion-at-shanghai-expo>
- Yu, E. (29 Nisan 2016). *How authentic is Hong Kong's bamboo scaffolding pop-up bar?* CNN. <https://edition.cnn.com/travel/article/hong-kong-bamboo-scaffolding-beer/index.html>

**DENİZ YANAŞMA YAPILARI USTURMAÇALARININ TEMAS DURUMLARININ
BASİTLEŞTİRİLMİŞ METODLAR İLE DEĞERLENDİRİLMESİ**
EVALUATION OF THE CONTACT CONDITIONS OF MARINE STRUCTURES
FENDERS WITH SIMPLIFIED METHODS

Temel TEMİZ

Assist. Prof. Dr. Yalova Üniversitesi, Mühendislik Fakültesi, Yalova, Türkiye
Yalova University, Engineering Faculty, Department of Civil Engineering, Yalova, Turkey.
ORCID: 0000-0002-4013-7218

ÖZET

Yanaşma yapıları olarak ifade edebileceğimiz liman, iskele gibi açık denize komşu yapılara yanaşan tekne, gemi gibi taşıtların sisteme uyguladığı hareketli yüklerin sönmelenmesinde kullanılan elemanlar usturmaça olarak tanımlanmaktadır. Bu elemanlar gemilerin limana bağlanması sırasında oluşabilecek çarpma kaynaklı hasar etkilerini en aza indirme bakımından büyük önem taşımaktadır. Büyük önem taşıyan bu elemanların zamana bağlı deformasyonlar nedeniyle düzenli olarak kontrollerinin ve testlerinin yapılması gerekmektedir, bu kontrollere bağlı olarak da ekonomik ömrünü tamamlamış olanlarının değiştirilmesi sonucu ortaya çıkmaktadır. Kullanıldıkları deniz yapısı boyunca çok sayıda uygulanması gereken bu büyük bütçeli elemanlar için ortaya ciddi bakım ve yatırım maliyetleri çıkmaktadır. Bu çalışmada ülkemizde de yaygın olarak kullanılan usturmaça örneklerinden iki farklı boyut ve tip seçilmiştir. Birinci tip hücre tipi usturmaça olarak geçerken diğeri arkadan çelik destek ayaklı diğere nazaran daha uygun maliyetli bir tasarıma sahiptir. Bu elemanların tam yüzey temas durumu, düşük seviyeli temas durumu ve açısız darbe durumu değerlendirilerek, uzun dönemli kullanımda ekonomik ömürleri bakımından değerlendirilmeleri yapılmıştır. Değerlendirme ilk olarak temas durumlarına karşı usturmaça reaksiyon kuvvetlerinin basit metotlar ile belirlenmesi ve seçilen usturmaçaların enerji, reaksiyon ve sapma eğrilerinin performanslarının ortaya konması şeklindedir. Tam temas, düşük seviyeli darbe, açısız darbe, kapasite ve kesit kontrolü gibi durumlar incelendiğinde, seçilen her iki kesitinde şartları sağlamasına rağmen Tip 2'nin çok güvenli sonuçlar verdiği görülmüştür. Usturmaça sistemlerinin uzun süreli bakım maliyetleri açısından değerlendirilmesi yapıldığında ise benzer yük ve yükleme durumları için iki tip usturmaça sisteminin de kullanılmasında herhangi bir mahsur bulunmadığı, bununla birlikte ilk yatırım maliyeti daha yüksek olan hücre tipinin (Tip 2) uzun süreli kullanımda diğere nazaran %20 oranında daha uygun maliyetlerle değerlendirilebileceği ifade edilebilir. Sonuç olarak, teknolojinin geldiği nokta itibarıyla üretilen yeni nesil güç sistemlerinin kontrollü ve yüksek manevra kabiliyeti özelliklerini barındırdıkları maliyet ve kullanım sürelerine bağlı olarak

seçimlerinin doğru yapılmasıyla tüm sistemlerin kullanılmasının uygun olacağı ifade edilebilir.

Anahtar Kelimeler: Usturmaça, Deniz Yanaşma Yapıları, Tam Temas Durumu, Düşük Seviyeli Darbe Durumu, Açısal Darbe Durumu

ABSTRACT

Equipment used in damping the moving loads applied to the system by vehicles such as boats and ships berthing to structures adjacent to the open sea, such as ports and piers, which we can express as berthing structures, are defined as fenders. This type of equipment is of great importance in reducing the effects of impact damage that may occur during the mooring of ships to the port. These types of equipment, which are of great importance, must be checked and tested regularly due to time-dependent deformations, and depending on these controls, the replacement of the ones that have completed their economic life occurs. In this study, two different sizes and types were selected from the fender samples, which are widely used in our country. While the first type is a cell-type fender, the other has a more cost-effective design than the other with steel support legs from the back. These types of equipment have been evaluated in terms of their economic life in long-term use as full surface contact state, low-level contact state, and angular impact state. The evaluation is first to determine the fender reaction forces against contact conditions with simple methods and to reveal the performance of the energy, reaction, and deflection curves of the selected fenders. When conditions such as full contact, low-level impact, angular impact, capacity, and section control are examined, it is seen that Type 2 gives very safe results, although it meets the conditions in both selected sections. When the fender systems are evaluated in terms of long-term maintenance costs, it can be stated that there is no problem in using both types of fender systems for similar load and loading situations. however, it can be stated that the cell type with a higher initial investment cost can be evaluated as 20% more affordable than the other in long-term use. As a result, it can be stated that the new generation power systems produced as of the point of technology have controlled and high manoeuvrability features, and it will be appropriate to use all systems if the selection is made correctly depending on the cost and usage period.

Keywords: Fenders, Marine Structures, Full Contact Condition, Low-Level Impact Condition, Angular Impact Condition

**1999 KOCAELİ DEPREMİ ÖNCESİ VE SONRASINDA İNŞA EDİLEN BİNALARIN
YAPISAL PERFORMANS DÜZEYLERİNİN DEĞERLENDİRİLMESİ**
EVALUATION OF STRUCTURAL PERFORMANCE OF BUILDINGS BUILT BEFORE
AND AFTER 1999 KOCAELİ EARTHQUAKE

Hasan SESLİ

Dr. Öğr. Üyesi, Yalova Üniversitesi, Mühendislik Fakültesi, İnşaat Mühendisliği Bölümü
Asst. Prof. Dr., Yalova University, Faculty of Engineering, Department of Civil Engineering
ORCID NO: 0000-0003-3328-5922

ÖZET

İçerisinde birçok fay parçasını barındıran ve Türkiye'nin en önemli aktif tektonik unsuru olan Kuzey Anadolu Fay Zonu üzerinde yer alan Yalova ili, Kocaeli depreminde yapı hasarlarının yoğun olduğu ve ağır kayıpların verildiği bölgelerden biri olmuştur. 17 Ağustos 1999'da meydana gelen Kocaeli Depreminde Yalova İli sınırları içerisinde 8585 adet orta hasarlı ve 9570 adet ağır hasarlı bina tespit edilmiştir. Bunun neticesinde ise 17480 can kaybının 2504'ü sadece Yalova genelinde meydana gelmiştir. Bilimsel araştırmalar ve geçmişe dönük değerlendirmeler sismik aktivite alanı içerisinde yer alan Yalova'yı da içerisine alan Marmara Havzası'nın yeni yer hareketlerine maruz kalabileceğini ortaya koymaktadır. Olası Kocaeli depremi ölçeğinde bir depremde, Kocaeli depremine maruz kalan binalardan güçlendirilmiş binalar ve güçlendirilmemiş binalar, 1999-2011 tarih aralıklı bina stoku, 2011-2018 tarih aralıklı bina stoku ve 2018 sonrası bina stokunun yapısal davranışı ve performansının hangi seviyede olacağı ise bilinmemektedir. Bu çalışmada, Yalova ili özelinde 1999 depremine maruz kalmış ve belirli bir mevzuata bağlı kalmadan güçlendirilmiş veya güçlendirilmemiş binalar, 2011 yılına kadar yeterli yapı denetiminden geçmeden inşa edilmiş binalar ile 1998, 2007 ve 2018 yönetmeliğine tam olarak uygun inşa edilmiş binaların yapısal davranışları değerlendirilmektedir. Bu amaçla, projeye uygun olarak seçilecek örnek binaların malzeme ve yapısal elemanlarına dair bilgiler mevcut uygulama projeleri ile değerlendirildikten sonra binalara ait elde edilecek yapı bilgileri, uygun analitik ve sayısal yöntemler yardımıyla bilgisayar ortamında modellenmektedir. Bilgisayar ortamında hazırlanan bina modelleri üzerinde Yalova ilinin de içerisinde yer aldığı Kuzey Anadolu Fay Hattı üzerinde oluşan depremlerin bir benzeşimi olan yer hareketi kayıtları ve yeni deprem senaryolarının yapıların dinamik davranışı üzerindeki etkileri incelenerek yapıların olası depremler karşısındaki dinamik davranışları ortaya konulmaktadır.

Anahtar Kelimeler: Dinamik analiz, deprem, fay hattı, yapısal davranış.

ABSTRACT

Yalova Province, located on the North Anatolian Fault Zone, has been one of intensity region of heavy losses during the Kocaeli Earthquake on August 17, 1999. 8585 medium damaged and 9570 heavily damaged buildings were identified within the borders of Yalova Province. As a result of this, 2504 of 17480 deaths occurred only in Yalova. Scientific researches and historical evaluations reveal that the Marmara Basin, which includes Yalova, which is located in the field of seismic activity, may be exposed to new ground motions. For a possible earthquake like Kocaeli earthquake, the structural behavior and performance level of the strengthened buildings and non-strengthened buildings after the Kocaeli earthquake, buildings constructed between 1999 and 2011, building constructed between 2011 and 2018 years, and buildings constructed after 2018 are unknown. In this study, the structural behaviors of buildings that have been subjected to the 1999 earthquake in Yalova province and have been strengthened or not strengthened without according to any code or regulations, the structural behaviors of buildings that have been built in full compliance with the 1998, 2007 and 2018 earthquake codes and the structural behaviors of buildings built without adequate building supervision until 2011 are evaluated. For this purpose, after the information about the material and structural elements of the reference buildings to be selected in accordance with the project are evaluated with the current application projects, the buildings are modeled with the computer-aided environment using appropriate analytical and numerical methods. The dynamic behavior of the buildings against possible earthquakes are revealed using dynamic analysis software under the effects of the ground motion records, which is a simulation of the earthquakes occurring on the North Anatolian Fault Line, in which Yalova is located, and the effects of the new earthquake scenarios.

Keywords: Dynamic analysis, earthquake, fault line, structural behavior.

GÜCÜNKAYA GRANİTOİDİNDEKİ MAFİK DAYKLARIN PETROLOJİSİ
PETROLOGY OF MAFIC DYKES WITHIN THE GÜCÜNKAYA (AKSARAY)
GRANITOIDS

Bahattin GÜLLÜ

Dr., Aksaray Üniversitesi Mühendislik Fakültesi Jeoloji Mühendisliği Bölümü
Dr., Aksaray University Engineering Faculty, Department of Geological Engineering
ORCID ID: 0000-0002-3629-1124

ÖZET

Çalışma alanı İç Anadolu Temel Birimleri (İATB) güneyinde Aksaray ili doğusunda yer almaktadır. Bu çalışma ile bölgede granit/granodiyorit bileşimli Gücünkaya granitoidi içerisinde K-G ve K30°-50°D/85°-89° KB-GD arasında değişen yönelimlerine sahip mafik damar kayalarının petrografik ve jeokimyasal özelliklerinin ortaya konulması amaçlanmıştır. Mafik damar kayaları petrografik olarak diyorit porfir, mikro-diyorit porfir ve mikro-gabro porfir bileşimlidir. Mafik damar kayaları genel olarak holokristalin hipidyomorf porfirik dokusal özelliği gösterir. Diyorit porfirlerin ana mineralojik bileşimini plajiyoklaz (An₄₄-An₅₂), biyotit, amfibol ve kuvars oluşturur. Benzer mineralojik bileşime sahip mikro-diyorit porfirlerde piroksen mineralleri gözlenmektedir. Mikro-gabro porfir türü kayalarda kuvars minerali gözlenmez ve piroksen mineralleri biraz daha baskındır. Diyorit porfirlerde magma homojen karışımını işaret eden dokusal özellikler yoğun olarak gözlenmektedir. Mafik damar kayalarının tamamı subalkali olup, toleyitik-kalkalkali (baskın olarak kalkalkali) geçiş karakteri sunarlar. Ortalama SiO₂ içeriği % 52-59 arasında değişen mafik damar kayalarının ortalama Mg# değerleri diyorit porfirlerde 58.0, mikro-diyorit porfirlerde 61.0 ve mikro-gabro porfirlerde 66.2'dir. Mikro-gabro porfir ve mikro-diyorit porfirlerdeki yüksek Mg# daha mafik bir kaynağı işaret etmektedir. Mafik damar kayalarının tamamı düşük A/CNK oranlarıyla (< 0.8) baskın metalümidirler. Okyanus Ortası Sırt Granitoidlerine (ORG) göre normalize edilen örümcek diyagramda; diyorit porfirlerde büyük iyon yarıçaplı litofil elementlerde (LIL) bir zenginleşme, kalıcılığı yüksek elementlerde (HFS) ise tüketilme göze çarpmaktadır. Mikro-diyorit porfir ve mikro-gabro porfir türü kayalarda ise LIL ve HFS elementlerce tüketilme gözlenir. Kondrit'e göre normalize edilen nadir toprak element dağılımında, mikro-diyorit porfir ve mikro-gabro porfirlerden farklı olarak diyorit porfirlerde gözlenen hafif nadir toprak elementlerce zenginleşme, diyorit porfirlerin yerleşiminde kıtasal kabuk etkileşiminin izlerini yansıtmaktadır. Sonuç olarak, elde edilen sınırlı petro-kimyasal verilere dayanarak Gücünkaya (Aksaray) granitoidindeki diyorit porfirlerin manto kaynaklı bir ürünün granitoid magması ile etkileşerek kristallendiği söylenebilir. Ayrıca, Mikro-diyorit porfir ve mikro-gabro porfirlerin ise ana granitik kütleli oluşturan magma odasını daha

derinden yeniden besleyen manto karakterli mafik ürünler olarak bölgedeki Üst Kretase-Alt Paleosen magmatizmasının geç evre ürünlerini temsil edebileceği düşünülmektedir.

Anahtar Kelimeler: İç Anadolu Temel Birimleri (İATB), mafik damar kayaları, diyorit porfir, mikro-diyorit porfir, mikro-gabbro porfir, Gücünkaya granitoid.

ABSTRACT

The study area is located in the east of Aksaray province in the south of Central Anatolian Basement Units (CABU). The aim of this study reveals the petrographic and geochemical properties of mafic vein rocks with a direction ranging between N-S and N30°-50°E/85°-89° NW-SE within the granitoid/granodiorite-composition Gücünkaya granitoid. Mafic vein rocks are diorite porphyry, micro-diorite porphyry and micro-gabbro porphyry in composition as a petrographically. Mafic vein rocks have holocrystalline hypidiomorph porphyric textural features. Plagioclase (An₄₄-An₅₂), biotite, amphibole and quartz form the main mineralogical composition of the diorite porphyries. Pyroxene minerals are observed in micro-diorite porphyries with similar mineralogical compositions. Quartz is not observed in micro-gabbro porphyry and pyroxene minerals are slightly more dominant. Magma mixing textural features are intensely observed in all of the diorite porphyries. All of the mafic vein rocks are sub-alkaline and show a tholeiitic-calc-alkaline (predominantly calc-alkaline) transitional character. Average Mg# values of mafic vein rocks with an average SiO₂ content between wt%52-59 are 58.0 in diorite porphyries, 61.0 in micro-diorite porphyries and 66.2 in micro-gabbro porphyries. High Mg# in micro-gabbro porphyry and micro-diorite porphyry indicates a more mafic source. All of the mafic vein rocks are predominantly metalluminous with low A/CNK ratios (< 0.8). There is an enrichment in large ion lithophile elements (LIL) and depletion in high field strength elements (HFS) in diorite porphyries in the spider diagram normalized to the Ocean Ridge Granitoids (ORG). Depletion LIL and HFS elements are observed in micro-diorite porphyry and micro-gabbro porphyry type rocks. The enrichment of light rare earth elements observed in diorite porphyries, unlike micro-diorite porphyry and micro-gabbro porphyry, reflect the fingerprints of continental crust interaction of diorite porphyries in the chondrite normalized rare earth element spider diagram.

In conclusion, based on the limited petro-chemical data obtained, it can be said that the diorite porphyries in the Gücünkaya (Aksaray) granitoid were crystallized by interacting with the granitoid magma of a mantle-derived product. In addition, it is thought that micro-diorite porphyry and micro-gabbro porphyry may represent the late-phase products of Upper Cretaceous-Lower Paleocene magmatism in the region as mafic mantle products re-feeding the magma chamber forming the main granitic mass more deeply.

Keywords: Central Anatolia Basement Unit (CABU), mafic vein rocks, diorite porphyry, micro-diorite porphyry and micro-gabbro porphyry Gücünkaya granitoid.

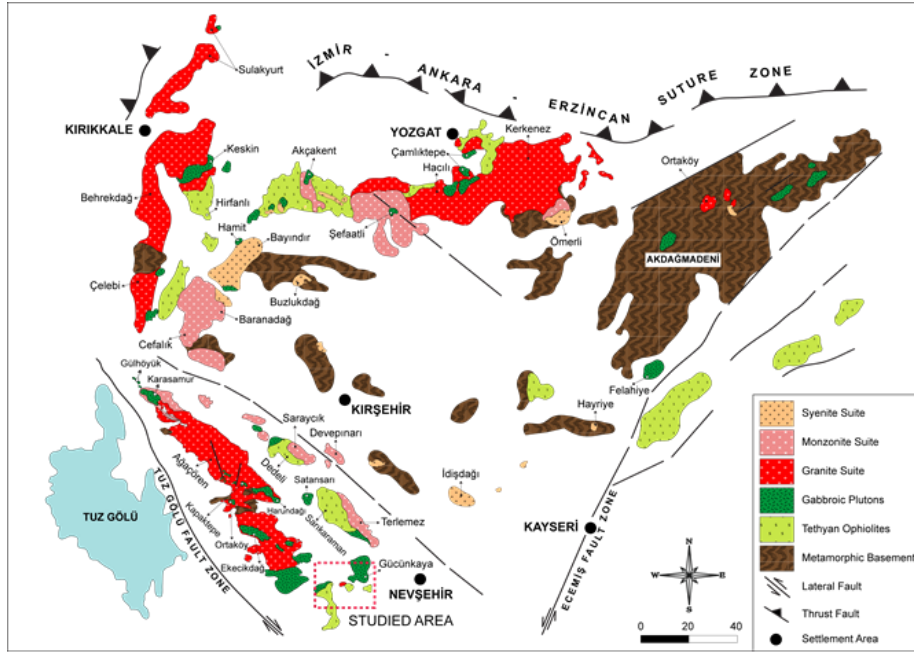
GİRİŞ

Granitik kütlelerin kristallenme veya kristallenme sonrası süreçlerinde uygun fiziko-kimyasal koşullar oluştuğunda plütonlar mafik ve/veya felsik damar kayaları ile kesilebilirler. Bu damar kayalarının felsik bileşimlerini aplit ve pegmatitler oluştururken mafik olanlar ise genel bir ifade ile mafik damar kayaları oluştururlar. Felsik damar kayaları daha çok magma kristallenme sürecinin geç eveleri hakkında bilgi verirler. Mafik damar kayaları ise magmatik kayaların kimyasal çeşitliliği, magma kristallenmesinde jeodinamik süreçler, magma odalarının yeniden beslenmesi ve mafik-felsik magmaların etkileşimlerini (magma mingling/mixing) anlamamıza yardımcı olabilecek önemli bilgiler içerirler (Fernandez ve Barbarin, 1991; Barbarin ve Didier, 1992; Wiebe ve diğ., 2004; Barbarin, 2005; Mafik damar kayaları magma odasının reolojik özelliklerine ve mafik magmanın hacmine bağlı olarak farklı şekillerde etkileşime girebilirler (Jayananda ve diğ., 2009). Özellikle granitik magmaların yerleşimleri esnasında mafik magma enjeksiyonları bazen ana magmatik kütlelerin jeokimyasal ve dokusal özelliklerini etkiler. Özellikle felsik-mafik magma karışım süreçleri sözkonusu ise karışım sürecine mafik bileşen olarak katılan uç üyelerin tahmininde mafik damar kayaları önemli bilgiler içerirler. Son yıllarda farklı karakterdeki (kalkalkaliden potassiğe kadar değişen) plütonların petrojenetik karakterleri incelenirken, ilişkili oldukları mafik sinplütonik dayklara da odaklanılmıştır (Frost ve Mahood, 1987; Harrison ve diğ., 1990; Castro et al. 1990; Ghani, 1998; Barbarin, 2005, Jayananda ve diğ., 2009; Kumar, 2020).

Bu çalışmada İç Anadolu Temel Birimleri (İATB) güneyinde yer alan Aksaray ili doğusundaki Gücünkaya granitoidleri (Güllü, 2003; Güllü ve Yıldız, 2012) içerisindeki mafik daykların petrografik ve jeokimyasal özelliklerinin ortaya konularak kökenlerine ve ana granitik magma ile ilişkilerine yaklaşımda bulunulabilmesi amaçlanmıştır.

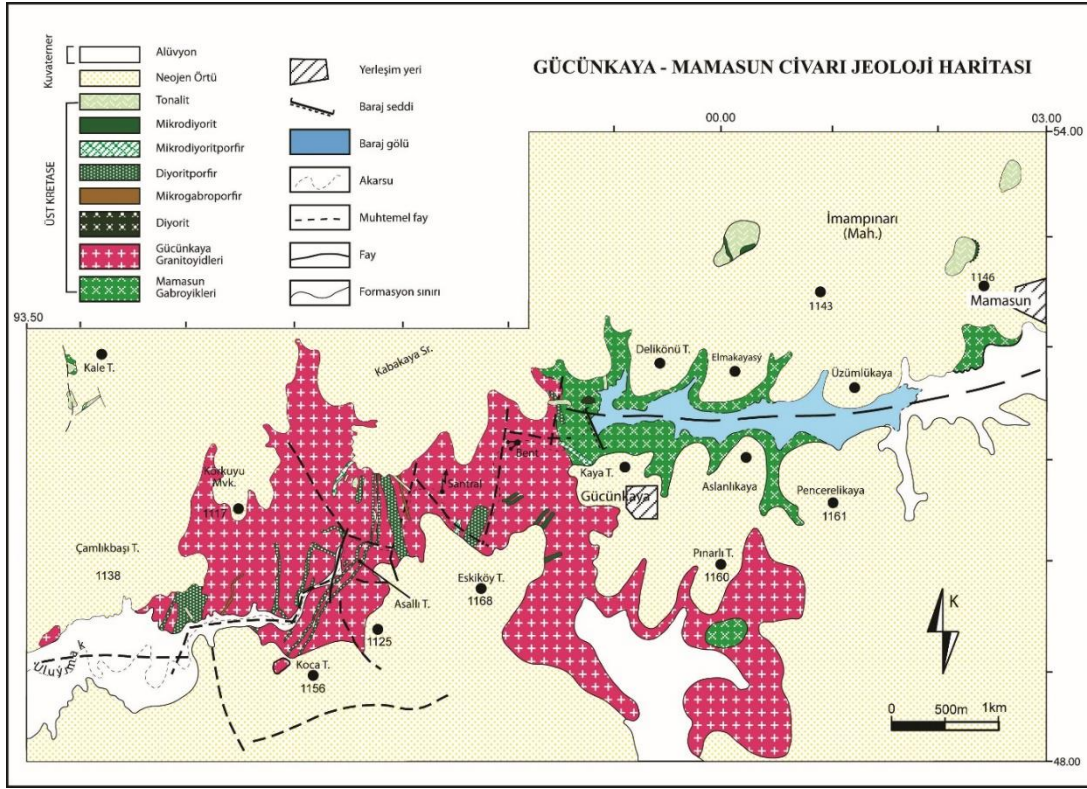
Geological Setting

Orta Anadolu Erken Senozoyik magmatizmasının baskın ürünlerini temsil eden granitoidler topluca Orta Anadolu Granitoidleri (Göncüoğlu ve diğ., 1991) olarak adlandırılmaktadır. Orta Anadolu Granitoidleri yüzeyleme alanları dikkate alınarak batı, iç ve doğu grubu olarak üç bölgeye ayrılmıştır (Erler ve diğ., 1991; Akıman ve diğ., 1993). Gücünkaya granitoidleri batı grubu granitoidleri oluşturan Ağaçoören İntrüzif Takımı'nın (Kadioğlu, 1996; Kadioğlu ve Güleç, 1995; 1998 Kadioğlu, 1996) güney ucunda yüzeylemektedir (Şekil 1).



Şekil 1. Basitleştirilmiş İATB jeoloji haritası (Kadioğlu ve diğ., 2006'dan alınmıştır).

Gücünkaya Granitoidleri, biyotit granit ve granodiyorit türü magmatik kayalardan oluşmaktadır. Gücünkaya yöresinde amfibol minerallerinin artmasıyla granodiyoritik bir bileşim sergiler. Kuvars, ortoklas, plajiyoklaz, biyotit ve amfibol minerallerinin ana bileşeni oluşturduğu kayada boyutları 1cm'den 25 cm'ye kadar değişen, mafik mikrogranüler anklavlar yer almaktadır. Gabroik kayalar ile dokanak halde bulunan granitoidlerin merkezi ve doğu kısmında boyutları 10 cm ile 150-200 cm arasında değişen ve yer yer km'lerce uzanan mafik damar kayaları mevcuttur (Şekil 2)



Şekil 2. Çalışma alanı jeoloji haritası (Güllü, 2003'ten alınmıştır).

Diyorit porfir, mikro-gabro porfir ve mikro-diyorit porfirden bileşimli mafik damar kayaları yer koyu yeşil-siyah renkli ve porfiro afanitik dokuludurlar. Bölgede K-G yönündeki mafik damar kayalarının hemen hemen tamamını diyorit porfirler oluştururken mikro-gabro porfir ve mikro-diyorit porfir türü damar kayaları ise, $K32^{\circ}-52^{\circ}D$, $88^{\circ}KB-GD$ yöneliminde en iyi asallı tepe civarında gözlenirler (Şekil 3).

MATERYAL VE METOD

Çalışma kapsamında alterasyondan etkilenmemiş veya en az etkilenmiş ana kaya ve onları kesen mafik damar kayalarından örnekleme yapılarak örneklere ait ince kesitler hazırlanmıştır. Petrografik incelemesi yapılan mafik damar kayalarından seçilen 10 adet örnek öğütülerek örneklerin ana element oksit, iz element ve nadir toprak analizleri yapılmıştır. Analizlerden bazıları Ankara Üniversitesi Yer Bilimleri Uygulama ve Araştırma Merkezinde (YEBİM) bazıları da ACME analitik laboratuvarında yaptırılmıştır.



Şekil 3. Gücünkaya Granitoyidleri içerisindeki mafik damar kayaları

BULGULAR

Petrografi

Mafik damar kayalarından diyorit porfirlerin ana bileşenlerini plajiyoklaz ($An_{32}-An_{46}$), amfibol ve biyotit oluşturmaktadır. Kayada çok az miktarda kuvars ve ikincil olarak gelişmiş epidot, klorit mineralleri gözlenir. Yer yer körfez ve kemirilme dokusunun (Şekil 4a) gözlemlendiği diyorit porfirlerde kuvars-hornblend ocellar (Şekil 4b) ve iri plajiyoklaz fenokristalleri içinde lata biçimli küçük plajiyoklaz oluşumları (Şekil 4c) gibi magma karışımına işaret eden dokusal özellikler gözlenmektedir.

Mikro-diyorit porfirlerde ana bileşenleri plajiyoklaz ($An_{44}-An_{52}$), amfibol, oluştururken çok az miktarda piroksen minerali gözlenmektedir. Kayada alterasyon süreçlerinin izlerini yansıtan ikincil epidot ve klorit mineralleri gözlenmektedir. Plajiyoklaz minerallerinde sossuritleşme nedeniyle epidot ve titanit agregaları gözlenmektedir.

Mikro-gabro porfirler oldukça ince taneli, grimsi-koyu yeşil renktedir. Plajiyoklaz ($An_{56}-An_{58}$), hornblend ve piroksen ana bileşeni oluşturmaktadır. Mikrokristalin porfirik dokulu olarak gözlenen kayada piroksen mineralleri ojittir.



Şekil 4. Diyorit porfirlerde gözlenen kuvars minerallerinde a) kemirilme, b) kuvars hornblend ocellar ve c) iri plajiyoklaz fenokristalleri içinde gelişen lata biçimli plajiyoklaz oluşumları

Jeokimya

Mafik damar kayalarının jeokimyasal özelliklerinin belirlenebilmesi amacı ile 10 adet örneğin tüm kaya jeokimyasal analizi yapılmıştır. Analiz sonuçları Tablo 1’de verilen mafik damar kayalarından diyorit porfirler % 55-59, mikro-diyorit porfirler %53-54 ve mikro-gabro porfirler ise %52-53 arasında SiO₂ içeriğine sahiptirler. Diğer ana element oksit içeriğine bakıldığında da mikro-diyorit porfirler ile mikro-gabro porfirlerin benzer jeokimyasal içeriğe sahip olduğu görülürken diyorit porfirlerin daha felsik karakteri yansıttığı görülmektedir.

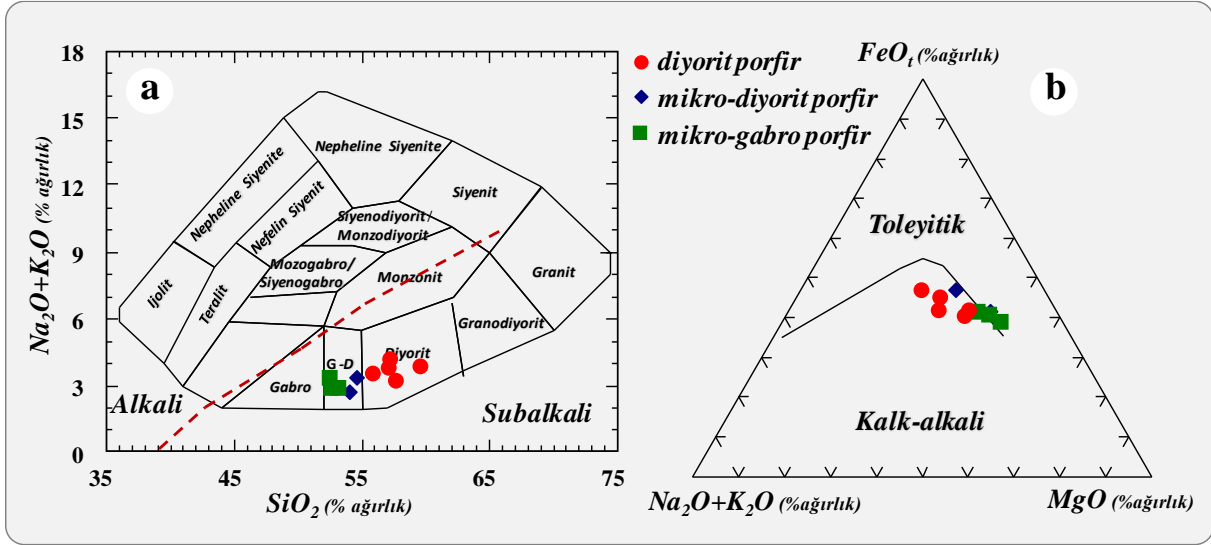
INTERNATIONAL AEGEAN CONFERENCES
ON INNOVATION TECHNOLOGIES & ENGINEERING-VI
 December 20-22, 2022

Tablo 1. Mafik damar kayalarına ait jeokimyasal analiz sonuçları

ELEMENT		Diyorit porfir					Mikro-diyorit porfir		Mikro-gabro porfir		
		MDK-2	MDK-3	MDK-4	MDK-8	MDK-9	MDK-7	MDK-1	MDK-10	MDK-6	MDK-5
SiO ₂	%	57.05	59.48	57.14	55.74	57.61	54.55	53.99	52.40	52.59	53.05
Al ₂ O ₃	%	15.50	15.73	15.76	14.75	13.33	15.02	12.83	14.46	13.89	11.79
Fe ₂ O ₃	%	8.25	7.64	7.77	7.94	8.22	9.36	9.10	9.19	8.89	9.44
MgO	%	5.17	3.88	5.53	6.93	6.95	6.10	8.76	8.24	8.75	10.42
CaO	%	8.10	7.51	7.76	9.04	8.64	9.05	10.15	9.88	10.45	10.10
Na ₂ O	%	2.94	2.71	3.00	2.69	2.37	3.11	2.50	3.07	2.74	2.55
K ₂ O	%	0.88	1.16	1.22	0.84	0.89	0.28	0.25	0.27	0.21	0.35
TiO ₂	%	0.57	0.58	0.53	0.51	0.46	0.59	0.47	0.52	0.50	0.39
P ₂ O ₅	%	0.07	0.08	0.07	0.06	0.06	0.05	0.04	0.04	0.04	0.03
MnO	%	0.15	0.15	0.13	0.14	0.15	0.18	0.17	0.16	0.16	0.17
Cr ₂ O ₃	%	0.03	0.03	0.03	0.04	0.05	0.02	0.05	0.03	0.05	0.05
LOI	%	1.6	1.4	1.5	1.5	1.5	1.9	1.8	1.9	1.8	1.9
TOPLAM	%	100.30	100.30	100.40	100.19	100.23	100.20	100.07	100.17	100.04	100.20
Ba	ppm	199.0	265.5	258.0	193.0	192.7	73.5	64.3	65.3	64.5	56.5
Ni	ppm	31.3	22.0	35.0	66.7	41.0	37.0	70.8	70.0	90.0	64.5
Sc	ppm	34.7	31.0	32.0	36.7	42.0	41.0	48.0	43.0	44.0	53.0
Mo	ppm	3.9	4.8	3.8	3.5	3.9	3.3	2.9	2.5	2.6	2.3
Cu	ppm	8.7	10.2	9.5	15.8	81.5	6.3	66.3	11.3	17.1	114.9
Pb	ppm	2.0	2.9	2.9	2.0	2.0	0.4	0.4	0.4	0.4	0.4
Zn	ppm	28.3	34.5	27.5	21.7	26.0	23.0	16.3	14.5	13.0	12.5
Co	ppm	26.7	21.8	26.2	30.1	30.4	32.2	37.4	36.9	37.2	42.0
Cs	ppm	1.2	1.6	1.7	1.2	1.2	0.5	0.5	0.6	0.5	0.6
Ga	ppm	17.1	18.6	16.2	14.6	14.9	16.6	13.0	13.5	12.8	10.9
Hf	ppm	1.7	2.3	2.0	1.6	1.7	1.0	0.8	0.7	0.8	0.6
Nb	ppm	2.5	3.6	3.6	2.6	2.5	0.5	0.6	0.6	0.6	0.5
Rb	ppm	31.6	42.9	44.0	30.4	31.6	8.1	7.1	7.7	6.2	9.2
Sn	ppm	6.0	8.5	2.5	2.3	6.0	7.0	4.3	1.3	1.5	1.0
Sr	ppm	196.9	212.4	186.6	158.5	168.3	191.9	141.6	150.2	134.3	123.1
Ta	ppm	0.3	0.4	0.4	0.3	0.3	0.1	0.1	0.1	0.1	0.1
Th	ppm	3.4	5.0	4.9	3.3	3.3	0.3	0.2	0.2	0.2	0.2
U	ppm	1.2	1.8	1.8	1.2	1.2	0.1	0.1	0.1	0.1	0.1
V	ppm	227.3	205.0	192.5	198.0	212.7	284.5	251.5	256.3	240.5	250.0
W	ppm	1.2	1.5	0.5	0.4	1.0	1.7	0.9	0.6	0.4	0.4
Zr	ppm	49.3	65.2	57.8	46.7	46.4	25.0	20.8	19.3	21.1	13.1
Y	ppm	16.5	18.8	14.4	14.5	15.6	16.3	14.1	12.6	13.3	10.6
La	ppm	8.2	11.9	11.4	8.1	8.1	1.3	1.2	0.9	1.2	0.7
Ce	ppm	19.1	27.3	25.8	18.6	19.1	4.3	3.9	3.1	3.5	2.8
Pr	ppm	1.9	2.6	2.4	1.9	1.8	0.6	0.5	0.5	0.5	0.3
Nd	ppm	8.0	10.8	9.2	7.5	7.7	4.0	3.4	2.8	3.3	1.9
Sm	ppm	2.0	2.6	2.2	1.9	1.9	1.4	1.2	1.1	1.2	0.9
Eu	ppm	0.65	0.80	0.61	0.57	0.61	0.56	0.46	0.40	0.44	0.31
Gd	ppm	2.50	2.97	2.41	2.26	2.29	2.12	1.79	1.66	1.76	1.25
Tb	ppm	0.41	0.47	0.38	0.37	0.38	0.39	0.33	0.31	0.33	0.25
Dy	ppm	2.77	3.17	2.46	2.50	2.53	2.68	2.30	2.12	2.27	1.62
Ho	ppm	0.60	0.69	0.51	0.52	0.58	0.61	0.53	0.46	0.49	0.40
Er	ppm	1.68	1.88	1.47	1.48	1.60	1.70	1.48	1.34	1.39	1.17
Tm	ppm	0.27	0.31	0.24	0.24	0.26	0.27	0.24	0.21	0.23	0.18
Yb	ppm	1.69	1.91	1.50	1.53	1.64	1.67	1.51	1.34	1.43	1.18
Lu	ppm	0.30	0.34	0.25	0.25	0.29	0.30	0.26	0.22	0.23	0.20

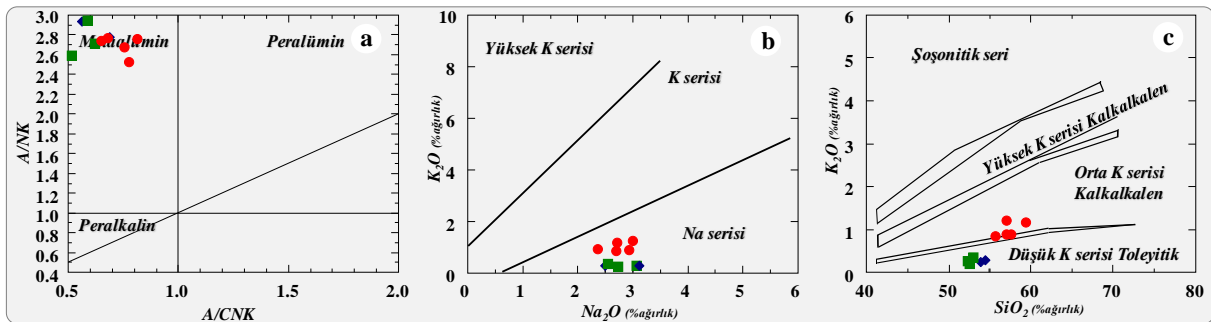
Toplam alkalilere karşı silika diyagramında mafik mafik damar kayaları diyorit ile gabro/diyorit alanında yer alırlar. Jeokimyasal adlama diyagramındaki adlamalar petrografik

tanımlamaları desteklemektedir (Şekil 5a). Farklı magma kaynaklarının ayrımı için de $\text{Na}_2\text{O}+\text{K}_2\text{O}$ 'ya karşı SiO_2 diyagramında kayaların tamamı sub-alkali alanda yer almaktadır (Şekil 5a). Sub-alkali kayaların ayrımı için önerilen AFM diyagramında ise hafif toleyitikten kalkalkaliye geçişi temsil etmektedirler (Şekil 5b). Alüminyum doygunlukları dikkate alındığında 1'den küçük A/CNK oranına sahip mafik damar kayaları baskın olarak metalümin karakterlidirler (Şekil 6a).



Şekil 5. a) Mafik damar kayalarının toplam alkali – silika adlama diyagramında (Cox ve diğ., 1979) (alkali-subalkali ayırım çizgisi Irvine ve Baragar, 1971'e göredir) ve b) AFM diyagramında (Irvine ve Baragar, 1971) dağılımları

$\text{K}_2\text{O}-\text{Na}_2\text{O}$ diyagramında Na sersisi karakterde (Şekil 6b) olan kayalar $\text{K}_2\text{O}-\text{SiO}_2$ diyagramında ise düşük K serisi toleyitik- kalkalkalen sınırında yer almaktadırlar (Şekil 6c).

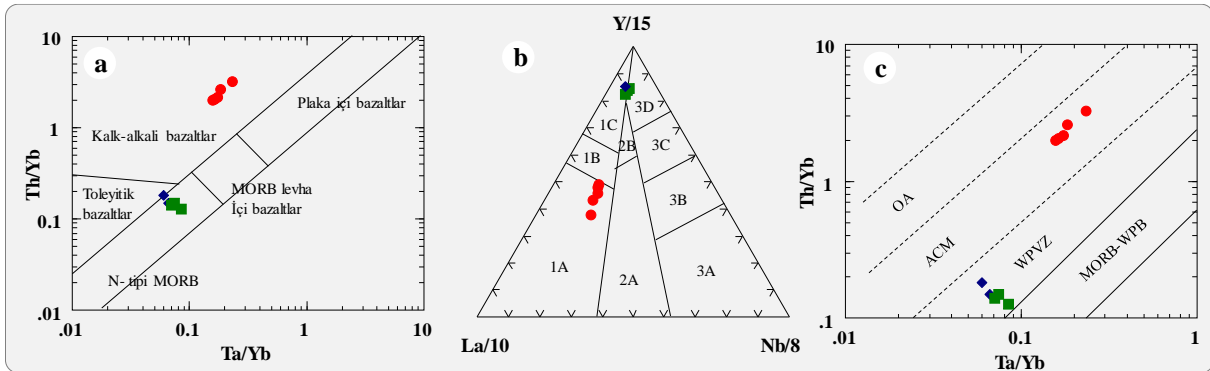


Şekil 6. Mafik damar kayalarının a) A/NK-A/CNK diyagramlarında (Maniar ve Picolli 1989), b) Na_2O 'e karşı K_2O değişim diyagramında (Middlemost, 1975) ve c) K_2O 'e karşı SiO_2 değişim diyagramında (Rickwood, 1989) dağılımları

TARTIŞMA ve SONUÇLAR

Mafik kayaların kökenlerine yaklaşımda bulunabilmek amacı ile bazı karakteristik iz elementlere dayalı diyagramlardan faydalanılmıştır. İnceleme alanındaki mafik damar kayaları Th/Yb-Ta/Yb diyagramına aktarıldığında mikro-gabro porfirlerin ve mikro-diyorit porfirlerin toleyitik bazaltlar alanında, diyorit porfirlerin ise kalkalkali bazaltlar alanında yer aldığı görülmektedir (Şekil 7a). Mafik damar kayalarındaki Nb (0.5-3.6ppm), La (0.7-11.9ppm) ve Y (10.6-18.8ppm) değerleri kullanılarak oluşturulan La/10-Y/15-Nb/8 üçgen diyagramında (Cabanis ve Lecolle, 1989) mikro-gabro porfir ve mikro-diyorit porfir kayaların Şekil 6a'daki dağılıma benzer şekilde volkanik yay toleyitleri alanında yer aldığı diyorit porfirlerin ise kalkalkalen bazaltlar alanında yer aldığı gözlenmiştir (Şekil 7b). Her iki diyagramda özellikle diyorit porfirlerin kalkalkalen seride yer alması, diyorit porfirleri oluşturan magmanın ana kütleli oluşturan granitik magma ile etkileşimini yansıtmaktadır. Petrografik olarak diyorit porfirlerde gözlenen magma karışım dokuları bunu desteklemektedir.

Mafik damar kayaları Th/Yb-Ta/Yb tektonik ortam ayırtlama diyagramında ise mikro-gabro porfir ve mikro-diyorit porfirlerin levha içi volkanik zon alanında diyorit porfirlerin ise aktif kıtasal kenar alanında yer almaktadır (Şekil 7c).

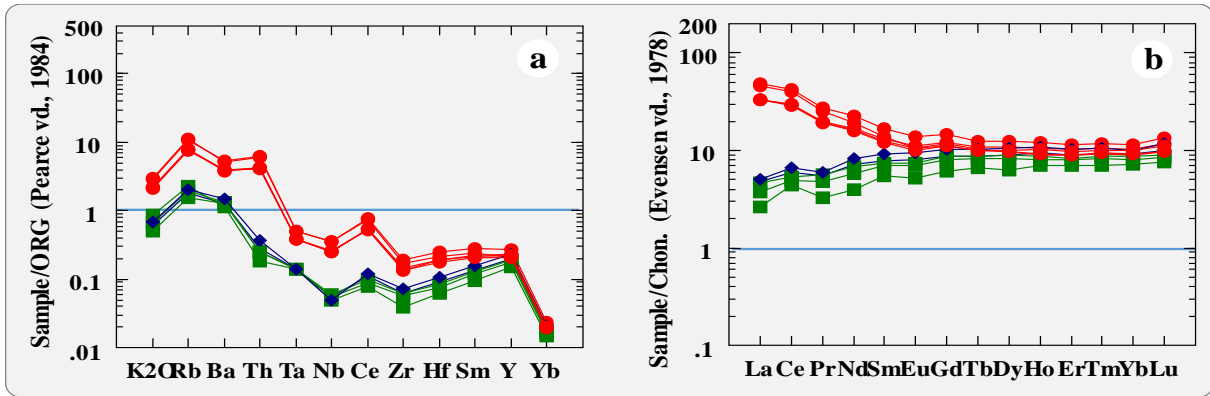


Şekil 7. Çalışma alanı mafik damer kayalarının a) Th/Yb-Ta/Yb diyagramında (Pearce, 1982), b) La/10-Y/15-Nb/8 üçgen diyagramında (Cabanis ve Lecolle, 1989), c) Th/Yb-Ta/Yb diyagramına adapte edilmiş Gorton ve Schandl (2000) diyagramında dağılımları (1A: kalk-alkali bazaltlar, 1B: 1A ve 1C alanları kısmen kapsar, 1C: volkanik yay toleyitleri, 2A: kıtasal bazaltlar, 2B: yayardı havzası bazaltları, 3A: kıta içi rifti alkali bazaltları, 3B,C: E tipi okyanus ortası sırtı bazaltları, 3D: N tipi okyanus ortası sırtı bazaltları; OA: okyanusal yay, ACM: aktif kıta kenarı, WPVZ: levha içi volkanik zon, WPB: levha içi bazaltlar)

ORG'ye normalize edilen iz element dağılım desenine bakıldığında diyorit porfirlerin, mikro-diyorit porfirler ve mikro-gabro porfirlere benzer ancak biraz daha zenginleşmiş iz element deseni sundukları gözlenir (Şekil 8a). Diyorit porfirlerdeki özellikle Rb ve Ba zenginleşmesi kıtasal kabukla kirlenmenin sonucu olabileceği gibi ana granitoid magmasıyla homojen

karışımı da yansıtabileceği düşünülmektedir. Toleyitik/kalkalkalen geçişli karakter sunan mafik damar kayalarındaki belirgin negatif Nb anomalisi de kısmen kıtasal kirlenmeyi işaret etmektedir (Baş ve Terzioğlu, 1986).

Kondite normalize edilen nadir toprak element dağılım desenlerin de diyorit-porfirlerdeki hafif nadir toprak elementlerindeki zenginleşme kıtasal kabuk ve/veya granitik ana kütle ile etkileşimi işaret etmektedir (Şekil 8b). Bunun dışında tüm mafik damar kayalarında gözlenen yataya yakın değişimler tüketilmiş üst manto kaynağına işaret etmektedir (Wilson, 1989).



Şekil 8. Mafik damar kayalarının a) ORG'ye göre normalize edilen iz element dağılım ve b) Kondrit'e normalize edilen nadir toprak element dağılım desenler (ORG değerleri Pearce ve diğ., 1984; Kondrit değerleri Evensen ve diğ., 1978'e göredir).

Çalışmadan elde edilen sınırlı petro-kimyasal veri ışığında Gücünkaya (Aksaray) granitoidi içerisindeki mafik daykların kökensel olarak tüketilmiş üst manto malzemesine benzer bir kaynaktan türediği düşünülmektedir. Granitoid magmasını yeniden besleyen bu üst manto malzemesinin bir kısmı granitoid magması ile etkileşime girerek (magma mixing?) kalkalkalen karakterli hibrit bir karışım ürünü olacaktır. Ana felsik magmadan daha mafik olan bu hibrit malzeme felsik magmanın kristallenmeye yüz tuttuğu anda gelişen erken evre kırıkları içerisinde enjekte olarak sin-plütonik daykları oluşturabilecektir (Fernandez ve Barbarin, 1991). Gerek arazi gerekse petrolojik verilerle karışım ürünleri karakterini yansıtan diyorit porfirler sin-plütonik daykları temsil etmektedir. Granitik magma odasını daha derinden besleyen ve onlarla etkileşime girmeden kristallenme sürecini henüz tamamlamış/tamamlamakta olan granitik kütle içerisindeki geç evre kırıklarına enjekte olan mafik magma da bölgedeki mikro-diyorit porfir ve mikro-gabro porfir türü damar kayalarını oluşturmuş olabilir.

Öncel ve sınırlı veri setleriyle, granitoid kütlelerindeki mafik daykların kökeni sorunsalına Gücünkaya (Aksaray) granitoidi örneği ile yaklaşımda bulunmayı amaçlayan bu çalışma sonuçlarının, izotop ve radyometrik yaş verileriyle desteklenmesi mafik damar kayalarının kökenleri ile ilgili daha kesin veriler sağlayabilecektir.

Katkı Belirtme

Çalışmanın arazi ve yorumlama aşamalarında tartışarak olumlu eleştirilerinden faydalandığım Dr. Öğr. Üyesi Mustafa YILDIZ (Aksaray Üniversitesi) ve Prof. Dr. Yusuf Kağan KADIOĞLU'da (Ankara Üniversitesi) teşekkür ederim.

KAYNAKLAR

- Akıman, O., Erler, A., Göncüoğlu, M.C., Güleç, N., Güven, A., Türel, T.K., Kadioğlu, Y.K., 1993. Geochemical Characteristics Of Granitoids along the Western Margin of The Central Anatolian Crystalline Complex and Their Tectonic Implications. *Geol. J.*, 28,371-382.
- Barbarin, B., Didier, J., 1992. Genesis and evolution of mafic microgranular enclaves through various types of interaction between coexisting felsic and mafic magmas. *Trans. Roy. Soc. Edinburgh, Earth Sciences*, v.83, pp.145-153
- Barbarin, B., 2005. Mafic magmatic enclaves and mafic rocks associated with some granitoids of the central Sierra Nevada batholith, California: nature, origin, and relations with the hosts. *Lithos*, v.80, pp.155-177.
- Baş, H., Terzioğlu, N., 1986. Jeokimya Ortamlar, Editör Ayhan Erler, TJK Yerbilimleri Eğitim Dizisi, 15-92.
- Cabanis, B., Lecolle, M., 1989. Le diagramme La/10-Y/15-Nb/8 un outil pour la discrimination des series volcaniques et la mise en evidence des processus de melange et/ou de contamination crustale, *C. R. Acad Sci. Ser. 2*, 309, 2023-2029.
- Castro, A., De La Rosa, J.D., Edryd Stephen, W., 1990. Magma mixing in the sub-volcanic environment: petrology of the Gerena interaction zone near Seville, Spain. *Contrib. Mineral. Petrol.*, v.105, pp.9-26.
- Cox, K.G., Bell, J.D. ve Pankhurst, R.J., 1979. *The interpretation of Igneous Rock*. George Allen and Unwin, London.
- Erler, A., Akıman, O., Unan, C., Dalkılıç, F., Dalkılıç, B., Geven, A. ve Önen P., 1991. Kaman (Kırşehir) ve Yozgat Yörelerinde Kırşehir Masifi Magmatik Kayaçlarının Petrolojisi ve Jeokimyası, *Tübitak, Doğa-Tr. J. of Eng. and Env. Sc.*, 15, 76-100.
- Evensen, N.M., Hamilton, P.J., O'nions, R.K., 1978. Rare Earth Abundances in Chondritic Meteorites. *Geochim. Cosmochim. Acta*, 42, 1199-1212.
- Fernandez, A.N., Barbarin, B., 1991. Relative Rheology of Coeval Mafic and Felsic Magmas: Nature of Resulting Interaction Processes. Shape and Mineral Fabrics of Mafic Microgranular Enclaves, in: Didier, J. and Barbarin, B. (Eds), *Enclaves and Granite Petrology: Developments In Petrology*, 13, Elsevier, 263-275.
- Frost, T.P., Mahood, G.A., 1987. Field Chemical and Physical Constraints on Mafic-Felsic Magma Interaction in The Lamark Granodiorite, Sierra Nevada, California, *Geol. Soc. Am. Bull.*, 99, 272-291.

- Ghani, A.A., 1998. Occurrence of Synplutonic Dykes from Perhentian Kecil Island, Besut, Terengganu. *Warta Geol.* 24, 65–68.
- Gorton, M.P., Schandl, E.S., 2000. From continent to island arcs: a geochemical index of tectonic setting for arc related and within plate felsic to intermediate volcanic rocks. *The Canadian Mineralogist*, 38, 1065-1073.
- Göncüoğlu, M.C., Toprak, V., Kuşçu, İ., Erler, A. ve Olgun, E., 1991. Orta Anadolu Masifinin Batı Bölümünün Jeolojisi, Bölüm 1-Güney Kesim: Tpa0 Rapor No. 2909, 140 s., yayınlanmamış.
- Güllü, B., 2003. Mamasun Barajı (Aksaray) magmatik kayalarının jeolojik, petrografik ve Jeokimyasal İncelemesi. 163 s. Niğde Üniv. Fen Bilimleri Enstitüsü (yayımlanmamış).
- Güllü, B., Yıldız, M., 2012. Mamasun (Aksaray) Petrogenetic Characterization of Mamasun Gabbroids. *KSU Journal of Eng. Sci.*, vol. 15(1), pp. 28-42.
- Harrison, T.N., Reavy, R.J., Finch, A.A., Brown, P.E., 1990. Co-existing mafic and felsic magmas in the early Proterozoic rapakivi granite suite of Southern Greenland. *Bull Geol Soc Denmark* 38: 53–58
- Irvine, T.N., Baragar, W.R.A., 1971. A Guide to the Chemical Classification of the Common Volcanic Rocks: *Canadian J. Earth Sci.*, v. 8, s. 523-548.
- Jayananda, M., Miyazaki, T., Gireesh, R.V., Mahesha, N., Kano, T., 2009. Synplutonic mafic dykes from late Archaean granitoids in the Eastern Dharwar Craton southern India *J. Geol. Soc. India*, 73, pp. 117-130.
- Kadioğlu, Y.K. 1996. Genesis of Ağaçören Intrusive Suite and Its Enclaves (Central Anatolia): Constraints From Geological, Petrographic, Geophysical and Geochemical Data. PhD Thesis, Middle East Technical University, 242p. Ankara (unpublished).
- Kadioğlu, Y.K., Güleç, N., 1995. Ağaçören (Aksaray) İntüzif Takımının Petrolojisi. *Ç.Ü.20.Yıl Sempozyumu Bildiri Özleri*, 35s.
- Kadioğlu, Y.K., Güleç, N. 1998. The role of anorthite contents on the generation of granitoid, enclaves and gabbro in the Ağaçören Intrusive Suite: Central Anatolia, Turkey, *Minerl. Mag.*, 2A, 733-734.
- Kadioğlu, Y.K., Dilek, Y., Foland, K.A., 2006. Slab break-off and syncollisional origin of the Late Cretaceous magmatism in the Central Anatolian crystalline complex, *Geological Society of America*, 409, pp 381-415.
- Kumar, S., 2020. Schedule of Mafic to Hybrid Magma Injections Into Crystallizing Felsic Magma Chambers and Resultant Geometry of Enclaves in Granites: New Field and Petrographic Observations From Ladakh Batholith, Trans-Himalaya, India. *Front. Earth Sci.* 8:551097. doi: 10.3389/feart.2020.551097.
- Maniar, P.D., Piccoli, P.M., 1989. Tectonic Discrimination of Granitoids, *Geo. Soc. American. Bul.*, 101, 635-643s.
- Middlemost, E.A.K., 1975. The basalt clan. *Earth Sci. Rev.* 11, pp. 337-364.

INTERNATIONAL AEGEAN CONFERENCES
ON INNOVATION TECHNOLOGIES & ENGINEERING-VI
December 20-22, 2022

- Pearce, J.A., 1982, Trace Elements Characteristic of Lavas from Destructive Plate Boundaries, Thorpe, R.S., (ed), Andesites, Wiley, Chichester, p525-548.
- Pearce, J.A., Harris, N.B.W., Tindle, A.G., 1984. Trace-Element Discrimination Diagrams for the Tectonic Interpretation of Granitic Rocks. Journal of Petrology, 25, 956-983.
- Rickwood, P.C., 1989. Boundary lines within petrologic diagrams which use oxides of major and minor elements. *Litos*, 22, pp. 247-263.
- Wiebe, R.A., Manon, M.R., Hawkins, D.P., McDonough, W.F., 2004. Late-stage mafic injection and thermal rejuvenation of the Vinalhaven granite, Coastal Maine. *Jour. Petrol.*, v.45, pp.2133-2153.
- Wilson, M., 1989. *Igneous Petrogenesis*. Unwin Hyman, London.

**SOUND DETECTION AND CLASSIFICATION IN A NOISY ENVIRONMENT
USING PCA AND ICA IN THE TIME DOMAIN AND TIME-FREQUENCY DOMAIN**

Levent AYMAN

ASELSAN Inc., Defence System Technologies

ORCID ID: 0000-0002-3884-0190

Osman Taha ŞEN

Istanbul Technical University, Faculty of Mechanical Engineering, Department of Vibration and Acoustic

ORCID ID: 0000-0002-8604-3962

ABSTRACT

The subject of machine learning is a popular research topic, as evident from numerous ongoing research projects. This topic has become the center of most recent research activities and has been applied in several disciplines, where the classification of sound signals is one of these domains. In the sound signal classification, the precision of the process improves for signals, where the signal to noise ratio is high. Thus, multiple methods exist for extracting features from acoustic signals containing various sources and measured by several microphones. Consequently, the accuracy of source detection process improves, by training neural networks with these features.

This paper aims to investigate the performance of different sound source classification algorithms via neural network approach. The clean acoustic source signals are passed through a pre-trained neural network, which are obtained by using the proposed method for detecting and classifying sounds in a noisy environment. The mixed acoustic signals, which contain multiple sound signal components are passed through the trained neural network without any pre-processing. Thus, methods for noise reduction and source separation, such as Empirical Mode Decomposition (EMD) and Principal Component Analysis (PCA) are utilized. The Independent Component Analysis (ICA) technique, which is typically applied to electroencephalography (EEG) or electrocardiogram (ECG) signals, are also studied in order to separate the sound sources contained in a noise-cleaned acoustic signal. As a result of the study, it is determined that PCA and ICA are more applicable. Furthermore, the performance of time-frequency domain investigation is found to be superior when compared to time domain analysis. The obtained sound sources are classified using the pre-trained YAMNET network, and the results' accuracy is determined. Finally, it is observed that when the same acoustic signal is classified without the proposed methods, only the dominant sound is found to be classifiable.

Keywords: Classification, PCA, ICA, Source Separation, Noise Reduction.

ÖZET

Makine öğrenmesi, bu konuda yürütülen güncel araştırma projelerinin sayısından da anlaşılacağı üzere, popüler bir araştırma konusudur. Güncel araştırma faaliyetlerinin merkezi haline gelen makina öğrenmesi konusu, ses sinyallerinin sınıflandırılmasının da içinde olduğu pek çok disipline uygulanmaktadır. Ses sinyali sınıflandırmasında, sinyal/gürültü oranının yüksek olduğu durumlarda, işlemin başarısı ve kesinliği artmaktadır. Bu nedenle, çeşitli kaynakları içeren ve birden fazla mikrofon tarafından ölçülen akustik sinyallerin özniteliklerinin çıkarılması için birçok yöntem geliştirilmiştir. Sonuç olarak, sinir ağları bu özniteliklerle eğitilerek kaynak bulma işleminin doğruluğu artırılabilir.

Bu çalışmada, yapay sinir ağı yaklaşımı aracılığıyla farklı ses kaynağı sınıflandırma algoritmalarının performanslarının araştırılması amaçlanmaktadır. Bu amaçla akustik kaynaklardan yayılan temiz ses sinyalleri, gürültülü bir ortamdaki sesleri algılamak ve sınıflandırmak için çalışma kapsamında önerilen yöntem ile önceden eğitilmiş bir sinir ağından geçirilmiştir. Birden fazla ses sinyali bileşeni içeren karışık akustik sinyaller ise herhangi bir ön işleme tabi tutulmadan eğitilmiş sinir ağından geçirilmiştir. Çalışma kapsamında, Ampirik Mod Ayırıştırma (EMD) ve Temel Bileşen Analizi (PCA) gibi gürültü azaltma ve kaynak ayırma yöntemleri kullanılmıştır. Ayrıca, genellikle elektroensefalografi (EEG) veya elektrokardiyogram (EKG) sinyallerine uygulanan Bağımsız Bileşen Analizi (ICA) tekniği de, gürültüden arındırılmış bir akustik sinyalde bulunan ses kaynaklarını ayırmak için uygulanmıştır. Çalışma sonucunda PCA ve ICA yaklaşımlarının daha uygulanabilir olduğu belirlenmiştir. Ayrıca, sinyallerin zaman-frekans tabanında incelenmesinin, sadece zaman tabanı analizine kıyasla daha üstün bir performans sergilediği görülmüştür. Elde edilen ses kaynakları önceden eğitilmiş YAMNET ağı kullanılarak sınıflandırılmış ve sonuçların doğruluğu tespit edilmiştir. Son olarak, aynı akustik sinyal önerilen yöntemler olmaksızın sınıflandırıldığında, sadece baskın sesin sınıflandırılabilir olduğu görülmüştür.

Anahtar Kelimeler: Sınıflandırma, PCA, ICA, Kaynak Ayırımı, Gürültü İndirgeme.

INTRODUCTION

Currently, machine learning applications is a major area of research in many fields, and the sound signal classification is an important application field of the machine learning. When the signal-to-noise ratio is high, which is a key factor on the determination of audio signal identification efficiency, detectability is improved. This can be accomplished through the use of techniques that reduce noise. According to a study on noise reduction, Empirical Mode Decomposition (EMD) is found to be a more effective approach than Wavelet Transform and Total Variation for the processing of heart sound signals [1]. Additionally, in a different study

Principal Components Analysis (PCA) was used to reduce noise to analyze separated single-lead electrocardiograms (ECG) [2].

In the case that the gathered sound signals include more than one sound source and reflection, a case that is referred to as the “cocktail problem” emerges. The “cocktail problem” is encountered frequently in the research literature, and a variety of methods are utilized in order to reach conclusions. Independent Component Analysis (ICA) is a technique that has been applied in numerous studies related to “cocktail problem”, either in time domain or time-frequency domain. Ikeda and Murata suggest that transforming the received signal from time domain to time-frequency domain, and implementing the ICA method leads to a more efficient source separation result [3]. In another study, ICA was successfully implemented for the purpose of analyzing EEG signals in time-frequency domain [4]. Finally, a study that proposes a different technique by combining ICA in time and frequency domains can be given as an example of ICA applications [5].

Artificial neural networks play a significant role in classification. Using testing, validation, and training datasets, these artificial neural networks can be trained. Furthermore, the classification result’s accuracy is also directly proportional to the size of the dataset. YAMNet can be given as an example of an artificial neural network. YAMNet is a neural network that has been pre-trained with the MobileNetV1 deep detachable convolution architecture. It is capable of using an audio waveform as input and making independent predictions for each of the 521 audio events in the AudioSet corpus [6].

In this article, a noisy environment is simulated by mixing the sound source signals with a random matrix structure. First, these mixed signals are whitened with PCA, then ICA is applied. The processed signals are then compared in time domain and time-frequency domain. The parsed signals and mixed signals are classified in the pre-trained YAMNet network and the classification results are given.

METHODS

To decrease the number of dimensions from a numerical measurement of several variables, PCA and ICA are techniques that are frequently used in multivariate statistical analysis. These techniques aim to simplify a statistical problem with the least amount of information lost through this dimensional reduction. These techniques are also employed in signal processing to separate a linear combination of signals produced by statistically independent sources.

Principal Component Analysis (PCA)

Principal Component Analysis (PCA), is a linear transformation technique. It is mainly utilized for dimension reduction and compression, and has applications in data analysis, finance, and bioengineering.

Using the potential correlation between features, PCA identifies patterns in the data. It identifies the vector with the highest variance in a high-dimensional dataset and then uses it to create a set of orthogonal vectors with the next highest variance. This new subspace has the same or fewer dimensions than the original. The algorithm allows the user to define the number of applied vectors. The first vector in the subspace can be thought of as the most “principal” component, and the following vectors of that as the next-most “principal”.

The PCA algorithm can be summarized in the following steps:

- The covariance matrix of the n -dimensional dataset X is constructed.
- The covariance matrix’s eigen-decomposition is found.
- The k number of eigenvectors that correspond to the first largest k eigenvalues are selected, where k is defined as the new dimensionality of the transformed dataset ($k \leq n$).
- A projection matrix W from the first k eigenvectors is constructed.
- The n -dimensional input dataset X is transformed using the projection matrix W to obtain the new transformation.

Independent Component Analysis (ICA)

Independent component analysis (ICA) is a computational and statistical method for identifying hidden factors underlying random variables, measurements, or signals. Though, it usually is not proper to feed the mixed signals directly to the ICA. To obtain the most accurate estimate of the independent components, it is recommended to pre-process the data. Following is a detailed explanation of the two most important pre-processing techniques.

- Centering

This is a straightforward subtraction of the mean from the input value X . Consequently, the centered mixed signals have a zero mean, which implies that input source signals also have zero mean.

- Whitening

Whitening is the second pre-processing step for the signal X . The aim here is to linearly transform X so that any possible correlations between the signals are eliminated and their variances are equal to unity.

The other steps of ICA can be summarized in the following steps:

- Weight Matrix Update
- Decorrelation
- Normalization
- Convergence Check

These steps will be repeated until Weight Matrix converge.

SIMULATION RESULTS

Three different, 5-second-long sound source files that are sampled at 44100 Hz are used to simulate the proposed methods. The sound source files include dog barking, rain sound, and traffic noise. Those signals are mixed by multiplying them with a random matrix. In addition, the mixed signals are normalized. The original signals and the obtained normalized mixed signals are depicted in Figures 1 and 2.

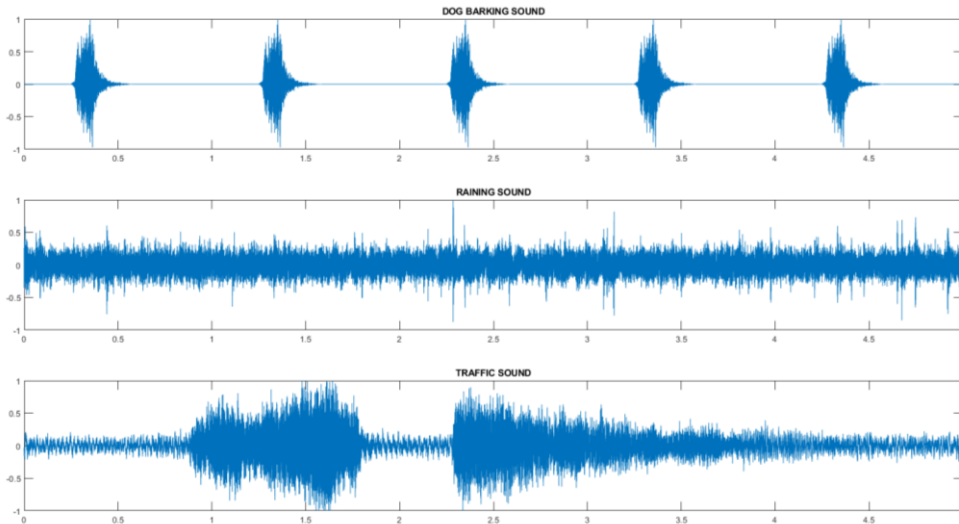


Figure 1 Original Signals

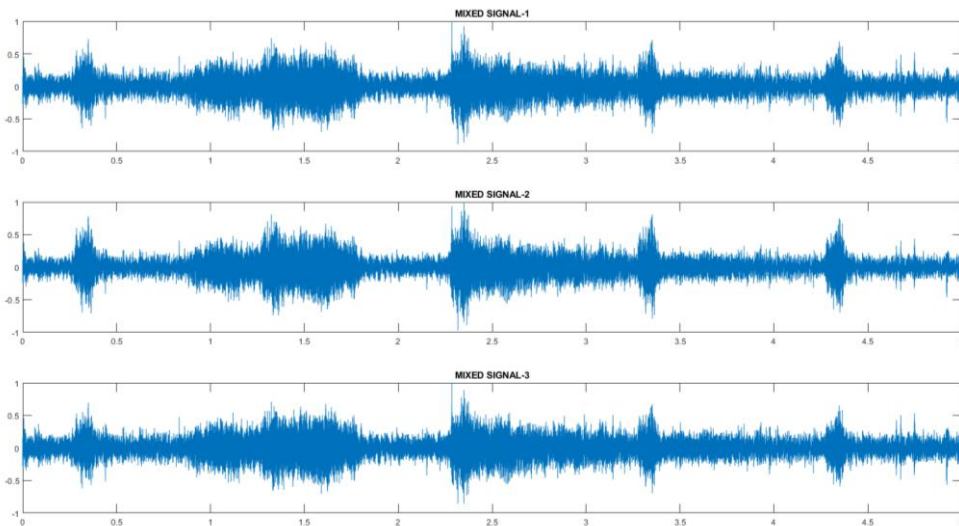


Figure 2 Mixed Signals

Results of Time Domain

First, a whitening process is applied to the mixed signals by applying PCA in time domain. Second, the source signals components are separated using the FastICA algorithm. The results are given in Figures 3 and 4 along with their spectrograms.

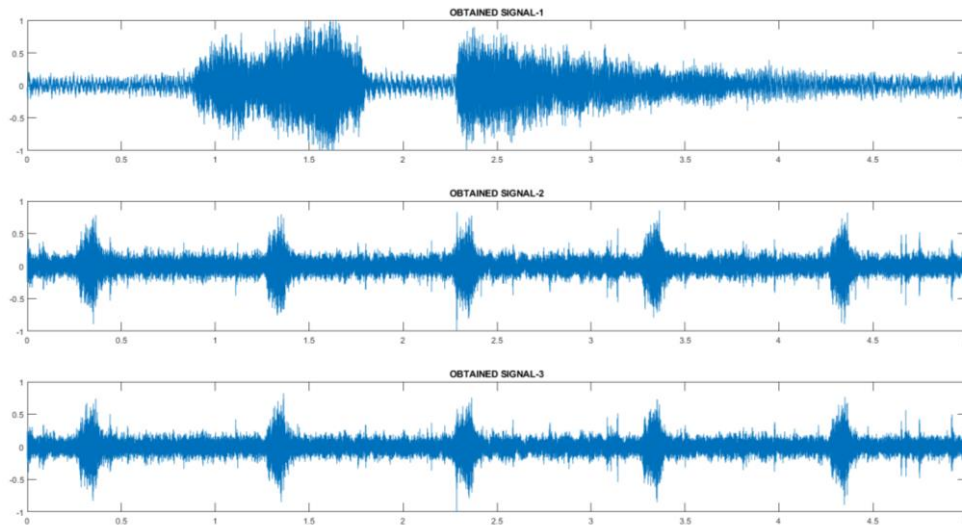


Figure 3 Obtained Signals in Time Domain

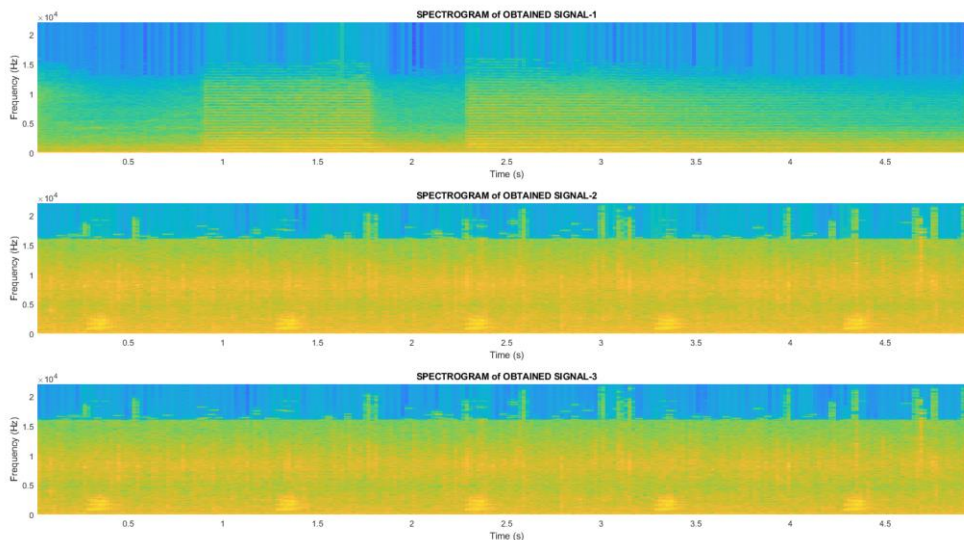


Figure 4 Spectrograms of Obtained Signals in Time Domain

Results of Time-Frequency Domain

As opposed to time domain investigation, the process in time-frequency domain is started by windowing and application of short-time Fourier transform in the 0.1–20 kHz frequency band. Subsequently, the input signal in time-frequency domain is spatially whitened with PCA dimension reduction. Finally, the signal is run through the complex-valued FastICA algorithm. The results are shown in Figures 5 and 6 along with their spectrograms.

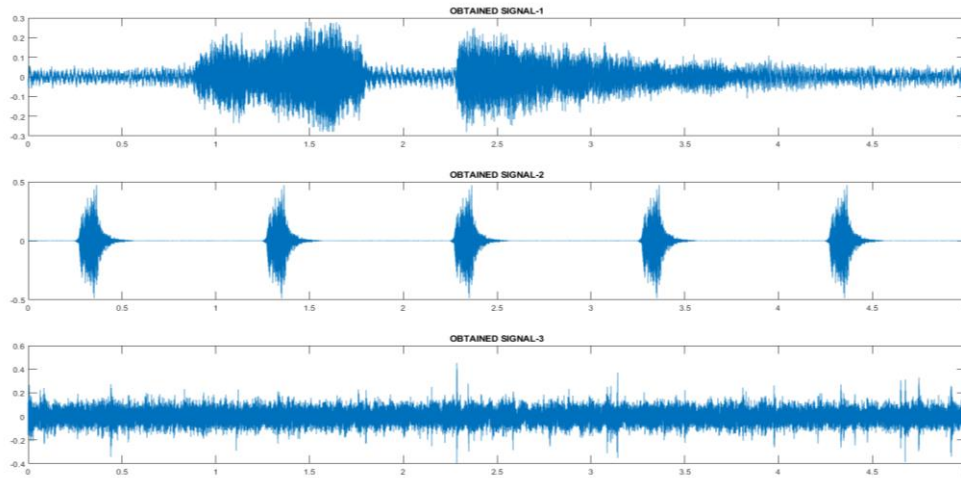


Figure 5 Obtained Signals in Time-Frequency Domain

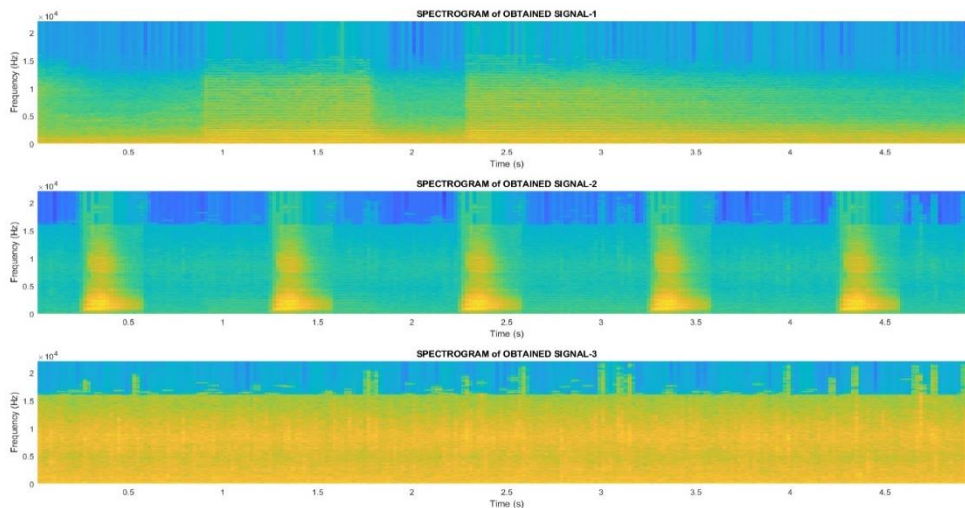


Figure 6 Spectrograms of Obtained Signals in Time-Frequency Domain

Results of Classification

To evaluate the results of classification, signals are processed 100 times through the following steps:

- Mixed signals are obtained using a new random mixing matrix.
- The time-domain algorithm is implemented.
- Time-frequency domain conversion is applied.
- Each of the output data (mixed, time domain, and time-frequency domain) is pre-processed and classified using YAMNet.

Based on the classification results of the mixed signals, it is observed that the generated mixed signals of dog, rain, and traffic sounds are classified as 64% vehicle, 32% toot, and 4% animal sound, respectively. Second, an accuracy of 88% is achieved for the category names dog, water, and vehicle, when the data obtained from processing in the time domain are classified. Finally, it is observed that the classification of the data obtained as a result of

processing in time-frequency domain yields to an accuracy of 100% for the dog, water, and vehicle category names.

CONCLUSION AND DISCUSSION

In this study, three different signals are combined to simulate a noisy environment. Afterwards, these mixed signals are processed through noise reduction techniques. These processed signals are then run through the FastICA algorithm in time domain and the complex-valued FastICA algorithm in time-frequency domain. These signals are the output of the algorithms executed on the pre-trained YAMNet neural network, and the classification results are obtained.

Analyzing these results reveals that working in time-frequency domain is superior to working in time domain. Examining the results of time and time-frequency domain investigations reveals that traffic sounds can be easily distinguished in both domains. Though, the precision of the classification is higher in time-frequency domain. In addition, although the number of iterations plays a role in the algorithms' processing time, the processing time in time domain is shorter than in time-frequency domain. However, processing time will be reduced if the frequency band can be tailored to the sounds that are desired to be detected.

These algorithms can be evaluated with actual environmental data in future research. In addition, a new neural network for classification can be obtained by classifying the desired signals using transfer learning.

REFERENCES

- [1] Salman, A. H., Ahmadi, N., Mengko, R., Langi, A. Z., & Mengko, T. L. (2015, November). Performance comparison of denoising methods for heart sound signal. In 2015 international symposium on intelligent signal processing and communication systems (ISPACS) (pp. 435-440). IEEE.
- [2] Palaniappan R, Khoon TE. Uni-channel PCA for noise reduction from ECG signals. Proc 1st International Bioengineering Conference 2004; 436-439.
- [3] Ikeda, S., & Murata, N. (1999). A method of ICA in time-frequency domain. In *in Proc. ICA*.
- [4] Hyvärinen, A., Ramkumar, P., Parkkonen, L., & Hari, R. (2010). Independent component analysis of short-time Fourier transforms for spontaneous EEG/MEG analysis. *NeuroImage*, 49(1), 257-271.
- [5] Nishikawa, T., Saruwatari, H., & Shikano, K. (2002, September). Comparison of time-domain ICA, frequency-domain ICA and multistage ICA for blind source separation. In 2002 11th European Signal Processing Conference (pp. 1-4). IEEE.
- [6] "Transfer Learning with YAMNet for Environmental Sound Classification | TensorFlow Core." TensorFlow, 26 Jan. 2022, www.tensorflow.org/tutorials/audio/transfer_learning_audio. Accessed 14 Dec. 2022.

**GELECEKTEKİ YOLCULARIN ARAÇ İÇİ MEKÂN KULLANIM İHTİYAÇLARI
VE OTONOM ARAÇ TASARIMI ÜZERİNDEKİ ETKİSİ**
FUTURE PASSENGER NEEDS IN INTERIORS AND ITS IMPACT ON AUTONOMOUS
VEHICLE

Rumeysa AKAR

Kocaeli University, Faculty of Technology, Department of Automotive Engineering,
ORCID: 0000-0002-3788-5725

Mehmet UÇAR

Kocaeli University, Faculty of Technology, Department of Automotive Engineering,
ORCID: 0000-0002-3363-438X

ÖZET

Teknolojinin hızla ilerlemesinin otomotiv sektörüne etkisinin en çok otonom araçlara yansıdığı görülmektedir. Sürücü ve yolcu ergonomisi de göz önüne alındığında otomotiv iç mekan tasarımının detaylı incelenmesi ve bu alana yoğunlaşılması gerekliliği ortaya çıkmaktadır. Yapılan çalışmalar ve sonuçları incelendiğinde aslında otonom araç denildiğinde çoğu çalışmanın çok yüksek teknolojiler içeren ve uygulandığında çok yüksek maliyetleri olacak araç tasarımları üzerine olduğu görülmektedir. Bu nedenle gelecekteki potansiyel otonom araç kullanıcılarının iç mekan beklentilerini anlamaya yönelik bir araştırma yapmak amaçlandı. Araştırmanın ilk adımı olarak belirlenen hedeflere yönelik çeşitli sorular içeren bir anket çalışması oluşturuldu. Anket çalışmasında en verimli sonucu almak adına bir araştırma yapıldı ve anket türü seçildi. Konuyu hiç bilmeyen insanlara bile fikir oluşturması adına tarafımızca tasarlanan görseller eklenerek anket tamamlandı.

Bu çalışmada Amerika, Asya, Avrupa gibi farklı pazarların beklentilerini anlamak hedeflendiği için anket ilgili ülkelerin yerel dillerine çevrilerek 25 farklı ülkeye ulaştırıldı. Toplamda 7053 yanıtı ulaşılarak hedeflenen geniş araştırmaya ulaşılmış oldu. Ülkelerden gelen sonuçlar, pazarlara göre sınıflandırılmanın yanı sıra, yaş, cinsiyet gibi demografik özelliklere göre de filtrelenerek analiz edildi. Farklı kullanım alışkanlıklarına sahip insanlardan alınan sonuçlara göre, araç iç mekanlarının nasıl kullanılmak istendiği, ergonomik anlamda beklentileri, ayrabilecekleri bütçeleri, güvenlik ve hijyen için neye ihtiyaç duydukları yorumlanmıştır. Böylece, otonom araçların iç tasarımıyla ilgili gerçekçi beklentilerin ne olduğunu analiz edilmiştir. Bu çalışmadan çıkarılan sonuçların sektördeki iç tasarıma bağlı çalışmalara yön vermesi amaçlanmaktadır.

Son olarak otonom araçlarla ilgili otomotiv sektöründeki beklentinin ne olduğunu anlamak ve sektörden olmayan insanların beklentileri ile karşılaştırmak amacıyla anket farklı bir formata

geçirildi. Bu formatı şirketin tüm ofislerindeki çalışanlarına ulaştırmak ve araştırmayı bu yönde zenginleştirmek hedeflenmektedir.

Anahtar Kelimeler: Otonom Araç, İç Mekân, Yüksek Teknoloji

ABSTRACT

It was seen that the effect of the rapid advancement of technology on the automotive sector was mostly on the studies on autonomous vehicles. In this sense, various researches were carried out in order to contribute to these studies and it was observed that there were few studies on automotive interiors. When the studies and their results were examined, it was observed that most of the studies on autonomous vehicles are on vehicle designs that contain very high technologies and will have very high costs when applied. For this reason, it was aimed to conduct a research to understand what the interior expectations of potential future autonomous vehicle users are. As the first step of the research, a questionnaire study containing various questions was created. In order to get the most efficient result in the survey study, a research was conducted and the survey type was selected. The survey was completed by adding visuals designed by us in order to create an idea even for people who do not know the subject at all.

Since it was aimed to understand the expectations of different markets such as America, Asia and Europe in this research, the survey was translated into the local languages of the relevant countries and delivered to 25 different countries. In total, 7053 responses were received and the targeted broad research was achieved. In addition to being classified according to markets, the results from the countries were also filtered and analysed according to demographic characteristics such as age and gender. According to the results received from people with different usage habits, how they want to use vehicle interiors, their expectations in terms of ergonomics, the budgets they can allocate, what they need for safety and hygiene, and what realistic expectations about the interior design of autonomous vehicles were analysed. It is aimed that the results of this research will guide the studies related to interior design in the sector.

Finally, the questionnaire was changed to a different format in order to understand what the expectations in the automotive sector are regarding autonomous vehicles and to compare them with the expectations of people who are not from the sector. It is aimed to deliver this format to employees in all offices of the company and to enrich the research in this direction.

Keywords: Autonomous Vehicle, Interior, High Technology

**ARI ALGORİTMASI KULLANILARAK ÖNDEN DÜMENLEMELİ BİR ARACIN
DÜMENLEME MEKANİZMASININ OPTİMİZASYONU**
OPTIMIZATION OF THE STEERING LINKAGE OF A FRONT-WHEEL-STEERING
VEHICLE BY USING THE BEES ALGORITHM

Abdullah ERDEMİR

MPG Makine Prodüksiyon Grubu Makine İml. San. ve Tic. A.Ş., Konya/TURKIYE
MPG Machinery Production Group Inc. Co., Konya/TURKIYE
ORCID NO: 0000-0002-7267-3111

Veysel ALVER

MPG Makine Prodüksiyon Grubu Makine İml. San. ve Tic. A.Ş., Konya/TURKIYE
MPG Machinery Production Group Inc. Co., Konya/TURKIYE
ORCID NO: 0000-0002-7917-8295

Mete KALYONCU

Prof. Dr., Konya Teknik Ü., Müh. ve Doğa Bil. Fakültesi, Makina Müh. Bölümü, Konya/TURKIYE
Prof. Dr. Konya Technical U., Faculty of Eng. and Natural Sci., Dep. of Mech. Eng., Konya/TURKIYE
ORCID NO: 0000-0002-2214-7631

ÖZET

Bu çalışmada, önden dümenlemeli bir aracın dümenleme mekanizmasının Arı Algoritması kullanılarak optimizasyonu gerçekleştirilmiştir. Burada dümenleme mekanizması olarak dört çubuk mekanizması kullanılmıştır. Dümenleme açıları dört çubuk mekanizmasının kinematik analizinden hesaplanmıştır. Genellikle araçların dümenleme mekanizmaları Ackerman geometrisi kullanılarak tasarlanmaktadır. Ackerman geometrisi, farklı yarıçapların çevrelerini takip etmeye ihtiyaç duyan bir dönüşün içindeki ve dışındaki tekerleklerin problemini çözmek için tasarlanmış dümenleme mekanizmasının geometrik düzenlemesidir. Ackerman geometrisinin amacı, dönüş sırasında bir eğri etrafındaki yolu takip ederken, lastiklerin yanlara kaymasını ve ilave yan yüklerin gelmesini önlemektir. Bunun geometrik çözümü, tüm tekerleklerin akslarının ortak bir merkez noktaya sahip daire yarıçapları olarak düzenlenmesidir. Ancak, aracın dönmesi sırasında Ackerman kuralı olarak bilinen ideal kuralın sağlanacağı her zaman garanti edilemez. Bu nedenle, boyutsal sentez, her iki dümenleme tekerinin araç dönerken Ackerman kuralına mümkün olduğunca uyması için sahip olması gereken dümenleme mekanizması boyutlarını belirlemeyi amaçlayan optimizasyon yoluyla yapılmıştır. Bu çalışmada, Ackerman kuralı ve dört çubuk mekanizması kinematik analizi ile elde edilen dümenleme açıları arasındaki hatayı en aza indirmek için Arı Algoritması kullanılmıştır. Optimizasyon sonucu elde edilen sonuçlar, Ackerman hatasını

azaltmış ve dümenleme mekanizması boyutlarında iyileştirme yapılabileceğini göstermiş ve grafikler halinde sunulmuştur.

Anahtar Kelimeler: Arı Algoritması, dümenleme mekanizması, Ackerman kuralı, boyutsal sentez, optimizasyon

ABSTRACT

In this study, the steering linkage of a front-wheel-steering vehicle was optimized using the Bee Algorithm. Here, a four-bar linkage is used as the steering linkage. Steering angles were calculated from the kinematic analysis of the four-bar linkage. Generally, steering linkages of vehicles are designed using Ackerman geometry. Ackerman geometry is the geometric arrangement of the steering linkage designed to solve the problem of wheels inside and outside of a turn that need to follow the circumferences of different radii. The purpose of Ackerman geometry is to prevent the tires from slipping sideways and causing additional lateral loads when following the path around a curve during a turn. The geometric solution to this is that the axles of all wheels are arranged as radii of circles with a common center point. However, it is not always guaranteed that the ideal rule, known as the Ackerman rule, will be met during vehicle rotation. Therefore, the dimensional synthesis has been done through optimization aiming to determine the steering linkage dimensions that both steering wheels must obey the Ackerman rule as much as possible while the vehicle is turning. In this study, the Bee Algorithm was used to minimize the error between the steering angles obtained by the Ackerman rule and the four-bar linkage kinematic analysis. The results obtained as a result of the optimization reduced the Ackerman error and showed that the dimensions of the steering linkage could be improved and presented in graphics.

Keywords: The Bees Algorithm, Steering linkage, Ackerman's rule, dimensional synthesis, optimization

1. GİRİŞ

Uzun yıllardan beri bilgisayar teknolojilerinin gelişmesiyle çok uzuvlu karmaşık mekanizmaların boyut sentezi problemleri çok gözde bir konu olmuştur [1]. Araçların yönlendirilmesi için kullanılan sistemler ise genellikle çok uzuvlu mekanizmalardır. Mekanizmaların karmaşıklaşması ile beraber doğrudan analitik çözüm elde edilmesi zor olduğundan çeşitli sayısal ve optimizasyon yöntemleri kullanılarak analiz ve tasarımlar gerçekleştirilir. Boyutlandırması uygun olmayan çok uzuvlu mekanizmaların kullanımı sonucunda araçlarda, Ackerman hatası oluşur ve bu da lastiklerin aşınmasına ve araca ilave yanal zorlamaların gelmesine sebep olur [2]. Bu durum, aynı zamanda aracın istenen yörüngede manevra yapamamasına ve manevra esnasında titreşimlerin oluşmasına yol

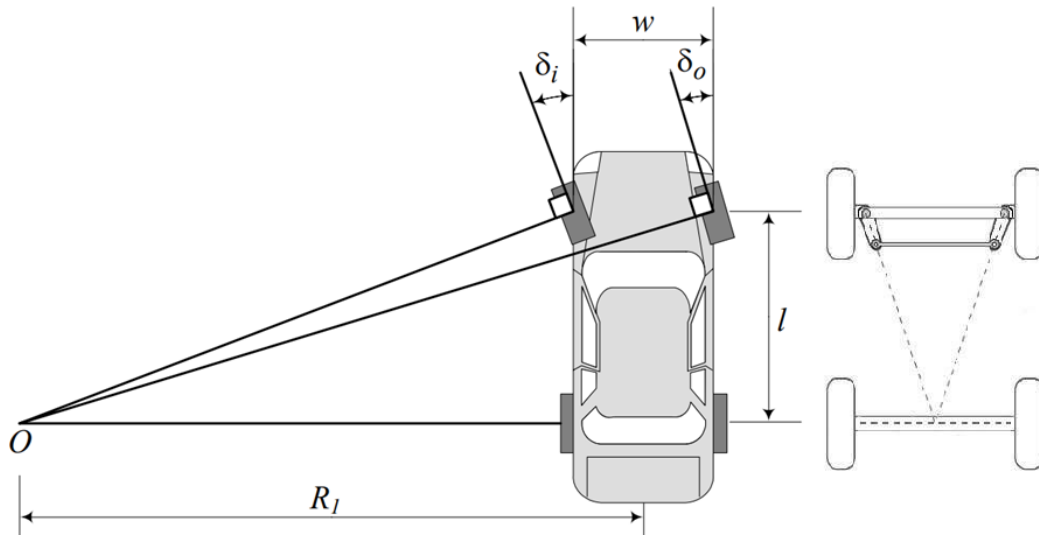
açmaktadır. Çok uzuvlu mekanizmalarda, istenilen yörüngeyi takip edilebilmesi için, Ackerman hatasını minimize eden uzuv boyutlarının belirlenmesi gerekir. Bu çalışmada konuda bilim insanlarını yapmış olduğu çok sayıda çalışma vardır [3-16]. Bu çalışmada, Ackerman hatasının minimum yapacak şekilde dört çubuk mekanizması olarak tasarlanan dümenleme mekanizmasının sentezi gerçekleştirilmiştir. Mekanizma boyutlarının optimizasyonunda birçok optimizasyon probleminde kullanılan Arı Algoritması [17-30] kullanılmıştır.

2. ACKERMAN GEOMETRİSİ

Bu çalışmada kullanılan sola dönen önden dümenlemeli bir araç Şekil 1’de görülmektedir. Araç çok yavaş hareket ettiğinde, iç ve dış tekerlekleri ilişkilendiren ve bunların kaymadan dönmesini sağlayan bir kinematik durum söz konusudur. Her lastik düzleminin merkezine giden normal doğru ortak bir noktada kesişmeli ve sıfır hızda kaymadan dönüş sağlamak için biri hariç tüm akslar yönlendirilebilir olmalıdır [2]. Bu geometrik ilişki Ackerman kuralı olarak adlandırılır ve Şekil 1’de ifade edilmiştir.

$$\cot \delta_o - \cot \delta_i = (w/l) \quad (1)$$

Denklem 1’de, w ; yönlendirilebilir tekerleklerin yönlendirme eksenleri arasındaki iz mesafesi, l ; ön ve arka dingil arasındaki dingil mesafesi, δ_i ; iç tekerleğin dümenleme açısı ve δ_o dış tekerleğin dümenleme açısıdır.

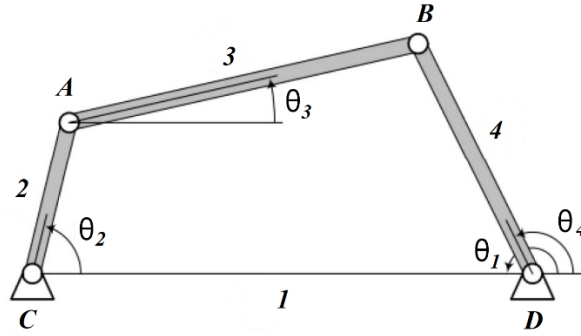


Şekil 1. Önden dümenlemeli bir araç [2] ve Ackerman geometrisi

3. DÖRT ÇUBUK MEKANİZMASI KONUM ANALİZİ

Araçların mekanik aksamalarında özellikle dümenleme mekanizmalarında kullanılan mekanizmaların çoğu dört çubuk mekanizmalarıdır. Bu mekanizma, Şekil 2’de görülmektedir. Bu mekanizmada, 1 nolu uzuv (\overline{CD}), tüm açıların ve değişkenlerin ölçüleceği referans uzuv

olarak kullanılır. 2 nolu uzuv (\overline{AC}), giriş uzvu olarak adlandırılır ve θ_2 giriş açısı tarafından kontrol edilir. 4 nolu uzuv (\overline{BD}), çıkış uzvu olarak adlandırılır ve konumu, θ_4 çıkış açısının bir fonksiyonu olarak tanımlanır. 3 nolu uzuv (\overline{AB}), 2 ve 4 nolu uzuvları bağlayan uzuv olup θ_3 açısal konumu ile tanımlanır. Çıkış uzvunun açısal konumu θ_4 , uzuvların uzunluklarının ve θ_2 giriş konumunun bir fonksiyonudur. θ_4 açısı aşağıdaki denklemler kullanılarak hesaplanabilir.



Şekil 2. Dört çubuk mekanizması

$$\theta_4 = 2 \arctan \left[\frac{-B \pm \sqrt{B^2 - 4AC}}{2A} \right] \quad (2)$$

Denklem 2'deki A, B ve C Denklem 3'te gösterilmiştir.

$$A = Z_3 - Z_1 + (1 - Z_2) \cos \theta_2, \quad B = -2 \sin \theta_2, \quad C = Z_1 + Z_3 - (1 + Z_2) \cos \theta_2 \quad (3)$$

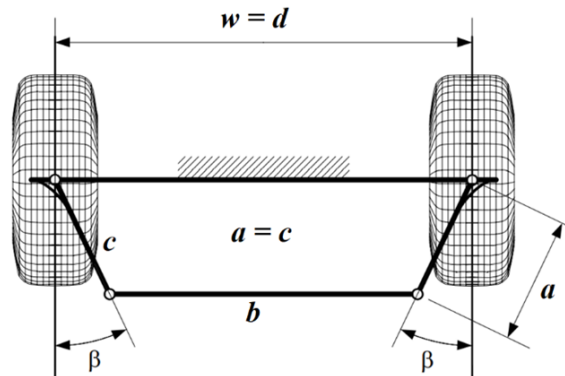
Dört çubuk mekanizmasının vektör poligonundan aşağıdaki denklemleri tanımlamak mümkündür.

$$Z_1 = d/a, \quad Z_2 = d/c, \quad Z_3 = (a^2 - b^2 + c^2 + d^2)/2ac \quad (4)$$

Denklem 4'te a; 2 nolu uzvun uzunluğu, b; 3 nolu uzvun uzunluğu, c; 4 nolu uzvun uzunluğu ve d; 1 nolu uzvun uzunluğudur. Bu denklemlerden dört çubuk mekanizmasının uzuv uzunlukları bilindiği sürece, giriş açısına bağlı olarak diğer uzuv açılarını ve çıkış açısını hesaplamak mümkündür.

$$Z_1 \cos \theta_4 - Z_2 \cos \theta_2 + Z_1 = \cos(\theta_4 - \theta_2) \quad (5)$$

Dört çubuk mekanizmasına ait bu denklemlerin dümenleme mekanizması olarak kullanılabilmesi için mekanizmaların birbirlerine göre uyarlanması gerekir. Şekil 3'te dört çubuk mekanizmasının dümenleme mekanizması olarak uyarlanması görülmektedir.



Şekil 3. Dört çubuk mekanizmasının dümenleme mekanizması olarak uyarlanması
Bu değerlendirmelerden sonra tekerleklerin dümenleme açıları β , θ_2 ve θ_4 'ün bir fonksiyonu olarak hesaplanabilir.

$$\delta_i = 90^\circ - \theta_2 - \beta \quad (6)$$

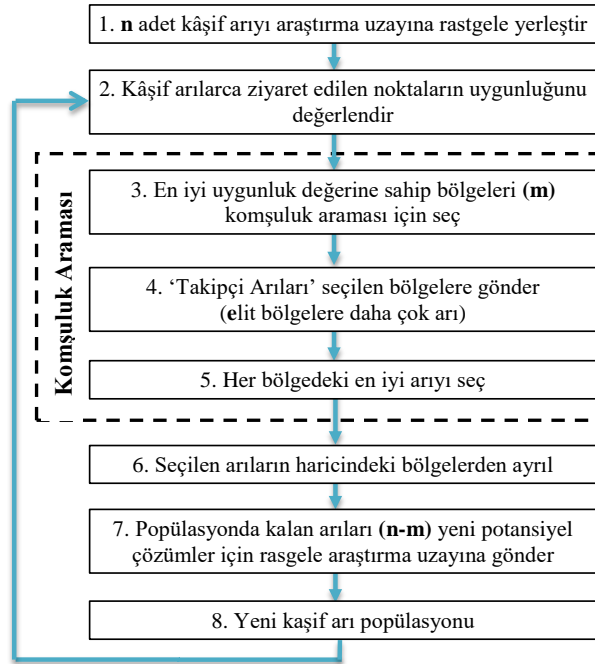
$$\delta_o = 90^\circ - \theta_4 + \beta \quad (7)$$

Denklem 6 ve 7'de, δ_i ; iç tekerleğin dümenleme açısı ve δ_o ; dış tekerleğin dümenleme açısıdır. Şekil 3'teki b boyutu ise d, β ve a'nın bir fonksiyonu olarak aşağıdaki gibidir:

$$b = d - 2a \sin \beta \quad (8)$$

4. ARI ALGORİTMASI

Bu bölümde, temel Arı Algoritması açıklanmıştır. Arıların kaynak (nektar, su vb.) arama davranışları, öğrenme, hatırlama ve bilgi paylaşma özellikleri sürü zekâsının en ilgi çekici araştırma alanlarından birisidir. Arı Algoritması [17-30], ilk olarak 2006 yılında D.T. Pham ve arkadaşları tarafından önerilmiş olup, bal arılarının kaynak arama davranışını taklit eden popülasyon tabanlı, sezgisel bir arama algoritmasıdır. Arı Algoritmasına ait akış şeması Şekil 4 'de verilmiştir.



Şekil 4. Arı Algoritması akış şeması

D.T. Pham ve ark. tarafından geliştirilen temel Arı Algoritması birçok parametre içermektedir. Bu parametreler: kâşif arı sayısı (n), ziyaret edilen n nokta içinden seçilen en uygun bölge sayısı (m), seçilen m bölge içindeki elit bölge sayısı (e), en iyi e bölgeye gönderilen arı sayısı (nep), kalan (m-e) bölgeye gönderilen arı sayısı (nsp), bölge boyutu (ngh) ve durdurma kriteri/iterasyon sayısı (itr)'dir.

Arı Algoritması n adet kâşif arının araştırma uzayına rastgele yerleştirilmesi ile başlar. 2. adımda, kâşif arılarca ziyaret edilen noktaların birbirlerine göre uygunlukları değerlendirilir. 3. adımda, n adet bölge içerisinde diğerlerine göre daha uygunluk değerine sahip m adet bölge seçilir. 4. ve 5. adımda, m adet bölge içerisinde en iyi uygunluk değerine sahip elit bölgeler (e) ve geriye kalan bölgeler (m-e) seçilir. Bu bölgelerin komşuluk arama boyutu (ngh) belirlenir. Seçilen bölgelerde komşuluk araması (bölge içinde en uygun noktaların araştırılması) için, daha umut verici çözümleri temsil eden en iyi e bölgeye seçilen diğer bölgelere göre daha fazla takipçi arı (nep), diğer bölgelere ise daha az takipçi arı (nsp) gönderilerek, detaylı arama yapılır. Her bölge içerisinde en uygun değere sahip arı seçilir. 6., 7. ve 8. adımda ise, her bölgede en uygun değere sahip arı haricindeki diğer arılar araştırma uzayından ayrılır. Popülasyondaki diğer arılar (n-m) yeni potansiyel çözümler elde etmek için tekrar, rastgele olarak, araştırma uzayına yerleştirilirler. Optimizasyon durdurma kriteri (itr) sağlanana kadar devam ettirilir. Her bir iterasyonun sonunda yeni popülasyon; seçilen her bir bölgenin temsilcileri ve rastgele arama yapan kâşif arılar olmak üzere iki parçadan oluşur.

5. DÜMENLEME MEKANİZMASININ OPTİMİZASYONU

Mekanizma sentezi, dış tekerleğin teorik olması gereken ve gerçekte gerçekleşen dümenleme açıları farkını ($\delta_{oT} - \delta_{oR}$) sifira olabildiğince yakın yapan, yani dört çubuk mekanizması konum analizinden elde edilen dümenleme açısı ile Ackerman kuralı tarafından tanımlanan açıları mümkün olduğunca yakın yapan dümenleme mekanizmasının boyutlarını belirlemeyi amaçlar. Bu doğrultuda optimizasyon çalışmalarında amaç fonksiyonu olarak hataların RMS değerini veren aşağıdaki fonksiyon kullanılmıştır:

$$Hata_{RMS} = \sqrt{\frac{1}{n} \sum_{j=1}^n (\delta_{oTj} - \delta_{oRj})^2} \quad (9)$$

Denklem 9’da n; dikkate alınan nokta sayısıdır. n değeri 100 olarak kabul edilmiştir. Bunun anlamı, amaç fonksiyonunda 100 farklı iç tekerlek dümenleme açısına karşılık gelen dış tekerlek dümenleme açısı hatasının RMS değerinin bulunduğuudur. Yapılan optimizasyon çalışmalarında giriş olarak, $R_1 \leq 5.8$ m dönüş yarıçapına denk gelen iç tekerlek dümenleme açısı kullanılmıştır. Dönüş yarıçapı 0’dan 5.8 metreye ulaşınca kadar artırılarak hata değerleri bulunmuştur. Ackerman kuralı için iç açıların ve dört çubuk mekanizması konum analizinden elde edilen θ_2 açısının aynı olduğu varsayılmış ve böylece δ_i ’nin tanımlanması sağlanmıştır. İç tekerlek dümenleme açısının bilinmesi ile gerçekleşen dış tekerlek dümenleme açısı (δ_{oR}) denklem 7 ve Ackerman kuralı için olması gereken teorik dış tekerlek dümenleme açısı (δ_{oT}) denklem 1 yardımıyla ile hesaplanmıştır. Daha sonra ($\delta_{oTj} - \delta_{oRj}$) bulunmuştur.

6. SAYISAL UYGULAMA

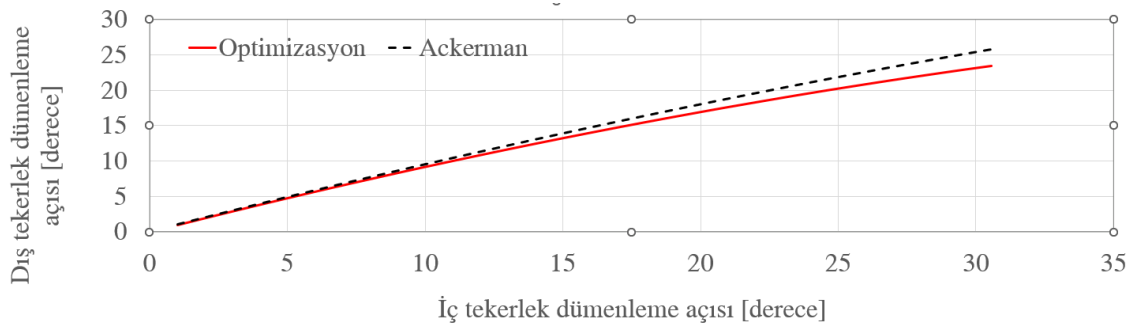
Bu çalışmada sayısal uygulama için kullanılan hali hazırda ticari olarak günlük hayatta kullanılan bir araca ait boyutlar Tablo 1’de verilmiştir. Arı Algoritmasının parametreleri Tablo 2’de gösterildiği gibi ayarlanmıştır. Şekil 5 ve 6’daki kesikli çizgiler Ackerman kuralına kesikli çizgiler ise optimizasyona göre oluşturulan dümenleme mekanizmasını temsil etmektedir. Şekil 5’e iç tekerleğin dümenleme açısına karşılık Ackerman kuralına ve dört çubuk mekanizmasının boyut optimizasyonuna göre elde edilen dümenleme mekanizmasına ait dış tekerlek dümenleme açısının değişimi görülmektedir. Ackerman kuralına göre oluşturulan dümenleme mekanizmasında iç tekerlek dümenleme açısı ile dış tekerlek dümenleme açısı arasında doğrusal bir ilişki söz konusu iken dört çubuk mekanizmasının boyut optimizasyonuna göre elde edilen dümenleme mekanizması sonuçlarına göre iç tekerlek dümenleme açısı ile dış tekerlek dümenleme açısı arasında doğrusal olmayan bir ilişki söz konusudur.

Tablo 1. Sayısal uygulama için kullanılan araca ait boyutlar

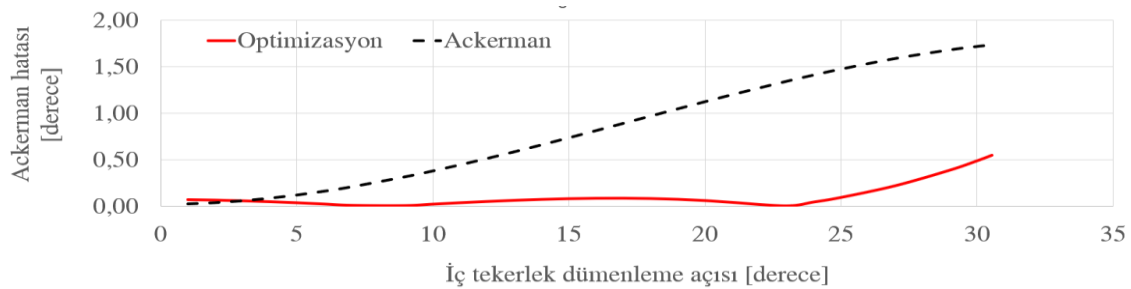
Aracın tekerlekler arası iz genişliği ($w = d$)	1619 mm
Aracın akslar arası mesafesi (l)	2939 mm

Tablo 2. Arı Algoritması parametreleri

n	m	e	nep	nsp	ngh	itr
20	10	5	10	7	0.01	1000



Şekil 5. Dış tekerlek dümenleme açısının değişimi



Şekil 6. Dış tekerlek dümenleme açısının Ackerman hatası

Şekil 6’da ise Ackerman kuralına ve dört çubuk mekanizmasının boyut optimizasyonuna göre elde edilen dümenleme mekanizmasına ait Ackerman hatasının iç tekerlek dümenleme açısına göre değişimi görülmektedir. Dört çubuk mekanizmasının boyut optimizasyonuna göre elde edilen dümenleme mekanizmasında dış tekerlek dümenleme açısı hatası Ackerman kuralına göre oluşturulan dış tekerlek dümenleme açısı hatasından oldukça küçüktür. Optimizasyon sonucunda hatanın RMS değerinde 0.9742’den 0.1771’e kadar bir azalma meydana gelmiştir. Tablo 3’te optimizasyon sonucu elde edilen dümenleme mekanizması boyutları verilmiştir.

Tablo 3. Optimizasyon sonucu bulunan boyutlar

	a=c [mm]	β [°]	b [mm]	d [mm]
Ackerman	350	15	1437	1619
Optimizasyon	500	20	1275	1619

7. SONUÇ

Bu çalışmada, önden dümenlemeli bir aracın dümenleme mekanizmasının Arı Algoritması kullanılarak optimizasyonu gerçekleştirilmiştir. Burada dümenleme mekanizması olarak dört çubuk mekanizması kullanılmıştır. Dört çubuk mekanizması konum analizinden elde edilen dümenleme açısı ile Ackerman kuralı tarafından tanımlanan açılar mümkün olduğunca yakın yapan dümenleme mekanizmasının boyutları optimize edilmiştir. Optimizasyon için amaç fonksiyonu olarak Ackerman hatasının RMS değeri dikkate alınmıştır. Optimizasyon sonucu hatanın RMS değerinde 0.9742’den 0.1771’e kadar bir azalma meydana gelmiştir. Bu, araç dönerken dümenleme mekanizması davranışının ideale daha yakın olduğu anlamına gelmektedir. Arı Algoritması, verilen kısıtlara göre en uygun olan değerlere yakınsamıştır. Gerçek hayata uygun boyutsal kısıtlamalar dikkate alınarak istenen davranışa yakın davranış gösteren optimum geometri bulunmuştur. Bununla birlikte, kısıtlamalarda farklı değişiklikler yapmak suretiyle teorik olarak daha iyi sonuçlar elde edilebilir fakat bu durumda daha küçük bir hata bulunsu bile, ortaya çıkan mekanizma gerçekleşemeyebilir. Sonuç olarak; Ackerman kuralı ve dört çubuk mekanizması kinematik analizi ile elde edilen dümenleme açıları arasındaki hata Arı Algoritması kullanılarak en aza indirilmiştir. Optimizasyon sonucu elde edilen sonuçlar, Ackerman hatasını azaltmış ve dümenleme mekanizması boyutlarında iyileştirme yapılabileceğini göstermiştir.

8. KAYNAKLAR

- [1]. Ouezdou, F. B., and S. Regnier, 1997 General method for kinematic synthesis of manipulators with task specifications, *Robotica* 15.06: 653-661.
- [2]. Jazar, R.N., 2017, *Vehicle Dynamics: Theory and Application*. Springer, Melbourne, 3rd edition.
- [3]. Slesongsom, S., Bureerat, S., 2016, Multiobjective optimization of a steering linkage. *J Mech Sci Technol* 30, 3681–3691. <https://doi.org/10.1007/s12206-016-0730-4>

- [4]. Stoicescu, A. P., 2013, On the optimization of an Ackermann steering linkage. *UPB Scientific Bulletin, Series D: Mech Engi*, 75(4), 5-9.
- [5]. Sheu, Jinn-Biau, Sheng-Lun Hu, and Jyh-Jone Lee, 2008, Kinematic synthesis of a four-link mechanism with rolling contacts for motion and function generation. *Mathematical and Computer Modelling* 48.5: 805-817.
- [6]. Zhou, B., Li, D., & Yang, F, 2009, Optimization design of steering linkage in independent suspension based on genetic algorithm. In *2009 IEEE 10th International Conference on Computer-Aided Industrial Design & Conceptual Design* (pp. 45-48). IEEE.
- [7]. Peñuñuri, F., et al, 2011, Synthesis of mechanisms for single and hybrid tasks using differential evolution. *Mechanism and Machine Theory* 46.10: 1335-1349.
- [8]. Quick, J., King, J., King, R. N., Hamlington, P. E., & Dykes, K., 2020, Wake steering optimization under uncertainty. *Wind Energy Science*, 5(1), 413-426.
- [9]. Bulatović, Radovan R., and Stevan R. Đorđević, 2004, Optimal synthesis of a four-bar linkage by method of controlled deviation. *Theoretical and applied mechanics* 31.3-4: 265-280.
- [10]. Pradhan, D., Ganguly, K., Swain, B., & Roy, H., 2021, Optimal kinematic synthesis of 6 bar rack and pinion Ackerman steering linkage. *Proceedings of the Institution of Mechanical Engineers, Part D: Journal of Automobile Engineering*, 235(6), 1660-1669.
- [11]. Bulatović, Radovan R., and Stevan R. Đorđević, 2012, Optimal synthesis of a path generator six-bar linkage. *Journal of mechanical science and technology* 26.12: 4027-4040.
- [12]. Babu, T. N., Rajkumar, E., Joshi, T., Patil, V., & Mukaddam, W, 2021, Design and topology optimization of a rack and pinion steering system using structural and vibrational analysis. In *IOP Conference Series: Materials Science and Engineering* (Vol. 1123, No. 1, p. 012060). IOP Publishing.
- [13]. Chang, Kuang-Hua, and Sung-Hwan Joo, 2006, Design parameterization and tool integration for CAD-based mechanism optimization. *Advances in Engineering Software* 37.12: 779-796.
- [14]. Qin, Gang, et al, 2012, Analysis and Optimization of the Double-Axle Steering Mechanism with Dynamic Loads. *The Open Mechanical Engineering Journal* 5: 26-39.
- [15]. Zhou, Bing, Dongsheng Li, and Fan Yang, 2009, Optimization design of steering linkage in independent suspension based on genetic algorithm. *Computer-Aided Industrial Design & Conceptual Design. CAID & CD 2009. IEEE 10th International Conference on*. IEEE.
- [16]. Felzien, Mark L., and D. L. Cronin, 1985, Steering error optimization of the MacPherson strut automotive front suspension. *Mechanism and machine theory* 20.1: 17-26.
- [17]. Pham, D.T., Koç, E., Ghanbarzadeh, A., Otri, S., Rahim, S., Zaidi, M., 2006, The Bees Algorithm - A Novel Tool for Complex Optimisation Problems, *2nd International Virtual Conference on Intelligent Production Machines and Systems*, 454-461.
- [18]. A Onder, O Incebay, MA Sen, R Yapici, M Kalyoncu, 2021, Heuristic optimization of impeller sidewall gaps-based on the bees algorithm for a centrifugal blood pump by CFD, *The International Journal of Artificial Organs*, 03913988211023773
- [19]. Bilgic HH, Sen MA, Yapici A, Yavuz H, Kalyoncu M, 2021, Meta-heuristic tuning of the LQR weighting matrices using various objective functions on an experimental flexible arm under the effects of disturbance, *Arabian Journal for Science and Engineering*, 1-14
- [20]. Fahmy, A. A., Kalyoncu, M. and Castellani, M., 2012, Automatic design of control systems for robot manipulators using The Bees Algorithm, *Proceedings of the Institution of Mechanical Engineers, Part I, Journal of Systems and Control Engineering*, 226(4), 497-508.
- [21]. Pham, D.T., Koç, E., Kalyoncu, M., Tinkır, M., 2008, Hierarchical PID Controller Design for a Flexible Link Robot Manipulator Using the Bees Algorithm, *Proceedings of 6th International Symposium on Intelligent Manufacturing Systems*, Sakarya, Turkey, October 14-16, 757-765.

INTERNATIONAL AEGEAN CONFERENCES
ON INNOVATION TECHNOLOGIES & ENGINEERING-VI
December 20-22, 2022

- [22]. Erdemir, A., Kalyoncu, M., 2019, Optimization of a Multi-Axle Steered Heavy Vehicle Steering Mechanism by using the Bees Algorithm and the Hooke-Jeeves Algorithms Simultaneously, The 1st International Symposium On Automotive Science And Technology (ISASTECH 2019), Ankara/Turkey, September 5-6, 613-622.
- [23]. Bilgic HH, Sen MA, Kalyoncu M, 2016, Tuning of LQR controller for an experimental inverted pendulum system based on The Bees Algorithm, Journal of Vibroengineering 18 (6), 3684-3694
- [24]. Sen MA, Kalyoncu M, 2016, Optimal tuning of a LQR controller for an inverted pendulum using the bees algorithm, J Autom Control Eng 4 (5)
- [25]. Sen MA, Tinkir M, Kalyoncu M, 2018, Optimisation of a PID controller for a two-floor structure under earthquake excitation based on the bees algorithm, Journal of Low Frequency Noise, Vibration and Active Control 37 (1), 107-127
- [26]. Acar O, Kalyoncu M, Hassan A, 2019, Proposal of a Harmonic Bees Algorithm for Design Optimization of a Gripper Mechanism, IFToMM World Congress on Mechanism and Machine Science, 2829-2839
- [27]. Pham, D.T., Kalyoncu, M., 2009, Optimisation of a Fuzzy Logic Controller for a Flexible Single-Link Robot Arm Using the Bees Algorithm, 7th IEEE International Conference on Industrial Informatics (INDIN 2009), Cardiff, UK, June 24-26, 475-480.
- [28]. Bakırcıoğlu V, Şen MA, Kalyoncu M., 2022, Numerical investigation and experimental verification of the proposed robot leg virtual model, Proceedings of the Institution of Mechanical Engineers, Part C: Journal of Mechanical Engineering Science, doi:10.1177/09544062221076769.
- [29]. Incebay O, Onder A, Sen MA, Yapici R, Kalyoncu M, 2022, Fuzzy-Based Modeling and Speed Optimization of a Centrifugal Blood Pump using a Modified and Constrained Bees Algorithm, Computer Methods and Programs in Biomedicine, 106867, ISSN 0169-2607, <https://doi.org/10.1016/j.cmpb.2022.106867>.
- [30]. Unal, R.E., Guzel, M.H., Sen, M.A., Kose, F., Kalyoncu M., 2022, Investigation on the cost-effective optimal dimensions of a solar chimney with the Bees Algorithm, Int J Energy Environ Eng, <https://doi.org/10.1007/s40095-022-00528-y>.

**KIZILÖTESİ NESNE ALGILAMA UYGULAMALARINDA VERİ ÇOĞALTMA
YÖNTEMİNİN PERFORMANSA ETKİSİ**
EFFECT OF DATA AUGMENTATION METHOD ON PERFORMANCE IN INFRARED
OBJECT DETECTION APPLICATIONS

Kevser İrem DANACI

Sivas Bilim ve Teknoloji Üniversitesi, Elektrik Elektronik Mühendisliği Bölümü
Sivas University of Science And Technology, Department of Electrical Engineering

ORCID NO: 0000-0002-4654-5140

Erdem AKAGÜNDÜZ

Dr., Orta Doğu Teknik Üniversitesi, Enformatik Enstitüsü
Dr., Middle East Technical University, The Graduate School of Informatics

ORCID NO: 0000-0002-0792-7306

ÖZET

Nesne tespit çalışmalarının giderek yaygınlaşmasıyla beraber kızılötesi görüntüler ile gerçekleştirilen hedef tespiti uygulamaları önem kazanmaya başlamıştır. Bu çalışmada etkili bir kızılötesi nesne tespit modeli geliştirmek için seçilen YOLOv3 ve YOLOv4 derin öğrenme modelleri üzerinden eğitimler gerçekleştirilmiştir. CAMEL, LTIR ve AALARTDATA isimli üç adet halka açık veri setinden toplamda 1000 adet kızılötesi görüntü seçilmiştir. Bu görüntüler modellerin tespit performansını artırmak adına çeşitli veri çoğaltma yöntemleri kullanılarak çoğaltılmıştır. Ayna görüntüsü alma, kenar doldurma, belli açılarla döndürme, sağdan/soldan kırpma ve gama düzeltmesi gibi yöntemler uygulanarak 1000 adet kızılötesi görüntü verisi 48000 adet görüntü verisine çoğaltılmıştır. Bu veri çoğaltma yöntemleri sayesinde hem eğitim için gerekli olan verinin artırılması, hem de verinin karmaşıklığı artırılarak modellerin aynı nesnenin farklı pozisyonlarını görmeleri sağlanmıştır. Çalışma kapsamında elde edilen 1000 adet görüntüde yer alan insan ve araçlar, modellerin eğitimi için YOLO formatında etiketlenmiştir. Bu etiketleme formatı nesnelerin sınıfını, nesneyi içine alan sınırlayıcı kutunun orta noktasını ve bu kutunun ölçülerini barındırmaktadır. Geri kalan 47000 görüntü, Python programlama dili ile önceki 1000 görüntünün etiketleri kullanılarak otomatik olarak işaretlenmiştir. Sonuç olarak 48000 adet görüntüye sahip artırılmış ve 1000 adet görüntüye sahip artırılmamış olmak üzere iki adet veri seti elde edilmiştir. Bu veri setleri 2-1-1 oranında sırasıyla eğitim seti, doğrulama seti ve test seti olarak ayrılmıştır. YOLOv3 ve YOLOv4 modelleri, transfer öğrenme yöntemi ile önceden eğitilmiş ağırlıklar kullanılarak hem artırılmış hem de artırılmamış veri setleri ile 100 adım olacak şekilde eğitilmiştir. Test veri setleri incelendiğinde artırılmış veri setinin modellerdeki tespit performansını her nesne sınıfı için artırdığı gözlenmiştir. Tüm sınıflar

için ortalama performans (mAP), artırılmış veri seti sayesinde YOLOv3 ve YOLOv4 için sırasıyla %56,04 ve %80,80 daha yüksek olduğu hesaplanmıştır.

Anahtar Kelimeler: Derin öğrenme, kızılötesi görüntüler, nesne tespiti, veri çoğaltma.

ABSTRACT

With the increasing prevalence of object detection studies, target detection applications with infrared images have become important. In this study, selected YOLOv3 and YOLOv4 deep learning models were trained to develop an effective infrared object detection model. A total of 1000 infrared images were selected from three publicly available datasets CAMEL, LTIR and AALARTDATA. These images were reproduced using various data augmentation methods in order to increase the detection performance of the models. By applying methods such as mirror image, edge filling, rotation with certain angles, right/left cropping and gamma correction, 1000 infrared images were augmented into 48000 images. Thanks to these data augmentation methods, both the data required for training and the complexity of the data were increased, allowing the models to see different positions of the same object. Within the scope of the study, people and vehicles in the 1000 images obtained were labelled in YOLO format for the training of the models. This labelling format contains the class of objects, the midpoint of the bounding box containing the object, and the dimensions of this box. The remaining 47000 images are automatically labelled using the Python language and the previous labels of 1000 images. As a result, two datasets were obtained, augmented with 48000 images and non-augmented with 1000 images. These datasets are divided into training set, validation set and test set with a 2-1-1 ratio. YOLOv3 and YOLOv4 models have trained 1000 epochs with transfer learning method using pre-trained weights with both augmented and non-augmented datasets. When the test datasets were examined, it was observed that the augmented dataset increased the detection performance of the models for each object class. The mean average precision (mAP) for all classes was calculated to be 56.04% and 80.80% higher for YOLOv3 and YOLOv4, respectively, thanks to the increased dataset.

Keywords: Deep learning, infrared images, object detection, data augmentation.

**DÜZGÜN OLMAYAN AÇISAL SINIR TABAKASINI İÇEREN PARABOLİK
PROBLEMİN ASIMPTOTİĞİ**
ASYMPTOTICS OF A PARABOLIC PROBLEM WITH A NONSMOOTH ANGULAR
BOUNDARY LAYER FUNCTION

Asan OMURALİEV

Prof. Dr., Kırgızistan-Türkiye Manas Üniversitesi, Fen Fakültesi, Uygulamalı Matematik ve Enformatik Bölümü
*Prof. Dr., Kyrgyz Turkiye Manas University, Science Faculty, Department of Applied Mathematics and
Informatics*

Ella ABYLAEVA

Dr., Kırgızistan-Türkiye Manas Üniversitesi, Fen Fakültesi, Uygulamalı Matematik ve Enformatik Bölümü
Dr., Kyrgyz Turkiye Manas University, Science Faculty, Department of Applied Mathematics and Informatics

ORCID NO: 0000-0001-6999-5059

ÖZET

Bu çalışmada düzgün olmayan açısall sınır tabakası fonksiyonunu içeren parabolik problemin çözümünün asimptotiği kurulmuştur. Daha önce çalışılan çalışmaların aksine, üretilen algoritma basittir. Regularize edici fonksiyonun seçimi nedeniyle, çözümün asimptotiğinin yapısını ve oluşturma algoritmasını basitleştirmek mümkün olmuştur. Bizim tarafımızdan oluşturulan asimptotikler, yalnızca üç sınır katmanını içermektedir. Oysa, Butuzov'un çalışmalarında oluşturulan çözümün asimptotiği beş sınır katmanı bileşeni içerir.

Problemin konulması aşağıdaki gibidir:

$$\begin{aligned} L_\varepsilon u &\equiv \varepsilon \partial_t u - \varepsilon^3 a(x) \partial_x^2 u + \varepsilon b(x) \partial_x u + c(x, t) u(x, t, \varepsilon) = f(x, t), \\ &(x, t) \in \Omega \\ u|_{t=0} &= h(x), \quad u|_{x=0} = u|_{x=1} = 0 \end{aligned} \quad (1)$$

bu yerde $\varepsilon > 0$ - küçük parametre, $\Omega = (0 < x < 1) \times (0 < t \leq T)$.

$\varepsilon \rightarrow 0$ da tüm başlangıç sınır koşullarının kaybolduğuna dayanarak, çözümün asimptotiklerinde $t = 0, x = l - 1, l = 1, 2$ boyunca sınır katmanları ortaya çıkar. Düzenleyici değişkenler aşağıdaki gibi tanımlanarak girilmiştir:

$$\begin{aligned} \xi_l &= \frac{\varphi_l(x, t)}{\varepsilon^2}, \quad \eta = \frac{\psi(x, t)}{\varepsilon}, \quad \tau = \frac{t}{\varepsilon^2}, \\ \varphi_l(l - 1, t) &= 0, \quad \psi(x, 0) = 0 \end{aligned} \quad (2)$$

ve genişletilmiş fonksiyon $\tilde{u}(M, \varepsilon)$, $M = (x, t, \xi, \eta, \tau)$, $\xi = (\xi_1, \xi_2)$

$$\begin{aligned} \tilde{u}(M, \varepsilon)|_{\theta=v(x, t, \varepsilon)} &\equiv u(x, t, \varepsilon), \\ \theta &= (\xi, \eta, \tau), v(x, t, \varepsilon) = \left(\frac{\varphi(x, t)}{\varepsilon^2}, \frac{\varphi(x, t)}{\varepsilon}, \frac{t}{\varepsilon^2} \right), \varphi = (\varphi_1, \varphi_2) \end{aligned} \quad (3)$$

konulmuştur. Gerekli türevler bulunarak ve işlemler yapılarak (1) problemin yerine aşağıdaki problem konulmuştur.

$$\begin{aligned} \widetilde{L}_\varepsilon u^2 \equiv & \varepsilon \partial_t \tilde{u} + \frac{1}{\varepsilon} \sum_{l=1}^2 (\partial_t \varphi_l - b(x) \partial_x \varphi_l) \partial_{\xi_l} \tilde{u} + (\partial_t \psi - b(x) \partial_x \psi) \partial_\eta \tilde{u} - \frac{1}{\varepsilon} \partial_\tau \tilde{u} \\ & - \frac{1}{\varepsilon} \sum_{l=1}^2 (\partial_x \varphi_l)^2 a(x) \partial_{\xi_l}^2 \tilde{u} - \varepsilon (\partial_x \psi)^2 \partial_\eta^2 \tilde{u} - \varepsilon a(x) L_\xi \tilde{u} + c(x, t) \tilde{u} \\ & - \varepsilon^2 a(x) L_\eta \tilde{u} - \varepsilon^3 a(x) \partial_x^2 \tilde{u} - \varepsilon b(x) \partial_x \tilde{u} = f(x, t), \quad M \in Q, \\ & \tilde{u}|_{t=\tau=\eta=0} = h(x), \quad \tilde{u}|_{x=l-1, \xi_l=0} = 0, \\ & Q = \Omega \times (0, \infty)^3. \end{aligned}$$

Konulan problem artık regülerdir ve ileride tanımlanacak olan fonksiyonlar sınıfında çözülecektir.

Anahtar Kelimeler: parabolik problem, asimptotik, düzgün olmayan fonksiyon.

ABSTRACT

In this paper, we construct a regularized asymptotics for a solution of any order with a nonsmooth angular boundary layer function. In contrast to the previously studied works, our algorithm is simple. Due to the choice of the regularizing function, it was possible to simplify the structure of the asymptotics of the solution and the construction algorithm. The asymptotics constructed by us consists of only three boundary-layer functions. Whereas the asymptotics of the solution constructed, for example, in Butuzov's works contains five boundary-layer components.

Let us consider the problem:

$$\begin{aligned} L_\varepsilon u \equiv & \varepsilon \partial_t u - \varepsilon^3 a(x) \partial_x^2 u + \varepsilon b(x) \partial_x u + c(x, t) u(x, t, \varepsilon) = f(x, t), \\ & (x, t) \in \Omega \\ u|_{t=0} = & h(x), \quad u|_{x=0} = u|_{x=1} = 0 \end{aligned} \tag{1}$$

where $\varepsilon > 0$ is a small parameter, $\Omega = (0 < x < 1) \times (0 < t \leq T)$.

Based on the fact that at $\varepsilon \rightarrow 0$ all initial-boundary conditions are lost, boundary layers appear along $t = 0, x = l - 1, l = 1, 2$ in the asymptotics of the solution.

We introduce regularizing variables and extended function:

$$\begin{aligned} \xi_l = \frac{\varphi_l(x, t)}{\varepsilon^2}, \quad \eta = \frac{\psi(x, t)}{\varepsilon}, \quad \tau = \frac{t}{\varepsilon^2}, \\ \varphi_l(l - 1, t) = 0, \quad \psi(x, 0) = 0 \end{aligned} \tag{2}$$

$$\begin{aligned} \tilde{u}(M, \varepsilon), \quad M = (x, t, \xi, \eta, \tau), \quad \xi = (\xi_1, \xi_2) \\ \tilde{u}(M, \varepsilon)|_{\theta=v(x,t,\varepsilon)} \equiv u(x, t, \varepsilon), \\ \theta = (\xi, \eta, \tau), v(x, t, \varepsilon) = \left(\frac{\varphi(x, t)}{\varepsilon^2}, \frac{\varphi(x, t)}{\varepsilon}, \frac{t}{\varepsilon^2} \right), \varphi = (\varphi_1, \varphi_2) \end{aligned} \quad (3)$$

By finding the necessary derivatives and performing operations, problem (1) was replaced by the following problem:

$$\begin{aligned} \widetilde{L}_\varepsilon u^2 \equiv \varepsilon \partial_t \tilde{u} + \frac{1}{\varepsilon} \sum_{l=1}^2 (\partial_t \varphi_l - b(x) \partial_x \varphi_l) \partial_{\xi_l} \tilde{u} + (\partial_t \psi - b(x) \partial_x \psi) \partial_\eta \tilde{u} - \frac{1}{\varepsilon} \partial_\tau \tilde{u} \\ - \frac{1}{\varepsilon} \sum_{l=1}^2 (\partial_x \varphi_l)^2 a(x) \partial_{\xi_l}^2 \tilde{u} - \varepsilon (\partial_x \psi)^2 \partial_\eta^2 \tilde{u} - \varepsilon a(x) L_\xi \tilde{u} + c(x, t) \tilde{u} \\ - \varepsilon^2 a(x) L_\eta \tilde{u} - \varepsilon^3 a(x) \partial_x^2 \tilde{u} - \varepsilon b(x) \partial_x \tilde{u} = f(x, t), \quad M \in Q, \\ \tilde{u}|_{t=\tau=\eta=0} = h(x), \quad \tilde{u}|_{x=l-1, \xi_l=0} = 0, \\ Q = \Omega \times (0, \infty)^3. \end{aligned}$$

The problem presented is now regular and will be solved in the functions class, which will be defined later.

Keywords: Parabolic problem, asymptotic, nonsmooth function.

**YÜKSEK YOĞUNLUKLU VURGULU IŞIK TEKNOLOJİSİNİN KURU İNCİRDE
AFLATOKSİN DEGRADASYONU VE BAZI KALİTE PARAMETRELERİ
ÜZERİNE ETKİSİ**
EFFECT OF HIGH INTENSITY PULSED LIGHT TECHNOLOGY ON AFLATOXIN
DEGRADATION AND SOME QUALITY PARAMETERS IN DRIED FIGS

Hasan YARIM

Ege Üniversitesi, Fen Bilimleri Enstitüsü, Gıda Mühendisliği Anabilim Dalı
Ege University, Institute of Science, Department of Food Engineering
ORCID NO: 0000-0002-0184-6177

Taner BAYSAL

Prof. Dr., Ege Üniversitesi, Mühendislik Fakültesi, Gıda Mühendisliği Bölümü
Assoc. Prof., Ege University, Faculty of Engineering, Department of Food Engineering
ORCID NO: 0000-0003-1039-6275

ÖZET

İncir (*Ficus carica* L.), ılıman iklim koşullarında yetişen bir bitki olup Akdeniz kıyılarının karakteristik bir meyvesidir. Türkiye, incir üretimi ve ihracatında Dünya çapında birinci sırada yer almaktadır. Geleneksel olarak güneşte kurutulan incirler, işlem sırasında hızlı bir şekilde nem içeriği düşürülemediğinden ve hijyenik olmayan ortam koşullarından dolayı mikrobiyal gelişime açıktır. Bu durum, küf toksini olan mikotoksinlerin oluşmasına yol açmaktadır. Mikotoksinlerden biri olan aflatoksinin varlığı kuru incirde en sık karşılaşılan kalite problemlerinin başında gelmekte ve Türkiye'nin mevcut ihracat potansiyeline karşı büyük bir tehdit oluşturmaktadır. Bu çalışmada, aflatoksin standart çözeltisi ile kontamine edilmiş kuru incirler ısısal olmayan, yenilikçi bir teknoloji olan yüksek yoğunluklu vurgulu ışık (HIPL) teknolojisiyle işlenmiştir. HIPL işleminde farklı enerji dozlarının (3, 6, 9, 12 J/cm²) aflatoksin degradasyonu üzerine etkisi araştırılmıştır. 3, 6, 9, 12 J/cm² enerji dozlarında işlenen kuru incirlerde gerçekleşen toplam aflatoksin degradasyonunun sırasıyla %14.79±0.29, %21.68±6.69, %19.60±0.33, %23.33±1.06 olduğu tespit edilmiştir. Genel olarak, artan enerji dozuna bağlı olarak aflatoksin degradasyonu (%) da yükselmiştir (p<0.05). Ancak, 6 ve 9 J/cm² uygulamaları arasında anlamlı bir fark yoktur (p>0.05). Çalışma kapsamında ayrıca HIPL teknolojisinin kuru incirdeki kalite özellikleri üzerine etkisi araştırılmıştır. HIPL ile işlem görmüş örneklerin nem içeriği, su aktivitesi, suda çözünür kuru madde (SÇKM) içeriği, pH, renk özellikleri, toplam fenolik madde içeriği gibi kalite özelliklerindeki değişimler incelenmiştir. Toplam renk farkı, en yüksek 6 J/cm² enerji dozunda, en yüksek toplam fenolik madde içeriği 138.80±8.55 mg GAE/100 g KM ile 12 J/cm² enerji dozunda tespit edilmiştir. Bu çalışma, "Yenilikçi ışık teknolojisi uygulamalarının

kuru incirde aflatoksin degradasyonuna etkisi” konusunda hazırlanan Yüksek Lisans tezinin bir bölümünü oluşturmaktadır.

Anahtar kelimeler: Kuru incir, Aflatoksin, HIPL

ABSTRACT

Fig (*Ficus carica* L.) is a plant that grows in mild climate conditions and is a characteristic fruit of the Mediterranean coast. Turkey ranks first in the world in fig production and export. Traditionally sun-dried figs are susceptible to microbial growth due to unhygienic environmental conditions and not being able to quickly reduce their moisture content during sun drying. This leads to the formation of mycotoxins, which are mold toxins. The presence of aflatoxin, one of mycotoxins, is one of the most common quality problems in dried figs and poses a great threat to the current export potential of Turkey. In this study, dried figs contaminated with aflatoxin standard solution were processed with high intensity pulsed light (HIPL) technology, which is an innovative non-thermal technology. The effect of different energy doses (3, 6, 9, 12 J/cm²) on aflatoxin degradation in the HIPL process was investigated. Total aflatoxin degradation in dried figs processed at energy doses of 3, 6, 9, 12 J/cm² was found to be 14.79±0.29%, 21.68±6.69%, 19.60±0.33%, 23.33±1.06%, respectively. In general, the aflatoxin degradation in percentage terms increased with increasing energy dose (p<0.05). However, the difference between 6 and 9 J/cm² applications was not significant (p>0.05). The effect of HIPL technology on the quality characteristics of dried figs was also investigated. The changes in quality properties such as moisture content, water activity, water-soluble dry matter (Brix) (%) content, pH, color properties, total phenolic matter content of the HIPL treated samples were investigated. The highest total color difference was obtained at 6 J/cm² energy dose, and the highest total phenolic content was found to be with 138.80±8.55 mg GAE/100 g KM at 12 J/cm² energy dose application. This study constitutes a part of the MSc thesis on "The effect of innovative light technology applications on aflatoxin degradation in dried figs".

Keywords: Dried figs, aflatoxin, HIPL

**DOKU MÜHENDİSLİĞİ UYGULAMALARI İÇİN YENİ BİR HİDROJEL SİSTEMİN
ÜRETİMİ: CHIA TOHUMU MÜSİLAJININ MİKRODALGA DESTEKLİ
METAKRİLASYONU**

DEVELOPMENT OF A NOVEL HYDROGEL SYSTEM FOR TISSUE ENGINEERING
APPLICATIONS: MICROWAVE ASSISTED METHACRYLATION OF CHIA SEED
MUCILAGE

Saime Nur KARASU

Erciyes Üniversitesi, Mühendislik Fakültesi, Biyomedikal Mühendisliği Anabilim Dalı
Erciyes University, Faculty of Engineering, Department of Biomedical Engineering

ORCID NO: 0000-0003-3336-0355

Yavuz Nuri ERTAŞ

Dr, Erciyes Üniversitesi, Mühendislik Fakültesi, Biyomedikal Mühendisliği Anabilim Dalı
Dr, Erciyes University, Faculty of Engineering, Department of Biomedical Engineering

ORCID NO: 0000-0002-6791-7484

Tuğrul Tolga DEMİRTAŞ

Dr, Erciyes Üniversitesi, Eczacılık Fakültesi, Temel Bilimler Anabilim Dalı
Dr, Erciyes University, Faculty of Pharmacy, Department of Basic Pharmaceutical Sciences

ORCID NO: 0000-0002-7806-6195

ÖZET

Günümüzde doku mühendisliği çalışmalarında dokuların rejenerasyonunu sağlamak, desteklemek ve fonksiyonlarını restore etmek için doğal ve sentetik biyomalzemeler kullanılmaktadır. 3 boyutlu (3B) biyobaskı sistemlerinde hücre, büyüme faktörü gibi biyoaktif bileşenler ile karıştırılması sonucu biyomürekkep olarak da kullanılabilen biyomalzemelerin kemik, kırık, deri vb. doku rejenerasyonunu sağlaması için hücrelerin doğal ortamlarında içinde bulunduğu ekstrasellüler matriks (ECM) yapısını ve fonksiyonlarını taklit etmesi kritik öneme sahiptir. ECM yapısı ile benzerlik gösteren biyomalzemeler, hücre yapışma ve çoğalmasında destekler, ECM oluşumunu artırarak doku rejenerasyonunu sağlar. Aynı zamanda biyomalzemelerin yeterli mekanik dayanıma sahip olması, bu sayede yeni gelişen dokuları desteklemesi gerekmektedir. Ayrıca biyomalzemeler, 3B biyoyazıcı sistemleri için basılabilir özelliğe sahip olmalıdır. Ancak bu özelliklerin yeterli seviyede sağlanamamasından dolayı doku mühendisliğinde kullanılan biyomalzemelerin sayısı sınırlıdır ve doku rejenerasyonunu sağlayacak yeni biyomalzemelerin geliştirilmesine ihtiyaç duyulmaktadır. Bu çalışmanın amacı, 3B biyoyazıcı sistemlerde kullanılan biyomalzeme (bio-ink) açığını gidermek üzere chia tohumu müsülajının mikrodalga destekli metakrilasyonu sağlanarak yeni bir bio-ink olan chiaMA sentezi gerçekleştirmektir. Chia tohumları su ile temas ettiği zaman, ağırlığının 27

katına varabilen müsilaaj salınıımı gerçekteştirir. Lifli yapıda bulunan amino asit, yağ asitleri ve polisakkarit açısından zengin içeriğe sahip olan chia tohumu müsilaajı ECM yapısı ile birçok benzer özelliğe sahiptir. Çalışmada chia müsilaajına ait karboksil grupları ve hidroksil grupları, EDC-NHS kimyası kullanılması ve farklı kuvvetlerde mikrodalga enerjisi uygulanması sonucu 2-aminoetil metakrilat hidroklorürde (AEMA) bulunan amin gruplarına bağlanarak metakrilatlanması sağlanmıştır. Ardından lityum fenil-2,4,6-trimetilbenzoilfosfinat (LAP) kullanılarak foto-çapraz bağlanan chiaMA hidrojellerinin SEM, FTIR, HNMR, XRD ve TGA analizleri ile yapısal ve morfolojik karakterizasyonu sağlanmıştır. %2.5 ve %5 konsantrasyonlarında hazırlanan chiaMA hidrojellerinin reoloji ve mekanik dayanım analizleri gerçekleştirilmiştir. Ek olarak, doku mühendisliğinde kullanılan 3 boyutlu biyobaskı sistemleri için viskozite analizi elde edilmiş ve 3B biyobaskı cihazında optimizasyonu sağlanmıştır.

Anahtar kelimeler: Biyobasım, Biyomalzeme, Biyomürekkap, Chia Tohumu Müsilajı, Doku Mühendisliği

ABSTRACT

In tissue engineering, synthetic and natural biomaterials have been used to repair/regenerate human tissues. In designing biomaterials which is also can be used as bioink by mixing with cells and bioactive compounds such as growth factors in 3D bioprinting systems, mimicking structure and functions of extracellular matrix (ECM) is critical for tissue regeneration. Biomaterials that have similar properties of ECM can promote cell attachment and proliferation, therefore regenerate the tissue by increasing ECM growth. Also, biomaterials should have sufficient mechanical strength, thus they can support newly developing tissues. In addition, they should be printable for 3D bioprinting systems. However, biomaterials in tissue engineering are limited due to lack of necessary properties. Therefore, new biomaterials which will provide better tissue regeneration are required. This study aims to synthesize chiaMA hydrogel as a novel biomaterial (bio-ink) to overcome some of the limitations of tissue engineering. Once chia seeds get contact with water, they start to generate mucilage up to 27 times of seeds. Fiber structured chia seed mucilage has similar properties to ECM with rich amino acid, fatty acid and polysaccharide components. Briefly, chia seed mucilage was methacrylated using EDC-NHS chemistry via microwave technique by applying different microwave powers to the carboxyl and hydroxyl groups of chia seed mucilage and amine groups of 2-aminoethyl methacrylate hydrochloride (AEMA). The chiaMA hydrogel was obtained by photocrosslinking by using lithium phenyl-2,4,6-trimethylbenzoylphosphinate (LAP). ChiaMA hydrogel was structurally and morphologically characterized by SEM, FTIR, HNMR, XRD and TGA analyses. Moreover, rheological and mechanical analyses with 2.5% and 5% concentrations of chiaMA were performed. Viscosity analysis was also carried out for

the developed biomaterial and further optimization of chiaMA as a bioink material in tissue engineering was validated.

Keywords: Bioink, Biomaterial, Bioprinting, Chia Seed Mucilage, Tissue Engineering

**INVESTIGATION OF PHOTOCATALYTIC COLOR REMOVAL OF REACTIVE
BLUE 203 USING H₂O₂/UV PROCESS**

REAKTİF BLUE 203 BOYARMADDESİNİN H₂O₂ / UV PROSESİ İLE
FOTOKATALİTİK RENK GİDERİMİNİN İNCELENMESİ

Semiha EREN

Dr., Bursa Uludağ Üniversitesi, Mühendislik Fakültesi, Tekstil Mühendisliği Anabilim Dalı
Dr., Bursa Uludağ University, Engineering Faculty, Department of Textile Engineering

ORCID NO: 0000-0002-2326-686X

Aliye AKARSU ÖZENÇ

Doktora Öğrencisi, Bursa Uludağ Üniversitesi, Mühendislik Fakültesi, Tekstil Mühendisliği Anabilim Dalı
PhD Student, Bursa Uludağ University, Engineering Faculty, Department of Textile Engineering

ORCID NO: 0000-0001-5603-5913

Merve ÖZTÜRK

Doktora Öğrencisi, Bursa Uludağ Üniversitesi, Mühendislik Fakültesi, Tekstil Mühendisliği Anabilim Dalı
PhD Student, Bursa Uludağ University, Engineering Faculty, Department of Textile Engineering

ORCID NO: 0000-0001-8356-2321

ABSTRACT

Sustainability, energy and water saving in the textile industry are among the most researched topics in recent years. Textile dyehouses are the areas where water and energy are used the most. Textile waste waters harm the nature ecologically as well as aesthetic concerns. The treatment and recovery of textile wastewater is very important for the environment and human health. The stability of the dyestuffs under acidic and basic conditions, their resistance to aerobic degradation, heat and light make it difficult to be treated with conventional treatment methods. Physical, chemical and biological methods are used in the treatment of wastewater containing dyestuffs. There are various advanced oxidation processes for wastewater treatment based on the principle of catalytic production of hydroxyl radicals. The advantage of advanced oxidation processes is greater than conventional wastewater treatment methods. The most important advantage of the advanced oxidation method is that it is suitable for the easy degradation of a wide variety of toxic organic compounds. The high oxidation potential of hydroxyl radicals, which are known to react with some pollutants in water, play an important role in organic degradation. When hydrogen peroxide interacts with UV, it forms hydroxyl radicals (OH•), which is a very active species. In this experimental study, photocatalytic reaction of Reactive Blue 203 dyestuff using H₂O₂ (hydrogen peroxide) / UV (Ultraviolet), which is one of the advanced oxidation processes used in industrial wastewater

treatment. discoloration has been investigated. The pH, temperature, conductivity and COD values of the samples were examined and the results were interpreted.

Keywords: UV, color removal, photocatalytic effect.

ÖZET

Tekstil endüstrisinde sürdürülebilirlik, enerji ve su tasarrufu son yılların en çok araştırılan konu başlıkları arasında yer almaktadır. Tekstil boyahaneleri suyun ve enerjinin en çok kullanıldığı alanlardır. Tekstil atık suları estetik kaygılarının yanısıra ekolojik olarak doğaya zarar vermektedir. Tekstil atık sularının arıtılması ve geri kazanılması çevre ve insan sağlığı için çok önemlidir. Boyarmaddelerin asidik ve bazik şartlar altında kararlı olmaları, aerobik parçalanmaya, ısı ve ışığa karşı dayanıklılık göstermeleri konvansiyonel arıtma yöntemleriyle arıtılmasını zorlaştırmaktadır Boyarmadde içeren atıksuların arıtılmasında fiziksel, kimyasal ve biyolojik yöntemler kullanılmaktadır. Hidroksil radikallerinin katalitik üretimi prensibine bağlı atık su arıtmaları için çeşitli ileri oksidasyon prosesleri vardır. İleri oksidasyon proseslerinin avantajı, klasik atık su arıtma yöntemlerine göre daha fazladır. İleri oksidasyon yönteminin en önemli avantajı, çok çeşitli toksik organik bileşiklerin kolaylıkla degradasyonuna uygun olmasıdır. Suda bulunan bazı kirleticiler ile reaksiyona girdiği bilinen hidroksil radikallerinin yüksek oksidasyon potansiyeline sahip olmaları organik bozunmada önemli rol oynamaktadır. Hidrojen peroksit UV ile etkileşim sağladığında oldukça aktif bir tür olan hidroksil radikalleri ($\text{OH}\cdot$) oluşturmaktadır. Bu deneysel çalışmada endüstriyel atık su arıtımında kullanılan ileri oksidasyon proseslerinden biri olan H_2O_2 (hidrojen peroksit) / UV (Ultraviyole) kullanılarak Reaktif Blue 203 boyarmaddesinin fotokatalitik olarak renk giderilmesi araştırılmıştır. Numunelerin pH, sıcaklık, iletkenlik ve KO_2 değerleri incelenmiş sonuçlar yorumlanmıştır.

Anahtar Kelimeler: UV, renk giderimi, fotokatalitik etki.

1. INTRODUCTION

The textile industry is one of the most water-consuming sectors. Approximately 100- 150 liters of clean water is used for finishing only 1 kilogram of textile surface (Yiğit et al., 2021). The waste water resulting from the finishing processes contains various chemicals and dyestuffs. Since the dyestuffs in textile wastewater are in complex and high molecular weight structures, their biodegradability is generally very low (Kim et al., 2004; Gao et al., 2007; Verma et al., 2012). If the waste waters of the industry are not treated and the dyestuffs are left untreated, they can be used as lakes, rivers, etc. pollutes water resources and indirectly harms the environment and human health. The World Health Organization (2002) has

associated the pollution of air, soil and water with industrial wastes with a heavy burden of disease.

There are physical, chemical and biological methods for the treatment and cleaning of wastewater. One of the most commonly used methods in the purification of dyestuffs is the chemical treatment method. This method can be divided into advanced oxidation process (AOP) and chemical oxidation. Sufficient amount of hydroxyl ($\bullet\text{OH}$) radicals may be formed in advanced oxidation processes (Holkar et al., 2016). Since hydroxyl radicals have very high oxidation potential, they play an important role in organic degradation (Eren, 2018). Due to the limited lifetime of hydroxyl radicals, they are produced by combinations of oxidizing agents (such as Hydrogen peroxide (H_2O_2), Ozone (O_3)) or with the support of various methods (such as Ultraviolet, ultrasound) (Deng and Zhao, 2015). These methods are common because they do not produce sludge and the reaction takes place in a short time. The reaction of hydroxyl radicals under UV light is given below (Alebouyeh et al., 2003; Costa et al., 2004; Bahrama et al., 2017; Eren, 2018).



In this study, color removal of reactive blue 203 dyestuff was observed with the addition of H_2O_2 under UV light. During the studies, the pH, conductivity and temperature values of the dyestuff were observed.

2. MATERIALS AND METHODS

Reactive Blue 203 dyestuff, whose molecular structure is given below, was chosen for this experimental study. 40 g/L H_2O_2 (Merck) was used for the bleaching process. The stock dyestuff solution was chosen as 1.5 g/L. Catalase enzyme (Rudolf Duraner Rucolex HTK) was used to finish the H_2O_2 activity remaining in the solution after UV treatments. COD measurement kits (Merck) were used to make COD measurements.

After the stock solution was prepared, H_2O_2 was added and the solution was placed in the UV cabinet. The UV cabin contains 18 UV lamps with a wavelength of 470 Watt and 254 nm in total. Samples were taken from the solution every 5 minutes, and the pH, conductivity and temperature values of the samples were checked.

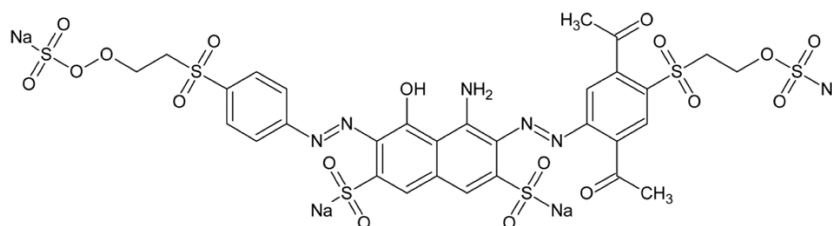


Figure 1 Molecular Structure of Reactive Blue 203 Dyestuff

Applied Tests

Temperature and conductivity measurements; conductivity was measured in the WTW Cond 3210 measuring device, and pH measurements were made in the WTW PH 3210 model pH measuring device. Color measurements were made on the Spectroquant Pharo 300 model spectrophotometer device, and COD measurements were made with Standard Methods.

3. RESEARCH AND FINDINGS

In the color measurements, the characteristic visible wavelength wavelength of the dyestuff was determined as λ_{max} 603 nm. The color removal of the samples taken every 5 minutes according to this wavelength was calculated according to this absorbance value. In Figure 2, the absorbance values obtained by the photocatalytic method are given. When Figure 2 is examined, it is seen that the photocatalytic method is successful in color removal. The increase of hydroxyl radicals with the addition of H₂O₂ resulted in color removal.

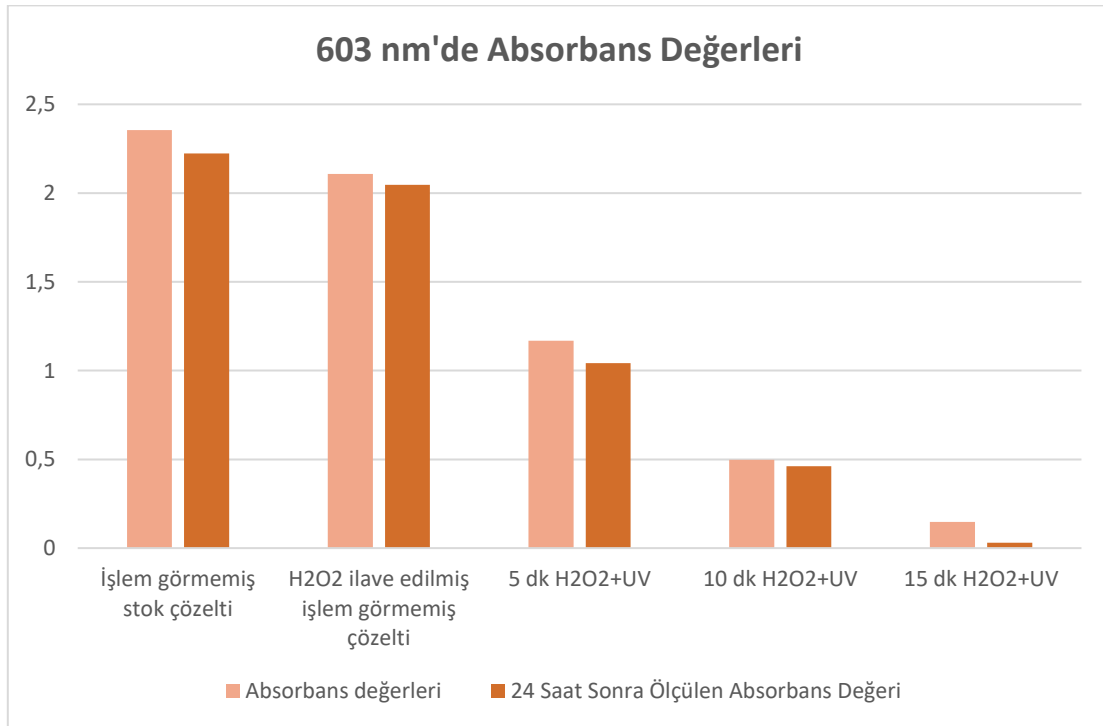


Figure 2. Absorbance values of Reactive Blue 203 dyestuff under UV light

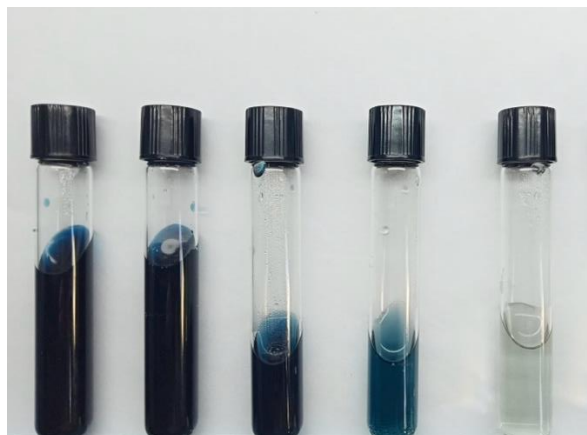


Figure 3. Decolorization of Reactive Blue 203 dyestuff (From left to right; Stock solution, untreated solution with added H₂O₂, 5 min H₂O₂+UV, 10 min H₂O₂+UV, 15 min H₂O₂+UV)

As a result of the photocatalytic process, the pH, temperature and conductivity values of each sample were recorded. Due to the products formed as a result of decomposition in dyestuff treatment, it has caused variability in pH and conductivity values. The increase in temperature values occurred with the heating of the UV cabinet as a result of the heating of the lamps.

Table 1. Temperature, pH, conductivity values of the samples

Sample	Temperature (°C)	pH	Conductivity(μS/cm)
Stock solution	13,6	10,6	179,3
Untreated solution	13,6	9,9	182,5
5 min H ₂ O ₂ +UV	14,5	9,6	197
10 min H ₂ O ₂ +UV	15,2	7,7	248
15 min H ₂ O ₂ +UV	16,1	6,8	334

The COD removal result is given in Table 2. While color removal was 99% successful in the study, COD removal was 3.5%.

Sample	KO _i _{first}	KO _i _{End}
Reaktif Blue 203	406,402	392,388

4. RESULTS

In this experimental study, photocatalytic decolorization of Reactive Blue 203 dyestuff was investigated. While color removal with UV/ H₂O₂ process was 99% successful, COD removal color removal was not that successful. With the addition of 40 g/L H₂O₂, the color removal process was successful after 15 minutes.

REFERENCES

- Alebouyeh, A., Alebouyeh, H. and Moussa, Y. (2003) Critical effect of hydrogen peroxide in photochemical oxidative decolourisation of dyes: Acid Orange 8, Acid Blue 74 and Methyl Orange, *Dyes and Pigments*, 57, 67-75. doi:10.1016/S0143-7208(03)00010-X
- Bahrama, M., Salamia, S., Moghtadera, M., Moghadama, P.N., Fareghia, A.R., Rasoulb, M. and Salimpourb S. (2017) Photocatalytic Degradation of Anionic Azo Dyes Acid Orange 7 and Acid Red 88 in Aqueous Solutions Using TiO₂-containing Hydrogel, *Analytical and Bioanalytical Chemistry Research*, 4(1), 53-63. doi:10.22036/abcr.2017.41098
- Costa, F.A., Reis, E.M., D, Azevedo, J.C. and Nozaki, J. (2004) Bleaching and photodegradation of textile dyes by H₂O₂ and solar or ultraviolet radiation, *Solar Energy*, 77, 29-35.
- Deng, Y., & Zhao, R. (2015). Advanced oxidation processes (AOPs) in wastewater treatment. *Current Pollution Reports*, 1(3), 167-176.
- Eren, S., (2018). CI Reaktif Black 5 Boyarmaddesinin Fotokatalitik Renk Giderimi. *Üniversitesi Mühendislik Fakültesi Dergisi* 23.1: 139-152.
- Gao, B. Y., Yue, Q. Y., Wang, Y., & Zhou, W. Z. (2007). Color removal from dye-containing wastewater by magnesium chloride. *Journal of Environmental Management*, 82(2), 167-172.
- Holkar, C. R., Jadhav, A. J., Pinjari, D. V., Mahamuni, N. M., & Pandit, A. B. (2016). A critical review on textile wastewater treatments: possible approaches. *Journal of environmental management*, 182, 351-366.
- Kim, T. H., Park, C., Yang, J., & Kim, S. (2004). Comparison of disperse and reactive dye removals by chemical coagulation and Fenton oxidation. *Journal of hazardous materials*, 112(1-2), 95-103.
- Pollutants, W. W. (2002). Biological Agents, Dissolved Chemicals, Nondissolved Chemicals, Sediments, Heat. *WHO CEHA*.
- Verma, A. K., Dash, R. R., & Bhunia, P. (2012). A review on chemical coagulation/flocculation technologies for removal of colour from textile wastewaters. *Journal of environmental management*, 93(1), 154-168.
- Yiğit, İ., Eren, S., Özcan, H., Avinc, O., Eren, H. A. (2021) An investigation of process parameters on colour during the dyeing of polyester in supercritical carbon dioxide media, *Coloration Technology*, 137(6), 625-644. doi: <https://doi.org/10.1111/cote.12553>

**INVESTIGATION OF DYEING POLYESTER WITH DISPERSE DYE IN THE
PRESENCE COMB-LIKE POLYCARBOXYLATES DISPERSANT**

Mohammad Amin Sarli

Ege University, Faculty of Engineering, Department of Textile Engineering

Arif Taner ÖZGÜNEY

Prof. Dr., Ege University, Faculty of Engineering, Department of Textile Engineering

Eylen Sema DALBAŞI

Doç. Dr., Ege University, Faculty of Engineering, Department of Textile Engineering

ABSTRACT

A series of comb-like polycarboxylates (PC) were synthesized and their performance was evaluated as dye dispersant. The PCs were prepared in different molecular weights and side-chain densities by copolymerization of methacrylic acid and an ethoxylated macromonomer. The dye dissolution, dispersive ability, and particle size of CI Disperse Blue 79 were studied in the presence of PCs. Polymers with lower side-chain density resulted in a higher dye dissolution, which could be due to more effective adsorption of dispersant on the dye surface. Moreover, the dyeing performance of the prepared dye dispersions on polyester was investigated. Spectrophotometric results of dyed fabrics demonstrated that there was an optimum side chain density and molecular weight for the PCs to improve both dye solubility and dispersive ability. This was also confirmed by particle size analysis and turbidity measurements. Overall, PCs exhibited good dispersing performance and could overcome the commercial one.

Keywords: Polycarboxylate, Dispersant, Dyeing, Disperse dye.

INTRODUCTION

Dispersing agents are chemicals that migrate to the solid-liquid interface and cause the stability of solid particles in liquid media by preventing agglomeration [1]. Alteration in surface free energy of the solid particle is the main mechanism of dispersion for small dispersants whereas high molecular weight dispersants have anchor groups that afford strong adsorption of polymer onto the particle [2]. Water-soluble comb-like PCs contain polyethylene or polypropylene oxide side chains which are attached to the acrylic-based backbone. They can adsorb to a solid particle by electrostatic attraction, hydrogen bonding, or van der Waals interactions. Side-chains are responsible for the steric hindrance effect. Chemical moiety and length of side-chains, side-chain density, and molecular weight of PCs are important variables in the design of PC dispersants [3].

EXPERIMENTAL

Chemicals

Methacrylic acid and nonylphenol polyethylene glycol (n=10), CI Disperse Blue 79, and sodium polynaphthalene sulfonic formaldehyde (PNS) were of industrial grade and purchased from the Lucite International, Kimiagaran Emrooz, Enacol, and Dystar. Cyclohexane and ammonium persulfate were provided by Petrochem and BASF, respectively. All other chemicals were of analytical grade and purchased from Merck.

Synthesis of dispersants

The synthesis of PCs consisted of two steps that have been reported in our previous work [4]. The first step was to synthesize the macromonomer which was going to be used as side-chain, and the second one was the solution copolymerization process. Briefly, the macromonomer was synthesized by esterification of methacrylic acid with nonylphenol polyethylene glycol. Then, the macromonomer was copolymerized with different concentrations of monomers and initiator to obtain polymers with different side-chain density and molecular weight. The chemical structure of synthesized polycarboxylates is presented in Figure 1.

Solubility measurement of dye

Dye suspensions were prepared at different concentrations of PCs. They were shaken in an incubator shaker at 25, 45, and 65 °C. Sampling was performed over time while dye dispersions were being shaken. Then, they were filtered and dissolved in acetone and the concentration of dissolved dye was calculated thanks to UV-Visible spectroscopy. Finally, the kinetic parameters of dye dissolution in the presence of different PCs were calculated.

Dyeing of polyester fabrics

Dye dispersions were prepared by the solution method using different dispersant concentrations as reported by [5]. The dyeing of polyester fabrics was carried out with a high-

temperature method. After dyeing, reduction clearing was performed on dyed samples and their color characteristics were evaluated by colorimetric analysis.

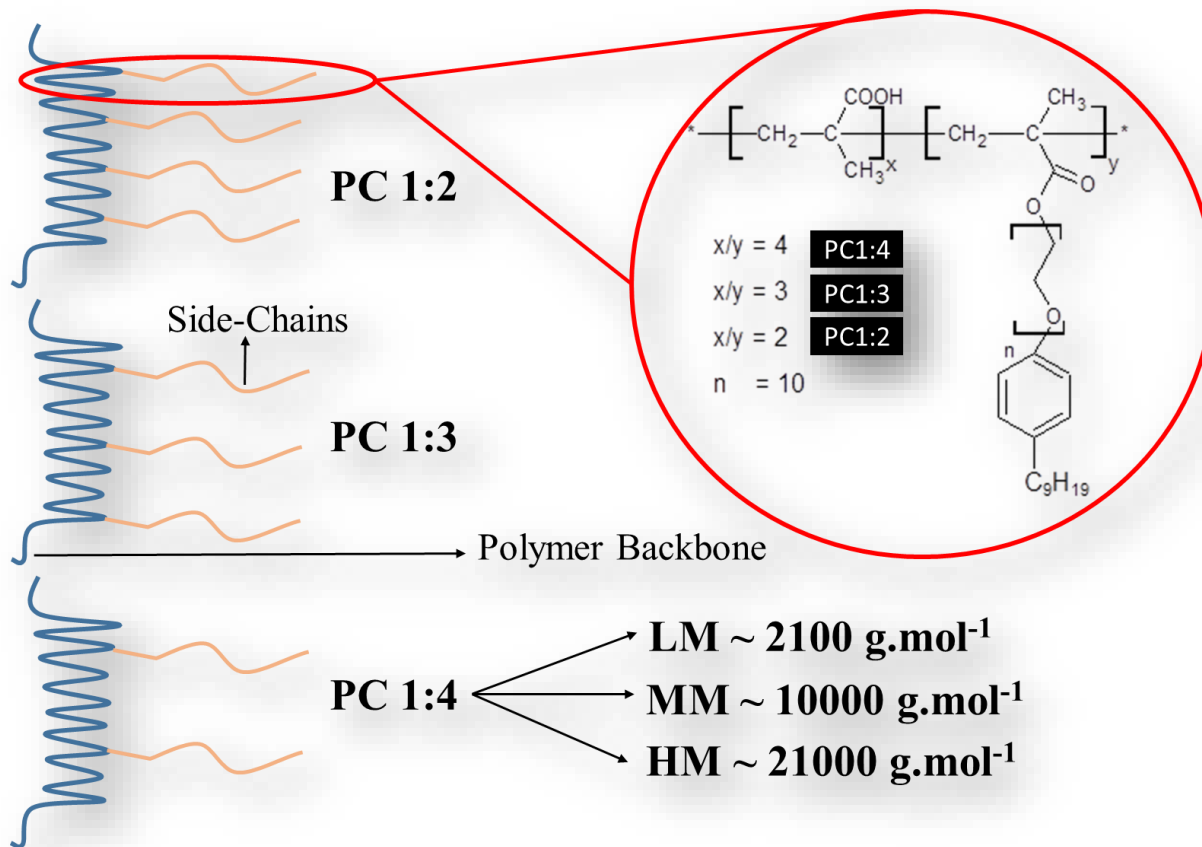


Fig. 1. The schematic representation of synthesized PCs and their general chemical structure.

Dye dispersion stability

Dye dispersions were prepared by milling of the used disperse dye in the presence of the best concentration of dispersants. Milling was carried out for 20 hours in a ball mill. Then, dye dispersions were diluted for further analysis including turbidimetry and particle size analysis.

Investigation of heat stability of dye dispersions

In this section, different dye dispersions were prepared and charged to the capsules of the dyeing machine. The dyeing process condition (temperature and time) were applied to the samples. Notably, no polyester fabrics were inserted inside the capsules. Eventually, sampling was done for turbidimetry, particle size analysis, and dye solubility measurements.

RESULTS AND DISCUSSION

The effect of PCs on dye dissolution

Samples were prepared by adding the disperse dye powder to water in the absence and presence of PCs. They were shaken and heated at different temperatures. The effect of PC type (Molecular weight and side-chain density) and PC concentration was investigated on dye dissolution at 25, 45, and 65°C. The concentration of dissolved dye in water was measured over time. Results revealed that there is almost no solubility of dye at 25 °C and it slightly increased as the temperature elevated to 45 and 65 °C. However, the dissolution of dyes increased with the addition of PCs. The maximum dissolution of disperse dye was less than 0.9 mg/l at 65°C while in the presence of PC1:4M, the dissolution was raised to 2 mg/l. Moreover, increasing the dispersant concentration improved the solubility of dye up to 6 mg/l. Besides, the PC with the medium molecular weight (PC1:4M) could enhance the dissolution the most.

The effect of PCs on polyester dyeing

In order to find the optimum PC concentration, polyester fabrics were dyed using different concentrations of dispersants. Results of reflectance spectrophotometry for dyed fabrics revealed that the higher the PC concentration was, the higher K/S value was obtained. Figure 2 is depicted to illustrate a better comparison between dispersants. As can be seen, higher K/S values are achieved by PC1:3 that demonstrated that there is an optimum side-chain density for polycarboxylates as a dyeing additive. Unlike dye dissolution results, PC1:4M was not the best dispersant for the dyeing of polyester. This might be due to elevated hydrophilicity of dyes by PC1:4M. As polyester fibers have hydrophobic nature, the high solubility of dyes would have a negative impact on dyeing of polyester using disperse dyes. The dyed polyester fabrics along with measured K/S is reported in Figure 2.

The effect of PCs on particle size and dye dispersion stability

Dispersants with good dispersive ability prevent dye agglomeration and lead to the production of dispersions with small particle sizes. The particle size of dye in the presence of different types of PCs and PNS were measured which were 3.6, 2.9, 3.3, 4.1, 3.1, and 3.1 µm for PNS, PC1:2, PC1:3, and PC1:4L, PC1:4M and PC1:4H, respectively. According to the results, all dispersants have the ability to prevent dye agglomeration but not all dispersants show similar efficiency in reducing particle size. A suitable dispersant should also stabilize particles for longer times. To this aim, the turbidity values of dyes were measured over time. Finding demonstrated that PDC1:3 had the highest initial and final turbidity.

Thermal treatment on the stability of dye dispersions prepared with PCs

In order to discover the advantages of PCs over commercial PNS, prepared dye dispersions with different dispersants were heated to 130 °C in a dyeing machine. The results of analyzing

dye dispersions showed that average particle size was increased for PNS and there is also a reduction of turbidity values for it, whereas dispersions prepared with PCs possessed higher turbidity values and lower particle size. Thus, the results indicated that the performance of PNS decreases at high temperatures. The poor heat stability of PNS at 130 °C has also been reported by investigating the sediment thickness of dye baths [6].

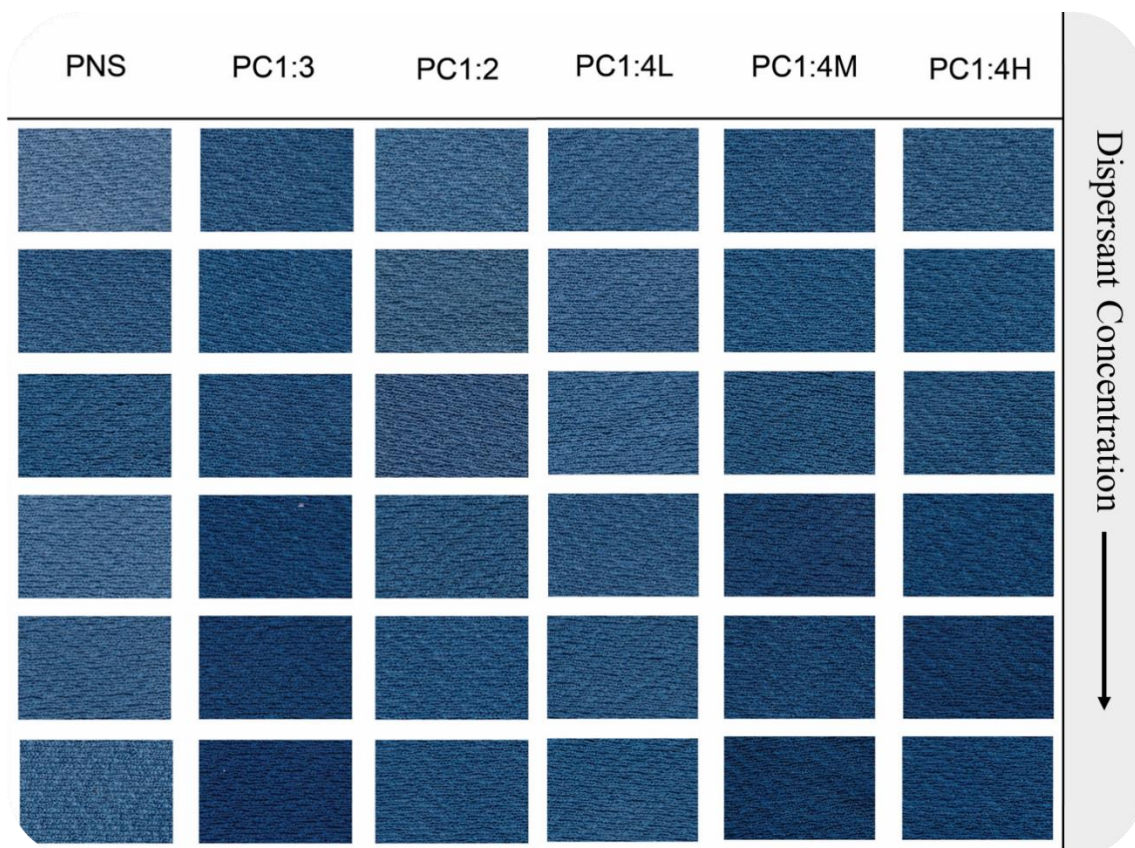


Fig. 2. Effect of dispersant type on color strength of dyed polyester

CONCLUSION

This study showed that comb-like polycarboxylate structures could be used as dispersing agents for dyeing with disperse dyes. However, the chemical structure of polycarboxylate should be optimized to give the best dispersing efficacy. In this regard, various PCs were synthesized with different molecular weight and side-chain density, and their performance was evaluated in improving disperse dye solubility, dispersive ability, and dyeing of polyester fabrics. Results indicated there was an optimum side-chain density and molecular weight for polycarboxylates. Moreover, an engineered PC could overcome conventional dispersing agents based on naphthalene sulfonate.

Acknowledgement

This study is supported by Ege University Scientific Research Projects Coordination Unit (in Turkey), Project Number: FHD-2020-22211

REFERENCES

- [1] D. M. Nunn, *The dyeing of synthetic-polymer and acetate fibres*. Dyers Company Publications Trust, 1979.
- [2] S. Farrokhpay, "A review of polymeric dispersant stabilisation of titania pigment," *Adv. Colloid Interface Sci.*, vol. 151, no. 1–2, pp. 24–32, 2009.
- [3] L. Ferrari, L. Bernard, F. Deschner, J. Kaufmann, F. Winnefeld, and J. Plank, "Characterization of Polycarboxylate-Ether Based Superplasticizer on Cement Clinker Surfaces," *J. Am. Ceram. Soc.*, vol. 95, no. 7, pp. 2189–2195, 2012.
- [4] H. Gharanjig, K. Gharanjig, and A. Khosravi, "Effects of the side chain density of polycarboxylate dispersants on dye dispersion properties," *Color. Technol.*, vol. 135, no. 2, pp. 160–168, 2019, doi: 10.1111/cote.12391.
- [5] H. Gharanjig, K. Gharanjig, and S. Tafaghodi, "Stability of Dye Dispersions in the Presence of Some Eco-Friendly Dispersing Agents," *J. Surfactants Deterg.*, vol. 16, no. 6, pp. 849–856, Nov. 2013, doi: 10.1007/s11743-013-1493-x.
- [6] Y. Qin, D. Yang, and X. Qiu, "Hydroxypropyl Sulfonated Lignin as Dye Dispersant: Effect of Average Molecular Weight," *ACS Sustain. Chem. Eng.*, vol. 3, no. 12, pp. 3239–3244, Dec. 2015, doi: 10.1021/acssuschemeng.5b00821.

BAL TAKVİYELİ NANOLİFLER
HONEY REINFORCED NANOFIBERS

AYŞE ÖZKAL

Dr., Pamukkale Üniversitesi, Mühendislik Fakültesi
Dr., Pamukkale University, Faculty of Engineering

MERVE DÖNMEZ

Pamukkale Üniversitesi, Fen Bilimleri Enstitüsü
Pamukkale University Institute of Science and Technology

ÖZET

Günümüzde nano teknolojik gelişmeler neticesinde nano ölçekli malzemelerin her alanda kullanımında artış görülmektedir. Nano ölçekli malzemeler içinde önemli bir yere sahip olan nanolifler yüksek yüzey alanı ve gözeneklilikleri sebebiyle malzemenin sahip olduğu antimikrobiyel, fizikokimyasal, mekanik vb. özellikleri daha etkili hale getirmektedir. Bu sebeple nanolifler yara iyileştirme, doku mühendisliği, ilaç salınımı ve kök hücre tedavisi gibi biyomedikal alanlarda etkili kullanım alanına sahip olabilirler. Bal ise yüzyıllardır biyomedikal alanlarda çeşitli hastalıkların tedavisinde özellikle yara iyileştirmede kullanılmakta olan bir ajandır. Üstün özelliklere sahip bu malzemenin nanolif formuna getirilerek etkinliğinin artırılması mümkündür. Bu çalışmada önce nanolif üretimi, nanolif üretim yöntemleri arasında önemli bir yere sahip olan elektro lif çekim yöntemi hakkında bilgi verilmiştir. Daha sonra kısaca bal ve ticarileşmiş olan çeşitli formlardaki ballı ürünler hakkında bilgi verilmiştir. Son olarak bal takviyeli nanolifli çalışmalar ile ilgili literatür taraması yapılmıştır. Bu tarama sonucunda ticarileşmiş bal takviyeli nanolifli ürün tespit edilememiştir. Literatür taraması sonucunda elde edilen bazı çalışmalarda kullanılan polimerler, katkı maddeleri, bal çeşidi ve konsantrasyonu, yapılan karakterizasyonlar, çalışmaların amacı ve elde edilen sonuçlar özetlenmiştir. Çalışmalardan elde edilen sonuçlara göre bal takviyeli nanoliflerin özellikle yara iyileştirmede potansiyel bir kullanım alanına sahip olabileceği kanaatine varılmıştır. Bu derleme çalışmasının bundan sonra yapılması planlanan deneysel çalışmalar için yol gösterici olması beklenmektedir.

Anahtar Kelimeler: Bal, Nanolif, Elektro lif çekimi, Yara iyileştirme

ABSTRACT

Today, as a result of nano-technological developments, there is an increase in the use of nano-scale materials in every field. Nanofibers, which have an important place among nano-scale materials, have antimicrobial, physicochemical, mechanical, etc. properties due to their high

surface area and porosity. making features more effective. For this reason, nanofibers can have effective use in biomedical fields such as wound healing, tissue engineering, drug release and stem cell therapy. Honey, on the other hand, is an agent that has been used for centuries in the treatment of various diseases in biomedical fields, especially in wound healing. It is possible to increase the efficiency of this material, which has superior properties, by bringing it into nanofiber form. In this study, firstly, information about nanofiber production and electro spinning method, which has an important place among nanofiber production methods, is given. Afterwards, information is given about honey and honey products in various forms that have been commercialized. Finally, a literature review on honey-reinforced nanofiber studies was conducted. As a result of this scanning, commercialized honey-reinforced nanofiber product could not be detected. The polymers used in some studies, additives, honey type and concentration, characterizations, the purpose of the studies and the results obtained are summarized as a result of the literature review. According to the results obtained from the studies, it was concluded that honey-reinforced nanofibers may have a potential use especially in wound healing. This review is expected to be a guide for future experimental studies.

Keywords: Honey, Nanofiber, Electrospinning, Wound Healing

GİRİŞ

Balın ilaç olarak kullanılması tarihin eski zamanlarına kadar dayanmaktadır. Birçok rahatsızlığın iyileştirilmesinde kullanılması ve ayrıca doğal bir tatlandırıcı olarak da kullanılması onu dünyanın üzerinde değerli kılan özelliklerindedir (Andrej vd, 2018).

Hastalıkların tedavi edilmesinde büyük rol oynayan bal, eski uygarlıklar tarafından hangi hastalığı tedavi etmede kullanıldıysa günümüze ulaşacak şekilde belgelenmişlerdir. Eski Mısırlılar yara iyileştirmede ve pansuman malzemesi olarak kullanırken, Yahudi, Hıristiyan ve İslami dinlere göre bal kutsal kabul edilen ruhu ve aynı zamanda zihni canlandıran bir madde olduğu kabul edilmiştir. Eski Yunanlılarda ise ateş, ağrı ve yara tedavilerinde bal esaslı karışımların kullanılmış olup, 1.Dünya savaşı sonrasında Rus ve Çin yaralı askerlerin tedavilerinde balı esas olarak kullanmışlardır (Lee vd., 2011).

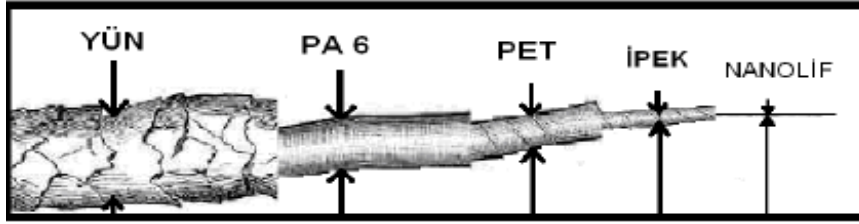
Arkeolojik bilgilere göre Mısırlılar, Yunanlılar ve Romalılar döneminde bal yara tedavilerinde kullanılmıştır. Fakat yeni dünya tıbbında olan gelişmelerle birlikte balın üzerine yapılan çalışmalar artırılmıştır. Farklı çalışmalar sonucunda ise balın içeriğindeki biyolojik bileşenlerde iyileşmeyi destekleyen birçok farklı biyoaktif bulunmaktadır (Yılmaz ve Aygin, 2009).

Bu araştırma yazısında ilk bölümünde nanomateryaller, nanolifler, özellikleri, üretim yöntemleri ve kullanım alanları özellikle elektro lif çekim yöntemi avantajları ve üretim

parametreleri, nanoliflerin biyomedikal alan uygulamaları anlatılmaktadır. Diğer bölümde balın geçmişten günümüze kullanım alanları, medikal uygulamaları, özellikleri ve balın farklı formlarda takviye edildiği akademik ve ticari uygulamalar anlatılmaktadır. Son bölüm ise bal takviye edilmiş nanoliflerin yer aldığı akademik çalışmalar, bu çalışmaların amacı, sonucu, karakterizasyon çalışmaları, kullanılan polimerler yer almaktadır. Bu çalışmanın amacı, literatürde bal takviye edilerek yapılmış olan nanolif (elektro lif çekim yöntemi ile üretilmiş) çalışmaları hakkında bilgi sahibi olmaktır.

1. NANOLİFLER VE KULLANIM ALANLARI

Ölçü birimi olarak kullanılan nanometre, metrenin milyarda birine ($10^{-9}m= 1nm$) denk gelmektedir. Nanoliflerin çapı belirtilmek istendiğinde bu ölçü birimi kullanılmaktadır. Büyük ölçeklerden nano ölçeklere doğru yaklaşıldıkça liflerin farklı özellikleri ortaya çıkmaktadır (Sazak Kozanoğlu, 2016). Nanoliflerin avantajları ve kazandırılan özellikler içerisinde; yüksek derecede yüzey alanı içermeleri, gözenekliliğin yüksek olması ve mekanik, elektriksel ve kimyasal özelliklerinin gelişmiş olması yer almaktadır (Alghoraibi ve Alomari, 2018).



Şekil 1: Nanolif ile diğer liflerin karşılaştırılmasının şematik gösterimi (Coşkun Üstündağ, 2009)

Nanoliflerin üretim yöntemleri; çekme (drawing), kalıp sentez (template synthesis), faz ayrımı (phase separation), kendiliğinden birleşme (self-assembly) ve elektroçirime (electrospinning) yer almaktadır (Oflaz, 2016). Endüstriyel ölçekte bir üretim için ise fibrilasyon, bicomponent, meltblowing, spunbond ve ayrıca elektro lif çekim yöntemleri tercih edilmektedir (Üstündağ Coşkun, 2009).

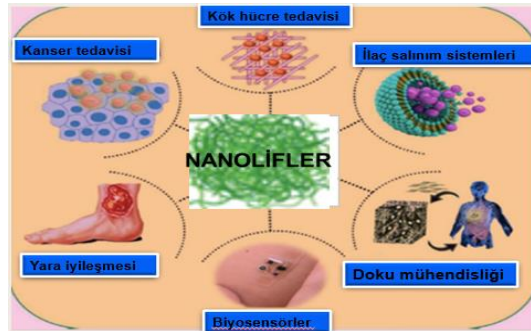
Nanolifler geçmişten günümüze birçok farklı alanda, farklı amaçlar için kullanılmaktadır. Özellikle sağlık, kozmetik, enerji ve çevre uygulamaları başta gelmektedir. Uygulama alanlarına örnek olarak; yara örtüleri, komposit malzemeler, filtreler, koruyucu kıyafetler, sensörler, doku mühendisliği, ilaç salınım sistemleri ve gıda takviyeleri verilebilir (Maliszewska ve Czapka, 2022).

Şekil 2’de nanoliflerin genel olarak kullanım alanları detayları ile birlikte gösterilmiştir. Tabloya göre teknik tekstillerin içerisinde yer alan tüm alanlarda kullanılabilme özelliklerine sahiptirler.



Şekil 2: Nanoliflerin kullanım alanları (Üstündağ Coşkun, 2009).

Nanolif ya da nanokompozit malzemelerin en yaygın kullanıldığı alanlardan biri içerisinde olan medikal ve sağlık uygulamaları içinde kanser tedavileri, kök hücre tedavileri, ilaç salınım sistemleri, yara iyileştirme tedavileri, biyosensör uygulamaları, kanser tedavileri ve doku mühendisliği uygulamaları yer almaktadır (Aras, 2019).

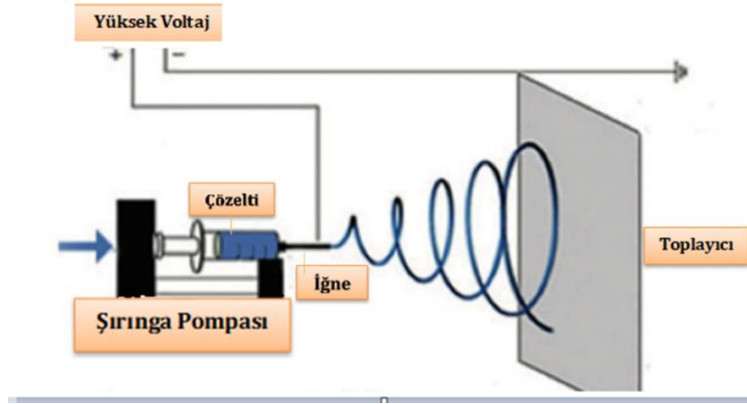


Şekil 3: Nanokompozit malzemelerin medikal olarak kullanıldığı alanlar (Aras, 2019)

2. ELEKTRO LİF ÇEKİM YÖNTEMİ

Nanolif üretiminde en çok kullanılan yöntemin elektro lif çekim sisteminin olması, diğer üretim yöntemlerine göre daha avantajlı bir üretim yöntemi olmasından kaynaklanmaktadır. Üretimde kullanılacak polimerlerin kısıtlı olması, istenilen incelikte lif elde edilememesi, üretim sürecinin karmaşıklığı ve süreksiz olması diğer üretim yöntemlerin seçilmemesindeki başlıca sebeplerdir (Ofiaz, 2016). Elektro lif çekim yönteminin endüstriyel olarak büyük ölçekli şekilde kullanabiliyor olması ve basitçe küçük sistemden büyük sisteme çevrilmesi avantajlardandır. Ayrıca elektro lif çekim üretim özelliklerinden yüksek üretim hızı, düşük maliyet, polimer olarak çok çeşitli malzemelerin kullanıma olanak sağlanması ve üretilen nanoliflerin tutarlı olması bu yöntemi, yaygın şekilde kullanılmaya yönlendirmiştir (Lee vd., 2018).

Elektro lif çekim yönteminin genel görüntüsü aşağıda yer alan şekildeki gibidir.



Şekil 4: Elektro lif çekim sisteminin şematik görüntüsü (Alghoraibi ve Alomari, 2018)

Temel prensibi şekilde de görüldüğü gibi polimer çözeltisinin ucundaki iğneye ve metal toplayıcıya birer elektrot bağlanır. Burada yeterli miktarda voltaj uygulandığında polimer çözeltisi ve metal toplayıcı elektrik yüklenir. Polimer çözeltisi metal toplayıcıya doğru çekilmeye başlar ve bu sırada iğnenin ucunda Taylor Konisi oluşturulur. Polimer çözeltisinin metal toplayıcıya kadar ulaşması sırasında polimer çözeltisinin içeriğinde yer alan çözücü madde buharlaşır ve metal toplayıcı üzerinde nanolif oluşumu gözlenir (Esentürk vd., 2016).

Taylor konisi oluşmadan önce, iğnenin ucuna doğru gelen polimer çözeltisi ya da eriyik polimer yüzey gerilimi ile asılı kalır ve damla oluşturur. Daha sonra iğnenin ucu ve metal toplayıcı arasında oluşan elektrik alan sayesinde, damla deforme olmaya başlar. Son olarak elektriksel kuvvetler damlanın yüzey geriliminin üstesinden gelmesiyle polimer jeti oluşur. Uygulanan voltaj ve iğnenin ucu ile metal toplayıcı arasında oluşan elektrik alan Taylor Konisi oluşumu için önemlidir (Aras, 2019).

Elektro lif çekim yöntemini etkileyen parametreler üç sınıfa ayrılmaktadır. İşlem değişkenleri içerisinde; çözelti besleme debisi, uygulanan voltaj, düze ve toplayıcı arasındaki mesafe ve toplama plakasının hareketi vardır. Çözelti/eriyik parametreleri; moleküler ağırlık, polimer yapısı ve çözelti özelliklerinden viskozite, dielektrik katsayısı, yüzey gerilimi ve iletkenliktir. Son olarak çevresel değişkenlerden sıcaklık, nem, hava akımı etkili olmaktadır.

Elektro lif çekim yöntemiyle üretilen liflerin yüzey morfolojileri Taramalı Elektron Mikroskobu (SEM) yöntemi ile ve liflerin polimer içeriğinin belirlenmesi için de Fourier Transform İnfrared Spektrometre (FTIR) kullanılmaktadır.

Elektro lif çekim yöntemiyle yapılmış bir nanolif, yara örtüsü olarak kullanıldığında yara üzerinde sağladığı faydalar; yüzey morfolojisinde görülen boşluklu yapılar ile deriye benzer bir yapı elde edilmesi, sağlanan geniş yüzey alanı ve gözeneklerin küçük olması, gözeneklilik

ile su buharı ve gazın geçişinin sağlanması son olarak da nano-boyutlu bir elyaf üretildiği için herhangi bir mikroorganizmanın yaranın içerisine girmesi engellenmektedir (Aras, 2019).

3. BALIN ÖZELLİKLERİ VE KULLANIM ALANLARI

3.1. Fiziksel Özellikleri

Üretildiği bölgeye ve o bölgede bulunan arı çeşidine ve bitki çeşidine göre değişiklik gösteren balın fiziksel özelliklerinde rengi, kokusu, tadı, saydamlığı ve viskozitesi değerlendirilebilir. Ayrıca balın içerisinde yer alan su miktarı, termal iletkenliği ve elektrik iletkenliği de çeşide göre değiştiği için fiziksel özellikler kategorisinde yer almaktadır (Aparna ve Rajalakshmi,1999).

3.2. Kimyasal Bileşenleri

Çiçeklerin sahip olduğu nektarlar bal arıları tarafından toplanır ve toplanan nektarlar arıların midesinde enzimler tarafından işlenir ve en son olarak da suyu uçurulan işlenmiş nektar bala dönüştürülmüş olur (Karadal ve Yıldırım, 2012). Balın kimyasal bileşenleri; nem (15%-20%), früktoz (38%-40%), glikoz (30%-32%), sakkaroz (5%-8%), trisakkaritler (1%-2%), tanımlanamayan (3%-4%) olarak ayrılır (Aparna ve Rajalakshmi,1999).

Bal genel olarak karbonhidrat, nitrojen bileşikler, aminoasitler, organik asitler, mineraller, pigmentler, vitaminler, polen ve sudan oluşmaktadır. İçerisinde bulundurduğu miktara göre de balın viskozitesi, nem alma kapasitesi, kristalleşmesi, rengi, tadı, yoğunluğu ve raf ömrü de değişmektedir (Hepsağ,2019).

3.3. Balın Karakteristik Özellikleri

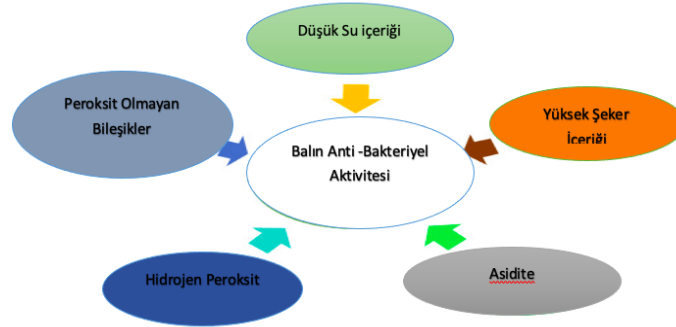
Antik çağlardan günümüze kadar çeşitli hastalıkların tedavisinde kullanılan bal, içeriğinde bulunan bileşenlerinden dolayı kendine has özellikleri barındırmaktadır. Bu özelliklerden bazıları ise antibakteriyel içerikli olması, antioksidan olarak kullanılabilmesi ve iltihaplanma önleyici olmasıdır (Scepankova vd., 2021).

3.3.1. Antibakteriyel Özelliği

Balın karakteristik özelliklerinden düşük su aktivitesi, asitliği ve yüksek ozmolaritesi ayrıca içeriğinde bulunan fenolik bileşikler ve hidrojen peroksit bakterilerin çoğalmasını ve yaşama süresini direkt olarak etkiler (Scepankova vd., 2021).

Yapılan bir araştırmaya göre özel bir bakteri türünün manuka balı ile işlem görmesinin ardından elektron mikroskopuyla analiz edildiğinde, bu bakterilerin çoğalmasında duraklama gözlenmiştir. Bu analiz ile balın, bakterilerin hücre döngüsünün ilerleyişini durdurmak için etkili olduğu anlaşılmıştır (Lee vd., 2011).

Antibakteriyel özelliği ile birçok tedavide kullanılan balın içeriğinde hangi bileşikler bu özelliği bala kazandırıyor diye incelendiğinde elde edilen sonuçlara göre Hidrojen Peroksit, Metilglioksal ve Bee Defensin-1 en çok etkili olanlardır (Kwakman ve Zaat, 2012).



Şekil 8: Balın içerisinde yer alan, antibakteriyel özellik sağlayan bileşikler (Hossain vd., 2022)

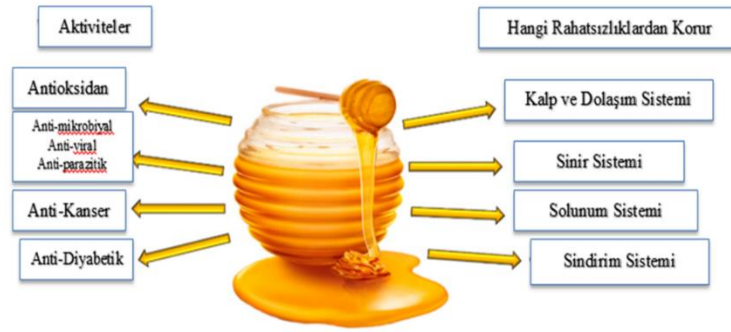
3.3.2. Antioksidan Aktivite

Bal, yüksek derecede duygusal, fiziksel ve zihinsel olarak yoğun stres altında kaldığında antioksidan olarak davranır. Balın sahip olduğu antioksidan kapasitesi birçok akut ve kronik rahatsızlığı önlemede etkili olmaktadır. İltihaplanma, alerji, diyabet, kanser ve kalp hastalıkları bu rahatsızlıklara örnek olarak verilebilir. Balın içeriğindeki C Vitamini, fenol bileşikleri, katalaz, peroksit, glikoz oksidaz enzimleri, flavonoidler ve karotenoidler antioksidan özellik taşırlar (Lewoehu ve Amare, 2019).

3.3.3. İltihaplanma Önleyici

Diğer karakteristik özelliği iltihaplanma önleyici olan bal, içeriğinde yer alan fenolik bileşikler sayesinde bu özelliğe sahip olduğu düşünülse de farklı ballarda incelenen fenolik bileşik düzeyi ile iltihaplanma karşıtı davranma arasında olumlu ya da olumsuz bir ilişki bulunamamıştır. Bal içerisinde yer alan diğer bileşenlerle birlikte böyle bir etkiye neden oluyor olabileceği düşünülmektedir (Scepankova vd., 2021).

Günümüz ticari uygulamalarında balın çeşitleri birçok değişik formda kullanılmaktadır. Bal bazlı jeller, yara örtüleri/sargı bezleri, merhemler, kremler, macunlar, şuruplar, göz damlaları ve pastiller ticari olarak üretilebilen örneklerdendir (Hossain vd., 2021).



Şekil 9: Tedavi etme sürecinde balın kullanıldığı rahatsızlıklar/hastalıklar
(Cianciosi vd.,2018)

Mekanik, kimyasal ya da termal etkiler derinin bütünlüğünün bozulmasına neden olduğunda, deride yaralanmalar meydana gelir. Bu yaraların iyileşmesi süreci ise dört adımda anlatılmıştır; kan akışının durdurulması, yaranın iltihaplanması, doku çoğalması ve doku yenilenmesidir.

Günümüz teknolojisi ile birlikte yara tedavileri, yara örtülerinin tasarımı ve işlevselliği artırılmıştır. İşlevsellik kriterleri olarak; biyoyumluluk, toksik yan etkilerinin olmaması, biyolojik olarak bozunabilme hızı ve örtünün içerisinde bulunan ilacın salınımı değerlendirilmektedir (Scepankova vd., 2021).

Aşınma, apse yatak yaraları, yanık, diyabet, travmatik ülserler, septik yaralar ve cerrahi yaralar gibi geniş ölçüde yara iyileştirmede etkili olan bal, enfeksiyonu temizlerken aynı zamanda ağrıyı da azaltmaktadır (Eteraf-Oskouei ve Najalafi, 2013).

Yapılan araştırmalara göre kalın bağırsak kanseri, kolon kanseri, rahim ağzı kanseri, mesane kanseri, pankreas kanseri, prostat kanseri, göğüs kanseri ve lösemi gibi kanser hastalıklarının tedavisinde farklı türlerde balların kullanılması ile, farklı dozlarda ve farklı zaman dilimlerine maruz bırakılarak veriler toplanmıştır. Manuka balı, kekik balı, akasya balı, tualang balı, orman balı ve çilek ağacı balı kullanılan ballardan bazılarıdır (Talebi vd., 2020).

Balın tedavi amacıyla kullanıldığı alanlardan biri de gözlerde oluşabilecek kornea yaralanmaları, gözdeki kimyasal ve termal yanıklardır. Yapılan bir çalışmada, tedaviye yanıt vermeyen bir göz bozukluğu olan 102 hastada, balın merhem olarak kullanılmasından sonra hastalardan 87 tanesi tedaviye olumlu sonuç verirken kalan 15 kişide ise hastalığın ilerlemediği kaydedilmiştir. Kızarıklık, şişlik, irin akıntısı ve bakterilerin tamamen yok edildiği süre azaltılmıştır (Eteraf-Oskouei ve Najalafi, 2013).

Yapılan çalışmalardan birinde Burkina Faso merkezinde, balın solunum yolu enfeksiyonlarında, doğum sonrası rahatsızlıklarda, adet sancılarında, farenjit tedavilerinde, kızamık rahatsızlığında tedavi edici olarak kullanıldığı belirlenmiştir. Başka bir çalışmada

yine balın günlük kullanımı ile endokrin sistemi üzerindeki olumlu etki, kandaki enzim ve mineral seviyelerinde olumlu yönde gelişmeler gözlenmiştir (Eteraf-Oskouei ve Najalafi, 2013).

Sinir sistemi rahatsızlıklarının tedavisinde, balın içeriğinde yer alan polifenoller çok önemli bir yere sahiptir. Nörotoksik olan maddelere karşı temizleyici olarak görev yapmaktadır, ayrıca yaşlanmaya karşı dirençlidir (Cianciosi vd.,2018).

4. BALIN TEDAVİ AMACIYLA KULLANILDIĞI FORMLAR

4.1. Bal Bazlı Hidrojeller

Balın içeriğinde bulunan prolin, arginin, metiyonin ve glisin yaranın iyileşmesi için gerekli olan kollajeni ve fibroblastı sağlar. Ayrıca yaranın iyileşebilmesi ortamın nem oranına da bağlı olduğundan yara örtülerinde ortam nemini koruyan hidrojellerin kullanılması çok önemlidir.

Bal bazlı hidrojeller ile yapılan araştırmalarda balın yanında kullanılan bazı içerikler; pektin, alginat, PVA, PVA/kitosan, kitosan/jelatin ve polivinilpirolidon(PVP)/ polietilenglikol(PEG) /proteinsiz agar'dır. Her bir yan içeriğin getirdiği sonuç farklı olmaktadır. Bal ve pektinin içeriğinde bulunduğu hidrojel, bir farenin derisinin tüm katmanlarının çıkartılıp alındığı bölgeye uygulandığında; yara yerinin daha hızlı oranda kapandığı ve daha düşük oranda iltihap hücrelerinin bulunduğu gözlemlenmiştir. Aynı şekilde oluşmuş bir yaraya bal ve alginat içerikli hidrojel ile müdahale edildiğinde; yaranın daha hızlı iyileştiği, kan damarlarının oluştuğu, epidermin geliştiği ve kollajen oluşumunun desteklendiği gözlemlenmiştir. PVA ve bal ile hazırlanmış bir hidrojelin laboratuvar ortamında insan fibroblast hücrelerinin analizinde antibakteriyel özellik, balın sürekli salınımı, nemli bir ortam sağladığı ve daha fazla hücrenin dağıldığı görülmüştür (Nezhad-Mokhtari vd., 2021).

4.2. Bal Bazlı Nanopartiküller

Yapılan çalışmalara göre, yaranın iyileşme sürecinde farklı aşamalarda etkili olan nanopartiküller bulunmuştur. Ancak çok az nanopartikülün hem iyileştirme hem de dezenfekte etme özelliği bir arada uyguladığı gözlemlenmiştir ve bunun için bu nanoparçacıklardan beklenti hem bakterileri öldürebilmesi hem de iyileşmeyi artırıcı özellikte olması gerekmektedir. Altın, gümüş ve bakır gibi metal iyonları ile balın içeriğindeki glikoz ve früktozun içeriğinde yer alan hidroksil grubu ile tepkimesinden sonra yeniden sodyum hidroksit ile tepkimesi ile nanopartikül oluşumu sağlanmaktadır. Altın/bal içerikli nanopartiküller; yaraların iyileştirilmesinde, dokuların yenilenmesinde ve hedeflenen ilaç salınımında kullanılmaktadır. Gümüş/bal içerikli nanopartiküller daha çok yanık yaralarının tedavi edilmesinde ve yaraların enfeksiyon tedavisinde kullanılmaktadır. Bakır/bal içerikli

nanoparküllerin kullanım alanı ise kronikleşmiş diyabet yaralarıdır, çünkü bakırın çeşitli mantar ve ilaca direnç gösteren bakterilere karşı yavaşlatıcı özelliği bulunmaktadır (Bahari vd., 2022).

4.3. Bal Bazlı Diğer Formlar

Balın esas olarak kullanıldığı krem, jel, merhem, sargı bezleri, şurup, göz damlaları ve pastil gibi çok çeşitli ticarileşmiş ve akademik çalışmalarda kullanılmış ürün bulunmaktadır. En çok kullanılan bal çeşidi ise Manuka balı iken adaçayı balı ve karabuğday balı da ilaç yapımında kullanılan diğer ballardandır. Sargı bezleri/yara örtüleri ülserden kaynaklanan vücut yaralarının, travmatik ve cerrahi yaraların iyileştirilmesi için kullanılmaktadır. Bal bazlı merhemler, daha çok cildin nemlendirilmesinde ve egzamalı ya da kaşıntılı cildin sakinleşmesi için kullanılmaktadır. Vücudun bağışıklığını koruması, fiziksel performansı artırması ve boğaz tahrişini azalması için de bal bazlı şuruplar üretilmektedir (Hossain vd., 2021).

5. BALIN FARKLI FORMLARDA TAKVİYE EDİLMİŞ TİCARİ VE AKADEMİK UYGULAMALARI

Balın farklı formlarda farklı amaçlar için kullanılması oldukça yaygınlaşmıştır. Bazı çalışmalar akademik ölçüde yapılarak ticarileşmemiş olsa da ticari ürün haline gelen pek çok bal içerikli ürün bulunmaktadır. Tablo 1’de bal takviyeli bazı ticari ürünler yer almaktadır.

Tablo 1. Bal takviyeli farklı formdaki ticari ürünler (Hossain vd., 2021)

Ürün adı	Ürün formu	Bal oranı (%)	İçerikte yer alan diğer maddeler	Sonuçlar/Etki Alanları
Activon	Jel	100	-	Diyabetik ayak ve bacak ülserlerin, travmatik ve cerrahi yara tedavileri, yanık tedavileri
Revamil	Jel	100	-	Damar yaralanmaları, enfekte olmuş, cerrahi ve kronik yaralar, diyabetik ayak yaraları, 1 ve 2.derece yanıklar
L-Mesitran Soft Medical Grade Honey	Jel	40	Hipoalerjenik lanolin, Propilen glikol, Polietilen Glikol 4000, E ve C Vitamini	Orta dereceli akıntılı yaralara kadar, ayak ve bacak yaraları, cerrahi ve kronik yaralar, 1.ve 2.derece kısmi yanıklar
ManukaPli	Jel	100	-	Ayak ve bacak yaraları, cerrahi ve kronik yaralar, 1.ve 2.derece kısmi yanıklar

INTERNATIONAL AEGEAN CONFERENCES
ON INNOVATION TECHNOLOGIES & ENGINEERING-VI
December 20-22, 2022

MANUKAtex	Sargı Bezi	100	-	Ayak ve bacak yaraları, cerrahi ve kronik yaralar, 1.ve 2.derece kısmı yanıklar
Actibalm Manuka Honey Lip Balm	Merhem	100	-	Uygulandığı bölgeye iyileştirme ve nemlendirme
Medihoney Barrier	Krem	30	Saf su,Hindistan Cevizi Yağı, Alman Papatyası özü, Çuha Çiçeği Yağı, Aloe Vera, E Vitamini	Deriyi korumaya, cilt tahrişini önleme
Medihoney	Macun	100	-	Yaranın iyileşmesi
Manuka honey and PropolisTM	Şurup	80	Propolis	Bağışıklık sistemi, toksinlerin atılması
Optimel Manuka+ Dry Eye Drop	Göz Damlası	98	Sodyum Klorid, Benzoik Asit	Aşırı dereceden orta dereceye kadar göz kuruluğu

Tablo 1’de yer alan ürünlerin hemen hepsinin jel, merhem, macun veya şurup formunda olduğu görülmektedir.

Tablo 2’de de henüz akademik çalışma halinde olan bazı bal takviyeli çalışma örnekleri özetlenmiştir.

Tablo 2. Bal takviyeli farklı formdaki akademik çalışmalar (Hossain vd., 2021)

Ürün adı	Ürün formu	İçerikte yer alan balın miktarı (%)	İçerikte yer alan diğer maddeler	Sonuçlar/Etki Alanları
Kanuka honey	Jel	90	Gliserin	Gül hastalığı
Leptospermum (Manuka balı)	Sargı bezi	80	Polivinil Alkol ve Boraks	Yara iyileşme
Leptospermum (Manuka Balı)	Sargı bezi	13	Kitosan, Gliserol, Su ve Sodyum Bikarbonat	Antibakteriyel etki

**6. BAL TAKVİYE EDİLEREK ÜRETİLMİŞ NANOLİFLER İLE İLGİLİ
AKADEMİK ÇALIŞMALAR**

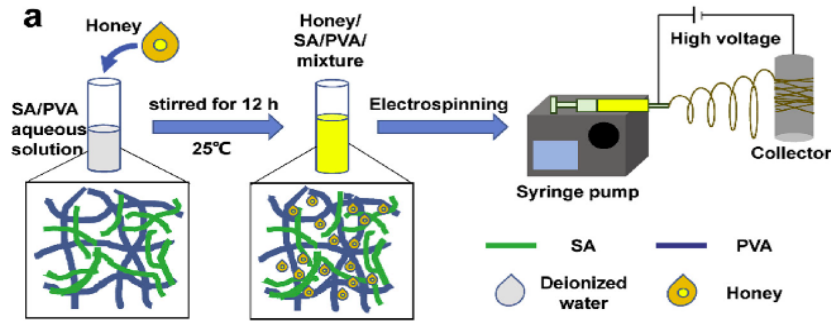
INTERNATIONAL AEGEAN CONFERENCES
ON INNOVATION TECHNOLOGIES & ENGINEERING-VI
December 20-22, 2022

Bir literatür taraması yapılarak bal takviye edilerek yapılmış olan nanolif üretimleri araştırılmıştır. Bu araştırma yapılırken çalışmaların ne amaçla yapıldığı, çalışmalarda kullanılan polimerler, çözümler ve diğer katkı maddeleri özellikle incelenmiştir. Çalışmalarda yapılan karakterizasyonlar ve çalışmaların genel sonuçları da sonraki deneysel çalışmalara ışık tutması amacıyla not edilmiştir (Tablo 3).

Amaç	Polimer, çözümler ve katkımlar	Yapılan Karakterizasyonlar	Sonuç	Kaynak
Yara örtüsü	Kitre (Kıvam artırıcı), Etil Selüloz, İnan-Balı, Etanol	SEM, FTIR, Şişme derecesi, bozunma testi, antioksidan ve anti bakteriyel aktivite tayini	Bal oranı arttıkça şişme derecesi düşmüş, nanolif çapı artmış, bozunma yeteneği gelişmiş, antibakteriyel özelliği, antioksidan özelliği artmıştır.	(Ghorbani vd., 2021)
Yara örtüsü	Selüloz Asetat/ Bal (Manuka Balı) DMF/ Aseton	SEM, FTIR, XRD analizi, çekme dayanımı, yüzey alanı ve gözenek büyüklüğü dağılımı, su buharı geçirme oranı, anti bakteriyel analiz, hücre yaşam testi	Bal oranı arttıkça nanolif çapı, hidrofilitate artmış ve yüzey alanı azalmıştır. Gözenek büyüklüğü artmış bunun sonucunda gaz ve su buharı transferi iyi seviyelerde gerçekleşmiştir. Kabul edilebilir seviyelerde antibakteriyel ve antioksidan özellikler sergilenmiştir.	(Ullah vd., 2020)
Yara örtüsü	Bal (Irak), Tripolifosfat(TPP), Kitosan, Kapsaisin, Altın nanopartikül, Buzlu asetik asit, saf su	SEM, antibakteriyel çalışma, sitotoksosite değerlendirme, yara iyileştirme değerlendirme	Kapsaisin takviyesi ile altın nanopartikül takviyesine göre daha etkili yara iyileştirme sağladı.	(Al-Musawi vd., 2020)
Yara örtüsü	Polietilenteraftalat (PET), Kitosan, Artvin Balı, Trifloroasetik asit (TFA)	SEM, FTIR, sitotoksosite değerlendirme, Islanma ve su içerme analizi	Üretilen liflerde toksik bir sonuç gözlenmemiştir. PET/bal ya da PET/kitosan-bal yara iyileştirmede iyi birer alternatif olarak değerlendirilmesi örnek gösterilmiştir.	(Arslan vd., 2014)
Yara örtüsü	Çin Akasya Balı, Polivinil Alkol (PVA), Sodyum Alginat (SA), Saf su	SEM, FTIR, şişme ve ağırlık kaybı testi, Antioksidan ve antibakteriyel ve sitotoksosite değerlendirme	Bal oranı arttıkça nanolif çapı artmıştır ve antioksidan aktivite artmıştır, gram pozitif bakteriler üzerinde daha etkili olduğu gözlemlenmiştir ve biyouyumlu bir yara örtüsü olduğu belirtilmiştir.	(Tang vd., 2019)
Yara örtüsü ve Gıda paketlenme	PVA, Sığır Jelatini, Muğla Çam balı, Asetik Asit, Saf Su	FTIR, SEM, Temas açısı ölçümü, Antioksidan aktivite değerlendirme	Nanolifler üretilebilmiş ve antioksidan aktivite gözlemlenmiştir. Üretilen nanolifler gıda paketlenmede, yara iyileştirme ve doku mühendisliğinde kullanılabilir.	(Parin vd., 2021)

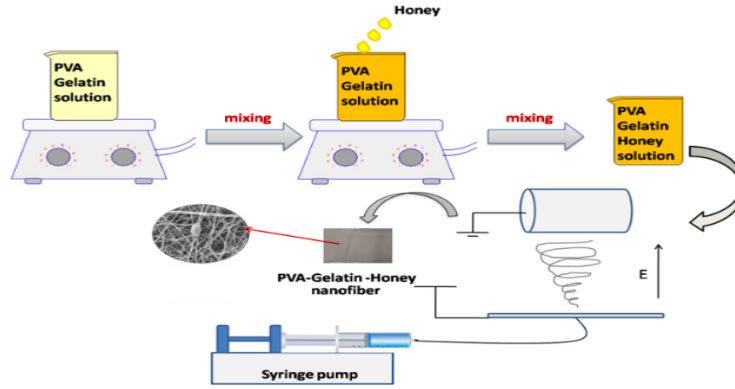
Yara örtüsü	Çörekotu, Hindistan Sundarbans Balı, Sarımsak, Sızma Zeyinyağı, PVA, Metanol	SEM, FTIR, Anti bakteriyel ve sitotoksosite değerlendirme, Termal analiz, absorbanans davranışı ölçümü	Antibakteriyel aktivite değerlendirme sonucunda birçok medikal alanda kullanılabilir olduğu belirtilmiştir.	(Uddin vd., 2022)
-------------	--	--	---	-------------------

Tang vd., 2019' a ait çalışmanın özeti Tablo 3'te verilmiştir. Araştırmacılar yara bezi üretmek amacıyla akasya balı takviye ederek dönen silindirik kolektör üzerine nanolifleri toplamışlardır. Bu çalışmaya ait şematik çizim Şekil 10'da verilmiştir.



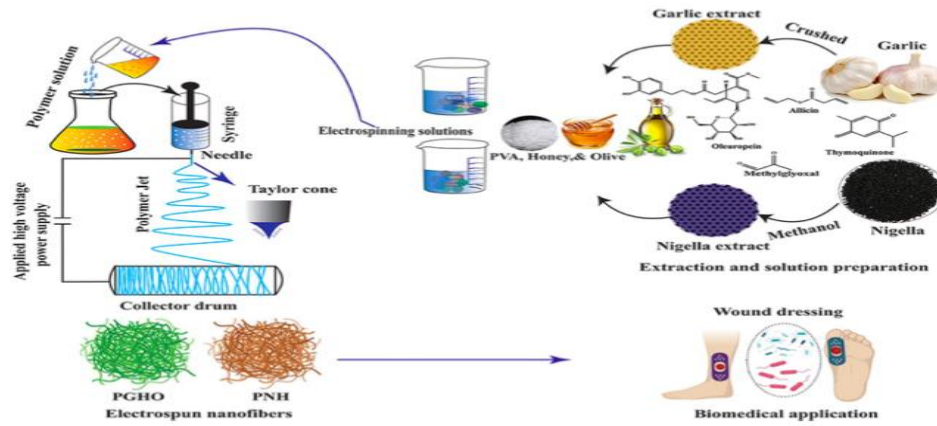
Şekil 10 : Akasya Balı/PVA/Sodyum Alginat ile yapılan çalışmanın şematik gösterimi (Tang vd., 2019)

Şekil 11'de Parin vd., 2021' e ait çalışmanın şematik görseli bulunmaktadır. Çalışmalarında PVA/Jelatin çözeltisine farklı oranlarda bal ekleyerek yara örtüsü amaçlı nanolif üretmişler ve sonuçta üretilen nanolifli yüzeyin yara örtüsü olarak kullanılabilme potansiyeli olduğu kanaatine varmışlar.



Şekil 11: PVA/Jelatin/Çam balı ile yapılan çalışmanın şematik gösterimi (Parin vd.,2021)

Çörekotu özü, bal ve PVA ile sarımsak özü, PVA, bal ve zeytin yağı ile ayrı ayrı üretimi yapılan nanoliflerin şematik olarak gösterimi Şekil 12’de verilmiştir. Bu çalışma Uddin ve arkadaşları tarafından 2022 yılında yapılmıştır. Bu çalışmada yeşil elektro lif çekim yöntemi kullanılmasının önemi de vurgulanmıştır, çünkü doğada yer alan özütler ile biyoyumlu ve toksik madde içermeyen bir çalışma yapılmıştır.



Şekil 12: Çörekotu/Bal/Sarımsak/Sızma Zeytin yağı/PVA ile yapılan çalışmanın şematik gösterimi (Uddin vd., 2022)

7.SONUÇLAR VE ÖNERİLER

Nano boyutlarda uygulamalar ile elde edilen avantajlar, endüstriyel uygulamalar ile yaygınlaştırılıp birçok kullanım alanı oluşturmaktadır. Medikal düzeyde oluşturulan uygulama alanları ise gelecek vadetmektedir. Burada avantajlarından dolayı elektro lif çekim yöntemi ön plana çıkmaktadır. Elektro lif çekim teknolojisinin günden güne gelişmesi, ayrıca çevreye ve insan sağlığına olan duyarlılığın artmasıyla birlikte yeşil üretim/yeşil elektro lif çekim

sistemleri geliştirilmektedir. Buna bağlı olarak üretim parametrelerinde toksik özellik içermeyen, doğal ve uyumlu polimerlerin seçilmesi en başta gelmektedir.

İncelenen akademik çalışmalar ışığında bal takviye edilerek elde edilen nanolifler üzerine bir ilginin olduğu görülmekte fakat çalışmaların yetersiz kaldığı gözlenmektedir. Bu çalışmalarda hem yapılması gereken analizler hem de kullanılacak olan çözeltinin içeriği çok az değişiklik göstermektedir. Farklı bölgelerde üretilen bal çeşitleri ile yapılacak bir çalışma ve kullanılacak ilave doğal polimer ve çözücüler ile yeşil elektro lif çekim yöntemi desteklenebilir.

Sadece nanolif boyutlarında değil, bal takviyeli hidrojel, nanopartiküller ya da diğer formlardan krem, macun, şurup gibi formlar ile de karşılaştırılma yöntemleri, karakterizasyon testlerinin yapılması ve sonuçları ile ilgili literatürde herhangi bir çalışma bulunamamıştır. Aynı balın kullanılmasıyla birlikte, farklı formlarda üretilmiş ürünlerin karşılaştırılması bir çalışma önerisi olarak sunulabilir.

REFERANSLAR

- Alghoraibi, I., & Alomari, S. (2018). Different methods for nanofiber design and fabrication. *Handbook of nanofibers*, 1-46.
- Al-Musawi, S., Albukhaty, S., Al-Karagoly, H., Sulaiman, G. M., Alwahibi, M. S., Dewir, Y. H., Soliman, D. A., & Rizwana, H. (2020). Antibacterial Activity of Honey/Chitosan Nanofibers Loaded with Capsaicin and Gold Nanoparticles for Wound Dressing. *Molecules*, 25(20), 4770.
- Alvarez-Suarez, J., Gasparrini, M., Forbes-Hernández, T., Mazzoni, L., & Giampieri, F. (2014). The Composition and Biological Activity of Honey: A Focus on Manuka Honey. *Foods*, 3(3), 420–432.
- Andrzej K. Kuropatnicki, Małgorzata Kłósek & Marek Kucharzewski (2018) Honey as medicine: historical perspectives, *Journal of Apicultural Research*, 57:1, 113-118.
- Aparna, A. R., & Rajalakshmi, D. (1999). Honey—its characteristics, sensory aspects, and applications. *Food Reviews International*, 15(4), 455-471.
- Aras, C. (2019). ÇÖREK OTU YAĞI KATKILI NANOKOMPOZİT POLİÜRETAN NANOLİFLİ YÜZEY ÜRETİMİ, KARAKTERİZASYONU VE YARA ÖRTÜSÜ OLARAK KULLANIM PERFORMANSININ ARAŞTIRILMASI. Yüksek Lisans Tezi, Uludağ Üniversitesi Fen Bilimleri Enstitüsü, Bursa.
- Arslan, A., Şimşek, M., Aldemir, S. D., Kazaroğlu, N. M., & Gümüşderelioğlu, M. (2014). Honey-based PET or PET/chitosan fibrous wound dressings: effect of honey on electrospinning process. *Journal of Biomaterials Science, Polymer Edition*, 25(10), 999-1012.

- Bahari, N., Hashim, N., Md Akim, A., & Maringgal, B. (2022). Recent Advances in Honey-Based Nanoparticles for Wound Dressing: A Review. *Nanomaterials*, 12(15), 2560
- Cianciosi, D., Forbes-Hernández, T., Afrin, S., Gasparri, M., Reboredo-Rodríguez, P., Manna, P., Zhang, J., Bravo Lamas, L., Martínez Flórez, S., Agudo Toyos, P., Quiles, J., Giampieri, F., & Battino, M. (2018). Phenolic Compounds in Honey and Their Associated Health Benefits: A Review. *Molecules*, 23(9), 2322.
- Coşkun Üstündağ, G. (2009). ELEKTROSPINNING YÖNTEMİ İLE BİYOMEDİKAL KULLANIMA YÖNELİK NANOLİF YÜZEY ÜRETİMİ VE UYGULAMASI. Yüksek Lisans Tezi, Uludağ Üniversitesi Fen Bilimleri Enstitüsü, Bursa.
- Esentürk, İ., Erdal, M. S., & Güngör, S. (2016). Electrospinning method to produce drug-loaded nanofibers for topical/transdermal drug delivery applications. *Journal of Faculty of Pharmacy of Istanbul University*, 46(1), 49-69.
- Eteraf-Oskouei, T., & Najafi, M. (2013). Traditional and modern uses of natural honey in human diseases: a review. *Iranian journal of basic medical sciences*, 16(6), 731.
- Ghorbani, M., Ramezani, S., & Rashidi, M. R. (2021). Fabrication of honey-loaded ethylcellulose/gum tragacanth nanofibers as an effective antibacterial wound dressing. *Colloids and Surfaces a: Physicochemical and Engineering Aspects*, 621, 126615.
- Hepsağ, F. (2019). DETERMINATION OF TOTAL PHENOLIC COMPOUNDS AND ANTIOXIDANT CAPACITY OF ANZER HONEY PRODUCED IN RIZE, TURKEY. *GIDA/The Journal of FOOD*, 44(4).
- Hossain, M. L., Lim, L. Y., Hammer, K., Hettiarachchi, D., & Locher, C. (2021). Honey-based medicinal formulations: A critical review. *Applied Sciences*, 11(11), 5159.
- Hossain, M. L., Lim, L. Y., Hammer, K., Hettiarachchi, D., & Locher, C. (2022). A Review of Commonly Used Methodologies for Assessing the Antibacterial Activity of Honey and Honey Products. *Antibiotics*, 11(7), 975.
- Karadal, F. & Yıldırım, Y. (2012). Balın Kalite Nitelikleri, Beslenme ve Sağlık Açısından Önemi . *Erciyes Üniversitesi Veteriner Fakültesi Dergisi* , 9 (3) , . Retrieved from <https://dergipark.org.tr/tr/pub/ercivet/issue/5830/77512>
- Kozanoğlu, G. S. (2006). ELEKTROSPİNİNİN YÖNTEMİYLE NANOLİF ÜRETİM TEKNOLOJİSİ. Yüksek Lisans Tezi, İstanbul Teknik Üniversitesi Fen Bilimleri Enstitüsü, İstanbul
- Kwakman, P. H., & Zaat, S. A. (2012). Antibacterial components of honey. *IUBMB life*, 64(1), 48-55.
- Lee, D. S., Sinno, S., & Khachemoune, A. (2011). Honey and wound healing. *American journal of clinical dermatology*, 12(3), 181-190.
- Lee, J. K. Y., Chen, N., Peng, S., Li, L., Tian, L., Thakor, N., & Ramakrishna, S. (2018). Polymer-based composites by electrospinning: Preparation & functionalization with nanocarbons. *Progress in Polymer Science*, 86, 40-84.

- Lewoyehu, M., & Amare, M. (2019). Comparative evaluation of analytical methods for determining the antioxidant activities of honey: A review. *Cogent Food & Agriculture*, 5(1), 1685059.
- Maliszewska, I., & Czapka, T. (2022). Electrospun Polymer Nanofibers with Antimicrobial Activity. *Polymers*, 14(9), 1661.
- Nezhad-Mokhtari, P., Javanbakht, S., Asadi, N., Ghorbani, M., Milani, M., Hanifehpour, Y., ... & Akbarzadeh, A. (2021). Recent advances in honey-based hydrogels for wound healing applications: Towards natural therapeutics. *Journal of Drug Delivery Science and Technology*, 66, 102789.
- Oflaz, K. (2016). MANYETİK NANOFİBER MEMBRANLAR. Yüksek Lisans Tezi, Selçuk Üniversitesi Fen Bilimleri Enstitüsü, Konya.
- Özdoğan, E., Demir, A., & Seventekin, N. (2006). Nanoteknoloji ve tekstil uygulamaları. *Tekstil ve Konfeksiyon*, 16(3), 160-168.
- Parin, F. N., Terzioğlu, P., Sicak, Y., Yildirim, K., & Öztürk, M. (2021). Pine honey-loaded electrospun poly (vinyl alcohol)/gelatin nanofibers with antioxidant properties. *The Journal of The Textile Institute*, 112(4), 628-635.
- Scepankova, H., Combarros-Fuertes, P., Fresno, J. M., Tornadijo, M. E., Dias, M. S., Pinto, C. A., ... & Estevinho, L. M. (2021). Role of honey in advanced wound care. *Molecules*, 26(16), 4784.
- Talebi, M., Talebi, M., Farkhondeh, T., & Samarghandian, S. (2020). Molecular mechanism-based therapeutic properties of honey. *Biomedicine & Pharmacotherapy*, 130, 110590.
- Tang, Y., Lan, X., Liang, C., Zhong, Z., Xie, R., Zhou, Y., ... & Wang, W. (2019). Honey loaded alginate/PVA nanofibrous membrane as potential bioactive wound dressing. *Carbohydrate polymers*, 219, 113-120.
- Uddin, M. N., Mohebbullah, M., Islam, S. M., Uddin, M. A., & Jobaer, M. (2022). Nigella/honey/garlic/olive oil co-loaded PVA electrospun nanofibers for potential biomedical applications. *Progress in Biomaterials*, 11(4), 431-446.
- Ullah, A., Ullah, S., Khan, M. Q., Hashmi, M., Nam, P. D., Kato, Y., ... & Kim, I. S. (2020). Manuka honey incorporated cellulose acetate nanofibrous mats: Fabrication and in vitro evaluation as a potential wound dressing. *International journal of biological macromolecules*, 155, 479-489.
- Yilmaz, A. C., & Aygin, D. (2020). Honey dressing in wound treatment: a systematic review. *Complementary therapies in medicine*, 51, 102388.
- Yokel, R.A., MacPhail, R.C. Engineered nanomaterials: exposures, hazards, and risk prevention. *J Occup Med Toxicol* 6, 7 (2011).

**ASFALT KAPLAMALARDA POLİFOSFORİK ASİTLİ VE SBS KOMPOZİT
POLİMERLERİN FARKLI ORAN VE KARIŞTIRMA SÜRELERİNDE DÜŞÜK
SICAKLIK PERFORMANS ANALİZİ**

LOW TEMPERATURE PERFORMANCE ANALYSIS OF POLYPHOSPHORIC ACID
AND SBS COMPOSITE POLYMERS IN ASPHALT PAVEMENTS WITH DIFFERENT
RATIO AND MIXING TIMES

Celaleddin Ensar ŞENGÜL

Dr., Devlet Su İşleri Genel Müdürlüğü, 14. Bölge Müdürlüğü, İstanbul, Türkiye

ABSTRACT

In asphalt pavements; the effect of polyphosphoric acid polymers and SBS composite polymers on low temperature cracking at different ratios and mixing times is investigated. Low temperature cracking is the main problem. NovoPrene-P and NovoPrene-S polymers are used in asphalt mixtures with their performance enhancing properties. NovaPrene-P is a liquid component and contains polyphosphoric acid (PPA). NovoPrene-S is an elastomeric based polymer modified bitumen additive produced from the combination of different polymers from the Styrene Butadiene Block Copolymer (SB-BK) family. NovaPrene-S is a diblock, triblock mixture high molecular weight SB block copolymer. With these additives, it is ensured that the asphaltene content in the mixture is managed or controlled. In order to manage the asphaltene issue, rate change should be investigated. The subject of this research is the investigation of low temperature cracking for different polymer contents. It was investigated whether lower polymer contents could be used for reinforced polymers in terms of low temperature cracking for different polymer contents. In this respect, the variation of low temperature performance was investigated depending on the polymer type. The more difficult to manage problem in asphalt pavement engineering is the low temperature cracking problem. Polyphosphoric acid polymers are predicted to improve a polymer synergy in terms of low temperature cracking resistance. Especially for polymeric materials, the subject of compositional synergy is one of the primary topics investigated. Polyphosphoric acid (PPA) has been tested as one of these tertiary ingredients. It is emphasized that the properties of PPA/SBS modified asphalt mixtures are better than only SBS modified asphalt mixtures. It is stated that the addition of PPA increases the rigidity of the asphalt mixture and therefore the high rutting, fatigue and water damage resistance provided at medium and high temperatures cannot be achieved in terms of cracking resistance at low temperatures. With the addition of PPA, the ratio of SBS, which has a general usage rate of 5%, can be reduced to 3% in bituminous binders, thus providing an economic advantage. On the other hand, by using the sulfur additive, which is cheaper than SBS, as the fourth component (sulfur/PPA/SBS

modified asphalt), thermal stability can be achieved at high temperatures, the distribution of SBS in bitumen can be improved, and the low temperature properties of the asphalt mixture can be improved. For this reason, it is thought that testing PPA-containing NovaPrene additives in asphalt mixtures at different addition rates will be beneficial in terms of literature, especially in terms of evaluating the low temperature problem, which has not been clearly determined in research.

Keywords: Asphalt pavements, polymer with polyphosphoric acid, SBS composite polymer, low temperature cracking.

ÖZET

Asfalt kaplamalarda; polifosforik asitli polimerler ve SBS kompozit polimerlerin farklı oran ve karıştırma sürelerinde düşük sıcaklık çatlaması üzerindeki etkisi araştırılmaktadır. Düşük sıcaklık çatlaması ana sorundur. NovaPrene-P ve NovaPrene-S polimerleri asfalt karışımlarda performans artırıcı özellikleri ile kullanılmaktadır. NovaPrene-P sıvı bileşenlidir ve polifosforik asit (PPA) içermektedir. İnorganik yapıda, yüksek doyumlukta bir polimer karışımıdır. NovaPrene-S ise Stiren Butadien Blok Kopolimeri (SB-BK) ailesinden farklı polimerlerin bileşiminden üretilen elastomerik tabanlı bir polimer modifiye bitüm katkısıdır. NovaPrene-S, diblok, triblok karışımı yüksek molekül ağırlıklı SB blok kopolimeridir. Bu katkılarla karışımdaki asfalten içeriğinin yönetilmesi veya kontrol edilmesi sağlanmaktadır. Asfalten konusunun yönetilmesi için, oran değişimi araştırılmalıdır. Bu araştırmanın konusu, farklı polimer içeriklerin farklı oranları için düşük sıcaklık çatlamasının araştırılmasıdır. Farklı polimer içerikleri için düşük sıcaklık çatlaması anlamında daha düşük polimer içeriklerinin güçlendirilmiş polimerler için kullanılıp kullanılmayacağı araştırılmıştır. Asfalt kaplama mühendisliğinde yönetilmesi daha zor ele alınan problem düşük sıcaklık çatlama problemi. Polifosforik asitli polimerlerin bir polimer sinerjisini düşük sıcaklık çatlama direnci anlamında geliştireceği öngörülmektedir. Özellikle polimerik malzemeler için bileşimsel sinerji konusu araştırılan öncül konulardandır. Polifosforik asit (PPA) bu üçüncül bileşenlerden birisi olarak denenmiştir. PPA/SBS modifiye asfalt karışımların özelliklerinin yalnızca SBS modifiye asfalt karışımlara göre daha iyi olduğu vurgulanmaktadır. PPA ilavesinin asfalt karışımının rijitliğini arttırdığı ve bu nedenle orta ve yüksek sıcaklıklarda sağlanan yüksek tekerlek izi, yorulma ve su hasarı direncinin düşük sıcaklıklarda çatlama direnci anlamında sağlanmadığı belirtilmektedir. PPA ilavesi ile genel kullanım oranı %5 mertebelerinde olan SBS'in bitümlü bağlayıcı içerisindeki oranı %3' seviyelerine kadar düşürülebilmekte ve böylece ekonomik avantaj sağlanabilmektedir. Diğer yandan, SBS'e göre daha ucuz olan sülfür katkısının da dördüncü bileşen olarak (sülfür/PPA/SBS modifiye asfalt) kullanılması ile yüksek sıcaklıklarda termal kararlılık sağlanabilmekte, SBS'in bitüm içerisindeki dağılımı geliştirilebilmekte ve asfalt karışımın düşük sıcaklık özellikleri de

geliştirilebilmektedir. Bu nedenle, PPA içeren NovaPrene katkılarının asfalt karışımlarda değişik katılma oranlarında denenmesinin literatür açısından yararlı olacağı, özellikle tartışmalı olan düşük sıcaklık probleminin değerlendirilmesi anlamında yarar sağlayacağı düşünülmektedir.

Anahtar Kelimeler: Asfalt kaplamalar, polifosforik asitli polimer, SBS kompozit polimer, düşük sıcaklık çatlaması.

INTRODUCTION

Because of heavy loads and increased traffic volume, modification of asphalt binder with different types of modifiers has become very common recently to enhance the asphalt pavement service life (Hossain & Wasiuddin, 2019). Polymer modification of asphalt binders has increasingly become the norm in the construction of modern asphalt pavements. Styrene butadiene styrene (SBS) is the widely used polymer for bitumen modification (Yıldırım, 2007). Former studies have shown that the strength of mixtures against rutting, fatigue, and moisture damage increases after utilizing SBS in the bitumen modification (Kök et al., 2013).

The content of polymer is usually in the range from 2 to 5% by weight of bitumen; a higher content of polymer is considered to be an economic disadvantage (Jaso et al., 2015). SBS is an elastomeric block copolymer. It has three chains: polystyrene, polybutadiene, and polystyrene. Polystyrene is a tough, hard plastic which gives durability and stiffness and polybutadiene gives rubbery properties. Polymer and maltenes control the low temperature properties of SBS modified asphalt binder. At high temperature, SBS modified asphalt binder shows the highest recovery on strain with non-recoverable creep compliance (Al-Adham & Wahhab., 2015)

In the case of incorporation of thermoplastic elastomers into asphalt, the butadiene phase of copolymer becomes swollen with the absorption of oil fractions (i.e., maltenes). Consequently, the original volume of the polymer increases by about 4 to 10 times. This phenomenon is the key to the development of a three-dimensional polymeric network in an asphalt blend, with the SBS passing elastomeric properties to the whole blend and maintaining its melting ability at high temperatures. There is a main disadvantage with the partial miscibility of these polymers. This negative aspect leads to limited compatibility of the polymer modified asphalt (PMA) with the polymer having a tendency to separate from the asphalt when stored at high temperatures without stirring (Jaso et al., 2015).

Besides the polymer modification, polyphosphoric acid (PPA) has been used as a means of producing modified binders for the last 30 years, and the interest to use it has increased in recent years (Asphalt Institute, 2005).

PPA is an inorganic polymer of orthophosphoric acid (H_3PO_4). PPA raises both the saturates and asphaltenes at the expense of the cyclics and resins. As saturates convert into asphaltenes, asphaltenes increase and molecular weight (M_w) decreases. PPA affects the dispersed phase and the matrix of asphalt and as a result the two main phases in asphalt stiffen (Baumgardner et al., 2005; Ye & Fu, 2014).

As a rule of thumb, the introduction of a small amount of PPA (0.5 wt.%) can change the temperature and aging resistances of straight run asphalts, by reacting with the destabilizing components formed during thermal processes (Edwards, Tasdemir and Isacsson, 2006). The same authors observed that the addition of PPA made asphalt stiffer at low temperatures, although to a lesser extent than with the addition of waxes. The positive effect on rutting parameters by increasing stiffness at higher temperatures was also discussed. The resistance to aging is also among the advantages of PPA modified asphalt binder (Daranga, 2009).

PPA changes the high service temperatures of asphalt, while the low service temperatures of such binders remain mostly unchanged. The main reason for the modification of asphalt with PPA is the limitation of the amount of polymer needed for improved processing conditions, viscosity at high temperature and storage stability. The value of the temperature parameter ($|G^*|/\sin\delta$) can be increased further with almost no effect on the minimum service temperature (Hampl et al., 2015).

Since the early 1990s, PPA has also been used in combination with various polymer modifiers to enhance the quality of paving asphalts. The elastomeric polymer of SBS is the commonly used polymer in combination with PPA. The intention of adding PPA to the SBS-modified binders is to reduce their polymer content, which leads to modified asphalt binders with lower modification costs and enhanced rheological properties (Xiao et al. 2014). Therefore the combination use of SBS and PPA has been very popular worldly in the preparation of asphalt pavement material (Zhang et al., 2021).

PPA/SBS MODIFIED BITUMEN PREPARING METHOD

The suitable addition of PPA improved the high-temperature properties of base asphalt evidently without negative effect on the low-temperature behaviour. The better rutting resistance of PPA/polymer modified asphalt and its mixture are reported in many publications and the reasonable PPA content in asphalt should be 0.5–1.1% (Dong, 2018).

PPA is more effective when SBS modified binder is used for PPA modification. Several researchers investigated PPA and SBS modified asphalt binders separately and in combination. Results indicated that PPA modification provides better results when it is added with SBS modified asphalt binder. As indicated above, PPA increases the creep recovery and the non-recoverable creep compliance, but the effects of PPA are not significant at low temperatures and SBS modification helps in this regard (Domingos & Faxina, 2014).

The maximum speed of the high shear mixer needs to be set at 4000 rpm at any set temperature at or below 200 °C to control the temperature during mixing (Hossain & Wasiuddin, 2019). In a study, bitumen was heated to 170 ± 5 °C. After that, SBS was added to shear at 5000 rpm for 40 min (adding the sulfur flour stabilizer at last 10 min for control group), then PPA was added to shear at the same speed for another 30 min. SBS was used at the rates of 2.5%, 3% and 3.5%. In decreasing proportions of SBS, PPA was used at 0.5%, 1%, and 1.5%, respectively (Yang et al., 2022).

The changes in chemical compositions due to the modifications of selected asphalt binders with Polyphosphoric Acid (PPA) and Styrene Butadiene Styrene (SBS) were examined. Arabian and canadian bitumens were selected and PPA/SBS modified bitumens prepared. PG 64-22+0.5% PPA + 2.00% SBS and PG 64-22 + 0.75% PPA + 2.00% SBS composite materials were prepared. It is concluded that PPA modification is good at lower dosage levels and even better with polymers combined. The maximum level of PPA modification should never cross the optimum level rather it is better to stay lower than the optimum (Alam & Hossain, 2017).

In a research, PPA/SBS modified bitumen was prepared using a high-speed shearing machine. First, the base bitumen was heated to 140 °C while blended with the set amount of furfural extract oil and stirred evenly. The uniformly stirred bitumen was then placed in a heating device for heating to 160 °C, and the set amount of DBP was added during uniform stirring. After that, the temperature was increased rapidly to 175 °C, and the SBS modifier was added during full, uniform stirring and allowed to swell for approximately 10 min. Then, add the set amount of PPA into the swelling, modified bitumen, use the high-speed shear to shear for 30 min at a speed of 5000 r/min, control the temperature at approximately 175 °C, and then add the set amount of stabilizer and continue mixing for 10 min. Finally, the prepared PPA/SBS modified bitumen product was developed continuously for 2.5 h. (Li et al., 2021).

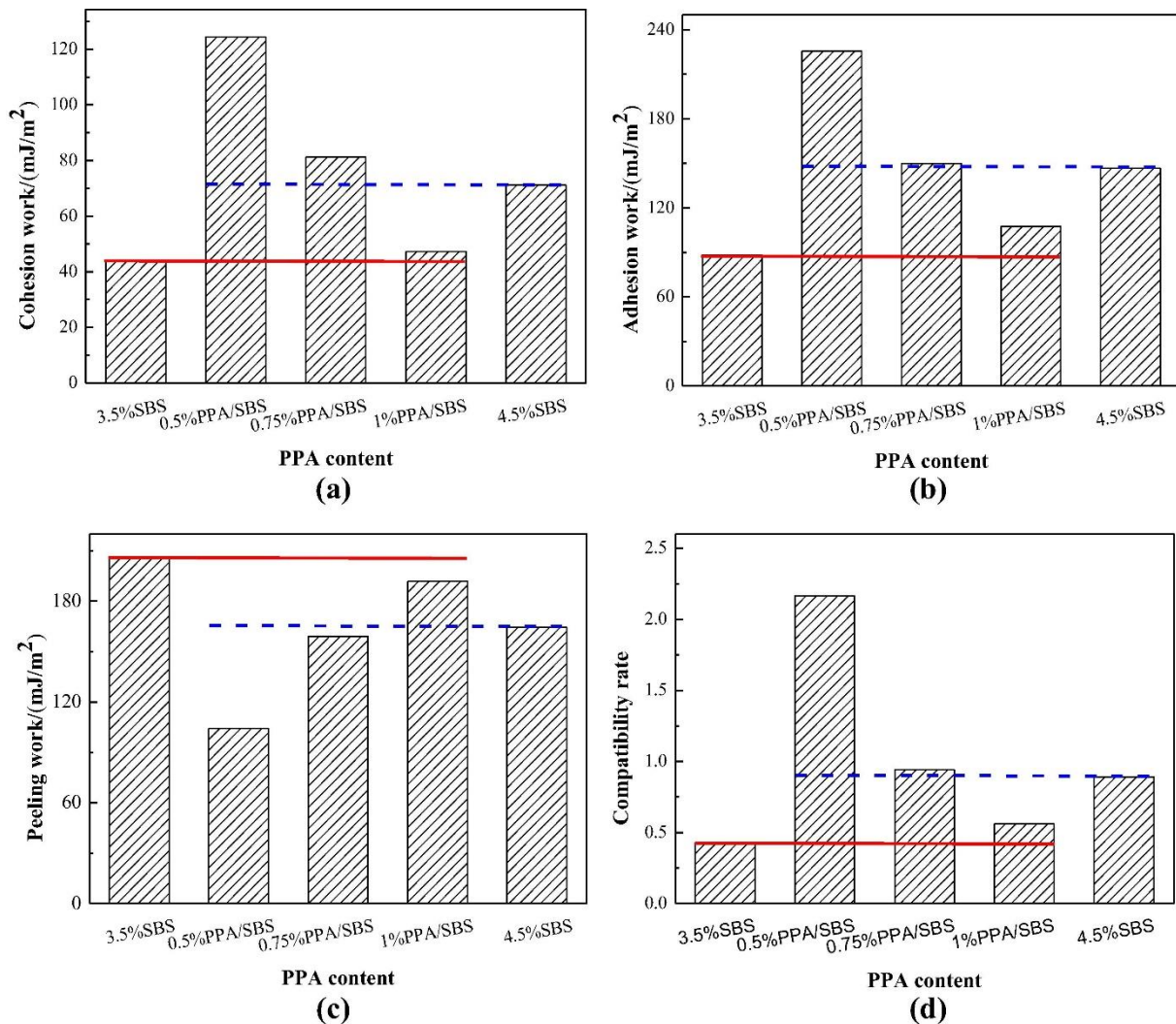


Figure 1. Adhesion index of PPA modified bitumens (Li et al., 2021).

The effect of base bitumen type, PPA type and raw materials content on the adhesion performance of polyphosphoric acid compounded SBS (PPA/SBS) modified bitumen was evaluated quantitatively using the contact angle test and surface free energy method. Three different bituminous materials, two types of PPA, SBS, stabilizer, compatibilizer and dibutyl phthalate (DBP) were used as raw materials to prepare PPA/SBS modified bitumen. The results indicate that the water damage resistance of SBS modified bitumen can be improved by adding PPA, but when the content exceeds a certain value, the water stability of PPA/SBS modified bitumen becomes worse. Increasing the content of PPA decreased the cohesion work, adhesion work and compatibility rate of PPA/SBS modified bitumen, while the peeling work increased. When the amount of extracted oil and SBS modifier are increased, the cohesion work, adhesion work and compatibility rate of PPA/SBS modified bitumen increased first and then decreased, whereas the peeling work decreased first and then increased. When the PPA content is 0.5%, and SBS content is 3.5%, the water damage

resistance of PPA/SBS modified bitumen is the strongest. The economic benefits are also considerable when using this material composition for PPA/SBS modified bitumen (Li et al., 2021).

Table 1. Modification parameters and modifier ratios used in some studies in the literature

SBS ratio (%)	PPA ratio (%)	Mixing time	Mixing temperature (°C)	Shearing speed (r/min)	Reference
4.0	0.8	SBS-bitumen one hour with high shear mixer and PPA-SBS modified bitumen 2 hour with mechanical mixer	180–190	8000	(Zhang et al., 2021).
2.0	0.5, 0.75	PPA/SBS modified bitumen was mixed for one minute with a stirring rod at 100 °C and put inside an oven heated at the 100 °C temperature for 10 min. Mixing repeated two more times to complete the blending process.	100	Manuel mixing	(Alam & Hossain, 2017).
2.8	0.4, 0.8, 1.2, 1.6	SBS-bitumen was stirred at 160 °C for 2 h, and then mixed further at 165–170 °C by a high-speed shearing machine at a speed of 5000 rpm for 45 min. PPA was added, using a high-speed shearing machine for 20 min. Place the mixtures in the oven at 170 °C for 60 min.	170	5000	(Ma et al., 2021).
2.5, 3.0, 3.5	0.5, 1.0, 1.5	Bitumen was raised to 170 ± 5 °C. After that, SBS was added to shear at 5000 rpm for 40 min, then PPA was added to shear at the same speed for another 30 min. Finally, the prepared composite modified asphalt was put into a vacuum drying oven, swelled at 170 °C for 1 h, and the bubbles were eliminated.	170	5000	(Yang et al., 2022)
2.5, 3.0, 3.5	0.5, 1.0, 1.5	SBS modification: bitumen was raised to 170 ± 5 °C with continuous stirring, then SBS was added and sheared at 5000 rpm for 40 min, and the stabilizer (sulfur flour, 0.2% of binder by weight) was added in the last 10 min; PPA modification: PPA was added and sheared at 5000 rpm for 30 min (SBS control group shear for 30 min without PPA addition); Swelling development: the prepared composite-modified BMA was placed in a vacuum drying oven at 170 °C for 1 h.	170	5000	(Liu et al., 2022)
3	0.4, 0.8, 1.2, 1.6	First, base asphalt were poured into a steel container when it heated to fluid state at 160°C; then a certain amount polymers (3.0 wt% SBS) were slowly mixed into asphalt at the speed of 4000 rpm for 40 min, after that PPA was added into these blends at the speed of 4000 rpm for 40 min. The PPA and polymers modified	160	4000	Liu, Zhou & Peng, 2020)

INTERNATIONAL AEGEAN CONFERENCES
ON INNOVATION TECHNOLOGIES & ENGINEERING-VI
 December 20-22, 2022

		asphalt were prepared in the lab through a high-speed shear mixer			
0.5, 2.0, 3.5	2	PPA is mixed and then SBS is mixed with PG 64-22 binder. The speed of the high shear mixer is set to 2,000 rpm. Mixing of PPA is done in two stages: first, the PPA is mixed with a mechanical mixer for 15 minutes; second, the mixed sample is sheared at 180°C for 30 minutes. Then 0.5%, 2%, and 3.5% SBS by weight of PG 64-22 are mixed with the 2% PPA modified PG 64-22. SBS is mixed with the base binder by a mechanical mixer for 15 minutes and then sheared for two hours with a high shear mixer at 180°C. The speed is set to 4,000 rpm.	180	4000 .	(Hossain &Wasiuddin, 2019)
4.0	0.2	SBS was gradually added to the melted bitumen under a high-speed shear mixer of 5500–6000 r/min. The mixture was stirred by a mechanical stirrer at 180 °C for 2 h while the rotation speed of mechanical stirrer was 300 r/min. The PPA was added to polymer modified bitumen at a level of 0.2% by weight at 180 °C. The mixture was heated and maintained at 180 °C and continuously mixed at 5500–6000 r/min for 30 min in a closed beaker to avoid any oxidation process.	180	5500–6000	(Rossi et al. 2015)
3.0, 2.5	0.75	Polymer modifier was blended stirring for 10 min to obtain (sbs mod. bit.) before shearing at a speed of 4000 r/min for 60 min at 175–180 C (for SBS modified). For composite modified binder, sheared for 30 min at the speed of 4000 r/min, under 160 C to produce PPA + SBS.	160	4000	(Liu et al., 2018)
3.5	0.5, 1.0, 1.5, 2.0	Base asphalt was heated up to 180°C; solubilizer and SBS-modifying agent which accounted for 3.5% of base asphalt mass were added. high-speed shearing emulsifying machine was used to operate at the speed of 4000 r/min for 40 min, and then stabilizer was added to shear for 5 min. It was put into a constant temperature oven at 160°C to grow for 1.5 hours.)en, PPA which accounted for 0.5%, 1.0%, 1.5%, and 2.0% of asphalt mass was added to it to be sheared at the speed of 1000 r/min for 10 min.	160	4000	(Li et al., 2019)
unspec ified	0.5, 1.0, 1.5, 2.0	The PPA modifier was added into the SBS-modified asphalt at 0.5%, 1.0%, 1.5%, and 2.0% of the weight of SBS-modified asphalt. The modified asphalt binders were prepared in a high-shear mixing instrument at around 190°C and at 4,000 rpm. After mixing for about 30 min, the modified asphalt binders were used for testing.	190	4000	(Du et al., 2020)

When the content of PPA is 0.5%, the cohesion work, adhesion work and compatibility rate of PPA/SBS modified bitumen are the largest, and the peeling work is the smallest. These results may be attributed to the chemical reaction between PPA and SBS modified bitumen. After adding a certain amount of PPA, the content of aromatics and resin changes drastically, which leads to the change in adhesion performance of SBS modified bitumen. Beyond this amount, the continued addition of PPA does not produce the ideal benefits (Alam & Hossain, 2017).

MORPHOLOGICAL PROPERTIES OF PPA/SBS MODIFIED BITUMENS

PPA and sulfur as the major modifiers in improving the high-temperature performance or storage stability of SBS- and SBR-modified asphalt have been used widely in practice (Zhang & Hu, 2013). Asphalt binder modified with SBS polymer was investigated and observed that aging causes both oxidation and SBS degradation. After aging, the colloidal instability index values increase for both the base binder and the SBS. Aging lowers the aromatics content and simultaneously increases the resins and asphaltenes contents, with insignificant change in the saturates contents. These types of changes have occurred because of the oxidation of asphalt binder and chemical reaction between the binder and SBS (Dehouche, Kaci and Mokhtar, 2012).

Due to the gelation of PPA, the aromatics content declines and the boundary layer between polymer and asphalt is destroyed to some extent and becomes very poor, so it would not be possible for the polymer particles to be swelled fully in the asphalt and the storage stability of the SBS-modified asphalt declines further by the addition of PPA. However, the storage stability of SBS-modified asphalt is improved significantly with the addition of sulfur. By chemical crosslinking, the polymer molecules are connected with each other by polysulfide bonds, a continuous polymer network is formed. In this process, the polymer molecule chain is spreaded out fully, the morphology changes greatly from the coarse particle to the filamentous polymer network, therefore the contact layer between polymer and asphalt increases further and the boundary layer becomes fine, the compatibility of the PMAs is improved obviously. The morphology of the SBS/PPA modified asphalt changes little compared to the SBS-modified asphalt, showing the poor compatibility between the polymer and asphalt (Figure 2). However it is still possible for the SBS modified asphalt to be stable by the addition of the proper amount of PPA and sulfur (0.5% PPA, 0.1% sulfur), and the filamentous polymer network is formed by chemical crosslinking.

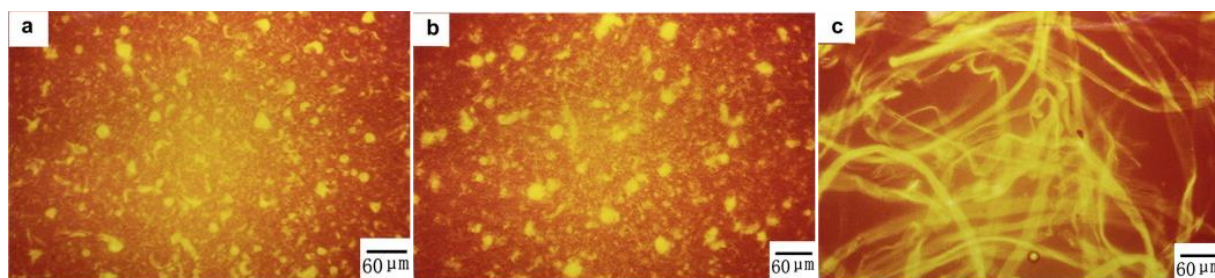


Figure 2. The morphology of the base and modified bitumens: (optical microscopy) at a magnification of 400. (a) The SBS modified bitumen (b) The SBS/PPA modified bitumen (c) SBS/PPA/sulfur modified asphalt. (Zhang & Hu, 2013).

Effects of PPA on high-temperature performance, temperature susceptibility, and anti-aging performance of SBS- PPA modified asphalt binders were evaluated. The addition of PPA enhanced the asphalt's resistance to temperature susceptibility. In addition, PPA played a significant role in improving asphalt performance at high temperatures. It indicated that the substitution of SBS polymers with PPA could enhance the binder's resistance to permanent deformation and temperature sensitivity, with a PPA content between 0.4% and 1.6%. Also, the increased G^* , failure temperature and R, and the decreased VTS and Jnr all indicated that a substitution of 5% SBS with 1.6% PPA-SBS was feasible. Due to the degradation of SBS polymer in the aging process, the PPA-SBS composite modified asphalt performed better after aging when the dosage of PPA increased, leading to the question of what is the optimum PPA content in real life considering both the cost and performance. After evaluating comprehensively the high-temperature performance, thermal-sensitivity and elastic recovery, the optimal content of PPA in PPA-SBS composite modified asphalt was considered between 0.8% and 1.2% (Ma et al., 2021).

PPA can improve the high-temperature performance of the SBS-modified asphalt evidently but decline the storage stability. Owing to the gelation of PPA, the phase separation of SBS becomes more serious. Sulfur can improve the storage stability and high-temperature performance of SBS-modified asphalt by chemical crosslinking. Because the compatibility between SBR and asphalt is very fine, so it is possible to modify further only by the addition of PPA and the PPA content is 2 wt%. For the SBS1301-modified asphalt, the compatibility between asphalt and SBS is modest. In the process of improving the storage stability by vulcanization, it is reasonable to improve the high-temperature property further before and after ageing by the addition of PPA, the content of sulfur and PPA is 0.1 wt% and 0.5 wt% respectively (Zhang & Hu, 2013).

MECHANICAL PROPERTIES OF PPA/SBS MODIFIED BITUMEN AND ASPHALT MIXTURES

The stiffness of asphalt binders can be increased by adding polyphosphoric acid (Gao et al., 2021). 0.1 to 0.5 wt% of PPA acts as a stiffener and cross-linker when combined with SBS and reactive terpolymers (Olabemiwo et al., 2016). PPA facilitates resistance to aging for RTFO and PAV aged SBS modified binder, and thereby the combination of PPA and SBS polymer had better short-term aging resistance (Gao et al., 2021). There is a synergistic effect between SBS and PPA, resulting in improved stiffness and elasticity.

However, in some studies, it is stated that the low temperature properties of SBS modified bitumen are improved with the addition of PPA. In a study study, a PPA acid modifier was added to SBS-modified asphalt to improve low-temperature behavior. Fractional viscoelasticity model was used to describe the BBR results and calculate the damping ratio $\xi\xi$ and the dissipation energy ratio $\omega\omega$ of the different asphalt binders. The addition of PPA to SBS-modified asphalt binder altered its molecular structure and increased the stickiness at low temperatures. However, the structural changes were significantly restricted by the temperature. FTTR spectroscopy showed differences in the functional groups in the modified asphalt binders compared with the SBS-modified asphalt. There was indeed a reaction between the PPA modifier and the SBS-modified asphalt binder. The chemical bond ratio showed that the modifier significantly improved the low-temperature performance of the asphalt binders, within a certain range of PPA concentration. However, the effect was reduced or remained stable when the PPA content continued to increase (Du et al., 2020).

Changes in rutting and fatigue resistances of the PG 58-22 asphalt binder modified with SBS due to partial replacements of the SBS with the PPA additive were investigated. The MSCR and LAS tests were used to determine the rutting and fatigue characteristics of the binders, respectively. The complex modulus test was also used to relate the test results of the binders to the mixtures' stiffness parameter. The SBS content of the SBS binder and the PPA content of the SBS+PPA binders were kept constant at 6 and 1%, respectively. Two different SBS + PPA binders were investigated, for which the SBS contents were determined to be 2 and 4% as well as to have the same continuous PG and the same rotational viscosity (at 135°C) as the SBS binder, respectively. Based on the results of Jnr and R values at the nonlinear stress levels, it was found that the SBS4+PPA1- and SBS2+PPA1-modified binders have the highest and lowest rutting resistance, respectively. Rutting and fatigue resistances of the SBS-modified binder prepared by adding the SBS additive to the PG 58-22 base binder improve through partial replacement of the SBS with PPA such that the viscosity of the SBS binder is not changed. Although the results of the MSCR and LAS tests were found to be in good agreement with the stiffness parameter of the mixtures (Jafari, Babazadeh and Rahi, 2017).

Studies were carried out to examine if the addition of PPA will alter the thermal stability of SBS-MBs during storage, where the presence of air is limited. The addition of 0.4 wt% PPA reduces the rate of erosion in SP by $\approx 50\%$ after 14 days of storage. Similarly, the deterioration in δ and η^* reduces considerably in the presence of PPA. PPA successfully reduced property erosion during storage. To understand the interaction of PPA with binder and SBS modified binder, FT-IR analysis was carried out for the pure PPA, fresh SBS-MB with and without PPA, and 14 days stored SBS-MBs with PPA. A strong peak (P-O-P stretching) at 1012 cm^{-1} is observed for the PPA molecule. The PPA peak is still present in the SBS-MB, even though only 0.4 wt% of PPA was added in the SBS-MB. The presence of the PPA peak in the SBS-MB around 1000 cm^{-1} indicates the interaction between PPA and

SBS molecules. Hence, the PPA molecules interact with the C bond in the butadiene segment, making it more thermally stable. In general, the proton released by PPA stabilizes the charge by resonance. Considering that aspect, the erosion rate during thermal storage reduces due to the arrest of SBS molecules by protons from PPA (Singh, Pandey and Ravindranath, 2022).

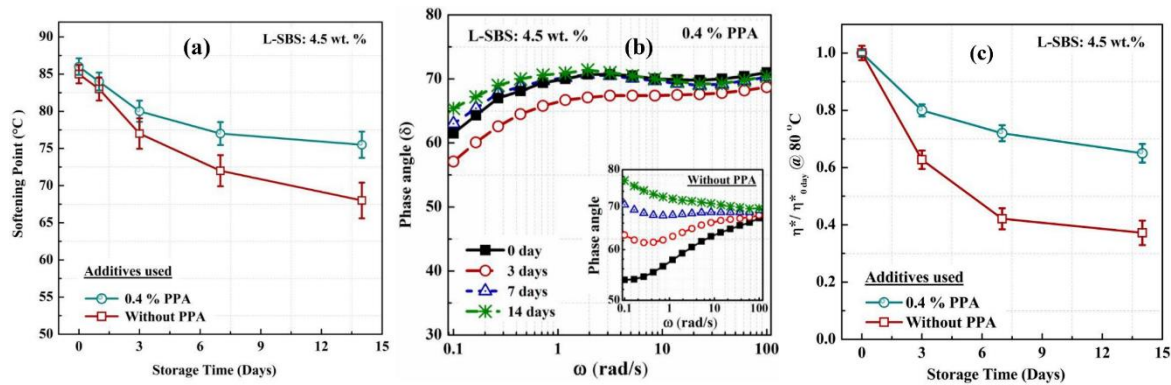


Figure 3. Some properties of SBS modified bitumens with and without PPA (a) Softening point (SP), (b) Phase angle (δ), and (c) Normalized (η^*) (Singh, Pandey and Ravindranath, 2022).

Creep response of PPA modified asphalt binders (base and polymer modified) and mixtures at intermediate and low temperature were investigated. BBR, TSRST were applied to evaluate creep at low temperature. Modified penetration test was proposed for intermediate temperature. Addition of PPA slightly decreased creep stiffness of both base and polymer modified asphalt binder before aging. While creep stiffness of binders cooperating PPA increased after aging (long and short term) when compared with binders without PPA. Modified penetration test indicated that creep rate of binder started at a lower point when indentation contacts happened, and its relationship with contact stress was well fitted through modification of Norton function. Besides, creep rate change at intermediate temperature was slower after adding PPA, especially for base binders whose creep rate declined a lot. In tensile stress restrained specimen test (TSRST), addition of PPA improved fracture strength and accelerated viscoelastic-elastic transition as well as weakened stress relaxation, which is undesired for low-temperature loading. Samples cracked earlier and faster within a small temperature range. Thus it possibly had negative effect on low temperature performance of asphalt mixtures and PPA is more applicable in SBR and SBS modified mixtures than base ones with respect to low temperature performance (Liu et al., 2018). The literature indicates that PPA improves the high-temperature rheological properties of asphalt binders with only minor effects on their properties at low temperatures (Jafari & Babazadeh 2016).

Due to the lower cost of PPA, the use of it in the preparation of SBS modified asphalt declines the SBS content to a great extent. Therefore, the great cost performance of PPA has been approved widely nowadays (Zhang & Hu, 2013).

The advantages described above can be achieved by adding PPA to SBS modified asphalt binders. Adding the PPA component to the asphalt binder separately causes labor and time loss. In this sense, testing the PPA/polymer additives developed as composites, for example NovaPrene additives, and expanding the subject in different addition conditions and rates are considered important especially in terms of the low temperature performance of the asphalt mixture.

CONCLUSIONS

In road pavement engineering, polymer modified asphalts are preferred more and more in order to meet the increasing stresses on the roads. Among the polymer asphalt additives, SBS is among the most widely used agents. SBS modified asphalt mixtures highly meet expectations such as rutting, fatigue and water damage resistance. However, SBS modified bitumen has some disadvantages such as high cost and storage stability.

With the latest technological developments, researches are carried out to further increase the performance of SBS modified asphalt mixtures. These researches are generally focused on producing composite materials with multiple additive applications and producing synergetic benefits. PPA/SBS modified asphalts can be presented as an example of composite materials. It is understood that the mechanical properties of asphalt mixtures can be improved at medium and high temperatures by adding PPA to SBS modified asphalts. However, there are recommendations that the addition of PPA is ineffective or has a negative effect due to the increased stiffness of the mixture at low temperatures.

Sulfur addition is recommended as a solution in order to prevent the ineffectiveness or negative effect of PPA addition at low temperature.

It is emphasized that the cost of PPA is lower than SBS, and the cost of asphalt mixture can be reduced by substituting PPA for SBS. In PPA/SBS/bitumen modification, the most effective rates for PPA can be given between 0.5% and 1%. 0.5% is more preferred. The SBS rate can be reduced from 5%, which is the common usage rate, to 3.5%.

REFERENCES

- Al-Adham, K., and Wahhab, H. A. (2018). Influence of Temperature on Jnr Values of Polymer Modified Asphalt Binders. *International Journal of Pavement Research and Technology*, 11, 603–610.
- Alam, S., & Hossain, Z. (2017). Changes in fractional compositions of PPA and SBS modified asphalt binders. *Construction and building materials*, 152, 386-393.

- Asphalt Institute. (2005). "Polyphosphoric acid modification of asphalt." IS 220, Lexington, KY
- Baumgardner, G. L., Masson, J. F. Hardee, J. R. Menapace, A. M. and Williams, A. G. (2005). Polyphosphoric Acid Modified Asphalt: Proposed Mechanisms. *Journal of Association of Asphalt Paving technologists*, 74, 283–305.
- Daranga, C. Clopotel, C. Mofolasayo, A., Bahia, H. Storage stability and effect of mineral surface on polyphosphoric acid (PPA) modified asphalt binders Presented During Poster Session, 88th Annual Meeting of the Transportation Research Board, Washington, D.C. (2009), 2-11
- Dehouche, N., Kaci, M. and Mokhtar, K. A. (2012) Influence of Thermo-oxidative Aging on Chemical Composition and Physical Properties of Polymer Modified Bitumens. *Construction and Building Materials*, 26, 350–356.
- Domingos, M. D. I., and Faxina, A.L. (2014). Creep-recovery Behavior of Asphalt Binders Modified with SBS and PPA. *Journal of Materials in Civil Engineering*, 26(4) 781–783.
- Dong, G. Performance and mechanism of asphalt modified with polyphosphoric acid and polyphosphoric acid/polymer. Doctor Thesis. Changan University. Xian. China, 2018.
- Du, J., Ai, C., An, S., & Qiu, Y. (2020). Rheological properties at low temperatures and chemical analysis of a composite asphalt modified with polyphosphoric acid. *Journal of Materials in Civil Engineering*, 32(5), 04020075.
- Edwards, Y., Tasdemir, Y., Isacson, U. Rheological effects of commercial waxes and polyphosphoric acid in bitumen 160/220 — low temperature performance. *Fuel*, 85 (7–8) (2006), 989-997
- Gao, L., Cai, N., Fu, X., He, R., Zhang, H., Zhou, J., & Liu, S. (2021). Influence of PPA on the Short-Term Antiaging Performance of Asphalt. *Advances in Civil Engineering*, 2021
- Hampl, R., Vacin, O., Jasso, M., Stastna, J., & Zanzotto, L. (2015). Modeling of tensile creep and recovery of polymer modified asphalt binders at low temperatures. *Applied Rheology*, 25(3), 32-39.
- Hossain, R., & Wasiuddin, N. M. (2019). Evaluation of degradation of SBS modified asphalt binder because of RTFO, PAV, and UV aging using a novel extensional deformation test. *Transportation Research Record*, 2673(6), 447-457.
- Jafari, M., & Babazadeh, A. (2016). Evaluation of polyphosphoric acid-modified binders using multiple stress creep and recovery and linear amplitude sweep tests. *Road Materials and Pavement Design*, 17(4), 859-876.

- Jafari, M., Babazadeh, A., & Rahi, M. (2017). Evaluating rutting and fatigue characteristics of binder containing SBS and PPA and their relationship with the mixture stiffness parameter. *Journal of Materials in Civil Engineering*, 29(9), 04017143.
- Jasso, M., Hampl, R., Vacin, O., Bakos, D., Stastna, J., & Zanzotto, L. (2015). Rheology of conventional asphalt modified with SBS, Elvaloy and polyphosphoric acid. *Fuel Processing Technology*, 140, 172-179.
- Kök, B. V., Yilmaz, M., & Geçkil, A. (2013). Evaluation of low-temperature and elastic properties of crumb rubber–and SBS-modified bitumen and mixtures. *Journal of Materials in Civil Engineering*, 25(2), 257-265.
- Li, B., Li, X., Kundwa, M. J., Li, Z., & Wei, D. (2021). Evaluation of the adhesion characteristics of material composition for polyphosphoric acid and SBS modified bitumen based on surface free energy theory. *Construction and Building Materials*, 266, 121022.
- Li, X., Pei, J., Shen, J., & Li, R. (2019). Experimental study on the high-temperature and low-temperature performance of polyphosphoric acid/styrene-butadiene-styrene composite-modified asphalt. *Advances in Materials Science and Engineering*, 2019.
- Liu, G., Zhang, W., Yang, X., & Ning, Z. (2022). Study on the Conventional Performance and Microscopic Properties of PPA/SBS-Modified Bio-Mixed Asphalt. *Materials*, 15(12), 4101.
- Liu, H., Chen, Z., Wang, Y., Zhang, Z., & Hao, P. (2018). Effect of poly phosphoric acid (PPA) on creep response of base and polymer modified asphalt binders/mixtures at intermediate-low temperature. *Construction and Building Materials*, 159, 329-337.
- Liu, S., Zhou, S., & Peng, A. (2020). Evaluation of polyphosphoric acid on the performance of polymer modified asphalt binders. *Journal of Applied Polymer Science*, 137(34), 48984.
- Ma, F., Li, C., Fu, Z., Huang, Y., Dai, J., & Feng, Q. (2021). Evaluation of high temperature rheological performance of polyphosphoric acid-SBS and polyphosphoric acid-crumb rubber modified asphalt. *Construction and Building Materials*, 306, 124926.
- Olabemiwo, O. M., Esan, A. O., Adediran, G. O., & Bakare, H. O. (2016). The performance of Agbabu natural bitumen modified with polyphosphoric acid through fundamental and Fourier transform infrared spectroscopic investigations. *Case Studies in Construction Materials*, 5, 39-45.
- Rossi, C. O., Spadafora, A., Teltayev, B., Izmailova, G., Amerbayev, Y., & Bortolotti, V. (2015). Polymer modified bitumen: Rheological properties and structural

- characterization. *Colloids and Surfaces A: Physicochemical and Engineering Aspects*, 480, 390-397.
- Singh, S. K., Pandey, A., & Ravindranath, S. S. (2022). Effect of additives on the thermal stability of SBS modified binders during storage at elevated temperatures. *Construction and Building Materials*, 314, 125609.
- Xiao, F., Amirkhanian, S., Wang, H., and Hao, P. (2014). "Rheological property investigations for polymer and polyphosphoric acid modified asphalt binders at high temperatures." *Construction and Building Materials*., 64, 316–323.
- Yang, X., Liu, G., Rong, H., Meng, Y., Peng, C., Pan, M., Ning, Z., & Wang, G. (2022). Investigation on mechanism and rheological properties of Bio-asphalt/PPA/SBS modified asphalt. *Construction and Building Materials*, 347, 128599.
- Ye, Q. and Fu, H. (2014). Rheological Properties of Polyphosphoric Acid Modified Asphalt Binder. *Indian Journal of Engineering and Material Sciences*, 21, 214–218.
- Yildirim, Y. (2007). Polymer modified asphalt binders. *Construction and Building Materials*, 21(1), 66–72.
- Zhang, F., & Hu, C. (2013). The research for SBS and SBR compound modified asphalts with polyphosphoric acid and sulfur. *Construction and Building Materials*, 43, 461-468.
- Zhang, F., Kaloush, K., Underwood, S., & Hu, C. (2021). Preparation and performances of SBS compound modified asphalt mixture by acidification and vulcanization. *Construction and Building Materials*, 296, 123693.

**ASFALT KAPLAMALARDA İŞLENEBİLİRLİK ARTIŞI İLE HIZLI SOĞUMAYLA
OLUŞAN DAYANIM KAYIPLARININ ÖNLENMESİ**
PREVENTION OF STRENGTH LOSSES CAUSED BY RAPID COOLING WITH
INCREASED WORKABILITY IN ASPHALT PAVEMENTS

Celaleddin Ensar ŞENGÜL

Dr., Devlet Su İşleri Genel Müdürlüğü, 14. Bölge Müdürlüğü, İstanbul, Türkiye

ABSTRACT

Low temperature cracking in asphalt pavements is one of the major pavement problems. Although problems such as water damage and rutting problems can be managed to a great extent with additives, the management of the low temperature problem is foreseen as a more complex problem. Compaction losses and problems may occur due to rapid cooling during pavement production. This means strength loss. In addition, the application of high temperatures can increase the level of damage, for example, gas incense in tunnel pavement courses. It is evaluated that some amine-derived chemicals improve the workability conditions of the mixtures. In this research, it is aimed to investigate the degree of improvement of the workability conditions of the selected amine type chemical additive (Pawma).

Keywords: Asphalt pavements, low temperature cracking, Marshall test, workability, cooling.

ÖZET

Asfalt kaplamalarda düşük sıcaklıktaki çatlamlar en önemli kaplama problemlerinden biridir. Su hasarı ve tekerlek izi gibi problemler katkı maddeleri ile büyük ölçüde çözülebilse de düşük sıcaklık probleminin yönetimi daha karmaşık bir problem olarak öngörülmektedir. Üstyapı üretimi sırasında hızlı soğuma nedeniyle sıkıştırma kayıpları ve sorunları meydana gelebilir. Bu dayanım kaybı anlamına gelir. Ayrıca, yüksek sıcaklıkların uygulanması, örneğin tünel kaplama tabakalarında bitüm dumanı salınımını, hasar seviyesini artırabilir. Bazı amin türevi kimyasalların karışımların işlenebilirlik koşullarını iyileştirdiği değerlendirilmektedir. Bu araştırmada, seçilen amin tipi kimyasal katkı maddesinin (Pawma) işlenebilirlik şartlarındaki iyileştirme derecesinin araştırılması amaçlanmıştır.

Anahtar Kelimeler: Asfalt kaplama, düşük sıcaklık çatlama, Marshall testi, işlenebilirlik, soğuma

INTRODUCTION

It is extremely important that asphalt mixes are compacted in situ as designed. Homogeneity issues and internal friction management are important for performance. In order to manage this issue, additive alternatives and constructive studies are carried out. In this context, it is understood that machinability-oriented contributions are and will be effective in performance management.

It is known that even a decrease in temperature values by 1°C can significantly change the measured performance value. It is known that the effect of these temperature drops creates more negative conditions than expected in the context of the relativity level of the void values formed in the field due to compression. Therefore, it is extremely important to improve the machinability and surface positivity conditions in order to ensure effective compaction at lower possible temperatures.

While the main problems such as water damage and rutting can be managed with additives, low temperature cracking problems seem more difficult to manage and show a more professional approach.

Especially design-related problems and unavoidable aggregate angularity and segregation problems make the problem more dramatic in the low temperature context.

In this study, the use of Pawma additive, whose workability-oriented feature is specified, as a domestic product in this sense, with extensive literature research, is presented as a synthesis study. A comprehensive literature study has been carried out and the literature on the Pawma contribution is given in this context. In addition, studies will be carried out with the experiments determined at this reporting point in the future. As stated in the literature, it is foreseen that an important field performance gain will be created with this directional function.

EVALUATION

The asphalt industry is striving to lower the mixing and compaction temperatures of the asphalt mix due to increased emissions, energy costs and workability. The production of Warm Mix Asphalt (WMA) is concerned with increasing the aggregate-bitumen composition and providing the appropriate viscosity of the bitumen for compaction and application of the mixture at low temperatures. The important advantages of Warm Mix Asphalt (WMA) are lower energy consumption, less pollution and workability. In general, the production temperature of the asphalt mixture depends on the characteristics of the asphalt. The effects of a certain amount by weight of Pawma, the selected warm mix asphalt additive, on the viscosity were evaluated in the Brookfield Rotational Viscometer device. In addition, the penetration and softening point measurements of the bitumen were obtained. The reduced viscosity of the bitumen will increase the production, workability and compaction of the

mixtures. In addition, the softening point and penetration values, the change in the sensitivity of the asphalt to temperature changes and the change in the road temperature of the asphalt are also in question. Asphalt mixtures can be applied at longer distances by reducing the cooling rate, and time can be saved in road construction. Pawma additive shows that the viscosity decreases, softening point and penetration value increase at the same rotation speed when additives are used. This will enable the road to be opened to traffic more quickly with the rapid results of the application (Şahin & İpek, 2019).

As a WMA additive, PAWMA was used for bitumen modification. PAWMA Warm Mixture Asphalt Additive is a type of amidoamine derivative produced by İstanbul Teknik. The chemical definition is defined as the hydrated alumina silicate of alkali metals and used before blending with bitumen. The bitumen temperature is not changed for the mixture but the mixture is prepared by decreasing the aggregate temperature by 30°C. The amount of use is between 0.2% and 0.5% of the bitumen weight. PAWMA was produced with amine compounds as well as peel inhibitor additives. It affects the structure of bitumen in a positive way and can not be said that the chemical properties of bitumen. It can increase peel strength and indirect tensile strength of asphalt (İstanbul Teknik, 2022-a).



Figure 1. Pawma additive (İstanbul Teknik, 2022-a).

Tablo 1. Pawma technical properties (İstanbul Teknik, 2022-a)

	Properties	Unit
Structure	Amidoamine derivative	
Physical appearance at 20 °C	Liquid	
Colour	Yellow - Orange	
Intensity	0.93 ± 0.2	g/cm ³
Ph	7-8	
Flash point	>150	°C
Viscosity at 25 °C	150	mPas

The additive feature is defined in the technical information given by the manufacturer. Energy savings are achieved due to low mixing temperature. Resources are used efficiently. A safe working environment is provided for worker health in the tunnels. In the time between laying and compaction, asphalt remains better workable. It does not spoil the chemical structure of asphalt, does not reduce the softening point of bitumen and does not cause rutting. Reduces aging of bitumen due to low production temperature. It offers application convenience. More efficient compression is achieved. Due to the low gas emission, the negative effects on worker health and the environment are reduced. Low operating temperature allows more comfortable and careful use of asphalt plant and machinery. It reduces work accidents. PAWMA is compatible with TeraGrip anti-stripping additive. If used together, the amount of TeraGrip can be reduced by up to 30% (İstanbul Teknik, 2022-a).

Table 2. Stripping performance values at different pawma additive ratios (İstanbul Teknik, 2022-a).

Stripping Strength Test, %	Test results	KTŞ 2013 Limits (Part 403-411)	Standard
Pure AC 50/70 with Bitumen	35-40	≥ 60	TS EN 12697-11 (app-A)
With AC 50/70 Bitumen and 0.3% Pawma Additive	95-100	≥ 80	TS EN 12697-11 (app-A)
With AC 50/70 Bitumen and 0.5% Pawma Additive	95-100	≥ 80	TS EN 12697-11 (app-A)

Table 3. Adhesion test performance values at different pawma additive ratios (İstanbul Teknik, 2022-b).

Adhesion Test (with Vialit Method) Number of Gravels Falling, %	Test results	KTŞ 2013 Limits (Part 403-411)	Standard
Pure AC 50/70 with Bitumen	30	≤ 10	TS EN 12697-11 (app-B)
With AC 50/70 Bitumen and 0.3% Pawma Additive	8	≤ 5	TS EN 12697-11 (app-B)
With AC 50/70 Bitumen and 0.5% Pawma Additive	5	≤ 5	TS EN 12697-11 (app-B)

The results of the Indirect Tensile Strength (ICM) Test with Bitumen without Additives at 140°C and the Indirect Tensile Strength (ICM) Test with 0.5% Additive (Pawma) at 140°C; shows that this value has increased from 82.6 to 86.7 (İstanbul Teknik, 2022 b). This value is evaluated as the additive increases the resistance to water damage as in stripping and vialite tests, and improves the workability conditions even at lower temperatures by creating an increase in performance in the mechanical test.

Pawma-1 is a liquid warm mix asphalt additive produced in our country and added to bitumen. It was used in field experiments and gave positive results (Kim et al., 2014).

The rheological and microstructural properties of chemical and wax warm additives in bituminous mastics with a recently launched additive named as PAWMA was evaluated. Then, outcomes of PAWMA concluded and compared with the results of Zycotherm and Sasobit modified bitumen along with properties of conventional wax additive. Furthermore, modified and unmodified bitumen's properties were checked and assessed by using standard testing Methodologies. The dynamic shear rheometer (DSR) test was done by using The Strategic Highway Research Program procedure for unaged and aged modified bitumens at moderate in-service temperatures ranges from 16 to 34 °C and at higher temperatures between 46 and 82 °C respectively. A bitumen penetration grade of 60/70 had been used as the indication binder in the production of mastic and bitumen specimens. In the preparation of limestone powder and mastics, were added by weight of bitumen to the base bitumen around 60%. Three different warm admixture contents including 0.2, 0.4 and 0.6% for PAWMA, 1, 3 and 5% for Sasobit, and mastics to Zycotherm at the concentrations of 0.07%, 0.10% and 0.15% were added as per weight of bitumen. In conclusion, although there was reduction in the mixing temperature for warm mastics, PAWMA displayed comparable rheological and micro-structural properties to reference mastic's properties. In terms of catana-phase structure and topography roughness of micro structural properties these were, apparently altered by Sasobit. The usage of the aforementioned proportions of chemical additives had not a notable influence on the nano-scale structure and AFM topography as compared to reference mastic (Mansoori & Modarres, 2020). It is understood that economic gains will be achieved by lowering the mixing temperatures.

Stability and ITSM values increased in warm mix asphalts, but tensile strength and creep modulus values were found to decrease. With the addition of hydrated lime, the tensile strength and creep performances of warm mix asphalts increased and results close to the control samples were obtained. While the Pawma-1 additive increased the fatigue strength slightly, the Leadcap additive decreased it a small amount. Fatigue performances of Leadcap modified mixtures were improved with lime additive. It would be beneficial to use hydrated lime additive together, as it has been seen that positive results were obtained in all tests applied to Leadcap modified mixtures. In Pawma-1 added mixtures, hydrated lime negatively

affected the indirect tensile stiffness modulus and fatigue performance, while it had a positive effect in other experiments. SBS modified mixtures with hydrated lime were found to give the best results (İstek, 2017).

The impacts of WMA additives (such as Sasobit®, Zeolite®, PAWMA®, and Kaowax®) and recovered asphalt pavement (RAP) materials on the mechanical and durability performance of HMA were investigated by (Mansoori & Modarres, 2020). As control mixtures, the characteristics of WMA & HMA containing 50% RAP were evaluated. Following that, the impact of WMA additions on the characteristics of each kinds of mixes with or without RAP were studied. At 25 °C, indirect tensile stress was applied, resilient modulus was measured at many temperatures of 5 °C, 25 °C, and 40 °C, dynamic creep was measured at 54.4 °C, and semi-circular bending fracture was measured at 25 °C. These experiments were carried out to assess the asphalt mixtures' mechanical properties, while the tensile strength ratio (TSR) was employed to assess the durability of WMA additions enhance asphalt mixture fracture energy, allowing up to 50% of RAP to be included in asphalt mixtures without affecting their mechanical performance, as indicated by the results. In the study, it was found that the fracture energy value of asphalt mixtures may be increased by up to 50% by adding WMA additives, without affecting the mechanical properties of the asphalt. In semicircular bending experiment for each type of mixtures, with or without RAP. Zeolitecontaining mixtures had the greatest strain energy values in both types of mixtures. In addition, the reduction in TSR values was observed in mixtures with Zeolite (Yousefi et al., 2021).

Additives: Different commercial WMA additives were used for SMA production. PAWMA® (A1), Licomont BS 100® (A2) and Evotherm M1® (A3) additives were received from the producers and added to bitumen at the recommended rates according to producers' technical sheets. Firstly, Marshall specimens were prepared for 50/70 bitumen as a control mixture. After that, Marshall specimens were prepared with the modified bitumens which were produced by adding A1, A2, and A3 at the rates of 0.3%, 3.0%, 0.4% of bitumen weight according to producers' technical sheets respectively. Effect of various WMA additives on SMA design parameters was investigated and results derived from the experimental study were compared with the control samples. According to the results of the WM-SMA Marshall tests, each of the additives reduced the SMA stability and increased the flow value within the specification limits. All additives increased the voids in mineral aggregates (VMA) and the voids filled with asphalt (VFA) of the mixtures, while the other additives reduce them. It was observed that WM-SMA prepared according to the manufacturer's catalog with the WMA additives lowered the mixing temperature by about 15 °C. This decrease in the mixture temperature means fuel savings and less harmful gas release during production in the asphalt plant (Aktaş, Aytekin and Aslan, 2019).

A1 is a kind of amidoamine derivative additive produced by Istanbul Teknik Company. It provides that asphalt mixture has longer workability and that a better compaction of asphalt is obtained. The chemical description is given as hydrated alumina silicate of alkali metals. It is used before mixing with bitumen. According to the manufacturer, the bitumen temperature for the mixture is not changed, but the mixture is prepared by reducing the aggregate temperature by 30°C. Usage amount is between 0.2% and 0.4% of the weight of the bitumen. Also, according to the manufacturer's recommendation, the dosage of the additive should be decided on site depending on the application type, whether or not the asphalt is modified, environmental conditions such as ambient temperature and wind. Since each application differs from the other, a standard dosage table is not available and the dosage should be determined according to local conditions. A1 additive is produced with amine compounds as well as anti-stripping additives. It affects the structure of the bitumen positively and does not disturb the chemical properties of bitumen. Asphalt increases stripping strength and indirect tensile strength. Since it does not contain water as it is zeolite-based or foam-activated admixtures, there is no water sensitivity (Istanbul teknik, 2018).

One of the scientific developments put into practice in asphalt production is warm mix asphalt technology. With the warm mix asphalt technology, asphalt production is possible at lower temperatures. In this study, Pawma-1 (0.35%) and Low Energy and Low Carbon-Dioxide Asphalt Pavement (Leadcap) (1.5%) warm mix asphalt additives and Styrene-Butadiene-Styrene (SBS) (2%) additives were used and tested in the mixture samples. In addition, the effects of using hydrated lime as filler in warm mix asphalts were also investigated. In the study, bitumen (B50/70) obtained from TÜPRAŞ refinery and limestone type crushed stone material obtained from Elazığ Hankendi region as aggregate were used. After the modified binders were prepared, the optimum bitumen ratios were determined according to the Marshall method and the mixture samples were prepared. In half of the mixture samples, 2% hydrated lime was used instead of filler. Marshall stability and yield test (ASTM D-1559) was applied on the prepared samples. Stability increased in mixtures prepared with Leadcap, Pawma-1 and SBS additives. It has been observed that hydrated lime increases the stability of warm mix asphalts. It was determined that the SBS modified mixtures with slaked lime gave the most positive results (İstek & Alataş, 2019).

In experiments on Pawma-1 modified binders, it was observed that the viscosity and penetration decreased, while the softening point increased (İstek & Alataş, 2017).

CONCLUSIONS

It is foreseen that the Pawma additive will make a great contribution in terms of adhesion and mixing homogeneity in this concept, especially considering the machinability-oriented definition. In the context of literary studies, it is seen that important contribution mechanisms

are provided in this direction. In this respect, expanding the scope of the study will create an important scientific field.

It is thought that the additive is compatible with slaked lime and can be successfully used in the interaction of amine-derived lime as a new synergy model.

It is evaluated that wet and dry adhesion will develop and this issue can be revealed by adhesion tests. It is understood that this improvement will automatically lead to an increase in indirect tensile strength and low temperature cracking resistance.

The workability advantages of the additive and the improvement of the possible reduction in compaction and strength properties of the mixture against possible temperature drops will be examined in terms of low temperature cracking and Marshall Parameters. This research studies to answer the question of how much can be done with the effect of workability in front of the strength losses that may occur due to fast cooling. The additive, which is considered as a workability enhancer within the scope of the research, can be used as in three different ratios in the recommended usage ratios. As the usage amount options, low, medium and high ratios may be applied as the common usage rates of the additive. It was decided to use 0.2%-0.4%-6% ratios. P1, P2, P3 notations will be used as the usage ratio symbol. Optimum mixing parameters were determined with the realized Marshall design. In order to simulate temperature drops and workability in the field, 3 briquettes may be preferred and produced in each option at the optimal bitumen values determined. Three identical briquettes could be produced for the selected P1, P2, P3 additive ratios. In addition, three briquettes would be produced in each option in the control condition. Production can be made under the conditions of 135°C, 140°C, 145°C, and 150°C as the mixing temperature. In the samples where Modified Lottman conditioning can be used as water damage conditioning, low temperature cracking resistance tests and workability-oriented mixture performance may be examined at this selected performance problem.

In terms of the scope of the study, it is predicted that it would be appropriate to choose these parameters and the examination method according to our Marshall design values that were previously carried out.

REFERENCES

- Aktaş, B., Aytekin, Ş., & Aslan, Ş. (2019). Evaluation of typical wma additives on design parameters of SMA mixtures. *Revista de la Construcción*, 18(3), 409-417.
- İstanbul Teknik. (2018). Pawma Warm Mix Asphalt Additive. Retrieved July 7, 2018, from <https://www.istanbulteknik.com/en/asphalt-products/pawma-warm-mix-asphalt-additive>

- İstanbul Teknik. (2022-a). Karayolları Asfalt Çözümleri, chrome-extension://efaidnbmnnnibpcajpcglclefindmkaj/https://www.istanbulteknik.com/pdf/karayolu_asfalt.pdf (20. 12.2022)
- İstanbul Teknik. (2022-b) Pawma İşlenebilirlik Arttırıcı Katkı
<https://www.istanbulteknik.com/tr/urunDETAY/25/pawma-islenebilirlik-arttirici-katki>
(20.12.2022)
- İstek A, Alataş T. (2019). Farklı İlik Karışım Katkıları İle Hazırlanan Marshall Numunelerinin Özelliklerinin İncelenmesi, Uludağ Üniversitesi Mühendislik Fakültesi Dergisi, 24(3)
- İstek A. (2017). Farklı İlik Asfalt Katkılarının Bitümlü Karışımların Mekanik Özelliklerine Etkisi, Doktora Tezi, T.C Fırat Üniversitesi Fen Bilimleri Enstitüsü, Danışman: Doç. Dr. Taner Alataş İnşaat Mühendisliği Programı: Ulaştırma Tezin Enstitüye Verildiği Tarih: 27 Mart 2017.
- İstek, A., & Alataş, T. (2017). Farklı ılık asfalt katkılarının bitümlü bağlayıcıların mekanik özelliklerine etkisi, *International Conference on Advanced Engineering Technologies*, 840-849. Bayburt, Türkiye.
- Kim, S., Lee, S. J., Yun, Y. B., & Kim, K. W. (2014). The use of CRM-modified asphalt mixtures in Korea: Evaluation of high and ambient temperature performance. *Construction and Building Materials*, 67, 244-248.
- Mansoori, S., & Modarres, A. (2020). Rheological and micro-structural properties of bituminous mastics containing chemical and wax warm additives. *Construction and Building Materials*, 248, 118623.
- Şahin, S. N. A., & Metin, İ. P. E. K. (2019). The effect of pawma addition on bitumen viscosity, penetration and softening point from warm mix asphalt additives. In *4th International Conference on Civil and Environmental Geology and Mining Engineering. Trabzon, Turkey*.
- Yousefi, A., Behnood, A., Nowruzi, A., & Haghshenas, H. (2021). Performance evaluation of asphalt mixtures containing warm mix asphalt (WMA) additives and reclaimed asphalt pavement (RAP). *Construction and Building Materials*, 268, 121200.

**INVESTIGATION OF HYDROGEOCHEMICAL PROPERTIES OF
GROUNDWATERS IN ŞEREFLİKOÇHİSAR PLAIN**

Murat KAVURMACI

Dr., Aksaray University, Engineering Faculty, Department of Geological Engineering
ORCID NO: 0000-0003-3625-9404

ABSTRACT

This study investigates the water quality and salinization potential of the freshwater aquifers surrounding Lake Tuz, one of the world's largest salt lakes. Lake Tuz is recharged by NaCl-rich groundwaters having a deep groundwater flow system. The average density of the lake water is 1173 kg/m³. The halite units of Lake Tuz have high Na₂O (41.97 %) and Cl (39.61 %) contents. As a result of mixing at different rates of Na-Cl and Ca-HCO₃ type water facies emerged different type water facies such as Na-HCO₃, Na-SO₄, and Ca-Cl in the region. The groundwater closer to Lake Tuz has the characteristics of Na-Cl facies. The results of the study showed that depending on the distance from Lake Tuz, the characteristics of groundwater change from Na-Cl to Na-HCO₃ and Ca-HCO₃ facies. Usually, Cl⁻, Na⁺, and HCO₃⁻ ions are more dominant. Aquifers with high chlorine concentrations in the western part of the lake may contain ions of up to 4,000 milligrams per liter. Groundwaters closer to Lake Tuz have a ratio of Na⁺/Cl⁻ between 0.44 and 0.78, while Na⁺/Cl⁻ ratios away from the lake are between 1 and 1.91. These groundwaters with a smaller Na⁺/Cl⁻ ratio than seawater (0.85) are classified as brackish water. The ratio of saltwater intrusion into wells changes from 3.3 to 14.1 % in the first 20 m of depth. Electrical conductivity, sodium, chlorine, and salinity contents of groundwater near Lake Tuz exceeded the World Health Organization and European Union standards. Thirty of the water samples are not suitable for drinking and agricultural irrigation due to the very high sodium and salinity levels. Salt Lake, which has high ion concentration and salinity values, negatively affects the water quality of freshwater aquifers. These aquifers were also mainly contaminated by the groundwater that has a high salt content as a result of water-rock interaction.

Keywords: Groundwater, hydrogeochemistry, isotope, Lake Tuz, Şereflikoçhisar

1. INTRODUCTION

Lake Tuz (LT), located in Central Anatolia, Turkey, is one of the largest hyper-saline lakes of the World. Lake Tuz formed from the evaporation of saline groundwater that has a high salt content as a result of its interaction with large salt beds and continental evaporites (MTA, 1976). During the geophysical assessment of the lake basin for petroleum exploration, the salt domes with a thickness of 1000 meters were detected (Yildiz and Soganci, 2010). The

salinization of groundwater is one of the most serious problems of the region. The Sereflikochisar (one of the districts of Ankara-Turkey) plain in the study area has documented over the past decade an increase in chloride in the monitoring wells (Kavurmaci, 2013). The salt content in freshwater can change with the dissolution of minerals containing more Cl⁻ (Hem, 1985; Kesler, 1994). In generaly, NaCl-type water and increasing chloride concentrations may indicate a strong salt-water intrusion in coastal areas (Wang and Jiao, 2012). High chloride concentrations in groundwater can be considered as definite proof of the salt-water intrusion (Hem, 1985). One of the biggest indicators of salt-water intrusion is the increase in electrical conductivity (EC). Particularly excessive increases have occurred in the chloride level and EC in the observation well closest to Lake Tuz. This situation is the result of salt-water intrusion. The reason for this are; increased pumping from wells and increased irrigation wells. Sereflikochisar aquifer could be affected by increasing salinity in the east part of the study area due to the upward or lateral movement of the saltwater interface because of greater water withdrawals (Kavurmaci, 2013). Hydrogeological studies have previously been undertaken in the research area to determine the most efficient use of available groundwater potential (Herzog, 1954; Camur and Mutlu, 1996; Oney, 1999). However, these studies mainly focused on determining the basic hydrogeological characteristics of the study area using limited data, and did not take into account the impact of the lake on the groundwater quality.

This study revealed the extent of pollution by Lake Tuz and groundwaters with high salt content in the region. In this way, the people of the region will have healthier drinking water. At the same time, more product yield will be achieved in agricultural activities.

2. MATERIAL and METHODS

2.1. The Study Area

The study area, covering 550 km² is located at in Central Anatolia between 33° 23' and 33° 37' E longitude and 39° 03' and 38° 45' N latitude (Figure 1). The average annual temperature of the region is 11.9 °C, the average altitude is 1050 m., and the average annual precipitation is 340 mm. The study area is topographically flat. Agriculture is carried out in an area of 150 km² in the region where 35,000 people live.

The most significant water body in the region is Lake Tuz. Lake Tuz is the shallowest lake in Turkey, with a mean surface area of 1665 km². The average water level of the lake is 40 cm, and its topographic altitude is 905 m. During the wet periods, the water level in southern sections of the lake can reach 120 cm. Despite its very large rainfall area of 11900 km², the lake is generally recharged by NaCl-rich groundwater rising due to tectonic movements recharging the lake (Kavurmaci, 2013). Lake Tuz is a salt lake formed as a result of continental evaporation (MTA, 1976). The dissolved substances in the shallow parts of the lake have been reported to range from 300g/L to 350 g/L and they were as low as 80 g/L in

the deeper area of the lake (Uygun and Sen, 1978). The lake is mostly dry during the summer with salt layers of 16-24 cm being formed in the lake area as a result of evaporation. There are three large saltworks, Kaldirim, Kayacik, and Yavsan extending along the shore of the lake. These factories produce 63 % of the total salt consumption in Turkey.

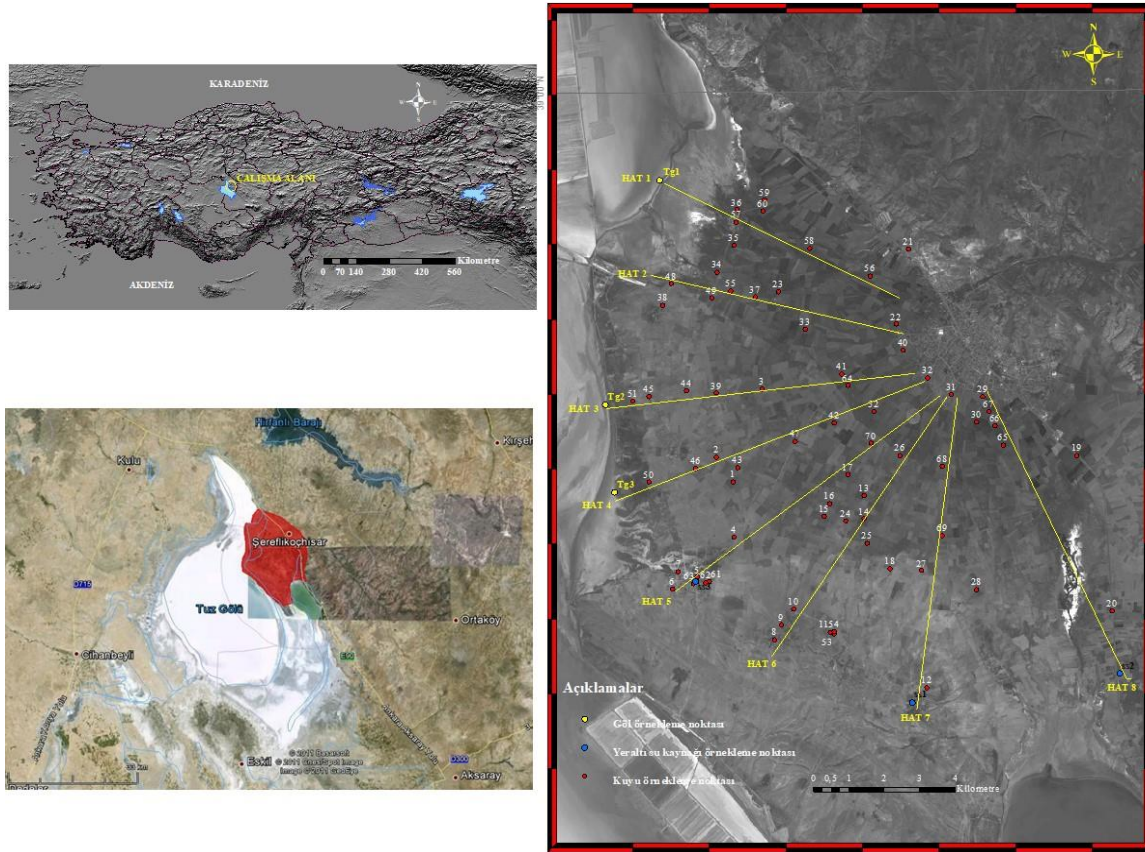


Figure 1. General view of the Tuz Lake and study area.

For chemical analysis and describing the extent of saltwater intrusion within the study area, we used 70 observation wells. However, water samples were collected from 3 parts of Lake Tuz and 3 spring water resources. Sampling was carried out in September 2011, May 2012, and September 2012.

2.2. Geological and Hydrogeological System

Lake Tuz Basin (LTB) evolved between the Late Cretaceous and Oligocene periods. The Central Anatolian Crystalline Complex rock unit is located at the bottom of the stratigraphic sequence (Goncuoglu et al., 1996) (Figure 2). Subsidence occurred during the Late Cretaceous and Middle Eocene, and it was followed by regression starting from the Late-Middle Eocene and lasting until the end of the Oligocene (Arikan, 1975). The LTB was filled with marine sedimentary units starting from the Late Cretaceous until the Middle Eocene and with continental sedimentary unit between the Late Eocene and the Quaternary (Dirik and Erol, 2000).

In the area, mainly flysch marine units represent the Upper Campanian until Middle Eocene; continental debris and coarse evaporites represent the Upper Eocene and Oligocene (Goncuoglu et al., 1996; Dellaloglu, 1997; Unluturk, 2000). The thickness of sedimentary mass in the region is approximately 2500 m (Goncuoglu et al., 1996). Salt deposit formed as a result of evaporation of salt-rich waters due to the regression in Oligocene-Miocene interval. As a result of strong tectonic movements, salt deposits formed as bends and diapiric structures.

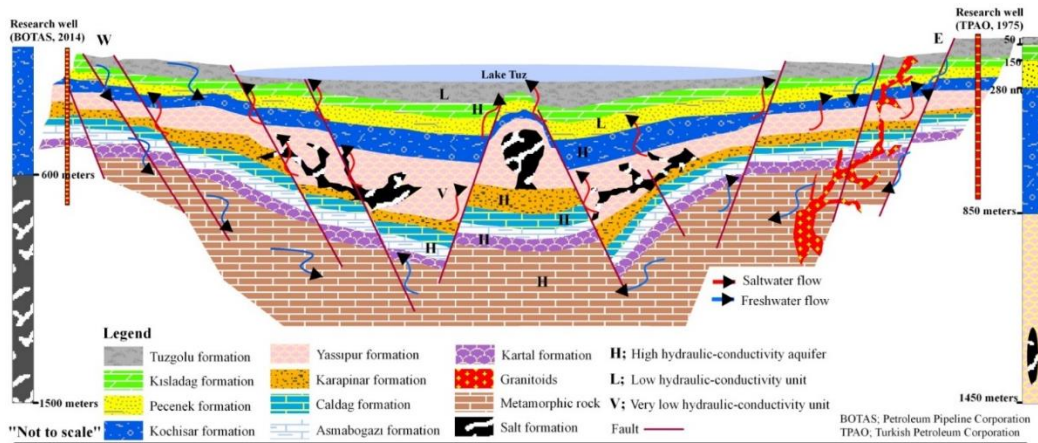


Figure 2. The cross-section shows the relationship between rock features and tectonic structures in the Lake Tuz Basin

3. RESULTS and DISCUSSION

3.1. Hydrogeochemical Evaluation

The some parameters are; temperature (T) 14.1 °C - 21.7 °C, total dissolved solid matter (TDS) 424 - 333803 mg/L, pH 6.1 - 8.1, electrical conductivity (EC) 536 - 295000 μ S/cm. Most of the groundwater samples contain total dissolved solids of up to 1000 mg/L. The groundwaters in the region can be categorized as brackish water type according to the total dissolved solids value. HCO_3^- , Cl^- , Mg^{2+} , SO_4^{2-} , Na^+ , and Ca^{2+} concentrations in groundwater samples changed between (81.2-3480.4), (28.5-1688.2), (49.2-1759.3), (129.3-2557), (42.1-459.3) and (2.6-477.2) mg/L, respectively (Table 1).

INTERNATIONAL AEGEAN CONFERENCES
ON INNOVATION TECHNOLOGIES & ENGINEERING-VI
 December 20-22, 2022

Table 1. Analysis results of water samples for September 2019

Örnek No	TDS (mg/L)	pH	EC (µS/cm)	HCO ₃ ⁻	SO ₄ ²⁻	Cl ⁻	Ca ²⁺	Na ⁺	Mg ²⁺	K ⁺	Örnek No	TDS (mg/L)	pH	EC (µS/cm)	HCO ₃ ⁻	SO ₄ ²⁻	Cl ⁻	Ca ²⁺	Na ⁺	Mg ²⁺	K ⁺
SK2	4551.0	6.9	5360.0	1556.9	47.8	1376.3	219.6	673.0	250.0	8.0	SK33	952.7	7.5	1040.0	575.3	222.0	114.0	78.4	154.0	65.9	4.4
SK3	3460.0	6.9	4130.0	759.8	289.9	1156.2	286.4	476.0	171.5	10.8	SK35	1828.0	7.6	2410.0	715.9	466.7	320.2	102.0	338.0	121.8	5.0
SK4	7306.2	7.1	7670.0	1021.8	526.7	2576.2	171.2	1474.0	381.3	6.5	SK36	1370.0	7.5	1804.0	580.5	330.4	200.6	106.8	180.4	78.6	18.8
SK5	12324.6	7.5	14890.0	411.5	1132.6	6032.4	309.2	2904.0	494.4	5.0	SK37	2542.5	7.4	3290.0	779.9	634.6	552.7	149.6	486.0	145.0	5.3
SK6	1547.0	7.6	2050.0	500.1	90.5	417.1	51.6	406.0	43.8	2.0	SK38	6617.4	7.2	7830.0	776.2	681.1	2197.1	220.0	1114.0	375.0	27.9
SK8	1674.0	7.2	2220.0	437.6	197.3	400.1	133.6	300.0	71.5	2.6	SK39	3394.8	6.8	4010.0	762.8	190.7	1069.6	232.4	456.0	158.8	11.6
SK9	3591.6	6.3	3710.0	2126.2	581.0	480.3	390.0	412.0	270.9	9.5	SK40	1098.0	7.5	1461.0	592.4	175.4	74.9	88.8	124.0	69.3	5.7
SK10	1893.0	7.0	2510.0	942.2	625.7	227.9	147.6	281.0	176.3	4.4	SK42	3821.2	7.4	4333.0	401.1	222.5	1241.4	118.0	812.0	112.6	12.1
SK11	716.0	7.3	948.0	533.6	74.9	76.0	72.4	91.4	35.0	1.6	SK43	3845.8	6.3	4755.0	504.0	146.6	1670.5	326.8	656.0	124.0	7.1
SK12	1113.0	7.3	1476.0	689.9	190.1	121.1	66.8	258.5	46.9	3.1	SK44	5297.2	7.3	6330.0	1258.4	224.2	1729.9	250.4	880.0	208.7	36.8
SK13	3485.0	7.2	4140.0	323.0	130.0	1223.7	200.4	506.0	154.4	6.6	SK45	9536.6	6.6	11330.0	1816.6	332.4	3479.4	373.2	1582.0	528.5	76.3
SK15	3903.2	7.0	4610.0	567.8	285.7	1312.4	278.0	600.0	160.0	3.6	SK46	5781.0	7.2	6800.0	849.1	195.3	2119.0	249.6	656.0	390.8	12.4
SK19	2692.5	7.0	3540.0	150.3	1842.8	190.6	608.0	300.0	97.3	3.7	SK47	3649.0	6.3	4320.0	1726.5	120.0	904.2	479.2	394.0	106.8	6.4
SK20	538.0	7.7	716.0	271.1	959.8	157.3	259.6	247.3	88.0	4.3	SK48	10676.4	7.5	13090.0	667.5	1352.4	3946.5	181.2	2564.0	453.8	40.4
SK21	4684.0	7.3	6210.0	322.6	578.4	2468.5	512.7	423.8	375.5	2.7	SK49	2437.5	7.2	3160.0	784.4	614.4	537.8	132.8	396.0	182.4	4.8
SK22	1274.0	7.2	1695.0	791.8	216.7	161.2	114.8	159.5	95.8	5.3	SK50	9782.6	6.9	11580.0	3366.8	347.6	3193.9	174.0	1604.0	711.6	152.6
SK23	1605.0	7.4	1586.0	634.8	370.8	274.1	116.4	300.0	83.4	5.3	SK51	7839.2	7.4	9340.0	931.7	1287.4	2554.9	235.2	1302.0	533.1	70.8
SK24	5297.2	6.2	6280.0	1670.0	243.4	1420.4	452.0	812.0	221.3	7.3	SK52	1105.0	7.2	1465.0	486.7	259.2	167.9	97.6	143.0	62.3	4.4
SK25	2782.3	7.2	3590.0	1318.0	377.8	531.4	72.0	726.0	103.3	4.0	SK69	4633.0	7.3	5360.0	230.0	211.1	1996.9	440.8	618.0	180.5	7.9
SK26	1233.0	7.5	1633.0	572.2	107.5	386.4	82.0	351.8	56.4	6.5	SK70	1901.0	7.6	2520.0	332.7	258.2	531.4	89.2	406.0	80.5	8.4
SK27	4264.0	7.1	5040.0	1236.1	263.0	1205.9	89.2	932.0	205.0	6.3	SS1	513.0	7.7	682.0	351.3	68.9	49.0	45.6	72.6	27.0	2.1
SK29	1638.0	7.2	2180.0	609.5	306.8	332.6	124.8	204.0	103.1	5.8	SS2	480.0	7.8	646.0	455.5	43.7	15.3	59.6	33.8	37.7	1.3
SK30	6469.8	7.1	6550.0	470.3	262.8	2441.3	374.4	1074.0	251.0	4.8	SS3	716.0	7.8	945.0	345.3	69.1	118.6	44.8	126.0	32.1	5.2
SK31	816.0	7.5	1085.0	480.0	126.8	92.7	67.2	93.6	51.1	4.4	TG1	333802.9	7.4	295000.0	1023.0	26560.0	182640.0	680.0	104670.0	13750.0	4480.0
SK32	1360.0	7.1	1810.0	743.5	233.2	194.9	150.8	188.5	71.5	5.6	TG2	322349.9	7.5	248000.0	670.0	28650.0	177450.0	720.0	98560.0	11670.0	4630.0

The dominant ion type was HCO₃⁻, Cl⁻, and Na⁺ during the all-season. Observation of the opposite trend of Ca⁺² and HCO₃⁻ concentrations shows the widespread deposition of CaHCO₃ minerals (Garrels and Mackenzie, 1976). The most striking examples of these changes were observed in the wells (SK35, SK36, SK26). The dominant facies type of SK35 and SK36 was MgSO₄ during the rainy period, but changed to NaHCO₃. Similarly, the dominant facies type of SK26 changed from CaSO₄ to NaCl. The main reasons for the alterations in the observed ion sequences are changes in seasonal rains, increments in the time in the deep groundwater circulation and ion exchanges that may occur during the interaction between the water and sodium enriched units.

The evaluation of a Piper diagram showed that, the hydrochemical facies of these waters were; NaCl, MgCl, NaHCO₃, MgHCO₃, CaSO₄, CaHCO₃, and MgSO₄. Further away from Lake Tuz, the hydrochemical facies of the water changes from NaCl to NaHCO₃ and CaHCO₃. Water samples (SK3, SK4, SK5, SK6, SK7, SK25, SK27, SK30, SK43, SK44, SK48, SK50, SK51, TG1, TG2, TG3) contain NaCl water types. Whereas other water samples (SK11, SK22, SK31, SK40, SK41, SS1, SS2, SS3) showed CaHCO₃ water types. The remaining water samples, which are plotted on the 9 th area of the Piper diagram, are characterized as mixed waters, where no ion exceeds 50 %. These samples are mixed waters.

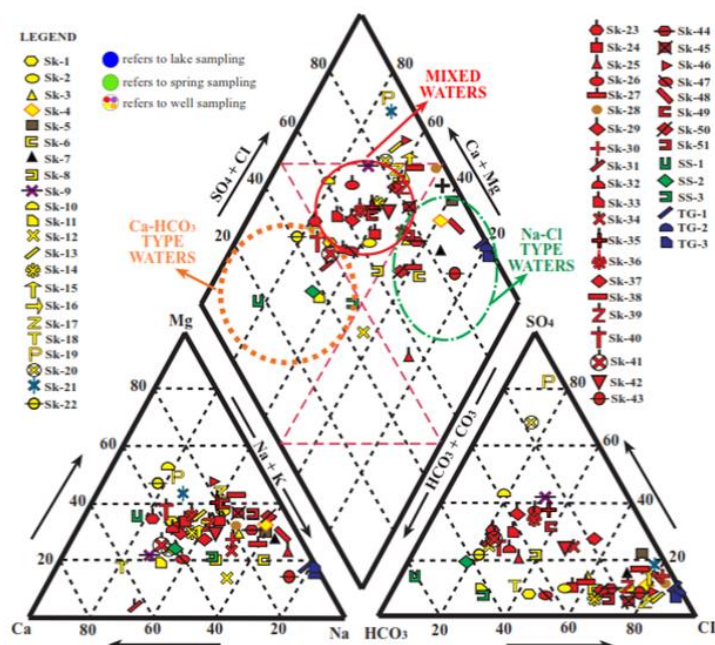


Figure 3. Classification in the trilinear diagram showing major ion chemistry of waters in the study area

The value of Na^+/Cl^- ratio in Lake Tuz is 0.58 (mg/L). Na^+/Cl^- ratio of the groundwater samples changed between 0.20 to 1.91. The brackish waters closer to lake showed Na^+/Cl^- values between 0.44-0.78 while these values measured in the range of 1-1.91 away from the lake. Na^+/Cl^- ratio of brackish waters is much smaller than in sea water (0.85). It is also not affected appreciably by ion exchange reactions. $\text{Ca}^{2+}/(\text{HCO}_3^- + \text{SO}_4^{2-})$ ratios of the brackish waters were detected entirely under 1. The value of $\text{Na}^+ / (\text{Na}^+ + \text{Ca}^{2+})$ ratio in Lake Tuz is 1(mg/L). $\text{Na}^+ / (\text{Na}^+ + \text{Ca}^{2+})$ ratio of the groundwater samples changed between 0.29 to 0.94. The brackish waters closer to lake showed $\text{Na}^+ / (\text{Na}^+ + \text{Ca}^{2+})$ values between 0.80-0.94. It refers to the salt-water intrusion which adversely affects the water quality of the aquifers.

3.2. Oxygen-18 ($\delta^{18}\text{O}$) and Deuterium ($\delta^2\text{H}$) relation

The $\delta^{18}\text{O}$ and $\delta^2\text{H}$ contents of samples in Lake Tuz range from -9.97 to -2.12 and -16.35 to -69.25, respectively. The data given in graphics is evaluated with respect to the Global Meteoric Water Line (GMWL) (Craig, 1961), the Mediterranean Meteoric Water Line (MMWL) (IAEA 1981) and Local Meteoric Water Line (LMWL) (IAEA, 2010) for Ankara. There is a deviation in the locations of wells (SK4, SK5, SK21, SK28, SK30, SK37, SK38) with respect to LMWL and GMWL (Figure 4). The deviation from GMWL signifies recharging from low elevations, evaporation, water-rock interaction, or external contamination. The leftwards movement on the $\delta^{18}\text{O}$ axis of the graphic indicates an increase in the elevation of the recharge area whereas the rightward movement shows an increase in water-rock interaction (Craig, 1961; Dansgaard, 1964).

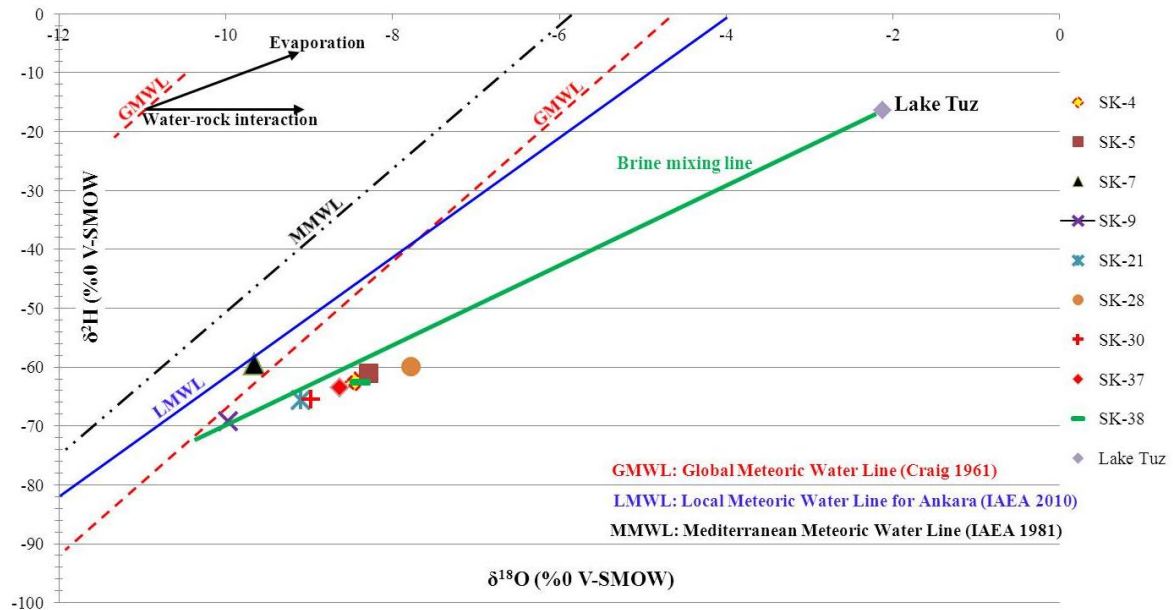


Figure 4. Stable isotopes of water expressed as $\delta^{18}\text{O}$ versus $\delta^2\text{H}$ for water samples from the study area.

An isotopic interaction between water and rocks is observed with the highest values being in the lake samples and the lowest in wells (SK7 and SK9). SK7 and SK9 sampling points plotted on the left of the graphic represent the highest recharge elevation, whereas, Lake Tuz sampling point represents the lowest recharge elevation. As the Lake Tuz sample is subjected to intense evaporation, it is enriched in both $\delta^{18}\text{O}$ and $\delta^2\text{H}$. Water samples with similar $\delta^{18}\text{O}$ isotope contents indicate that they are recharged by the same or similar elevations. The evaporation line is affected by several mechanisms such as; humidity, temperature, and salt concentration. The point at which the meteoric line is intersected with the evaporation line represents the initial isotopic composition of surface water before evaporation (Gat, 1981). The correlation coefficient calculated for the resulting regression between this initial point and the composition of Lake Tuz was found as 0.94.

Deuterium (d) excess values were calculated to be higher than 10 in SK7 and SK9; and lower than 10 in the water samples from other wells. The lower value of deuterium content indicates that most of the waters are recharged from the continental rainfall under low evaporation conditions.

Data from the shore area and inland area samples plot along a saltwater mixing line. Eight of the points along this line, with $\delta^{18}\text{O}$ higher than -7.7δ (‰), have a dissolved-solids concentration exceeding 2,500 mg/L. Wells (SK4, SK5, SK9, SK21, SK28, SK30, SK37, SK38) plot close to an extension of the saltwater mixing line fit to the shore area data, whereas SK7 plot on or near the GMWL.

3.3. Tritium (^3H) and chlorine relationship

The $\text{Cl}^- - ^3\text{H}$ graph illustrates the relationship between the residence time of water in the aquifers. The residence time increases along the horizontal axis (Cl^-) of the graph (Clark and Fritz, 1997). The wells closer to the lake (SK28, SK30, SK38) have a lower ^3H content due to their longer residence within the hydrologic system that is intensely faulted and fractured during the tectonic activity in the area. Thus, these waters have a deeper and long-lasting groundwater flow system when compared to others (Figure 5).

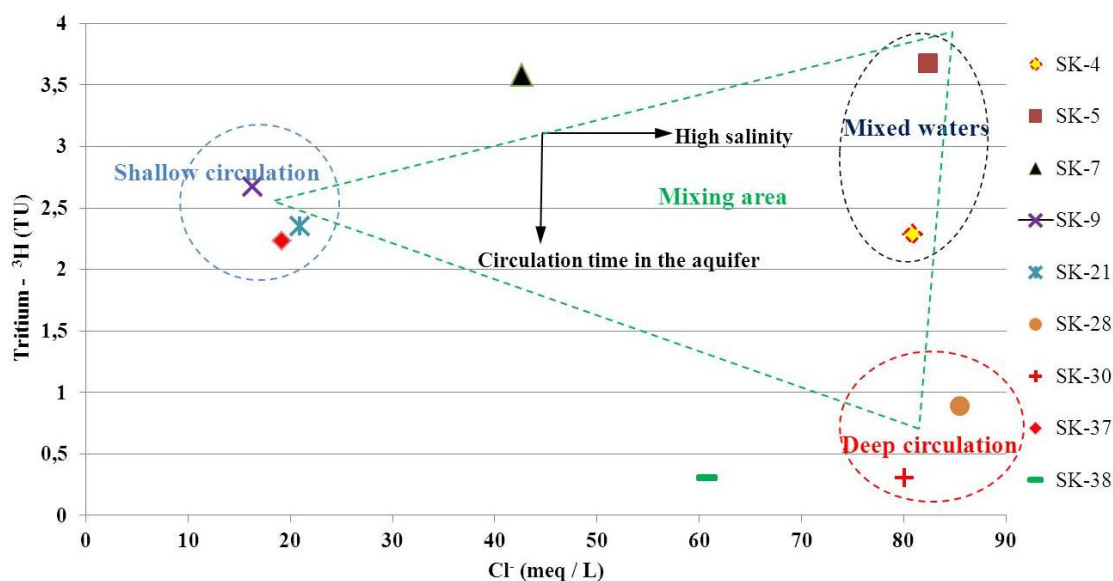


Figure 5. Tritium isotope ratio versus chloride for water samples from the study area

The $^3\text{H}-\text{Cl}^-$ diagram illustrates that the waters in the study area are clustered into three different types according to the residence time and flow duration. Other water sources possess higher ^3H and lower Cl^- contents. They represent young water with a shallower groundwater flow system and shorter water-rock interaction.

3.4. Investigation of electrical conductivity and chlorine values

Cl^- concentrations in the spatial distribution maps range from 81.2 to 3480.4 mg/L. EC was detected as above the limit value at a rate ranging from 800 to 14000 $\mu\text{S}/\text{cm}$. EC and Cl^- values in all of work area have exceeded the limit given in the drinking water standard supplied by the WHO. Cl^- and EC values decrease away from the lake (Figure 6).

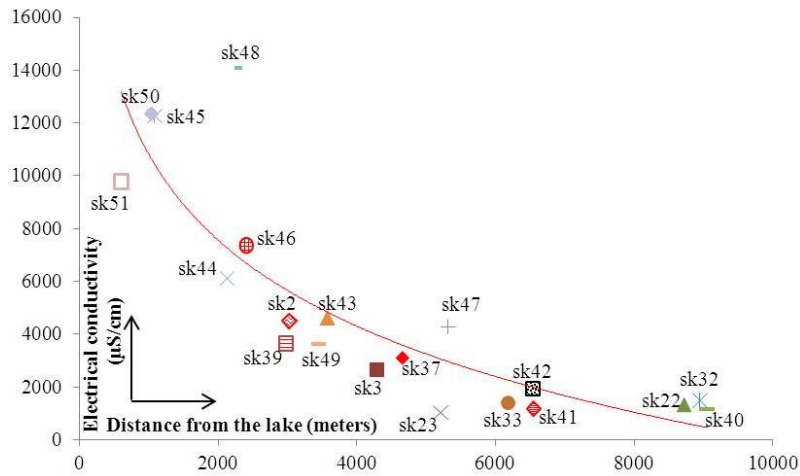


Figure 6. Relationship between electrical conductivity values and the distance from the lake of the wells

EC values in the wells (SK5, SK37, SK43, SK46, SK48, SK50, SK51) were measured 42480, 4023, 4504, 7141, 46448, 12212, and 10252 $\mu\text{S}/\text{cm}$, respectively. EC values in the wells (SK37, SK48, SK50, SK51) were measured 4916, 97036, 33132, and 33852 $\mu\text{S}/\text{cm}$, respectively at the altitude 894 m during the rainy period while these values were measured 4367, 83740, 29650, and 27382 $\mu\text{S}/\text{cm}$, respectively. EC values decrease in the research wells in the dry season while these values increase in the rainy season. Salt deposition in the tectonic system increases depending on the rise of evaporation during dry periods. As a result, a decrease on the permeability of the tectonic system is observed. The higher EC values found in the wells (SK5, SK48, SK50, SK51) and the sudden increase in EC values at different altitudes shows that the freshwater aquifers are contaminated by the Lake Tuz. Here, the contamination caused by saltwater intrusion also indicates the persistence of saltwater intrusion due to lithology.

4. CONCLUSIONS

This study presents important data concerning the salinization potential and water quality characteristics of aquifers surrounding Lake Tuz in Central Anatolia. Lake Tuz is recharged by groundwater with a high salt content interacting with salt formations. The average density of the lake water is $1173 \text{ kg}/\text{m}^3$. The halite units of Lake Tuz have high Na_2O (41.97 %) and Cl (39.61 %) contents. NaCl-rich groundwater rises upwards through tectonic systems and recharges the lake. The level of salinity may vary based on the location of tectonic features. Different flow behaviors arise from sedimentological and tectonic variations in the aquifer framework. The salt deposits decrease the conductivity of tectonic systems. This is supported by lower EC values observed during the dry seasons in wells (SK4, SK6, SK9, SK30, SK33, SK45, SK46, SK48, SK49, SK50, SK51) near the lake.

The groundwater close to Lake Tuz shows NaCl facies feature. Usually, Cl^- , HCO_3^- , and Na^+ ions are more dominant in dry periods. Higher concentrations of Cl, EC, and Na were observed, especially toward Lake Tuz. As the distance from the lake increases the concentrations of EC, Na and Cl decreased with the EC values rising with the increasing depth.

The water samples in the study area have been classified as saltwater in the wells (SK5, SK48), freshwater in the wells (SK11, SK20, SK31, SK33, SS1, SS2, SS3), and the rest as brackish water. According to the proportion of Cl^- ion values between wells and the lake, the saltwater mixing ratio of the wells (SK5, SK48, SK45, SK50, SK51) are calculated as 3.3, 2.2, 1.9, 1.7, and 1.4 %, respectively. The ratio of saltwater intrusion into wells SK5, SK48, SK45, SK50, and SK51 in the first 20 m of depth are 12.5, 14.1, 4.1, 4.6, and 3.3 %, respectively. The brackishwater groundwater area ($\text{TDS} > 1 \text{ g/l}$) extends about 3 km inland from Lake Tuz. Saltwater interference surface at a 1 km distance from the lake is 285 m in depth according to the Glover equation.

Thirteen water samples in the study area are not suitable for agricultural irrigation as they have very high sodium content and salinity value. Also, seventeen samples are not drinkable due to very high salinity and moderate sodium level. Excessive water supply from wells should be avoided for accelerating the saltwater intrusion. In addition, wells without legal permits should be closed. Dripping or sprinkler irrigation applications should be practiced on agricultural lands.

REFERENCES

- Arikan, Y., 1975, The geology and petroleum prospects of the Tuz Golu Basin. Bulletin of the Mineral Research and Exploration Institute of Turkey, 85, 17–44.
- Camur, M.Z., and Mutlu, H., 1996, Major ion geochemistry and mineralogy of Salt Lake (Tuz Gölü) Basin, Turkey. Chemical Geology, 127, 313–329.
- Craig, H., 1961, Isotopic variations in meteoric waters. Science, 133, 1702–1703.
- Dansgaard, W., 1964, Stable isotopes in precipitations. Tellus, 16, 436–468.
- Dellaloglu, A., 1997, Evolution of northern branch of neotethys between Ankara and Tuzgolu (Geotectonic evolution and stratigraphy of Haymana and Tuzgolu basins). PhD Thesis, Cukurova University, Adana, Turkey, 110 p. (in Turkish with English abstract)
- Dirik, K., and Erol, O., 2000, Tectonomorphologic evolution of Tuzgolu and Surrounding area, central Anatolia-Turkey. Workshop of Haymana-Tuzgolu-Ulukisla Basins, Aksaray, Turkey, Turkish Association of Petroleum Geologists Bulletin, Special Publication, Ankara, 5, 9–11 October, p. 27–46. (in Turkish with English abstract)

- Garrels, R.M., and Mackenzie, F.T., 1967, Origin of the chemical composition of some springs and lakes. In: R.F. Gould (ed), *Equilibrium Concepts in Natural Water Systems*, American Chemical Society, *Advances in Chemistry Series*, 6, 222–242.
- Gat, J.R., 1981, Isotopic fractionation. In: *Stable isotope hydrology, deuterium and oxygen-18 in the Water Cycle*. Report 210, IAEA, 13 p.
- Goncuoglu, M.C., Dirik, K., Erler, A., Yaliniz, K., Ozgul, L., and Cemen, I., 1996, Basic geological problems of the western part of the Tuzgolü basin. Report 3753, Turkish Petroleum Corporation (TPAO), Ankara, Turkey. (in Turkish with English abstract)
- Hem, J.D., 1985, Study and interperation of the chemical characteristics of natural water, USGS Water Supply Paper, 2254, U.S. Government Print Office, 263 p.
- Herzog, J.D., 1954, Sereflikochisar Report. Report 06–11, The General Directorate of State Hydraulic Works (DSI), Ankara, Turkey, 45 p.
- Kavurmaci, M.M., 2013, Investigation of hydrogeological and hydrochemical properties of groundwater in the Sereflikochisar basin and determination of environmental impacts of saltwater intrusion in the region. PhD Thesis, Aksaray University, Aksaray, Turkey, 232 p. (in Turkish with English abstract)
- Kesler, E.S., 1994, *Mineral Resources, Economics and the Environment*, Macmillan College MTA, 1976, Etude and feasibility research of the Tuzgolü basin. Report 5780, General Directorate of Mineral Research and Exploration of Turkey, Ankara, Turkey, 223 p. (in Turkish with English abstract)
- Oney, A., 1999, Hydrogeology etude report of the Tuz Lake east and Pecenekoðu basin. Report 16–02–99, The General Directorate of State Hydraulic Works (DSI), Ankara, Turkey, 93 p. (in Turkish with English abstract)
- Unluturk, H., 2000, Reassessment of the Tuzgolü-Haymana basin, TPAO Report 4082, Turkish Petroleum Corporation (TPAO), Ankara, Turkey, 86 p. (in Turkish with English abstract)
- Uygun, A., and Sen, E., 1978, Geochemistry of the brine of the Salt Lake (Central Anatolia-Turkey). *Bulletin of the Geological Society of Turkey*, 21, 113–120. (in Turkish with English abstract)
- Wang, Y., and Jiao, J.J., 2012, Origin of groundwater salinity and hydrogeochemical processes in the confined Quaternary aquifer of the Pearl River Delta, China. *Journal of Hydrology*, 438–439, 112–124.
- Yildiz, M., and Soganci, A.S., 2010, Evaluation of geotechnical properties of the salt layers on Lake Tuz, *Scientific Research and Essays*, 5, 2656–2663.

**ŞIRNAK ASFALTİT NUMUNESİNİN ÖNEMLİ KARAKTERİZASYON
ÖZELLİKLERİNİN BELİRLENMESİ**
DETERMINATION OF SIGNIFICANT CHARACTERIZATION FEATURES OF SIRNAK
ASPHALTITE SAMPLE

Öykü Bilgin

Doç. Dr., Şırnak Üniversitesi, Mühendislik Fakültesi, Maden Mühendisliği Bölümü
Doç. Dr., Sırnak University, Faculty of Engineering, Department of Mining Engineering
ORCID NO: 0000-0002-1276-5751

ÖZET

Asfaltit; petrol kökenli, kömür ile benzer özelliklere sahip, hidrokarbon esaslı bir enerji hammadesidir. Kalorifik değeri genel olarak 3000-6000 kcal arasında değişmektedir ve cevher hazırlama/zenginleştirme yöntemleri ile daha yüksek değerlere kadar ulaşabilmektedir. Türkiye'nin Güneydoğu Anadolu Bölgesinde Şırnak ili, bu önemli enerji hammaddesinin kaynağıdır. Bu bölgede asfaltitler; Avgamasya, Milli, Segürük, Nivekara, Karatepe, Seridahli, İspindoruk, Rutkekurat, Uludere-Ortasu, Silopi-Harbul, Silopi-Silip ve Silopi-Üçkardeşler filonları halinde bulunmaktadır. Şırnak ocaklarından çıkarılan asfaltitler yaygın olarak termik santrallerde elektrik üretim veya yöresel ısınma amaçlı enerji hammaddesi olarak kullanılmaktadır. Asfaltitden petrol elde edilmesi, içerisindeki kül ve kükürt oranlarının düşürülmesi ve asfaltit külü içerisindeki değerli ağır metallerin zenginleştirilerek kazanılmasına yönelik çalışmalar vardır. Bu çalışmada; Şırnak merkezinde faaliyet gösteren Avgamasya ocağından yerinde alınan asfaltit numunesinin; elek analizi, kimyasal analizi, standart kalitatif mineral analizi (X-Ray), taramalı elektron mikroskop (SEM), mikrokimyasal analiz (EDS) ve iz metal analizi (ICP-OES) sonuçları incelenmektedir. Asfaltit numunesinin ASTM D7582, ASTM D 4239, ASTM D5865, ASTM D5016, ASTM D5373, TS329ISO test standartları ile yapılan kimyasal analiz sonuçlarına göre; başlıca %0.48 nem, %46.06 kül, %6.45 toplam kükürt, % 4.70 organik kükürt, % 1.62 piritik kükürt, %16.70 sabit karbon ve 4280 kcal üst ısıl değerleri belirlenmiştir. Asfaltit numunesinin iz element analiz sonuçlarına göre; Mo, Ni, V, Zn, Cr, Ba, As, Sr, Cd, Se, Rb, Cu, Th, Ga, B, Co ve U gibi önemli metaller ppm seviyesinde tespit edilmiştir. X-Ray analizlerine göre içerisinde dolomit, kuvars, pirit, alkali feldspat, mika/illit minerali ve siderit gibi mineraller bulunmuştur. Asfaltit numunesinin farklı noktalarında uygulanan SEM ve EDS analizlerine göre; Zn, S, Al, Zn, Fe, Cd, Ca, Ti, Si, Ni, Mg ve V gibi elementlere rastlanmıştır.

Anahtar Kelimeler: Şırnak, asfaltit, kömür, karakterizasyon

ABSTRACT

Asphaltite is a petroleum-based, hydrocarbon-based energy raw material with similar properties to coal. Its calorific value generally varies between 3000-6000 kcal and can reach higher values with ore preparation/enrichment methods. Şırnak province in the Southeastern Anatolia Region of Turkey is the source of this important energy raw material. Asphaltites in this region; there are fleets in Avgamasya, Milli, Segürük, Nivekara, Karatepe, Seridahli, İspindoruk, Rutkekurat, Uludere-Ortasu, Silopi-Harbul, Silopi-Silip and Silopi-Üçkardeşler. Asphaltites extracted from Şırnak quarries are widely used in thermal power plants as an energy raw material for electricity generation or local heating. There are various studies on obtaining petroleum from asphaltite, reducing the ash and sulfur ratios in it, and enriching the valuable heavy metals in asphaltite ash. In this study; the asphaltite sample taken from the Avgamasya quarry operating in the center of Şırnak; sieve analysis, chemical analysis, standard qualitative mineral analysis (X-Ray), scanning electron microscope (SEM), microchemical analysis (EDS) and trace metal analysis (ICP-OES) results are examined. According to the chemical analysis results of the asphaltite sample made with ASTM D7582, ASTM D 4239, ASTM D5865, ASTM D5016, ASTM D5373, TS329ISO test standards; 0.48% moisture, 46.06% ash, 6.45% total sulfur, 4.70% organic sulfur, 1.62% pyritic sulfur, 16.70% fixed carbon and 4280 kcal upper calorific values were determined. According to the trace element analysis results of the asphaltite sample; important metals such as Mo, Ni, V, Zn, Cr, Ba, As, Sr, Cd, Se, Rb, Cu, Th, Ga, B, Co and U were detected at ppm level. According to X-Ray analysis, minerals such as dolomite, quartz, pyrite, alkali feldspar, mica/illite mineral and siderite were found in asphaltite. According to SEM and EDS analyzes applied at different points of the asphaltite sample; elements such as Zn, S, Al, Zn, Fe, Cd, Ca, Ti, Si, Ni, Mg and V have been encountered in sample.

Keywords: Şırnak, asphaltite, coal, characterization.

ZEYTİNİN TARIMSAL SU AYAK İZİNİN HESAPLANMASI: İZMİR ÖRNEĞİ
CALCULATION OF AGRICULTURAL WATER FOOTPRINT OF OLIVES: A CASE
STUDY FOR IZMIR

Fatma DENİZ

Mersin Üniversitesi, Mühendislik Fakültesi, Çevre Mühendisliği Bölümü
Mersin University, Engineering Faculty, Department of Environmental Engineering
ORCID NO: 0000-0001-6782-8169

Mehmet Ali MAZMANCI

Mersin Üniversitesi, Mühendislik Fakültesi, Çevre Mühendisliği Bölümü
Mersin University, Engineering Faculty, Department of Environmental Engineering,
ORCID NO: 0000-0003-0219-530X

ÖZET

Sınırlı doğal kaynaklarımızın en önemlisi sudur. Geçmişten günümüze insan nüfusu ve yaşam kalitesi arttıkça tüketilen ve kirletilen su hacmi artmış ve artmaya devam etmektedir. Su ayak izi kavramı herhangi bir ürünün üretimi ve/veya tüketimi aşamasında harcanan tatlı su hacmini ifade etmek için kullanılmaktadır. Tarımsal üretim, su ayak izinin fazla olduğu alanlardan biridir. Tarımsal üretimde su ayak izi değeri belirli bir mekana, zamana ve ürüne ait olarak bulunur. Bu şekilde aynı ürünün su ayak izi değerleri zamana ve mekana göre kıyaslanabilir. Su ayak izi hesaplamaları ile iklimsel değişikliğin bitki su tüketimine etkisi tespit edilip, sürdürülebilir tarım uygulamalarına destek olunabileceği düşünülmektedir.

Bu çalışmada İzmir İli'nde üretilen yağlık zeytinin 2012-2021 yılları için tarımsal yeşil su ayak izi hesaplamaları gerçekleştirilmiştir. Tarımsal su ayak izi hesaplamalarında CROPWAT programı kullanılmıştır. Kullanılan iklimsel veriler Meteoroloji Genel Müdürlüğü (MGM)'nden, bitki gelişimi ile ilgili veriler Tarımsal Araştırmalar ve Politikalar Genel Müdürlüğü (TAGEM)'nden ve zeytin üretimi yapılan alan ile zeytin üretim miktarları Türkiye İstatistik Kurumu (TÜİK)'nden temin edilmiştir. Etkili yağış miktarının hesaplanmasında USDA metodu, referans bitki su tüketim miktarı (ET_0) hesaplanmasında Penman-Monteith metodu kullanılmıştır.

Çalışma sonucunda İzmir'de yetiştirilen yağlık zeytin için tarımsal su ayak izinin sulama yapılmaması durumunda ortalama $3,54 \text{ m}^3/\text{kg}$ zeytin olduğu hesaplanmıştır. Bu değer, zeytin üretimi yapılan 19 ilin ortalamasının ($3,96 \text{ m}^3$ su/kg yağlık zeytin) altında olduğu bulunmuştur.

Anahtar kelime: Su ayak izi, Bitki su tüketimi, Yağlık zeytin

ABSTRACT

The most important of our limited natural resources is water. From past to present, as the human population and quality of life increase, the volume of consumed and polluted water has increased and continues to increase. The concept of water footprint is used to express the volume of fresh water consumed during the production and/or consumption of any product. Agricultural production is one of the areas where the water footprint is high. In agricultural production, the water footprint value is found in a specific place, time and product. In this way, water footprint values of the same product can be compared according to time and place. With water footprint calculations, it is thought that the effect of climate change on crop water consumption can be determined and sustainable agricultural studies can be supported.

In this study, agricultural water footprint calculations were carried out for the years 2012-2021 of olives for oil produced in Izmir. The CROPWAT program was used for agricultural water footprint calculations. The climatic data used were obtained from the Turkish State Meteorological Service (MGM), the data on crop development was obtained from the General Directorate of Agricultural Research and Policies (TAGEM), and the olive production area and olive production amounts were obtained from the Turkish Statistical Institute (TUIK). The USDA method was used to calculate the effective precipitation amount, and the Penman-Monteith method was used to calculate the references crop water evapotranspiration (ET_0).

As a result of the study, it has been calculated that the agricultural water footprint for olive oil grown in Izmir is $3.54 \text{ m}^3/\text{kg}$ rainwater on average in the absence of irrigation. It was found that this value is below the average water footprint (3.96 m^3 water/kg olives for oil) of 19 provinces where olive production is made in Turkey.

Keywords: Water footprint, crop water consumption, olive for oil

1. GİRİŞ

İnsan faaliyetleri sonucunda çok fazla su tüketilmekte ve kirlenmektedir (Hoekstra, Chapagain, Mekonnen, & Aldaya, 2011; UNESCO, 2009). Toplam su tüketimi ve kirliliği, toplumların ne tükettiği ve ne kadar tükettiğiyle ilgilidir. Yakın zamana kadar bir ürünün tüketiminin su kullanımına olan etkisinin aslında o ürünün üretiminde, tedarik zinciri boyunca gerçekleşen su tüketimini ve kirliliğini de kapsadığına dair çok az farkındalık vardı. Hoekstra ve Chapagain (2008), ürünlerin arkasındaki gizli su kullanımının ortaya çıkarılmasının, tüketim ve ticaretin su kaynaklarının kullanımı üzerindeki etkilerinin ölçülmesine yardımcı olabileceğini göstermiştir (Hoekstra & Chapagain, 2011; Hoekstra et al., 2011).

Herhangi bir ürün için su kaynaklarının kullanımı tüketicilerden mekansal olarak bağımsızdır. Çoğunlukla üretim aşamaları farklı yerlerde gerçekleşirken tüketim başka bir yerde gerçekleşmektedir (Chapagain, Hoekstra, Savenije, & Gautam, 2006; Hoekstra et al., 2011).

Bu nedenle bir ürünün tüketiminin dünyanın su kaynakları üzerindeki etkileri ancak tedarik zincirine bakılarak ve ürünün kökeninin izini sürerek bulunabilir (Hoekstra et al., 2011). Tedarik zinciri boyunca su tüketimini dikkate alma fikri, 2002 yılında Hoekstra tarafından “su ayak izi” kavramının uygulamaya konmasıyla başlamıştır (Hoekstra, 2003). Su ayak izi, üreticinin ve/veya tüketicinin yalnızca doğrudan su kullanımını değil, aynı zamanda dolaylı su kullanımını da içeren bir göstergedir. Kullanılan suyun kaynağına göre yeşil su ayak izi ve mavi su ayak izi, kirletilen su hacmine göre de gri su ayak izi olmak üzere üç gruba ayrılmaktadır. Yeşil su ayak izi yağmur suyu tüketimini, mavi su ayak izi yüzey ve yeraltı suyu tüketimini ifade etmektedir. Gri su ayak izi ise herhangi bir alıcı ortama verilen atık suyun o alıcı ortamın mevcut kalite standartlarına ulaşabilmesi için kirlettiği su miktarını, yani alıcı ortamın özümleme kapasitesini ifade etmektedir. Su ayak izi kavramı klasik su kullanım hesabından farklı olarak sadece hacimsel olarak değil, aynı zamanda zamansal ve mekânsal olarak da bilgi vermektedir (Hoekstra et al., 2011; Mekonnen & Hoekstra, 2011).

İnsan faaliyetleri arasında tarım, tatlı su ayak izinin %92'sini oluşturmaktadır (Rossi et al., 2019). Tarımsal su ayak izi hesaplamaları, tarımsal su tüketiminde mevcut durumun tespit edilmesi dışında sürdürülebilir tarım stratejilerinin belirlenmesinde de kullanılmaktadır (Ferrero, Araujo, Valdeón, Hun, & Mele, 2022; Mekonnen & Hoekstra, 2020). Bir ürünün tarımsal su ayak izi, bitkinin su tüketimi (evaporatranspirasyonu) ile hesaplanmaktadır. FAO tarafından geliştirilen CROPWAT 8.0 programı kullanılarak, Hoekstra'nın Su Ayak İzi Ağı yöntemiyle mavi ve yeşil su ayak izi hesaplanmaktadır. Son yıllarda tarımsal ürünler için su ayak izi çalışmaları artarak devam etmektedir (Ferrero et al., 2022; Mekonnen & Hoekstra, 2020; Muratoglu, 2020; Rossi et al., 2019).

Zeytin Akdeniz havzasında yetiştirilen önemli tarımsal ürünlerden biridir. Türkiye sahip olduğu zeytinlik alanı ile dünya genelinde 6. sırada yer almaktadır (TEPGE, 2021). Türkiye’de, 2021 yılı verilerine göre 6.589.146 dekar yağlık zeytin ve 2.302.531 dekar sofralık zeytin olmak üzere toplam 8.891.677 dekar zeytin ekili alan bulunmaktadır. İzmir Türkiye’de yağlık zeytin yetiştiriciliğinde 842773 dekar toplam ekili alan ile Aydın ve Muğla’dan sonra 3. sırada yer almaktadır (TÜİK, 2022).

Bu çalışmada, İzmir’de yetiştirilen yağlık zeytinin yağmur suyu ile beslenmesi durumunda, 2012-2021 yılları için yeşil su ayak izi hesaplamaları yapılmıştır.

2.MATERYAL VE METOD

İzmir, Türkiye'nin Ege Bölgesi'nde yer alan bir ilidir. 38.40 kuzey enlemi ve 27.19 doğu boylamında yer alan il, Akdeniz iklim kuşağında bulunmaktadır. Yıllık ortalama sıcaklığı 17.9 °C, yıllık ortalama yağış yüksekliği 713.8 mm'dir (MGM, 2022). Yaz mevsimi sıcak ve

kurak, kış mevsimi ılık ve yağışlıdır. İlin coğrafi olarak sahip olduğu çeşitlilik iklim özelliklerini etkilemektedir (İBB, 2022).

İzmir İli'nin tarımsal su ayak izinin hesaplandığı bu çalışmada 2012-2021 yıllarına ait iklimsel veriler Meteoroloji Genel Müdürlüğü (MGM)'nden (MGM, 2022), zeytin için ekili alan ve üretim miktarı verileri Türkiye İstatistik Kurumu (TÜİK)'nden (TÜİK, 2022) ve bitki gelişimi ile ilgili veriler Tarımsal Araştırmalar ve Politikalar Genel Müdürlüğü (TAGEM)'nden (TAGEM, 2017) temin edilmiştir.

Çalışmada CROPWAT-8.0 programında, sulama programı seçeneği uygulanmıştır. Etkili yağış miktarının hesaplanmasında USDA metodu, referans bitki su tüketim miktarı (ET_0) hesaplanmasında Penman-Monteith metodu kullanılmıştır. Penman-Monteith denklemi Eşitlik 1'de verilmiştir (Allen, Pereira, Raes, & Smith, 1998).

$$ET_0 = \frac{0.480\Delta(R_n - G) + \gamma \frac{900}{T+273} u_2 (e_s - e_a)}{\Delta + \gamma(1+0.34u_2)} \quad \text{Eşitlik 1}$$

Burada;

ET_0 : Referans evapotranspirasyon (mm/gün)

Δ : Buhar basıncı eğrisinin eğimi (kPa/°C)

R_n : Bitki yüzeyindeki net radyasyon (MJ/m²/gün)

G : Toprak ısı akısı yoğunluğu (MJ/m²/gün)

γ : Psikrometrik sabit (kPa/°C)

T : Günlük ortalama sıcaklık (°C)

u_2 : Rüzgar hızı (m/s)

e_s : Doymuş buhar basıncı (kPa)

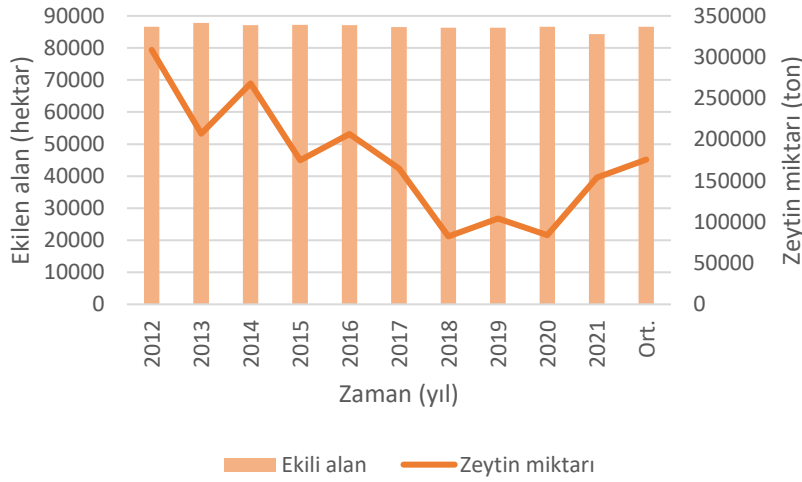
e_a : Gerçek buhar basıncı (kPa)

ifade etmektedir.

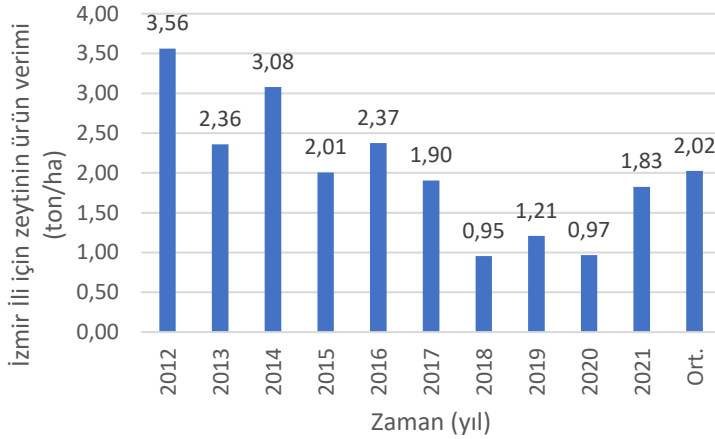
Meteoroloji verileri günlük veri olarak girilmiştir. Yeşil bileşen $SAI_{\text{yeşil}}$ (m³/ton)'i hesaplamak için zeytinin kullandığı yağmur suyu (yeşil su) miktarı mm cinsinden hesaplanmıştır. Yükseklik olarak hesaplanan su miktarı ürün verimine (ton/ha) bölünerek m³/kg birimine çevrilmiştir. Bitki veya ağaç yetiştirme sürecinin toplam su ayak izi yeşil, mavi ve gri bileşenlerin toplamıdır. Yapılan araştırmalar sonucunda Türkiye'de zeytin yetiştiriciliğinde mavi su kullanımının düşük seviyelerde olduğu görülmüştür. Bu çalışmada yıllık zeytin ağaçlarının sadece yeşil su ile beslenmesi durumu için su ayak izi hesaplaması yapılmıştır.

3. BULGULAR VE TARTIŞMA

Su ayak izi hesaplamasında kullanılmak üzere TÜİK'ten temin edilen, İzmir'de yağlık zeytin ekili alan ve bu alandan elde edilen yağlık zeytin miktarı verileri Şekil 1'de, birim alandan elde edilen yağlık zeytin miktarı olan ürün verimi verileri de Şekil 2'de verilmiştir.



Şekil 1. İzmir İli için yağlık zeytin ekili alan ve ürün miktarı verileri (TÜİK, 2022)



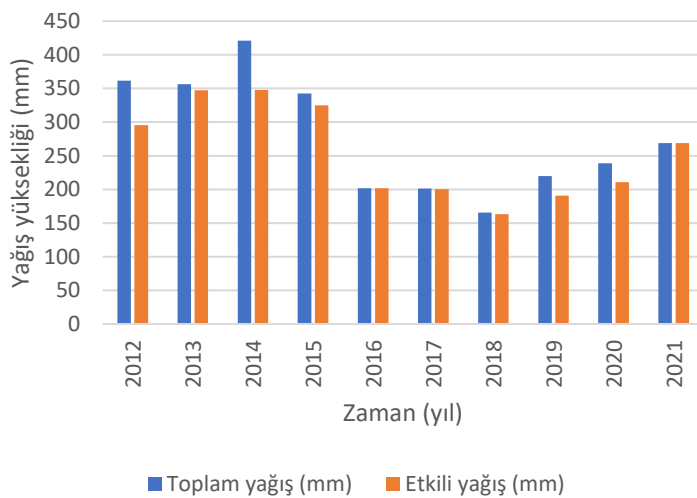
Şekil 2. İzmir İli için zeytinin ürün verimi (TÜİK, 2022)

Yeşil su ayak izi hesaplamasında etkili yağış miktarı kullanılmaktadır. Yıllara göre, zeytinin gelişim dönemine ait toplam yağış ve USDA metodu ile hesaplanan etkili yağış verileri Şekil 3'te verilmiştir. 2016 yılı ve sonrasında yağış yüksekliği önceki yıllara göre düşüş göstermiştir. Bu durum mavi su ile sulamanın yapılmadığı tarımsal ürünlerde verimin

düşmesine neden olabilir. Ürün veriminin düşmesi de su ayak izini arttırmaktadır. Zeytin üretim miktarlarındaki düşüşler yağış yüksekliği ile benzerlik göstermektedir. 2016 yılından itibaren zeytin üretim miktarı düşmüş, 2021 yılında tekrar artmıştır (Şekil 1).

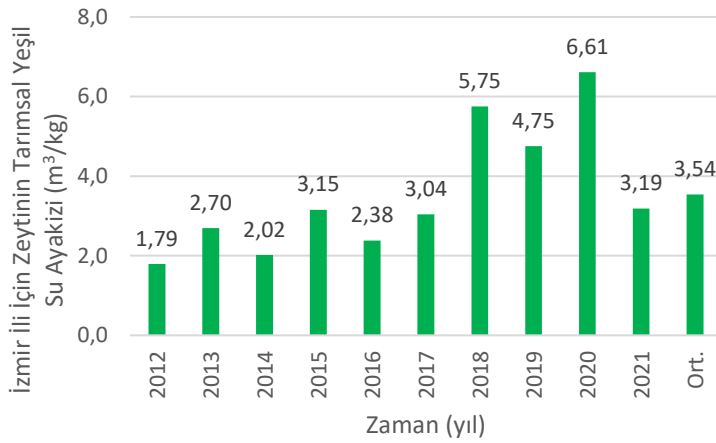
Zeytinde çiçek tomurcuğun farklılaşmasından meyve olgunlaşmasına kadar olan süreç, yaz aylarında başlayıp bir sonraki yıl sonbaharda sona ermektedir. Bu süreç zeytin çeşidine ve yetiştirme koşullarına göre 15-18 ay sürmektedir (Steduto, Hsiao, Fereres, & Raes, 2012). Bu durum zeytin yetiştiriciliğinde her yıl alınan ürün miktarında değişikliğe neden olmaktadır. Ekilen alan ve elde edilen ürün verilerinin yer aldığı Şekil 1'e baktığımızda, ekili alan miktarı yaklaşık aynı olmasına rağmen ürün miktarlarında bir yıl artma sonraki yıl azalma durumları gözlenmektedir. Bu durum zeytinin bir yıl fazla bir yıl az meyve veren bir bitki olmasından kaynaklanabilir. Ancak 2016 sonrasındaki azalmanın farklı nedenlere dayandığı düşünülmektedir.

Kış yağışının az olduğu yıllarda, yağmurla beslenen ağaçlarda çiçeklenme ve meyve tutumu süreci su eksikliğine karşı hassas olmaktadır. Bu nedenle ilkbaharda başlayan çiçek gelişiminden meyve tutumuna kadar su stresinden kaçınılmalıdır. İzmir'de yağlık zeytin üretiminde 2016 yılından sonra gözlenen düşüş, aynı dönemde azalan yağışla ilişkilendirilebilir. Zeytinde meyve tutumu çiçeklerin %2'sinden azdır. Uygun olmayan iklimsel koşullar bu oranı daha da düşürebilir. Zeytinler geç çiçek açtıklarından dolayı, düşük sıcaklıktan zarar görme riski önemli ölçüde azalmaktadır. Ancak Akdeniz iklim şartlarında sudan ve/veya yüksek sıcaklıktan etkilenme riski artmaktadır. Ayrıca meyve büyümesi de suyun çok daha az olduğu yaz mevsimine ertelenmektedir (Steduto et al., 2012). Tüm bu özellikler zeytin ağacından alınacak meyve miktarını etkilemektedir. Değişen iklim şartları ve buna bağlı olarak değişen ürün miktarı da su ayak izini etkilemektedir.



Şekil 3. İzmir için zeytin gelişim döneminde toplam ve etkili yağış yükseklikleri

Bu çalışmada İzmir’de yetiştirilen yağlık zeytin ağaçlarının yağmur suyu ile beslenmesi durumundaki yeşil su ayak izi, 2012-2021 yılları arası için hesaplanmıştır. Yapılan hesaplama sonucunda elde edilen değerler Şekil 4’te verilmiştir. En yüksek ve en düşük su ayak izi sırasıyla 1.79 ve 6.61 m³/kg, hesaplanan 10 yılın ortalama değeri ise 3.54 olarak bulunmuştur. Yıllara göre su ayak izi değerlerinde artış ve azalışlar görülmektedir. Bitki su tüketim miktarının ürün verimine bölünmesinden dolayı, su ayak izi değerleri ürün verimine göre artmakta ya da azalmaktadır. Şekil 2’de verilen ürün verimi verileri incelendiğinde verimin düşük olduğu yıllarda su ayak izinin yüksek, verimin yüksek olduğu yıllarda ise su ayak izi değerinin düşük olduğu görülmektedir. 2018, 2019 ve 2020 yıllarında su ayak izi diğer yıllara göre daha yüksek bulunmuştur.



Şekil 4. İzmir İli’nde yetiştirilen yağlık zeytin ağaçlarının su ayak izi

Rossi ve arkadaşları 2019 yılında yaptıkları çalışmada İtalya’da yağmur suyu ile beslenen zeytin ağaçlarının yeşil su ayak izini 1.024 m³/kg zeytin olarak rapor etmiştir. Salmoral ve arkadaşları 2011 yılında yaptıkları çalışmalarında İspanya’da yağmur suyu ile beslenen zeytin ağaçlarının yeşil su ayak izini 1971 m³/ton zeytin (1.971 m³/kg zeytin) olarak rapor etmişlerdir. Bu çalışmada İzmir’de yağmur suyu ile beslenen zeytin ağaçlarının yeşil su ayak izi ortalama 3.54 m³/kg zeytin olarak hesaplanmıştır. İtalya, İspanya ve Türkiye’de yetiştirilen zeytinin su ayak izi arasındaki fark, her bölgede birim alandan elde edilen zeytin miktarındaki farklılıktan ve/veya iklimsel farklılıktan kaynaklanabilir.

4. SONUÇ

Bu çalışmada İzmir’de yağmur suyu ile beslenen yağlık zeytin ağaçlarının yeşil su ayak izi değerleri 2012-2021 yılları için, CROPWAT programı kullanılarak hesaplanmıştır. Çalışma sonucunda İzmir’de yetiştirilen yağlık zeytin ağaçlarının yeşil su ayak izi ortalama 3.54 m³/kg

zeytin olarak hesaplanmıştır. Bu değerin, Türkiye’de zeytin üretimi yapılan 19 ilin yeşil su ayak izi değerlerinin ortalamasının (3,96 m³ su/kg yağlık zeytin) altında olduğu bulunmuştur. Su kaynaklarının zeytin tarafından en verimli şekilde kullanılabilmesi, zeytine uygun iklim şartlarına sahip bölgelerde zeytin yetiştiriciliğinin artırılması ile sağlanabileceği düşünülmektedir.

TEŞEKKÜR

Yazarlar, sağlanan mali destekten dolayı Mersin Üniversitesi Bilimsel Araştırma Projeleri Birimi’ne teşekkür eder (Proje No: 2015 AP4-1368).

KAYNAKÇA

- Allen, R. G., Pereira, L. S., Raes, D., & Smith, M. (1998). FAO Irrigation and drainage paper No. 56. *Rome: Food and Agriculture Organization of the United Nations*, 56(97), e156.
- Chapagain, A. K., Hoekstra, A. Y., Savenije, H. H., & Gautam, R. (2006). The water footprint of cotton consumption: An assessment of the impact of worldwide consumption of cotton products on the water resources in the cotton producing countries. *Ecological economics*, 60(1), 186-203.
- Ferrero, L. M. M., Araujo, P. Z., Valdeón, D. H., Hun, A. L. N., & Mele, F. D. (2022). Water footprint of lemon production in Argentina. *Science of the total environment*, 816, 151614.
- Hoekstra, A. Y. (2003). Virtual water trade: proceedings of the international expert meeting on virtual water trade, Delft, The Netherlands, 12-13 December 2002, Value of Water Research Report Series No. 12: UNESCO-IHE, Delft, The Netherlands.
- Hoekstra, A. Y., & Chapagain, A. K. (2011). *Globalization of water: Sharing the planet's freshwater resources*: John Wiley & Sons.
- Hoekstra, A. Y., Chapagain, A. K., Mekonnen, M. M., & Aldaya, M. M. (2011). *The water footprint assessment manual: Setting the global standard*: Routledge.
- İBB, İzmir Büyükşehir Belediyesi (2022). <https://www.izmir.bel.tr/tr/IzmirinCografyasi/220/255> adresinden, 15.12.2022 tarihinde erişilmiştir.
- Mekonnen, M. M., & Hoekstra, A. Y. (2011). National water Footprint accounts: the green, blue and grey water Footprint of production and consumption. Volume 1: Main Report.
- Mekonnen, M. M., & Hoekstra, A. Y. (2020). Sustainability of the blue water footprint of crops. *Advances in water resources*, 143, 103679.

- MGM. Meteoroloji Genel Müdürlüğü (2022). <https://mgm.gov.tr/> adresinden 12.11.2022 tarihinde erişilmiştir.
- Muratoglu, A. (2020). Assessment of wheat's water footprint and virtual water trade: a case study for Turkey. *Ecological Processes*, 9(1), 1-16.
- Rossi, L., Regni, L., Rinaldi, S., Sdringola, P., Calisti, R., Brunori, A., . . . Proietti, P. (2019). Long-term water footprint assessment in a rainfed olive tree grove in the Umbria Region, Italy. *Agriculture*, 10(1), 8.
- Steduto, P., Hsiao, T. C., Fereres, E., & Raes, D. (2012). *Crop yield response to water* (Vol. 1028): Food and Agriculture Organization of the United Nations Rome.
- TAGEM. Tarımsal Araştırmalar ve Politikalar Genel Müdürlüğü (2017). *Türkiye'de Sulanan Bitkilerin Bitki Su Tüketimleri*. <https://www.tarimorman.gov.tr/TAGEM/Belgeler/yayin/Tu%CC%88rkiyede%20Sulanan%20Bitkilerin%20Bitki%20Su%20Tu%CC%88ketimleri.pdf> adresinden 12.11.2022 tarihinde erişilmiştir.
- TEPGE, Tarımsal Ekonomi ve Politika Geliştirme Enstitüsü Müdürlüğü, T.C. Tarım ve Orman Bakanlığı. (2021). *Ürün Raporu, Zeytinyağı, 2021*.
- TÜİK, Türkiye İstatistik Kurumu (2022). Zeytin bitkisinin yıllık üretim verileri. <https://www.tuik.gov.tr/> adresinden 12.11.2022 tarihinde erişilmiştir.
- UNESCO, United Nations Educational, Scientific and Cultural Organization (2009). Water in a changing world: the United Nations world water development report 3. <https://unesdoc.unesco.org/ark:/48223/pf0000181993> adresinden 15.12.2022 tarihinde erişilmiştir.

**ANALYZE OF OIL AND GAS ACCIDENT ASSOCIATED WITH DRILLING
OPERATION USING FISHBONE DIAGRAM**

Slimani Sami

Research Laboratory on Surface and Interface Physics and Chemistry LRPCSI; Université 20 août 1955 Skikda,
Algeria

Zennir Youcef

Automatic Laboratory of Skikda, Université 20 août 1955 Skikda, Algeria

ABSTRACT

Oil and gas drilling is an important phase in petroleum industry life. It is the most important phase and the most expensive in terms of cost and time. This phase “drilling” associated with many constraints and incidents. The most common is lost-of circulation, fire explosion, blowout, explosion...etc. This paper analyze over than 26 incidents and accidents occurred around the world during the period between 2000 and 2018 based on reports and research articles, Fishbone Diagram is applied to analyze the causes that lead to accident. The results showed that the number of incidents doubled over the period 2012-2015 by 31%. also the results showed that explosion is the most common incident by 31%. finally in the period between 2016 and 2018 the number of fatalities has increased by 54%.

Keywords: Drilling incident, Fishbone Diagram, Fire explosion, Statistical analyses.

**SYNTHESIS, MOLECULAR STRUCTURES AND CATALYTIC ACTIVITIES OF
BIS-2,2-BIPYRIDINE PALLADIUM (II) DI CHLORIDE COMPLEXES IN
FORMATION OF C-C BOND**

Ibrahim Abdullah Albarakati

King Abdulaziz University, Faculty of Sciences

ABSTRACT

Pyridine heterocyclic compound synthesis continues to attract much attention due to their wide applicability on various fields including Pharmaceutical and Organic synthesis. Transition metals such as Palladium complexes have been used successfully for the preparation of very active hypertensive drugs Losartan and Valsartan. In recent years, remarkable progress has been recorded in Suzuki-Miyaura cross coupling reaction upon the discovery of very active and highly efficient catalysts. These catalysts Palladium with Phosphine or Carbene ligands- have been very promising due to their high efficiency in coupling reactions. In a quest to synthesize a more efficient catalyst, the combination of Palladium and Nitrogen containing ligands look promising due to their stability to air, non-toxicity and very convenient to handle.

Keywords: Suzuki cross coupling, Palladium

**TRANSFORM BASED RADIAL BASIS FUNCTION SCHEME FOR SOLVING
VARIABLE ORDER DIFFUSION EQUATION**

Rashid Ali

Department of Basic Sciences, University of Engineering & Technology Peshawar, Pakistan.

Marjan Uddin

Department of Basic Sciences, University of Engineering & Technology Peshawar, Pakistan.

Muhammad Taufiq

Department of Basic Sciences, University of Engineering & Technology Peshawar, Pakistan.

ABSTRACT

The solution of variable order fractional diffusion equations is accomplished in the current study using a localized meshless approach based on hybrid transform. To get around the time instability issue with meshless approaches, the time stepping operation is avoided. By including tiny local system matrices, the problem of improper conditioning associated with meshless differentiation matrices is removed. By combining the inverse Laplace transform with the trapezoidal rule of equal width, the answer is finally achieved as a contour integral along a smooth curve. The approach is tested using the time fractional diffusion equation for error analysis, convergence rate, and accuracy show a definite improvement.

Keywords: Fractional diffusion equation, Laplace transform, Meshless method.

INTRODUCTION

According to physicists, engineers, and mathematicians, several transversal applications may have been exquisitely created by applying fractional derivatives. For instance, non-linear seismic oscillations may be patterned in the fractional derivatives [1]. Without a problem, the most significant area of applied mathematics in the last ten years has been fractional calculus. Fractional derivatives and fractional integrals give more precise results for describing real-world events than the classical order. In particular, the domains of damping viscoelasticity, chemistry, communications, electrical, traffic systems, biology, signal processing, robotic technology, economics & finance, genetic algorithms, etc, have notable applications in modelling numerous physical phenomena. Significant advancements and discoveries in the subject of fractional calculus have been produced by several academics [2–9]. Fractional calculus is seen to be a very significant area of study by the majority of academics and scientists due to its many applications. Many fractional calculus academics have focused their research on fractional order partial differential equations. Analog realizations can only

describe situations of limited length, but analytical and numerical solutions are quite comparable and can explain examples of infinite length. The research findings of [11] enable reliable identification of the numerical and analogous outcomes of the process of diffusion with dissipation. Recent studies have shown that transient behaviours in some phenomena vary with geographical variation, temporal evolution, or even with spatiotemporal changes [10]. It will not be a productive and efficient way to comprehend transitory behaviours if we employ constant order fractional diffusion equations. Hence, the inconsistent order The solution to this problem has been provided using fractional diffusion equations. The Laplace transform eliminates the need for computationally challenging temporal time stepping. While the Laplace transform does away with the need for time marching, we still have to deal with the challenge of inverting the Laplace transform. Thanks to the work of Weideman and Trefethan [13] and López-Fernández [14], in which the outcomes of the Bromwich integral connected to the inverse Laplace transform are scientifically evaluated. If the number of n gets big enough, we obtain round-off errors that deviate from the right solution when we estimate the Bromwich integral using the traditional quadrature of n steps. Techniques based on local radial basis functions (RBFs) were presented in [12] to address the contour factor problem, the sensitivity and the problem of improper conditioning of global RBFs techniques. Efficiency, stability, and precision were achieved with the use of local radial basis functions (RBFs), which also generated good results smoothly.

METHOD ANALYSIS

A meshless technique based on hybridization and laplace transform is suggested in this section. The time variable is removed from the suggested technique via the Laplace transformation, and a time independent PDE localized meshless numerical scheme is then built. Our numerical method for estimating the form of the time fractional differential equation of order $0 < \alpha < 1$.

$$\partial_{0t}^{\alpha(x)} V = \frac{\partial}{\partial x} \left(k(x) \frac{\partial V}{\partial x} \right) - Vg(x, t) + f(x, t), \quad 0 < t \leq T \quad 0 < x < 1 \quad (1)$$

with the initial conditions,

$$V(0, t) = v_1(t) \quad V(1, t) = v_2(t), \quad 0 < t \leq T \quad (2)$$

and boundary conditions,

$$V(x, 0) = v_0(x), \quad 0 \leq x \leq 1 \quad (3)$$

Now applying laplace transform to (1)-(3) we have,

$$[Z^{\alpha(x)} - k(x)D_2 + g'(x, z)]v(x, z) = G(x, z), \quad x \in \Omega \quad (4)$$

$$\text{as } G(x, z) = f'(x, z) + Z^{\alpha(x)-1}v_0 \quad (5)$$

The solution $u(\mathbf{x}, t)$ of Problems (1)–(3) can be obtained by using inverse Laplace transform.

$$V(x, t) = \frac{1}{2\pi i} \int_{c-i\infty}^{c+i\infty} e^{zt} v(x, z) dz = \frac{1}{2\pi i} \int_{\psi} e^{zt} \hat{v}(x, z) dz, \quad c > c_0 \quad (6)$$

The complex contour integral (6) must be approximated along the selected path, which might be parabolic, hyperbolic etc, in order to solve problem (1)-(3). Due to the nature of slowly decaying transform $V(x, z)$, $z = \sigma + i\gamma$ as $|\gamma| \rightarrow \infty$, and contour integral of high oscillatory exponential factor, the numerical integration of Eq (6) is very hard to calculate. We employed two different sorts of contours for our approximation: parabolic and hyperbolic, respectively.

The parameterization of the parabolic contour in [15] is as

$$z = \mu(1 + is)^2,$$

for the path $s = \gamma + ic$, where $c > 0$ and $-\infty < \gamma < \infty$, the contour in parabolic form can be as,

$$z(\gamma) = \mu((1 - c)^2 - \gamma^2) + 2i\mu\gamma(1 - c). \quad (7)$$

The governing width parameter μ for the given contour is shown below,

$$\text{Where } \mu = \frac{\pi}{4\sqrt{8\Lambda+1}} \frac{m}{t}, \quad \Lambda \text{ can be calculated as } K = \frac{\sqrt{8\Lambda+1}}{M}, \quad \text{and } M = \frac{T}{t_0}$$

To calculate the error estimate order we have,

$$E_1 = |v_k(x, t) - v(x, t)| = O\left(\left(\frac{2\pi}{\sqrt{8\Lambda+1}}\right)M\right), \text{ while } M \rightarrow \infty \quad (8)$$

Where M is defined as $m = \frac{2M}{k}$, k is step size of trapezoidal rule and, m is the number of quadrature points.

The hyperbolic contour in [16] may be expressed as,

$$z(\gamma) = \omega + \lambda(1 - \sin(\delta - i\gamma)), \quad -\infty < \gamma < \infty, \quad (9)$$

here $0 < \delta < \beta - \frac{1}{2}\pi$, and $\frac{1}{2}\pi < \beta < \pi$, $\omega \geq 0$, $\lambda > 0$, see [15]

in which [15] the integral from (6) is given as,

$$v(x, t) = \frac{1}{2\pi i} \int_{-\infty}^{+\infty} e^{z(\hat{\eta})t} \hat{v}(x, z(\hat{\eta})) \dot{z}(\hat{\eta}) d(\hat{\eta}) \quad (10)$$

An error estimate is provided as,

$$E_2 = |v_k(x, t) - v(x, t)| = O(i(\rho_r M) e^{-\mu M}) \quad (11)$$

and $i(x) = \max(1, \log(1/x))$, $\mu = (1 - \theta) \bar{r}/b$, $\bar{r} = 2\pi r$, $r > 0$, $0 < \theta < 1$,

$$\rho_r = \theta \bar{r} \tau \sin(\delta - r) / b, \text{ where } \bar{r} = 2\pi r, \quad b = \cosh^{-1}(1/(\theta \tau \sin(\delta))),$$

$$\text{Where } \tau = t_o/T, \quad t_o \leq t \leq T, \quad o < t_o < T, \quad \lambda = \theta \bar{r} M / (bT) \text{ and } k = b/M.$$

Implementing the trapezoidal rule [15] to (10) produced the results shown below

$$v_k(x, t) = \frac{k}{2\pi i} \sum_{j=-M}^M e^{z_j t} v(x, z_j) \dot{z}_j \quad (12)$$

The step size in this case is k .

STABILITY

The stability of systems is explored by [17] in the discrete form, and the system is expressed as follows:

$$WU = j \quad (13)$$

W is a $N \times N$ sparse matrix that may be obtained in differentiation using a method based on local kernel. Stability constant, according to the system, is as follows:

$$C = \sup_{U \neq 0} \frac{\|U\|}{\|WU\|} \quad (14)$$

the value of C is finite when any kind of discrete norm $\|\cdot\|$ on \mathbb{R} is used. The preceding equation may be expressed as follows:

$$\|W\|^{-1} \leq \frac{\|U\|}{\|WU\|} \leq C \quad (15)$$

writing W in pseudo-inverse W^\dagger form, we have,

$$\|W^\dagger\| = \sup_{v \neq 0} \frac{\|W^\dagger v\|}{\|v\|} \quad (16)$$

now we can write the following,

$$\|W^\dagger\| \geq \sup_{v=W \neq 0} \frac{\|W^\dagger WU\|}{\|WU\|} = \sup_{U \neq 0} \frac{\|U\|}{\|WU\|} = C \quad (17)$$

Using Eqs. (15) and (17), the stability constant C 's limits are defined. Despite the computationally intensive nature of the calculation of the pseudo-inverse for the approximate solutions of system (13), the numeric stability is guaranteed in this. The MATLAB's `condst` function is giving the estimate L_∞ norm of W^{-1} , When it comes to square systems, we have,

$$C = \frac{\text{condst}(W')}{\|W\|_\infty} \quad (18)$$

This role is completed with the fewest possible calculations and is for our sparse differentiation matrix W .

APPROXIMATION BASED ON KERNEL

We use radial basis function to discretize the transformed problem (4). In bounded domain Ω , let $x_i, i = 1, 2, \dots, N$ be the center points and for each point $x_i, i = 1, 2, \dots, N$ there is a subdomain Ω_i . The function $v(x)$ can be approximated by creating local sub domain $\Omega_i, i = 1, 2, \dots, N$ by the following equation,

$$v(x_i) = \sum_{x_j \in \Omega_i} \lambda_j^i \phi^i(\|x_i - x_j\|) \quad (19)$$

Each node x_i has a local domain Ω_i that is surrounded by n other nodes. As a result, we get the following. Given are N linear systems, each of order $n \times n$.

$$\begin{pmatrix} v_1^i \\ v_2^i \\ \vdots \\ v_n^i \end{pmatrix} = \begin{pmatrix} \phi_{11}^i & \phi_{12}^i & \cdots & \phi_{1n}^i \\ \phi_{21}^i & \phi_{22}^i & \cdots & \phi_{2n}^i \\ \vdots & \vdots & \ddots & \vdots \\ \phi_{n1}^i & \phi_{n2}^i & \cdots & \phi_{nn}^i \end{pmatrix} \begin{pmatrix} \lambda_1^i \\ \lambda_2^i \\ \vdots \\ \lambda_n^i \end{pmatrix}, \quad i = 1, 2, \dots, N \quad (20)$$

which could be expressed as

$$v^i = \mathbf{B}^i \lambda^i \quad (21)$$

Here we have $\phi_{lm}^i = \phi^i(\|x_l - x_m\|), x_l, x_m \in \Omega_i$. \mathbf{B}^i is referred local interpolation matrix. From above we can approximate $\mathcal{L}v(x_i)$, which gives,

$$\mathcal{L}v(x_i) = \sum_{x_j \in \Omega_i} \lambda_j^i \mathcal{L}\phi^i(\|x_i - x_j\|) \quad (22)$$

(22) in vector form may be expressed as

$$\mathcal{L}v(x_i) = \mathbf{G}^i \cdot \lambda^i, \quad (23)$$

Where $\mathbf{G}^i = \mathcal{L}\phi^i(\|x_i - x_j\|), x_j \in \Omega_i$, expansion coefficients λ^i from equation (21) given by

$$\lambda^i = (\mathbf{B}^i)^{-1} v,$$

Put the λ^i value in (23),

$$\mathcal{L}v(x_i) = \mathbf{G}^i \cdot (\mathbf{B}^i)^{-1} v^i = \mathbf{H}^i v^i, \quad \mathbf{H}^i = \mathbf{G}^i \cdot (\mathbf{B}^i)^{-1} \quad (24)$$

Consequently, the approximate value of the arbitrary function in a local setting is given by

$$\mathcal{L}\hat{v} = \mathbf{H}\hat{v}, \quad (25)$$

\mathcal{L} is approximated by differentiation matrix \mathbf{H} of order $N \times N$, Every \mathbf{H} row has $N-n$ zero entries and n non-zero entries. In each local domain Ω_i there are n nodes. Similar methods may be applied to the boundary operator \mathbf{B} .

PROBLEM

This section begins with a description of the fractional differential equation issue that was the focus of this research, followed by some analytical solutions that may be used to better understand the nature of the problem.

$$\frac{\partial^\alpha u(x,t)}{\partial t^\alpha} = k \frac{\partial^2 u(x,t)}{\partial x^2} + f(x,t), \quad 0 < x < 1 \quad 0 \leq t \leq T \quad (26)$$

subject to the initial and boundary criteria listed below:

$$\begin{aligned} u(x, 0) &= 0 & 0 < x < 1 \\ u(0, t) = u(1, t) &= 0 & 0 \leq t \leq T \end{aligned}$$

We investigate the issue and offer a precise analytical response:

$$u(x, t) = t^2 \sin(2\pi x) \quad (27)$$

The related forcing term can be verified by

$$f(x, t) = \frac{2}{\Gamma(3-\alpha)} t^{2-\alpha} \sin(2\pi x) + 4\pi^2 t^2 \sin(2\pi x) \quad (28)$$

Table with different N values that shows error and convergence order and M = 40,

$\sigma = 0.1541, a = 0, b = 1$. we find convergence by the formula, $\log_{N_1/N_2} \frac{e_1}{e_2}$.

N	Error	convergence order
30	2.318E-05	
35	1.889E-05	0.12
40	1.670E-05	0.07

Figure displays both the exact and approximate results.

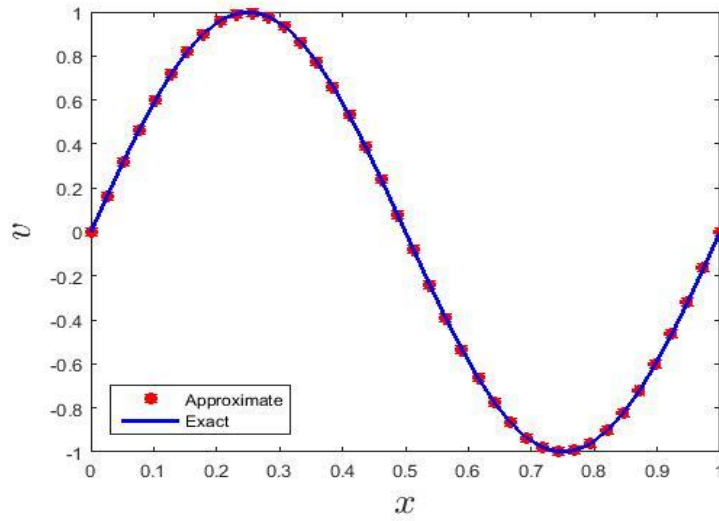


Table displaying several x values, the exact and approximately calculated results, and error.

'x'	Approximate results	Exact results	Error
0.0	0.0	0.0	0.0
0.0250000000000000	0.156449238010661	0.156434465040231	0.0000147731
0.0500000000000000	0.309030531504204	0.309016994374947	0.0000135361
0.0750000000000000	0.454001711027883	0.453990499739547	0.0000112131
0.1750000000000000	0.891009591714526	0.891006524188368	0.0000030677
0.2000000000000000	0.951058053545917	0.951056516295154	0.0000015435
0.2500000000000000	0.999999196945230	1.000000000000000	0.0000008031
0.2750000000000000	0.987686737343928	0.987688340595138	0.0000009671
0.3000000000000000	0.951054356306205	0.951056516295154	0.0000021599
0.3250000000000000	0.891004041297596	0.891006524188368	0.0000024831
0.3500000000000000	0.809014407001321	0.809016994374947	0.0000025873
0.4750000000000000	0.156433765786071	0.156434465040231	0.0000006993
0.5000000000000000	0.000000064656501	0.000000000000000	0.0000000646

CONCLUSION

In this study, a numerical method of calculating differential order fractional diffusion issues in a local environment is provided. This method makes use of the Laplace transform with RBF functions. The recommended numerical method worked well to approximate the difficulties. This method is effective for variable fractional order equations because it is not time-sensitive, in contrary to finite difference estimation for fractional order operators. By generating small size differentiation grids in local sub-domains and combining them as a single sparse matrix in the global domain, RBF may approximate spatially operators in multi-dimensions in the local environment.

REFERENCES

- [1] He, J. H. (1998, August). Nonlinear oscillation with fractional derivative and its applications. In *International conference on vibrating engineering* (Vol. 98, pp. 288-291).
- [2] Saad, K. M., & Gómez-Aguilar, J. F. (2018). Analysis of reaction–diffusion system via a new fractional derivative with non-singular kernel. *Physica A: Statistical Mechanics and its Applications*, 509, 703-716.
- [3] Morales-Delgado, V. F., Gómez-Aguilar, J. F., & Taneco-Hernandez, M. A. (2019). Analytical solution of the time fractional diffusion equation and fractional convection-diffusion equation. *Revista mexicana de física*, 65(1), 82-88.
- [4] Atangana, A., & Gómez-Aguilar, J. F. (2018). Fractional derivatives with no-index law property: application to chaos and statistics. *Chaos, Solitons & Fractals*, 114, 516-535.
- [5] Atangana, A., & Gómez-Aguilar, J. F. (2018). Decolonisation of fractional calculus rules: breaking commutativity and associativity to capture more natural phenomena. *The European Physical Journal Plus*, 133(4), 1-22.
- [6] Gómez-Aguilar, J. F., & Dumitru, B. (2014). Fractional transmission line with losses. *Zeitschrift für Naturforschung A*, 69(10-11), 539-546.
- [7] Gómez Aguilar, J. F., Atangana, A., & Morales-Delgado, V. F. (2017). Electrical circuits RC, LC, and RL described by Atangana–Baleanu fractional derivatives. *International Journal of Circuit Theory and Applications*, 45(11), 1514-1533.
- [8] Saad, K. M., Khader, M. M., Gómez-Aguilar, J. F., & Baleanu, D. (2019). Numerical solutions of the fractional Fisher’s type equations with Atangana-Baleanu fractional derivative by using spectral collocation methods. *Chaos: An Interdisciplinary Journal of Nonlinear Science*, 29(2), 023116.
- [9] Yépez-Martínez, H., & Gómez-Aguilar, J. F. (2019). A new modified definition of Caputo–Fabrizio fractional-order derivative and their applications to the multi step homotopy analysis method (MHAM). *Journal of Computational and Applied Mathematics*, 346, 247-260.
- [10] Hosseini, V. R., Yousefi, F., & Zou, W. N. (2021). The numerical solution of high dimensional variable-order time fractional diffusion equation via the singular boundary method. *Journal of Advanced Research*, 32, 73-84.
- [11] Sierociuk, D., Skovranek, T., Macias, M., Podlubny, I., Petras, I., Zielinski, A., & Ziubinski, P. (2015). Diffusion process modeling by using fractional-order models. *Applied Mathematics and Computation*, 257, 2-11.
- [12] Šarler, B., & Vertnik, R. (2006). Meshfree explicit local radial basis function collocation method for diffusion problems. *Computers & Mathematics with applications*, 51(8), 1269-1282.
- [13] Weideman, J., & Trefethen, L. (2007). Parabolic and hyperbolic contours for computing the Bromwich integral. *Mathematics of Computation*, 76(259), 1341-1356.

- [14] López-Fernández, M., Palencia, C., & Schädle, A. (2006). A spectral order method for inverting sectorial Laplace transforms. *SIAM journal on numerical analysis*, 44(3), 1332-1350.
- [15] Weideman, J., & Trefethen, L. (2007). Parabolic and hyperbolic contours for computing the Bromwich integral. *Mathematics of Computation*, 76(259), 1341-1356.
- [16] McLean, W., & Thomée, V. (2010). Numerical solution via Laplace transforms of a fractional order evolution equation. *The Journal of Integral Equations and Applications*, 57-94.
- [17] Uddin, M., & Ali, A. (2018). A localized transform-based meshless method for solving time fractional wave-diffusion equation. *Engineering Analysis with Boundary Elements*, 92, 108-113.

**STUDY OF THE EVOLUTION OF THE STRESS CONCENTRATION
COEFFICIENT AND THE STRESS INTENSITY FACTOR OF ABS SPECIMENS
CONTAINING A COMBINED DEFECT**

H. BOUHSISS

Ben M'sick Faculty of Sciences, Laboratory of Condensed Matter, Casablanca Morocco,
Laboratory of Control and Mechanical Characterization of Materials and Structures, National Higher School of
Electricity and Mechanics, BP Oasis, Hassan II University, Casablanca, Morocco

EN-NAJI

Ben M'sick Faculty of Sciences, Laboratory of Condensed Matter, Casablanca Morocco,
Laboratory of Control and Mechanical Characterization of Materials and Structures, National Higher School of
Electricity and Mechanics, BP Oasis, Hassan II University, Casablanca, Morocco

A.WAHID

M'sick Faculty of Sciences, Laboratory of Condensed Matter, Casablanca Morocco,
Laboratory of Control and Mechanical Characterization of Materials and Structures, National Higher School of
Electricity and Mechanics, BP Oasis, Hassan II University, Casablanca, Morocco

ABDELKRIM KARTOUNI

M'sick Faculty of Sciences, Laboratory of Condensed Matter, Casablanca Morocco,
Laboratory of Control and Mechanical Characterization of Materials and Structures, National Higher School of
Electricity and Mechanics, BP Oasis, Hassan II University, Casablanca, Morocco

M. EL GHORBA

M'sick Faculty of Sciences, Laboratory of Condensed Matter, Casablanca Morocco,
Laboratory of Control and Mechanical Characterization of Materials and Structures, National Higher School of
Electricity and Mechanics, BP Oasis, Hassan II University, Casablanca, Morocco

ABSTRACT

Plastics play an important role in our daily lives due to their ease of installation and relatively low production costs. At present polymers are ubiquitous in all facets of our lives, hence the imminent need to detect the mechanical behaviour of these said polymers. This research presents new developments in the field of fracture mechanics.

The present work will be devoted to the study of the mechanical behaviour of a polymer of type Acrylonitrile Butadiene Styrene (ABS) under uniaxial tensile loading focusing on the influence of stress concentrations on the behavior of the studied ABS structures containing a combined defect.

The knowledge of the mechanical behavior of the components is essential to predict their service life in order to avoid any fatal failure in service. In this context, our study is based on the evolution of the stress concentration coefficient and the stress intensity factor of single and double notched specimens.

In order to achieve this objective we have damaged the studied material (ABS) by the realization of combined hole + single notch and hole + double notch defects.

Mots clefs: Comportement mécanique, Coefficient de concentration de contrainte, ABS, traction, endommagement, durée de vie, Facteur d'intensité de contrainte, défaut critique

ANALYSIS OF THE BENEFITS OF PURWACENG AS A MEDICINAL PLANT

Shinta Dewi

Uin KH Abdurrahman Wahid Pekalongan Indonesia

ORCID: 0000-0001-9543-6840

ABSTRACT

Purwaceng is a commercial herbaceous 1 plant whose roots are medicinal as an aphrodisiac, diuretic, and tonic. The plant is native to Indonesia that lives endemic to mountainous areas such as the Dieng plateau in Central Java, Mount Pangrango in West Java, and mountainous areas in East Java. The purwaceng population is already rare because it has undergone massive genetic erosion, currently the plant is only found in the Dieng plateau.

Based on several studies from the purwaceng plant, purwaceng content was found such as coumarin derivatives, sterols, saponins, and alkaloids. Data from the Research Center for Medicinal and Aromatic Plants shows that other purwaceng content is lomonene compounds, kafaet acid, skualena, dianethole, isoorientin, anisketone, and hidrokinone. Based on the content in it, purwaceng is also believed to be one of the aphrodisiacs.

Purwaceng is included in herbal plants that can provide various health benefits, including: increasing male virility, increasing female sexual desire, overcoming fungal infections, improving blood circulation, pain and fever relief, preventing cancer and tumors, maintaining muscle health, increasing stamina, and anti-cold medicine. To get noticeable efficacy, Purwaceng should be taken regularly for 7-15 days. In addition, this plant is also efficacious in warming the body, nerves and muscles, eliminating colds and soreness, promoting urination, analgetic drugs (relieving pain), lowering heat, deworming, antibacterial and anti-cancer. The original Purwaceng has a distinctive taste, which is spicy, which is produced by its roots and seeds.

Keywords: Medicinal Plant, Aromatic, Purwaceng

**PECULIARITIES IN DETERMINING THE EFFECTIVENESS OF
ENVIRONMENTAL PROTECTION ACTIVITIES**

M. As. Michailov

Assoc. Prof. PhD – SWU “Neofit Rilski” – Bulgaria

ABSTRACT

Questions about the need for analysis and more precise assessments of the various environmental protection activities are discussed. An approach is proposed for a more categorical presentation of the benefit of these activities, i.e., to prove their effectiveness.

Keywords: Environmental Activities, Anthropogenic Impact On Watercourses, Effectiveness Of Environmental Protection Activities

INTRODUCTION

A few contemporary examples can be found in various publications, through which to provoke more serious reflections on the evaluation of actions in the field of environmental protection. Whatever methodology is applied in determining the meaning of all types of environmental protection activities, their benefit should be taken into account, i.e. their effectiveness.

It is imperative to understand "that environmental protection activities" are not just an appendage to the science of "ecology", but that it is a specific period in the development of the world during which specific evaluations of the effectiveness of human activities are imperative

i.e., is to assess the effectiveness of anthropogenic impact on the environment.

In ecology, one usually deals with concepts such as biotic, abiotic and anthropogenic factors. Through them, it is assumed that the various states, influences and impacts on ecosystems are covered.

But such concepts are also used in other sciences that also have interests in this field. That is why basic questions about the evaluations of the effectiveness of environmental protection actions are considered here, i.e. how the benefit of such type of activities is determined.

By answering such questions and summarizing them, we can hope for adequate assessments of the effectiveness of various environmental protection activities.

It is no longer enough to count the so-called biotic and abiotic factors of ecology among the commonly known factors. anthropogenic factors and thus be considered to end the nature and significance of environmental protection activities.

In this regard, it is worth commenting on the practice of explaining various laws from the field of ecology (law of the minimum, law of tolerance or law of the joint action of ecological factors [Shelford's law of tolerance] - fig.1) and not delving into the essence of conservation of the environment (as a specific scientific field, as a niche for economic realizations and social manifestations, etc.).

A more serious consideration of the role of basic laws in ecology and environmental protection is required, especially in relation to justification and evaluations of the effectiveness

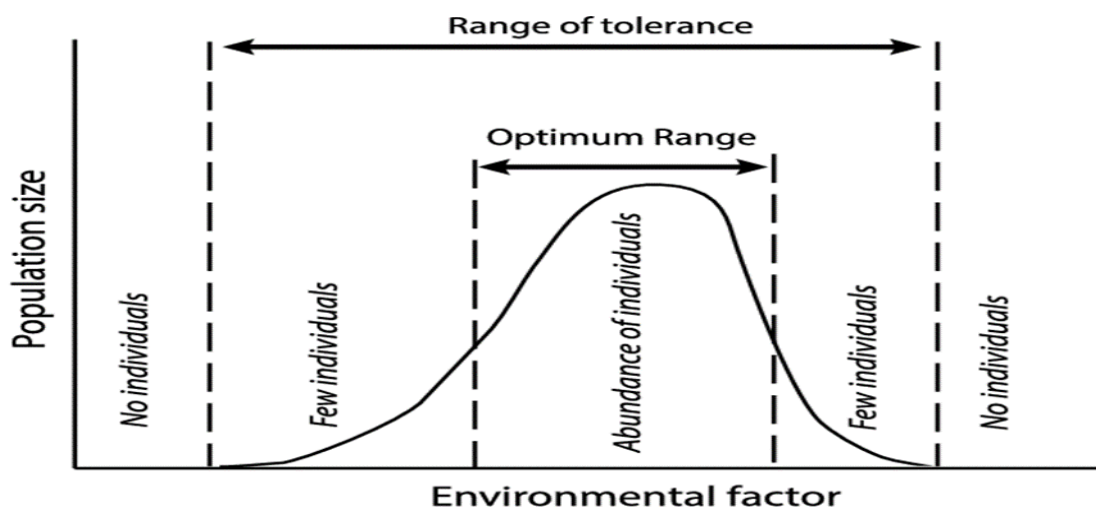


Fig. 1 Graphical representation of Shelford's Law of Tolerance [7]

of specific activities, through which to limit the anthropogenic impact (avalanche-like growing) in modern society.

MATERIALS AND METHODS

The popularization of campaign concepts in environmental protection activities cannot fulfill their essence and, what is more important, provide an opportunity for real evaluation of the effectiveness of such type of activities. The goal is not to report expenses, but to generate revenue.

In relation to the said situation, it is relevant to note the fact that still in the system of NSI (National Statistical Institute) [<https://nsi.bg/bg//2582-Ecology7.1.xls>] a platform "expenses for restoration and protection of the environment" is maintained.

It is imperative that this situation be changed. Conservation supports the restoration of the environment, but to realize this restoration, other activities must also be implemented.

Arguments for including data on "circulating water supply" in environmental protection activities are controversial, as such practices are part of the "rational use of water resources" and it does not make much sense to associate it with "environmental protection"

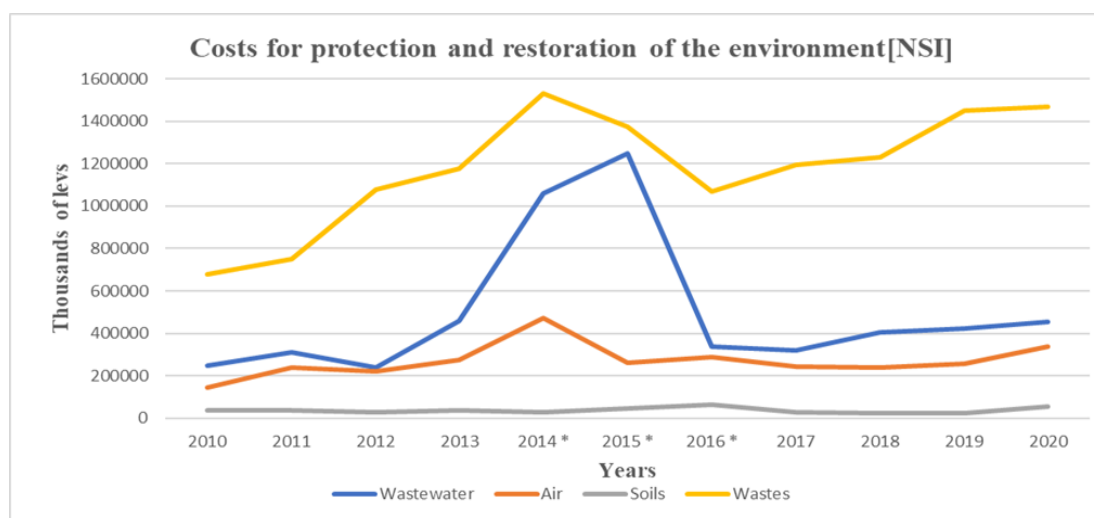


Fig. 2

The one shown in fig. 2 information on "expenses for environmental protection and restoration" in the period 2010-2020 provides an opportunity for a more serious consideration of this type of activity, for which it is important to explain their expediency, i.e. they need an economic evaluation of their benefit ie. for their effectiveness.

But if one looks more seriously into this information, one (rather unpleasant) finding can be made - less than 1% of all stated expenses [<https://nsi.bg/bg//2582-Ecology7.1.xls>] are allocated to research and educational activities.

Based on this finding, it should be summarized - the various activities in the field of environmental protection are not given serious attention, which can be taken as an argument for a much more serious attitude to the evaluations of the effectiveness of activities in the field of environmental protection.

By means of the following figure (fig. 3) one can very easily get an idea of the allocation of funds for these activities [<https://nsi.bg/bg//2582-Ecology7.1.xls>]. Based on such information,

the question of the meaning and evaluations of environmental protection activities arises. And the logical conclusion is that we cannot expect good results when the plans for achieving them are not sufficiently scientifically substantiated. On this occasion, we should pay attention to the justifications for the nature of environmental impact assessment (EIA) activities.

It is inexplicable why the law on environmental protection [*Environmental Protection law - <https://lex.bg/laws/>*] provides for environmental impact assessments, when through the implementation of "plans, programs and investment proposals for construction, activities and technologies or their changes, the implementation of which is possible significant impacts' on the environment.

It appears that this law applies to "significant impacts" but not to "minor" or other types of impacts.

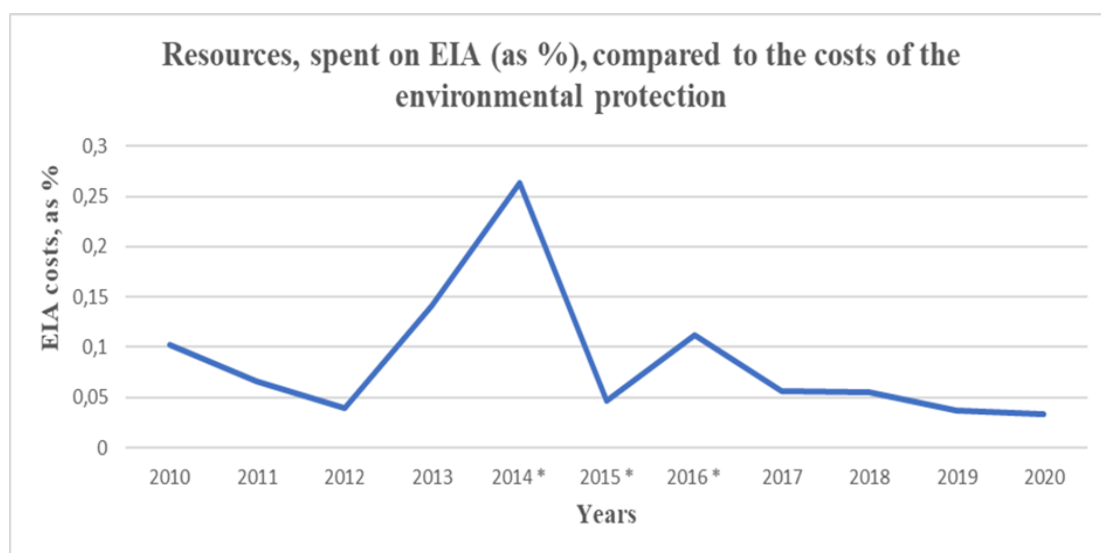


Fig. 3

Based on the stated arguments, a position should be clearly expressed in relation to the various environmental protection activities.

This specific activity needs a substantial scientific and research basis, based on which to implement practical programs and plans, according to specific justifications and evaluations of their effectiveness.

In accordance with the stated position, it is imperative to pay attention to the nature of environmental protection activities. In the conditions of the increasingly looming anthropogenic impact, it is especially imperative to delve into it, i.e. the perception of environmental protection activities as being easy to implement is deeply flawed.

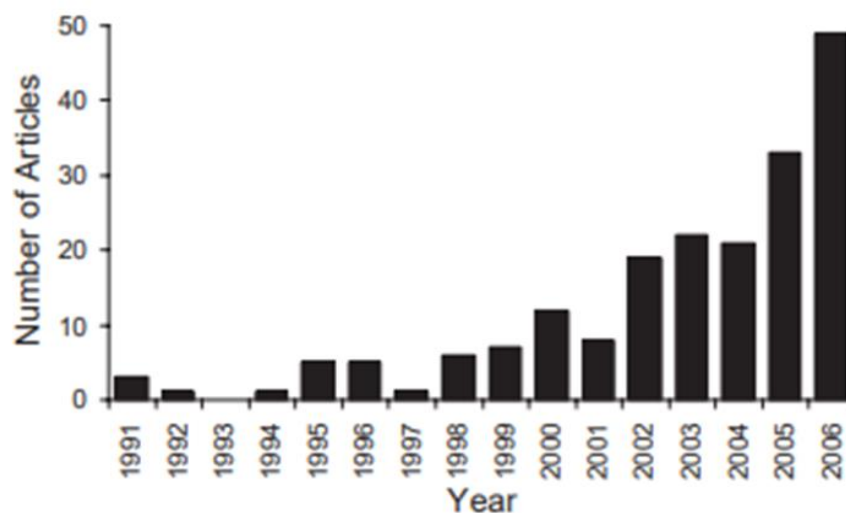
With the various activities in this area, it is imperative to evaluate their results, i.e. to evaluate their effectiveness. That is why it is expedient to take a much more serious approach and to analyze similar approaches applied in other branches of the Society's economy. In various editions and publications, mixing is allowed in the analyzes of environmental problems and problems in environmental protection activities.

For example, ideas for company development, business development, etc. continue to spread [Kotter John P.-1996] without considering the challenges that may arise from this in terms of environmental protection. The engagement of individual media and non-governmental structures with this type of activity does not correspond to the importance of the problem of increasing anthropogenic impact.

The analysis of the results of several events with an environmental focus (campaigns, NGO-initiatives, etc.) shows that such an approach is insufficiently effective. It is one thing to launch ideas for ecological thinking and solving environmental problems, and quite another to implement and manage environmental protection activities, i.e. to limit the negative anthropogenic impact.

As an example of the topicality of the discussed theme, it is worth paying more serious attention to the figure (fig. 4), commented on [Hydroecology and Ecohydrology: Past, Present and Future. Edited by P. J. Wood and all.].

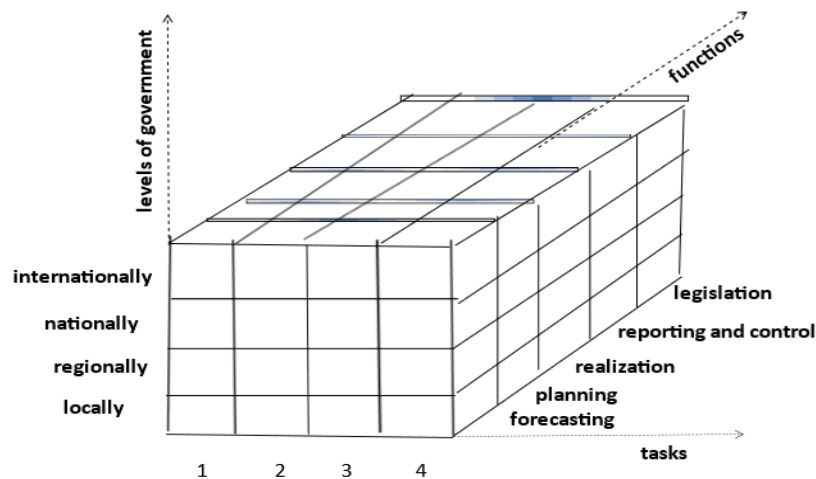
The increased interest in environmental topics (especially at the end of the XX century and the beginning of the XXI century) is impressive. In this regard, the considerations set out here are aimed at greater efficiency of environmental protection activities.



Number of peer-reviewed journal articles using the terms, ecohydrology and hydroecology (1991 - 2006)
according to [Hydroecology and Ecohydrology: Past, Present and Future. Edited by P. J. Wood, D. M. Hannah, J.P. Sadler. John Wiley & Sons Ltd. 2007]

Fig. 4

Given the stated position, it is suggested that the environmental protection activities described in this way should be viewed as all other human activities, according to the presented structural-functional management model [Hristov Hr.-1980] (fig. 5) i.e. regardless of the level (local, regional, national or international) of management activity, the type of tasks performed (scientific - research, design, construction - assembly activities, organizational, etc.) and functions (planning, implementation, control, legislation and etc.) the relevant actions for environmental protection must be carried out.



Structure and functional management model

Fig. 5

For this purpose, it is imperative to structure all attributes, as in other human activities - domestic, financial, social, industrial, etc. As with them, such structuring covers:

- scientific-research and methodical.
- organizational (executive – monitoring, control, etc.).
- legislative, etc.

In this way, it will be possible to differentiate their functions more correctly and to evaluate the achieved results.

On this basis, the following approach is proposed to overcome doubts about the benefits of environmental protection activities and to implement them as those committed to reducing and limiting the negative anthropogenic impact on the environment.

In this regard, we should pay attention to the rationale for the nature of environmental impact assessment (EIA) activities. It is inexplicable why the Environmental Protection Act [4] provides for provisions on environmental impact assessments, when through the implementation of “plans, programs and investment proposals for construction, activities and technologies or their amendments, the implementation of which is possible significant impacts” on the environment. It seems that this law applies to "significant impacts", but not to "minor" or other types of impacts.

Taking into account the stated position, it is imperative to pay attention to the nature of environmental protection activities. In the conditions of the more and more emerging anthropogenic impact, it is especially necessary to understand it, ie. the notion that environmental activities are easily feasible is deeply flawed.

In the centuries-old history of economic development, attention has always been paid to the value of output and to analyze similar approaches applied in other sectors of the Company's economy.. The value expressed the causal link between the price of the product produced and the costs necessary for its production.

On this basis, the value of each product can be represented as:

$$\mathbf{Pr_{ij}} = \mathbf{R_{ij}} + \mathbf{S_{ij}} + \mathbf{L_{ij}} \quad (1)$$

where: $\mathbf{Pr_{ij}}$ - the value of a any product (i) of a any company (j),
 $\mathbf{R_{ij}}$ - resources (raw materials) for a given product (i) of a company(j),
 $\mathbf{S_{ij}}$ - service (electricity, water, heating) in the production of a given product (i) of a company (j) ,
 $\mathbf{L_{ij}}$ - labor for the production of a any product (i) of a company (j).

It's clear, there are three main groups of factors in this relationship, all three of which are related to our environment. In general, the activities of all types of production should take into account these factors.

The assessment of raw materials (resources) is absolutely mandatory in the marketing of any activity related to the production of all types of products. Due to the limitations that stand out in the future, it is necessary to pay even more attention to this factor. No less important is the attitude towards the other two groups of factors. The inclusion of these factors is mandatory, both in the assessments of marketing activities and in those related to the protection of the environment.

The presented dependence (1) is general for all types of economic activities, as it covers and reflects the main influencing elements in the production of products. However, this does not cover all groups of factors relevant to environmental impact assessments.

Therefore, it is appropriate to work on the dependence to assess the effectiveness of different types of activities in marketing, from one side, and environmental protection, from the other.

RESULTS

Its additional provisions introduce such as "effectivity", "efficiency", "economy". They can help to refine some activities of the Court of Auditors [Law on the National Audit Office - www.lex.bg/bg/laws/ldoc], but for the needs of the proposed research it is appropriate to work with the effectiveness of the various types of activities:

$$\mathbf{Ete, ij} = \mathbf{Epr, ij} + \mathbf{Esup, ij} + \mathbf{Ele, ij} + \mathbf{Etr, ij} + \mathbf{Emar, ij} + \mathbf{Econs, ij} = \mathbf{max} \quad (2)$$

where:

Ete, ij - total efficiency of the activity for a given product (i) in a given company (j);

Epr, ij - efficiency in the production of a product (i) in a company (j);

Esup, ij - efficiency in providing support (service) activities ensuring the production of a product (i) in a given company (j), for example for electricity, water, heating and others.;

Ele, ij - labor efficiency in the production of a product (i) in a given company (j);

Etr, ij - efficiency in the transport of a product (i) in a company (j) to retail outlets or to consumers;

Emar, ij - efficiency in the realization of a given product (i) in a given company (j) on the market);

Econs, ij - efficiency at the consumer of a product (i) in a company (j) - (Are his needs met and to what extent).

As a variant of the above dependence, it can also be presented as a dependence for assessing the appropriateness of costs throughout the production-market-consumer chain:

$$C_{t, ij} = C_{p, ij} + C_{anc, ij} + C_{l, ij} + C_{tr, ij} + C_{mark, ij} + C_{cons, ij} = \min \quad (3)$$

where:

$C_{t, ij}$ - total cost of a product (i) in a company (j);

$C_{p, ij}$ - total costs of production of a product (i) in a company (j);

$C_{anc, ij}$ - total costs of providing ancillary activities, providing the production of a product (i) in a company (j), for example for electricity supply, water supply, heating, etc .;

$C_{l, ij}$ - total labor costs in the production of a product (i) in a given company (s);

$C_{tr, ij}$ - total transport costs of a product (i) in a company (j) to retail outlets or to consumers;

$C_{mark, ij}$ - total costs of selling a product (i) in a company (j) on the market;

$C_{cons, ij}$ - total costs to the consumer of a product (i) in a company (j) –
 (Are his needs met and to what extent).

DISCUSSION

By summarizing all of the above, it is possible to look for an opportunity to evaluate environmental activities, for example through the attitude

$$E = \frac{R}{C} \quad (4)$$

where: **E** - effectiveness of the various types of environmental activities:

R - revenues from the efficient production of goods and services;

C - costs incurred for the specified activities.

The great variety of activities in the Society, valued through the means of production and consumption, should be complemented by the activities of environmental protection, ie. and for this type of activities it is imperative to look for efficiency in their implementation.

The essential point in this idea is to evaluate the activities for environmental protection both in terms of the costs for them, but also in terms of the achieved results, ie.

$$E_{ep} = R_{ep} + C_{ep}, \quad (5)$$

where: **E_{ep}** - the efficiency of the implemented activities under environmental

protection;

Rep - revenues and profits from environmental protection activities
(including intangible);

Cep - the costs of these activities.

Through the above proposals and their implementation in practice, we can hope for better (more effective) results from the various activities in the field of environmental protection. In this connection it is pertinent to recall a quotation from Carl Jung (1875 – 1961), namely „We cannot change anything unless we accept it “[C.G.Jung-1985].

CONCLUSION

On this basis, the proposed equation (4) should be presented in the form

$$E = \frac{R+Rep}{C+Cep} \quad (6)$$

This provides an opportunity for more effective evaluation of the results of the various environmental activities and the same not to be considered only as an initiative of individual campaigns or initiatives of NGOs.

REFERENCES

1. Act 2002. Environmental Protection law (**Zakon za opazvane na okolnata creda - Obn.** ДВ. бр.91 от 2002г., ..., изм. и доп. ДВ. бр.102 от 2020г., изм. ДВ. бр.21 от 2021г.) <https://lex.bg/laws/ldoc/2135458102>
2. Act 2004. Law on the National Audit Office (Zakon za Smetnata palata – bul.) – <https://www.lex.bg/bg/laws/ldoc/2135219205>
3. Bojinov Todor and all. Ecology and economics. (Bojinov T.i kolektiv - Ecologia i ikonomica. bul. Zemizdat.) Sofia. 1990.
4. C. G. Jung - [Modern Man in Search of a Soul](#). 1985. ISBN 9780415255448.
5. Hydroecology and Ecohydrology: Past, Present and Future. Edited by P. J. Wood, D. M. Hannah, J.P. Sadler. John Wiley & Sons Ltd. 2007.
6. Hristov Hr. - Management of activities for the protection of the natural environment. (Hristov Hr. – Upravljenje na deinostite po opazvane na prirodната среда – bul.) SU "Kl. Ohridski", Sofia. 1980.
7. Kotter John P. – Leading change. Harvard business review press (1996) 2012, ISBN 978-1-4221-8643-5
8. National Statistical Institute - <https://nsi.bg/bg/content/2582 - Ecology 7.1.xls>.
9. Shelford's law of tolerance. – www.oxfordreference.com

HVDC LINKS: SOLUTION TO IMPROVE HVAC GRIDS

MANKOUR MOHAMED

Department of electro-technical and Automatic Engineering, University of Ahmed Zabana of Relizane, Algeria
ORCID ID: 0000-0002-8544-8909

MILOUDI MOHAMED

Department of electro-technical and Automatic Engineering, University of Ahmed Zabana of Relizane, Algeria

ABSTRACT

In order to enhance the traditional grids based on Alternate Current, this article will examine several HVDC (High Voltage Direct Current) system topologies that may be used. The investigation of DC-link failures and recovery scenarios based on a 12-pulse HVDC link system is also covered in the second part of this work. Given that the DC-link to ground fault is one of the most severe failures that may occur on an HVDC-link, two DC-fault scenarios are explored in order to understand how the system would behave in the presence of this fault type. One scenario occurs at the rectifier's transmitting end, and the other at the inverter's receiving end. The faults are primarily used to test the proposed DC fault prevention function and to analyze the dynamic performance of the recovery of the HVDC-link system following faults. Additionally investigated is the effect of the Voltage Dependent Current Order Limiter (VDCOL) function. The HVDC-link system is modeled and simulated using the digital real-time simulator laboratory (RT-Lab) platform. To achieve a high performance recovery from the fault, the preservation of system stability is explored. High performance recovery from the faults is demonstrated by the ramp-up recovery approach employed in the DC-bus voltage restoration supplied by the VDCOL-function and the validated functioning of the protection function against DC faults.

Keyword: HVDC link, Mono-polar link, AC grids, DC faults, DC protection function.

**ARTIFICIAL NEURAL NETWORK CONTROLLER FOR NONLINEAR
DYNAMICAL SYSTEMS**

Nurşah DİK

Undergraduate Student, Muğla Sıtkı Koçman University, Faculty of Engineering, Department of Electrical and
Electronics

ORCID: 0000-0002-0425-6316

Kemal UÇAK

Assis. Prof. Dr. Muğla Sıtkı Koçman University, Faculty of Engineering, Department of Electrical and Electronics
Engineering,

ORCID: 0000-0001-7005-7940

ABSTRACT

Artificial neural networks (NN) are one of the most powerful artificial intelligence techniques for estimating the unknown dynamics of systems due to their superior learning and adaptation capabilities. NNs can be used for estimation of the dynamics of an unknown system or directly as an adaptive controller architecture. For this reason, in this study, an adaptive neural network controller has been proposed for nonlinear dynamical systems. Since the control performance is directly dependent on the network structure, the controller performance for different number of neurons and activation functions has been evaluated on a time-varying nonlinear system. According to the acquired results, it can be concluded that activation function type has more effect on control performance than the number of neurons. The NN controller parameters are optimized via gradient descent algorithm. The NN controller has been assessed for nominal, measurement noise and parametric uncertainty cases that are significant for adaptive control architectures. The learning and adaptation ability of NN provides a robust adaptive controller for nonlinear dynamical systems.

Keywords: Adaptive Control, Activation Function, Artificial Intelligence, Learning Theory, Neural Network Controller.

1. INTRODUCTION

The generalization and learning abilities of NN provides a powerful tool for system identification problems. In addition to system identification problems, NN can be directly utilized to identify the unknown dynamics of controller architectures to force the closed-loop system output to the desired reference. Due to their learning capability, NN architectures are often deployed in adaptive control theory. In the case that the complexity and non-linearity of

the system increase, the classical controller becomes insufficient. Therefore, it is required to adapt the controller parameters depending on nonlinear behavior of the controlled system.

In technical literature, there are various NN controller structures for nonlinear dynamical systems. Yeşildirek and Lewis introduced a stable NN controller for state-feedback linearizable nonlinear system[1]. A robustifying term is added to the control law to interfuse robustness. The stability of the controller has been examined in the sense of Lyapunov. Mohamed et al utilized two NN architecture for model based NN controller utilized in nonlinear control systems[2]. One of the NN is deployed to identify the jacobian information required to adjust NN controller parameters via steepest descent and second NN is used to identify the unknown control law[2]. Yongquan et al proposed the combination of a fuzzy and PID type NN controller[3]. The fuzzy structure is utilized to inject nonlinearity to the error signal, then NN is used as a cascade block to the output of the fuzzy structure[3]. Chen and Narendra introduced an adaptive controller which is composed of a linear controller to ensure stability and NN controller to enhance transient state behavior of the controlled system[4]. Chen et al introduced a novel NN controller based on quadratic-type Lyapunov–Krasovskii functional for multi input multi output (MIMO) nonlinear time delay systems[5]. Ge et al presented a NN controller architecture which estimates the derivative of the controlled output via high-gain observer for nonlinear system[6]. Jacob and Murugan utilized NN to identify the dynamics of the controlled system for adaptation of PID controller parameters[7]. Kim and Lewis employed two separate NN as a controller and system model to control the nonlinear dynamics of robot arm[8]. Levin and Narendra considered a general NN controller for nonlinear dynamical systems in [9]. Lewis et al proposed a NN robot controller ensuring the stability and tracking performances[10]. Nahas et al introduced a NN based nonlinear internal model controller for SISO nonlinear systems[11]. Conjugate gradient algorithm has been used to optimize the NN parameters[11]. Ge et al introduced adaptive neural controller ensuring stability via backstepping design method for nonlinear systems with unknown time delays[12]. Wang et al proposed a deterministic learning based RBF NN controller, and persistence of excitation for RBF is analyzed[13]. Zhang et al introduced a backstepping NN controller nonlinear dynamical system to ensure stability[14]. Huaguang and Yongbing proposed a controller design methodology which combines the features of fuzzy logic, NN and linear control theory[15]. Hagan et al introduced various NN based controller architectures for nonlinear dynamical system in [16].

In this paper, model free NN controller has been utilized for nonlinear dynamical system. The NN controller performance has been tested for nominal, measurement noise, parametric uncertainty cases. The attained result indicates the powerful learning capability and generalization performance of the NN controller for nonlinear control systems.

The organization of this paper is as follows: an overview about MLP is given in section 2. The NN controller learning rules are derived in section 3. The controller performance is examined in section 4, and the paper is concluded a brief conclusion part in section 5.

2. AN OVERVIEW OF MULTI LAYER PERCEPTRON

NN's can be deployed to model the dynamics of any system by using input-output samples. Therefore, NNs can be considered as sample based model. The common MLP network topology is illustrated in Figure 1 where $w_{S,N}^h$ denotes input layer weights, $w_{1,S}^o$ is output layer weights, $h(\bullet)$ represents the activation function, b stands for bias, $\mathbf{\Pi}$ is input vector, \hat{y} indicates the output of the NN.

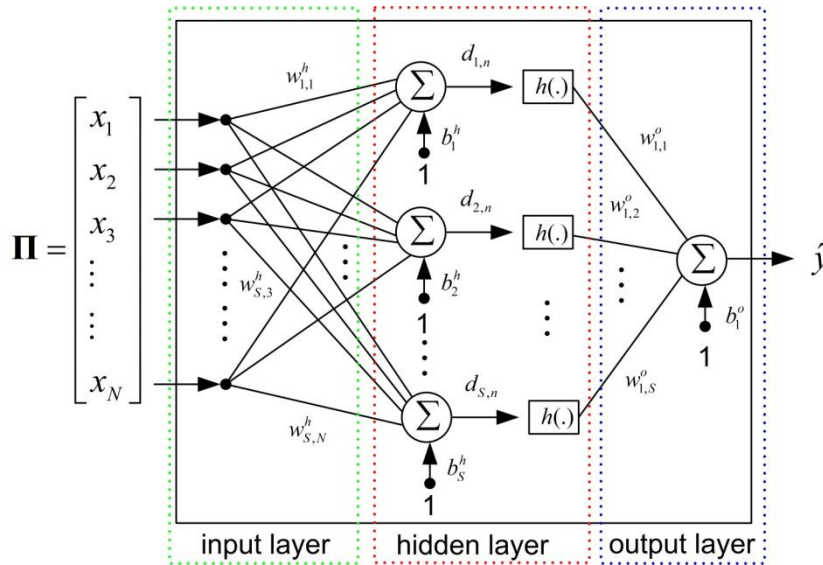


Figure 1. MLP Structure[17][18][19][20].

NNs are composed of weights in each layer and activation functions to provide nonlinearity. The network weights are initialized randomly at the beginning of the training. Then, using an objective function, the training error can be backpropagated to the weights to optimize the objective function and learn the dynamics of the system over input-output samples. The objective function to be optimized can be derived as follows:

$$J_m = \frac{1}{2} e_m^2(k), \quad e_m(k) = y(k) - \hat{y}(k) \quad (1)$$

where e_m is training error, y is actual output of system and \hat{y} denotes estimated system output (the NN output). The main aim in learning is to force the NN output to track the actual system output. Gradient based methods can be utilized to optimize the given objective function in (1). If the weight vector including all weights is considered as follows:

$$\mathbf{W} = [w_{1,1}^h \cdots w_{S,N}^h \cdots w_{1,S}^o \cdots b_s^h, b_1^o] \quad (2)$$

The weight vector can be optimized via Steepest descent as follows:

$$\mathbf{W}^{new} = \mathbf{W}^{old} + \Delta \mathbf{W}, \quad \Delta \mathbf{W} = \frac{\partial J_m}{\partial \mathbf{W}} \quad (3)$$

In order to enhance the learning capability of NN, in addition to weights, it is possible to optimize the parameters of the activation function. By using different learning algorithms such as Levenberg Marquardt, it is possible to enhance the convergence of the weights to their optimal values. The derivation of the learning rules are detailed in [19][20].

3. NEURAL NETWORK CONTROLLER

NNs can be utilized to identify the dynamics of control signal. For this purpose, NNs can be directly used as a controller as given in Figure 2 where $r(k)$ is desired reference signal, $y(k+1)$ is controlled output of the system and $u(k)$ is the control signal generated by NN controller, w_{mn} is input layer coefficients and v_n denotes the output layer weights and $h(\bullet)$ is activation function providing nonlinearity.

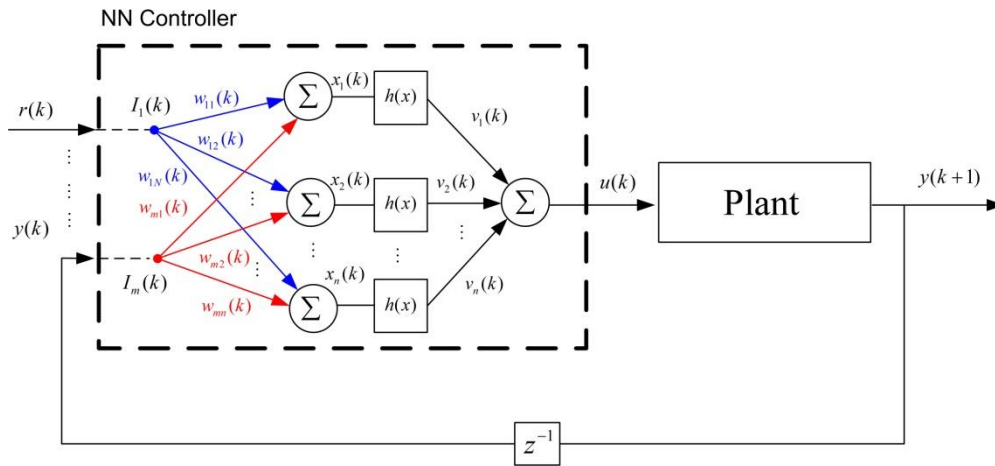


Figure 2. Neural Network Controller.

The control signal produced by NN controller can be derived as follows in matrix form.

$$u(k) = [v_1(k) \ v_2(k) \ \cdots \ v_n(k)] \begin{bmatrix} h_1(k) \\ h_2(k) \\ \vdots \\ h_n(k) \end{bmatrix} = [v_1(k) \ v_2(k) \ \cdots \ v_n(k)] h \begin{bmatrix} w_{11}(k) & w_{21}(k) & \cdots & w_{m1}(k) \\ w_{12}(k) & w_{22}(k) & \cdots & w_{m2}(k) \\ \vdots & \ddots & \ddots & \vdots \\ w_{1n}(k) & w_{2n}(k) & \cdots & w_{mn}(k) \end{bmatrix} \begin{bmatrix} I_1(k) \\ I_2(k) \\ \vdots \\ I_m(k) \end{bmatrix} \quad (4)$$

The objective function to optimize the tracking error is determined as

$$J = \frac{1}{2} e^2(k), \quad e(k) = r(k) - y(k) \quad (5)$$

The adjustable parameters of NN controller can be updated as follows:

$$\begin{aligned} \mathbf{V}^{new} &= \mathbf{V}^{old} + \Delta \mathbf{V} \\ \mathbf{W}^{new} &= \mathbf{W}^{old} + \Delta \mathbf{W} \end{aligned} \quad (6)$$

where $\mathbf{V} = [v_1 \dots v_n]$ and $\mathbf{W} = \begin{bmatrix} w_{11} \dots w_{m1} \\ \dots \dots \\ w_{1n} \dots w_{mn} \end{bmatrix}$. The objective function in (5) can be minimized via gradient descent as follows:

$$\Delta \mathbf{V} = \frac{\partial J}{\partial \mathbf{V}} = - \begin{bmatrix} \frac{\partial J}{\partial v_1} \\ \vdots \\ \frac{\partial J}{\partial v_n} \end{bmatrix} = -e \frac{\partial y}{\partial u} \begin{bmatrix} h_1(k) \\ \vdots \\ h_n(k) \end{bmatrix} \quad (7)$$

$$\Delta \mathbf{W} = \frac{\partial J}{\partial \mathbf{W}} = - \begin{bmatrix} \frac{\partial J}{\partial w_{11}} & \frac{\partial J}{\partial w_{21}} & \dots & \frac{\partial J}{\partial w_{m1}} \\ \frac{\partial J}{\partial w_{12}} & \frac{\partial J}{\partial w_{22}} & \dots & \frac{\partial J}{\partial w_{m2}} \\ \vdots & \ddots & \ddots & \vdots \\ \frac{\partial J}{\partial w_{1n}} & \frac{\partial J}{\partial w_{2n}} & \dots & \frac{\partial J}{\partial w_{mn}} \end{bmatrix} = -e \frac{\partial y}{\partial u} \begin{bmatrix} v_1(k) \frac{\partial h_1}{\partial x_1} I_1 & v_1(k) \frac{\partial h_1}{\partial x_1} I_2 & \dots & v_1(k) \frac{\partial h_1}{\partial x_1} I_m \\ v_2(k) \frac{\partial h_2}{\partial x_2} I_1 & v_2(k) \frac{\partial h_2}{\partial x_2} I_2 & \dots & v_2(k) \frac{\partial h_2}{\partial x_2} I_m \\ \vdots & \ddots & \ddots & \vdots \\ v_n(k) \frac{\partial h_n}{\partial x_n} I_1 & v_n(k) \frac{\partial h_n}{\partial x_n} I_2 & \dots & v_n(k) \frac{\partial h_n}{\partial x_n} I_m \end{bmatrix} \quad (8)$$

As can be clearly seen from the update rules in (7) and (8), in order to optimize the controller parameters, it is required to use system Jacobian ($\frac{\partial y}{\partial u}$). System Jacobian can be estimated via numerical derivations as follows:

$$\frac{\partial y(k)}{\partial u(k)} \cong \frac{y(k+1) - y(k)}{u(k) - u(k-1)} \quad (9)$$

By using different type of activation functions and neurons, it is possible to attain reasonable results. Various activation functions and their derivatives are shown in Table 1.

Table I. Various Activation Functions and their derivatives[16][19][20].

Activation Function	Mathematical Form	Derivative
Tanh	$h(x) = \frac{e^x - e^{-x}}{e^x + e^{-x}}$	$\dot{h}(x) = (1 - h(x)^2)$
Sigmoid	$h(x) = \frac{1}{(1 + e^{-x})}$	$\dot{h}(x) = h(x)(1 - h(x)^2)$
ReLU	$h(x) = \begin{cases} 0 & x < 0 \\ x & x \geq 0 \end{cases}$	$\dot{h}(x) = \begin{cases} 0 & x < 0 \\ 1 & x \geq 0 \end{cases}$
Leaky ReLU	$h(x) = \begin{cases} 0.01x & x < 0 \\ x & x \geq 0 \end{cases}$	$\dot{h}(x) = \begin{cases} 0.01 & x < 0 \\ 1 & x \geq 0 \end{cases}$
Parametric ReLU	$h(x) = \begin{cases} x & x > 0 \\ ax & x \leq 0 \end{cases}$	$\dot{h}(x) = \begin{cases} 1 & x > 0 \\ a & x < 0 \end{cases}$
Swish	$h(x) = x \operatorname{sig}(x)$	$\dot{h}(x) = h(x) + \operatorname{sig}(1 - h(x))$
Softplus	$h(x) = \ln(1 + e^x)$	$\dot{h}(x) = \frac{1}{1 + e^{-x}}$
Softsign	$h(x) = \frac{x}{1 + x }$	$\dot{h}(x) = \frac{1}{(1 + x)^2}$

4. SIMULATION RESULTS

The adaptation performance of the NN controller has been tested on the following nonlinear dynamical system. As can be clearly seen from its dynamics, the system dynamics are changed radically after $k=500$.

$$y(k+1) = \begin{cases} \frac{y(k)}{1 + y^2(k)} + u^3(k), & k \leq 500 \\ \frac{y(k)y(k-1)y(k-2)u(k-1)(y(k-2)-1) + a(k)u(k)}{1 + y^2(k-1) + y^2(k-2)}, & k > 500 \end{cases}, \quad (10)$$

The controller performance has been evaluated for different types of activation functions for $N=5$ (neuron number in hidden layer). The performance index given below is used to constitute Table 2 for various activation functions given in Table 1.

$$J_p = \sum_{k=1}^{\infty} \frac{1}{2} e^2(k) \quad (11)$$

Table II. Comparison of Activation Functions in Table 1 for N=5.

Activation Function	$J_p = \sum_{k=1}^{\infty} \frac{1}{2} e^2(k)$
Tanh	17.1791
Sigmoid	0.3807
ReLU	17.3049
Leaky ReLU	17.5271
Parametric ReLU	17.8806
Swish	23.5253
Softplus	0.4254
Softsign	18.0609

It has been observed that the type of the activation function is more effective than neuron numbers. As given in Table 2, Sigmoid and Softplus activation functions have superior performance if it is compared with other activation functions. Swish has the worst performance. The adaptation performance of the NN controller has been investigated for nominal, measurement noise and parametric uncertainty cases.

4.1. Nominal Case

The control performance of NN controller is illustrated in Figure 3. It is clearly seen that the system output tracks the desired reference signal accurately.

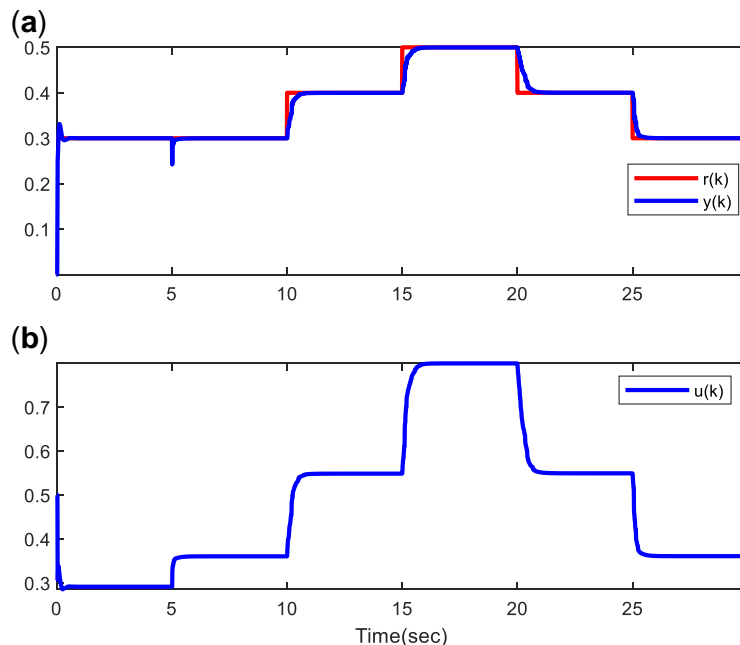


Figure 3. System Output and Reference Signal(a), Control Signal(b) for nominal case.

The evaluation of the NN weights are given in Figure 4. Depending on alternation of reference signal, the controller parameters are optimized to force to their sub/optimal values.

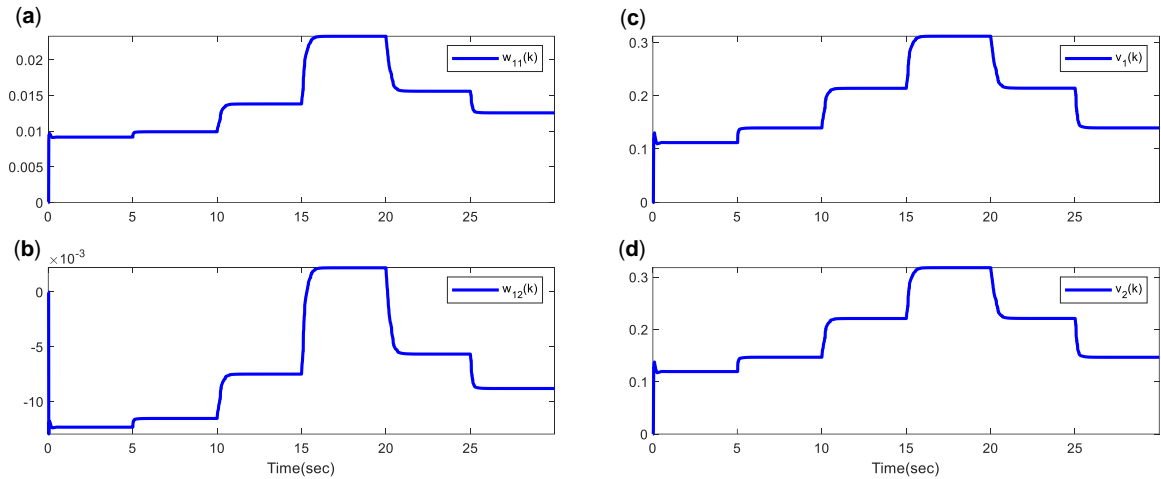


Figure 4. Weights of input(a,b) and output layers(c,d).

The system Jacobian and learning rate are shown in Figure 5.

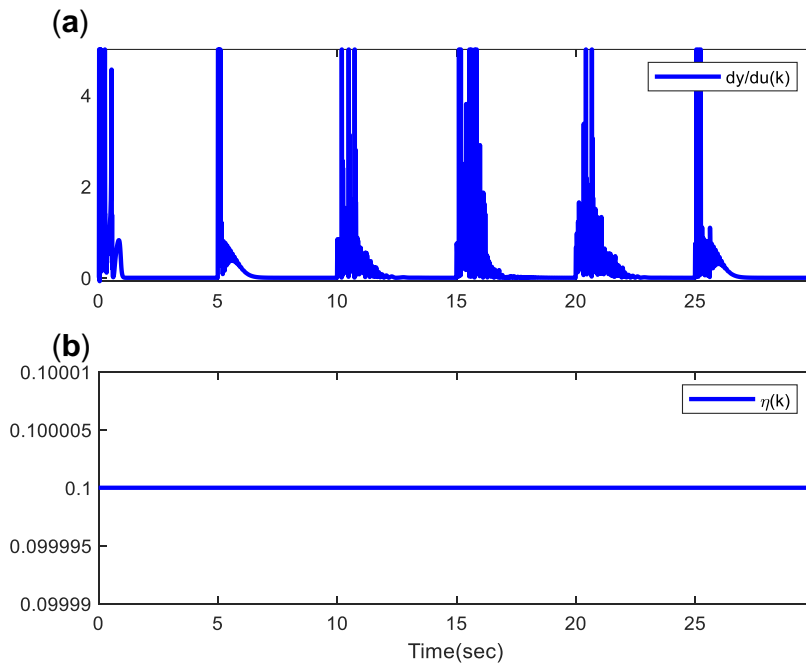


Figure 5. Jacobian(a) and Learning Rate(b).

4.2. Measurement Noise Case

The controlled output of the system is exposed to 30 dB measurement noise. The tracking performance of the closed-loop system is depicted in Figure 6. Thus, the robustness of the

NN controller for uncertainties resulting from measurement devices has been observed in Figure 6.

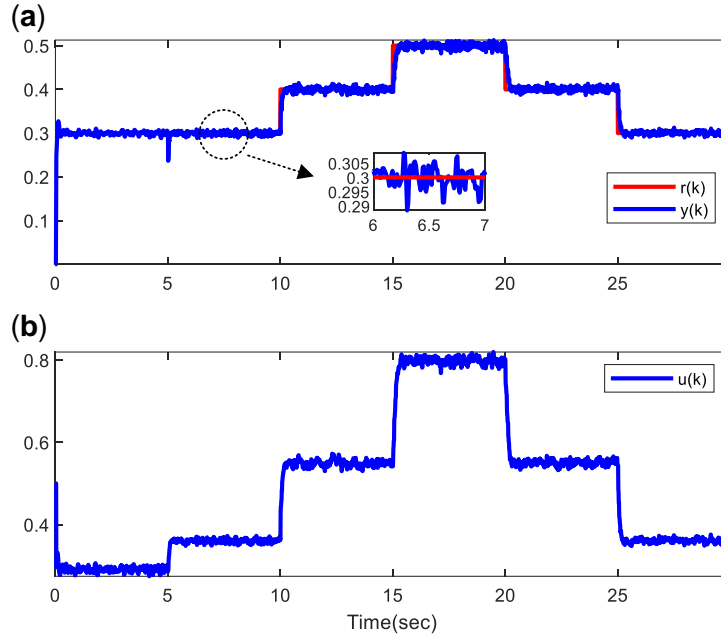


Figure 6. System Output and Reference Signal(a), Control Signal(b) for measurement noise case.

4.3. Parametric Uncertainty Case

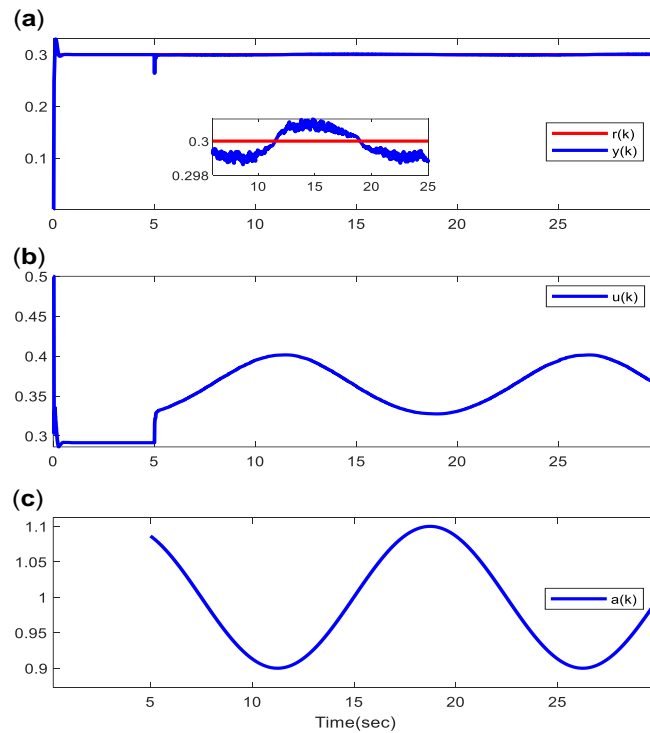


Figure 7. System Output and Reference Signal(a), Control Signal(b), uncertain parameter (c) for parametric uncertainty case.

In order to evaluate the robustness with respect to parametric uncertainty, $a(k)$ in (10) is chosen as uncertain parameter. The closed-loop system performance is depicted in Figure 7. Figure 7 (c) is uncertainty system parameter. The NN controller successfully rejects the parametric uncertainty in system dynamics.

5. CONCLUSION AND FUTURE WORKS

In this paper, the performance of MLP-NN controller has been examined on nonlinear dynamical system by considering various types of activation functions. The learning ability of NN provides a adaptation ability to NN controller against the uncertainties arised due to internal and external factors. The learning and control performance of NN controller is investigated for nominal, measuring noise and parametric uncertainty conditions, which are very important for control systems. The results show that the controller structure provides a very fast adaptation to uncertainties.

As future work, it is planned to adapt the weights with high-order learning rules to increase the convergence of the parameters.

REFERENCES

- [1] A. Yeşildirek and F. L. Lewis, "Feedback linearization using neural networks," *Automatica*, vol. 31, no. 11, pp. 1659–1664, 1995.
- [2] B. Mohamed, K. Kara, A. Oussama, and L. Hadjili, "Adaptive Neural Network PID Controller," *Proc. - 2019 IEEE Int. Conf. Environ. Electr. Eng. 2019 IEEE Ind. Commer. Power Syst. Eur. IEEEIC/I CPS Eur. 2019*, 2019.
- [3] Y. Yongquan, H. Ying, and Z. Bi, "A PID neural network controller," *Proc. Int. Jt. Conf. Neural Networks, 2003.*, vol. 3, pp. 1933–1938, 1933.
- [4] L. Chen and K. S. Narendra, "Nonlinear adaptive control using neural networks and multiple models," *Proc. Am. Control Conf.*, vol. 6, pp. 4199–4203, 2000.
- [5] B. Chen, X. Liu, K. Liu, and C. Lin, "Novel adaptive neural control design for nonlinear MIMO time-delay systems," *Automatica*, vol. 45, no. 6, pp. 1554–1560, 2009.
- [6] S. S. Ge, C. C. Hang, and T. Zhang, "Adaptive neural network control of nonlinear systems by state and output feedback," *IEEE Trans. Syst. Man, Cybern. Part B Cybern.*, vol. 29, no. 6, pp. 818–828, 1999.
- [7] R. Jacob and S. Murugan, "Implementation of neural network based PID controller," *Int. Conf. Electr. Electron. Optim. Tech. ICEEOT 2016*, no. 1, pp. 2769–2771, 2016.
- [8] Y. H. Kim and F. L. Lewis, "Neural Network Output Feedback Control of Robot Manipulators," *IEEE Trans. Robot. Autom.*, vol. 15, no. 2, pp. 301–309, 1999.
- [9] A. U. Levin and K. S. Narendra, "Control of Nonlinear Dynamical Systems Using Neural Networks: Controllability and Stabilization," *IEEE Trans. Neural Networks*, vol. 4, no. 2, pp. 192–206, 1993.

- [10] F. L. Lewis and A. Yesildirek, "Neural Net Robot Controller with Guaranteed Tracking Performance," *IEEE Trans. Neural Networks*, vol. 6, no. 3, pp. 703–715, 1995.
- [11] E. P. Nahas, M. A. Henson, and D. E. Seborg, "Nonlinear internal model control strategy for neural network models," *Comput. Chem. Eng.*, vol. 16, no. 12, pp. 1039–1057, 1992.
- [12] S. S. Ge, F. Hong, and T. L. Lee, "Adaptive Neural Network Control of Nonlinear Systems With Unknown Time Delays," *IEEE Trans. Automat. Contr.*, vol. 48, no. 11, pp. 2004–2010, 2004.
- [13] C. Wang and D. J. Hill, "Learning from neural control," *IEEE Trans. Neural Networks*, vol. 17, no. 1, pp. 130–146, 2006.
- [14] T. Zhang, S. S. Ge, and C. C. Hang, "Adaptive neural network control for strict-feedback nonlinear systems using backstepping design," *Automatica*, vol. 36, no. 12, pp. 1835–1846, 2000.
- [15] Z. Huaguang and Q. Yongving, "Modeling, identification, and control of a class of nonlinear systems," *IEEE Trans. Fuzzy Syst.*, vol. 9, no. 2, pp. 349–354, 2001.
- [16] M. T. Hagan, H. B. Demuth, and O. De Jesus, "An introduction to the use of neural networks in control systems," *Int. J. Robust Nonlinear Control*, vol. 12, no. 11, pp. 959–985, Sep. 2002.
- [17] S. Iplikci, "A comparative study on a novel model-based PID tuning and control mechanism for nonlinear systems," *Int. J. Robust Nonlinear Control*, vol. 20, no. 13, pp. 1483–1501, 2010.
- [18] K. Uçak, "A Runge – Kutta neural network-based control method for nonlinear MIMO systems," *Soft Comput.*, vol. 23, no. 17, pp. 7769–7803, 2019.
- [19] S. Haykin, *Neural networks: a comprehensive foundation*, 2nd ed. Pearson Prentice Hall, 1999.
- [20] M. Ö. Efe, "Neural Network -Based Control," in *The Industrial Electronics Handbook Intelligent Systems*, 2nd ed., B. M. Wilamowski and J. D. Irwin, Eds. CRC Press, 2011.

**ADAPTIVE SLIDING MODE CONTROLLER FOR INVERTED PENDULUM
SYSTEM**

Sima KÜÇÜKÇE

Undergraduate Student, Muğla Sıtkı Koçman University, Faculty of Engineering, Department of Electrical and
Electronics Engineering,
ORCID: 0000-0001-6999-5059

Kemal UÇAK

Assis. Prof. Dr. Muğla Sıtkı Koçman University, Faculty of Engineering, Department of Electrical and Electronics
Engineering,
ORCID: 0000-0001-7005-7940

ABSTRACT

Sliding Mode Controller (SMC) architectures are frequently utilized for the control of nonlinear dynamical systems owing to the robustness and stability features they provide. Switching functions providing a smooth transition can be deployed to overcome the chattering phenomenon in SMC. Time-varying sliding surfaces can be chosen so that the error dynamics of the controlled system can reach the sliding surface in a short time. For this purpose, in this study, the slope of the sliding surface and gain of the switching function are considered as adjustable parameters of the SMC. Model free adjustment mechanism based on steepest descent and Levenberg-Marquardt has been introduced to optimize the parameter of the sliding surface. Numerical differentiation has been preferred to estimate the system jacobian information. The control performance and robustness of the introduced adjustment mechanism has been evaluated on nonlinear inverted pendulum system for nominal, measurement noise, parametric uncertainty and input disturbance cases. The attained results indicate that the introduced adjustment mechanism for SMC parameters enhances the controller performance for uncertainties.

Keywords: Adaptive Control, Adaptive Sliding Surface, Nonlinear Inverted Pendulum, Sliding Mode Controller.

1. INTRODUCTION

In control systems, robustness is the most important factor that determines control performance and stability, both for traditional controller structures (PID, LQR, etc.) and for adaptive controller architectures. For this reason, the robustness of adaptation architectures affects the stability of adaptation mechanisms against uncertainty. Sliding Mode Controller (SMC) structure, one of the robust control method, is the most effective method used to

guarantee stability in control systems. Derived from the Lyapunov stability theorem, this controller mechanism provides effective performance in the control of nonlinear systems. Basically, the SMC structure contains two main phases called as reaching and sliding phases. For the reaching phase, the control signal that will lead the error dynamics from a random initial point to a predetermined stable sliding surface is derived over system and sliding surface dynamics. This control law is called as the equivalent control law. In addition to equivalent control law, in order to hold the system dynamics on sliding surface, it is required to use a discontinuous control law ensuring stability of the controller. For this reason, by applying a discontinuous control law (switching law) to bring back the system dynamics deviating from the surface, both the system dynamics are kept on the sliding surface and the stability is guaranteed. Due to the discontinuous control signal, various continuous switching structures have been proposed to overcome this natural phenomenon called chattering on the sliding surface, which causes high frequency components to contaminate the control signal.

Various SMC architectures have been presented in the technical literature. Tokat et al introduced a new sliding surface which is linear combination of original sliding surface and perpendicular surface to the original sliding surface[1]. Levant proposed a new single-input single-output (SISO) NCC structure with arbitrary degrees[2]. Tokat et al proposed to define a new sliding surface which is combination of original sliding surface and orthogonal surface to original sliding surface[3]. In architectures in which the effectiveness of time-varying linear sliding surfaces is insufficient, non-linear slip surfaces can be preferred. Tokat et al proposed a new technique to nonlinear sliding surface design for high-order systems, primarily based totally at the definition of a new coordinate axis[4]. A constant and non-linear sliding surface is offered on this newly described coordinate axis[4]. One of the main problem with inside the time-varying sliding surface design problem is to decide the best values of the design parameters relying at the initial condition[4][5]. When the initial conditions of the system change, the parameters of the time-varying sliding surface want to be recalculated to attain the preferred performance[4]. Therefore, a new SMC structure primarily based totally on a guide vector system has been proposed for the estimation of time-varying sliding surface parameters to respond to a change in system initial conditions[4]. Tokat et al utilized a time-varying nonlinear sliding surface changed into proposed by [6][7]. This nonlinear surface is then moved in the suitable direction the usage of a time varying function[6][7]. Kaya used the bee colony algorithm, which is a swarm algorithm, to optimize the parameters of the SMC[8]. Adaptation mechanisms may be used to enhance the overall performance of the SMC structure. Tokat et al proposed new methods with inside the SMC structure where in the slope of the linear sliding surface is adapted online[9]. Eray and Tokat used type 1 and type 2 fuzzy inference mechanisms to adapt the parameter of the time-varying sliding surface [10]. Aydın and Tokat provided a special-cause approach with the state-based sliding surface algorithm

for the control of the coupled tank system, in which state variables are described because the liquid ranges of the tanks[11].

In this article, the adaptive sliding mode control for inverted pendulum system is introduced. The slope of the sliding surface and gain of switching function are adjusted via model free adaptation mechanism based on gradient descent and levenberg marquardt. The adjustment mechanism has been assessed for nominal, measurement noise, input disturbance and parametric uncertainty cases. Thus, the effectiveness of the SMC on nonlinear dynamical system has been evaluated.

This paper is organized as follows: Sliding mode control is given in section 2. Adaptive sliding mode control is given in section 3. Simulations results are given in section 4. The paper ends with a brief conclusion and future works part in section 5.

2. FUNDAMENTALS OF SLIDING MODE CONTROL

SMC is a non-linear robust control method preferred against various external and internal factors affecting the control performance such as modeling errors, parametric uncertainties, disturbances and measurement noises. Since the control laws for SMC are derived over Lyapunov stability theory, SMC presents stable and robust performances for nonlinear dynamical systems. There are two main phases in sliding mode control[12][13]. These are the reaching and sliding phases. The reaching phase is the part of dragging the system error dynamics to the sliding surface, and the sliding phase is the part of the error dynamics going to the origin. Figure 1 shows the graphical representation of the SMC phases. The error dynamics of the controlled system tends to deviate from sliding surface due to model uncertainties, disturbances, measurement noise, parametric uncertainties etc. Switching control law ensuring the stability is required used in order to keep the system dynamics on the sliding surface. Sudden transitions in switching function can cause high frequency components on the control signal that are going to excite the high frequency dynamics of the controlled system. This phenomenon is called as "chattering"[14].

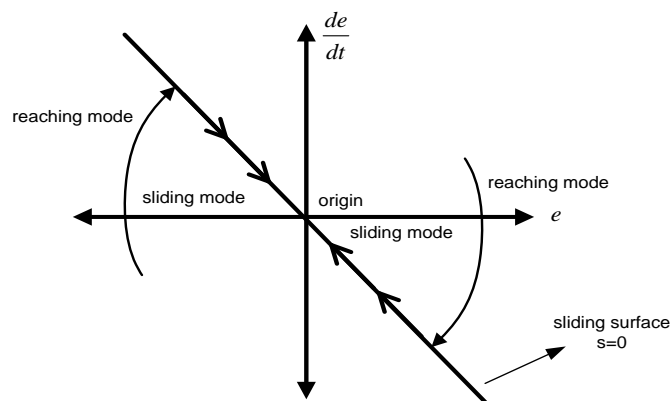


Figure 1. Reaching and sliding phases of sliding mode control [14][15]

Lets consider a second-order nonlinear system given below[16]:

$$\begin{aligned}\frac{dx_1(t)}{dt} &= x_2(t) \\ \frac{dx_2(t)}{dt} &= -f(X(t)) + g(X(t))u(t) = \frac{d^2x_1(t)}{dt^2} \\ y(t) &= x_1(t)\end{aligned}\quad (1)$$

In (1), the control signal is given as $u(t)$, $y(t)$ indicates the system output, $f(x(t))$ and $g(x(t))$ are nonlinear subdynamics of system and $x \in R^n$ stands for the state vector[16]. As can be clearly seen in the following equations, since the denominator term of the control signal will be $g(x(t))$, $g(x(t)) \neq 0$ has to be satisfied for the system in (1) to be controllable[16]. The system dynamics are forced to the following PD type sliding surface:

$$s(t) = \frac{de(t)}{dt} + \theta e(t) \quad (2)$$

where $e(t)$ given in (3) represents error states for controlled system output, θ is sliding surface parameter, and must satisfy Hurwitz condition($\theta > 0$) [12].

$$e(t) = r(t) - y(t) \quad (3)$$

and $r(t)$ denotes the desired reference. The following candidate Lyapunov function can be utilized to derive the control laws of SMC over $s(t)$:

$$V(t) = \frac{1}{2}[s(t)]^2 \quad (4)$$

The stable control laws can be derived by taking into account $V(t) > 0$ and $\frac{dV(t)}{dt} < 0$ for $s(t) \neq 0$ conditions[17][18][19]. The SMC law is composed of continuous (u_{eq}) and discontinuous parts(u_{sw}). In order to attain the continuous part of control law(u_{eq}), $\frac{ds(t)}{dt} = 0$ has to be satisfied as given below expression:

$$\begin{aligned}\frac{ds(t)}{dt} &= \frac{d^2e(t)}{dt^2} + \theta \frac{de(t)}{dt} = \frac{d^2r(t)}{dt^2} - \frac{d^2y(t)}{dt^2} + \theta \frac{de(t)}{dt} = 0 \\ \frac{ds(t)}{dt} &= \frac{d^2r(t)}{dt^2} + f(X(t)) - g(X(t))u_{eq}(t) + \theta \frac{de(t)}{dt} = 0 \\ u_{eq}(t) &= \frac{1}{g(X(t))} \left[\frac{d^2r(t)}{dt^2} + f(X(t)) + \theta \frac{de(t)}{dt} \right]\end{aligned}\quad (5)$$

The discontinuous part (u_{sw}) ensuring the stability can be derived as follows[20]:

$$u_{sw}(t) = \frac{1}{g(\mathbf{X}(t))} [\mu \text{sgn}(s(t))] \quad (6)$$

Thus, the combined SMC law can be rewritten as follows:

$$u(t) = u_{eq}(t) + u_{sw}(t) = \frac{1}{g(\mathbf{X}(t))} \left[\frac{d^2 r(t)}{dt^2} + f(\mathbf{X}(t)) + \theta \frac{de(t)}{dt} + \mu \text{sgn}(s(t)) \right] \quad (7)$$

The SMC architecture is depicted in Figure 2.

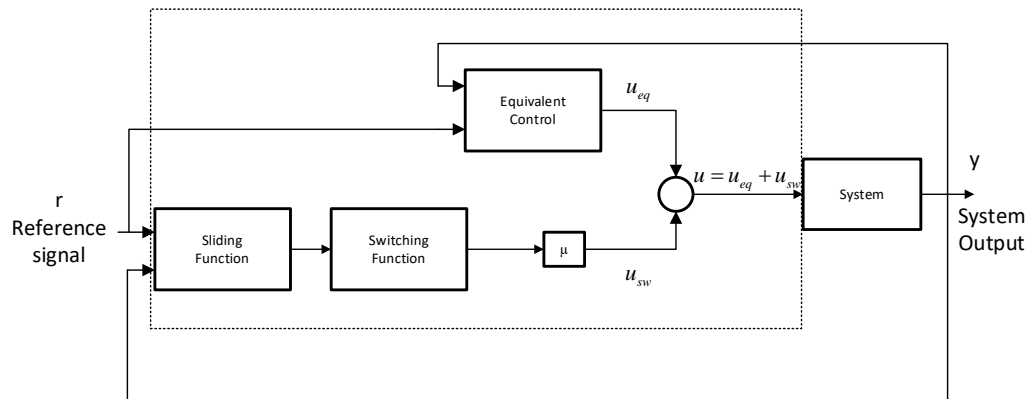


Figure 2. Architecture of SMC system [12][14].

Switching functions with smooth transition such as saturation, tanh etc given in Figure 3 can be used to overcome the chattering phenomenon.

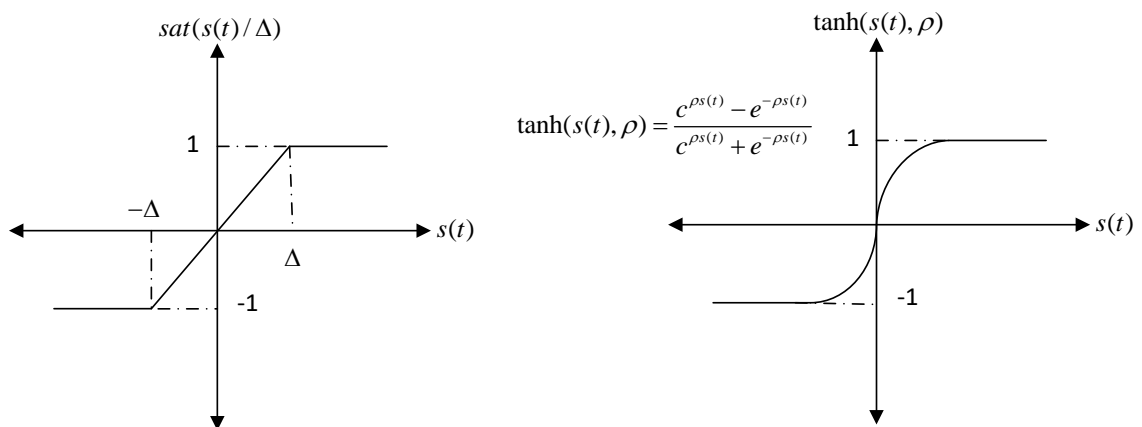


Figure 3. Chattering Free Switching Functions[14].

3. ADAPTIVE SLIDING MODE CONTROL

The introduced learning mechanism for SMC is illustrated in figure 4.

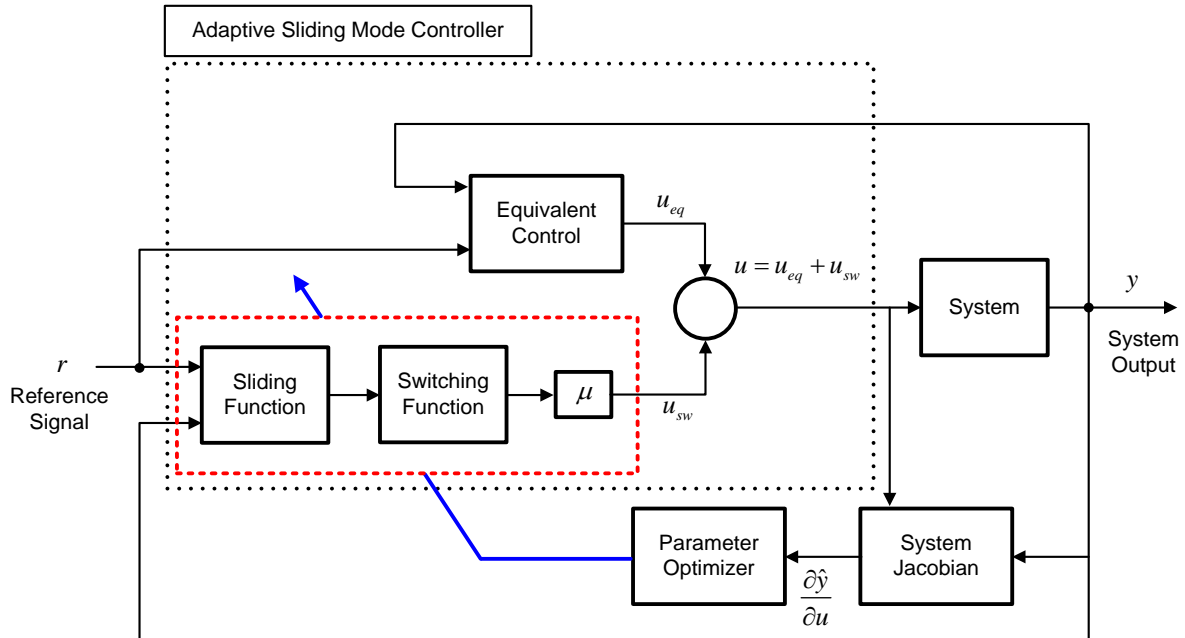


Figure 4. Learning mechanism for SMC

The aim of the adaptation mechanism is to optimize the sliding surface and switching function parameters in order to force the sliding surface the error dynamics of the system. Thus, the error dynamics can reach the stable sliding surface as soon as possible. The μ parameter is utilized to hold the system dynamics on sliding surface to provide robustness and stability to the control law. The θ and μ can be optimized as follows via Gradient descent.

$$\begin{aligned}
 \theta(k+1) &= \theta(k) + \Delta\theta(k) \\
 \Delta\theta(k) &= -\eta \frac{\partial J(k)}{\partial \theta(k)} = -\eta \left[\frac{\partial J(k)}{\partial u_{eq}(k)} \frac{\partial u_{eq}(k)}{\partial \theta(k)} + \frac{\partial J(k)}{\partial u_{sw}(k)} \frac{\partial u_{sw}(k)}{\partial f_{sw}(k)} \frac{\partial f_{sw}(k)}{\partial s(k)} \frac{\partial s(k)}{\partial \theta(k)} \right] \\
 \Delta\theta(k) &= -\eta \frac{\partial J(k)}{\partial e(k)} \frac{\partial e(k)}{\partial y(k)} \frac{\partial y(k)}{\partial u(k)} \left[\frac{\partial u(k)}{\partial u_{eq}(k)} \frac{\partial u_{eq}(k)}{\partial \theta(k)} + \frac{\partial u(k)}{\partial u_{sw}(k)} \frac{\partial u_{sw}(k)}{\partial f_{sw}(k)} \frac{\partial f_{sw}(k)}{\partial s(k)} \frac{\partial s(k)}{\partial \theta(k)} \right] \quad (8) \\
 \mu(k+1) &= \mu(k) + \Delta\mu(k) \\
 \Delta\mu(k) &= -\eta \frac{\partial J(k)}{\partial \mu(k)} = -\eta \frac{\partial J(k)}{\partial e(k)} \frac{\partial e(k)}{\partial y(k)} \frac{\partial y(k)}{\partial u(k)} \frac{\partial u(k)}{\partial u_{sw}(k)} \frac{\partial u_{sw}(k)}{\partial \mu(k)} \\
 \Delta\mu(k) &= \eta e(k) \frac{\partial y(k)}{\partial u(k)} f_{sw}(s, g)
 \end{aligned}$$

The update rules can derived via Levenberg-Marquardt as follows:

$$\begin{bmatrix} \theta(k+1) \\ \mu(k+1) \end{bmatrix} = \begin{bmatrix} \theta(k) \\ \mu(k) \end{bmatrix} - (J^T J + \eta I)^{-1} J^T e \quad (9)$$

$$J = \begin{bmatrix} \frac{\partial e}{\partial u} & \frac{\partial e}{\partial \theta} \\ \frac{\partial u}{\partial \theta} & \frac{\partial u}{\partial \mu} \end{bmatrix}$$

4. SIMULATIONS

The performance of the adaptive SMC has been tested on nonlinear inverted pendulum system illustrated in Figure 5.

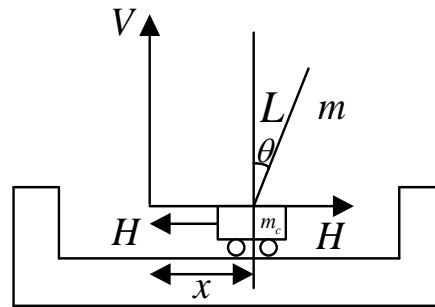


Figure 5. Inverted Pendulum System[12]

Adaptive SMC has been evaluated for nominal, measurement noise, input disturbance and parametric uncertainty cases. The dynamics of the IP can be expressed via the following differential equation set[12]:

$$f(x) = \frac{g \sin x_1 - m l x_2^2 \cos x_1 \sin x_1 / (m_c + m)}{l(4/3 - m \cos^2 x_1 / (m_c + m))} \quad (10)$$

$$g(x) = \frac{\cos x_1 / (m_c + m)}{l(4/3 - m \cos^2 x_1 / (m_c + m))}$$

where $g = 9.8m/s^2$, m_c is the vehicle mass, $m_c = 1kg$, m is the mass of pendulum bar, $m = 0.1kg$, l is one half of pendulum length, $l = 0.5m$, u is the control input[12].

4.1. Nominal Case

The tracking performance for staircase reference input is given in Figure 6 The control signal produced by SMC is given in Figure 6 (a). The evaluation of the θ and μ parameters are shown in Figure 6 (b).

Adaptive SMC forces the controlled output to track the desired reference signal as close as possible.

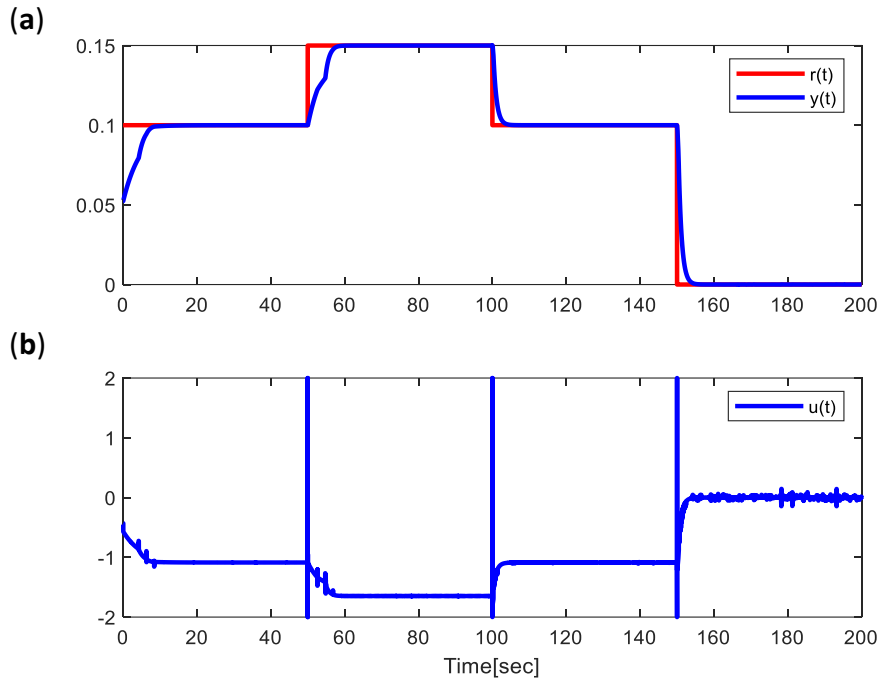


Figure 6. System Output (a) , and control signal (b) for nominal case.

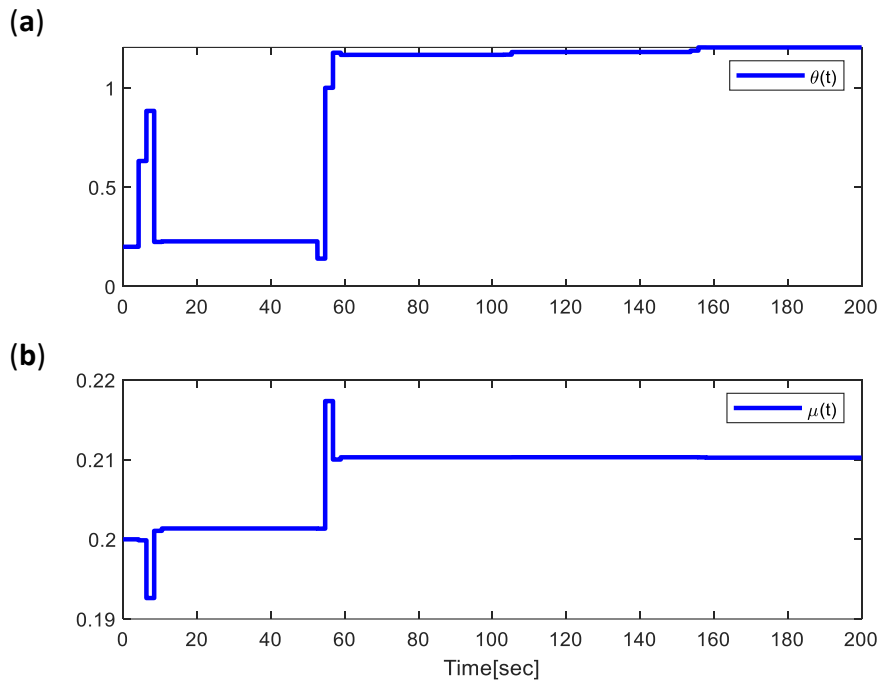


Figure 7. Evaluation of SMC parameters for nominal case.

4.2. Measurement Noise Case

In order to test the controller performance for measurement noise case, the controlled output of the system is exposed to a gaussian measurement noise. The control performance and the adaptive controller parameters are given in figure 8 (a) and (b) respectively.

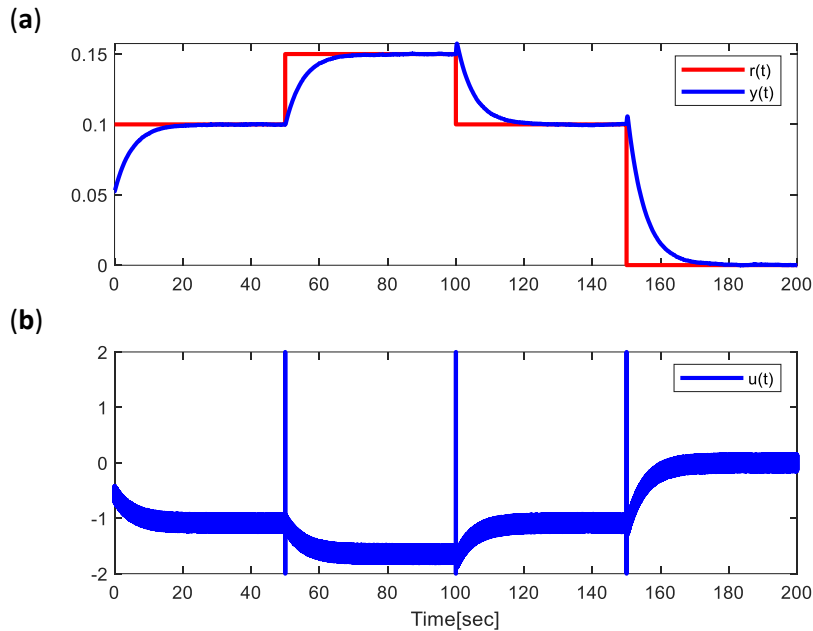


Figure 8. System Output (a) , and control signal (b) for measurement noise case.

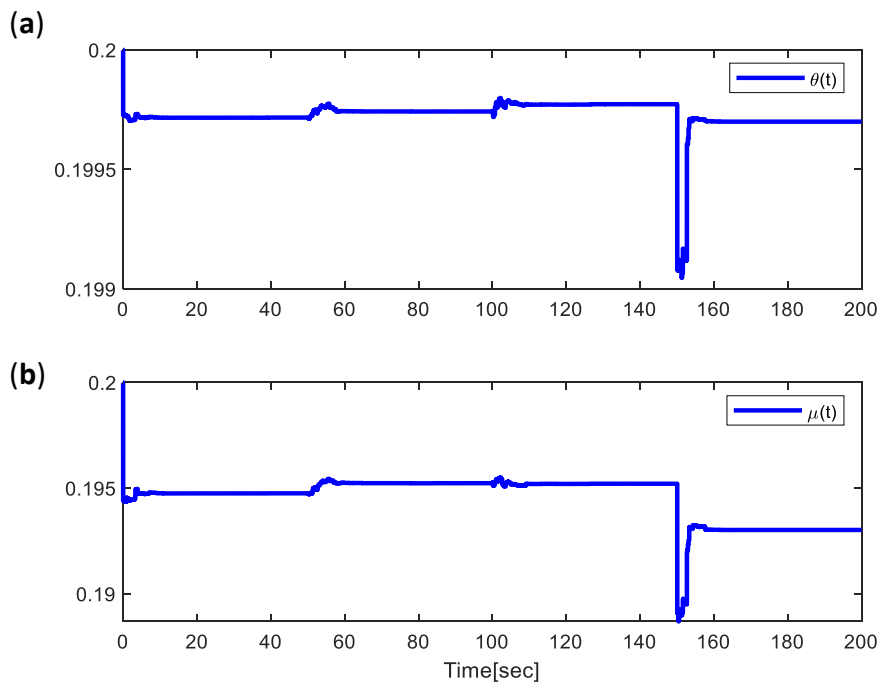


Figure 9. Evaluation of SMC parameters for measurement noise case.

4.3. Parametric Uncertainty Case

The robustness of the SMC has been examined for parametric uncertainty case. For this purpose, m is chosen as an uncertain parameters given as $m(t) = 0.1 + \frac{5}{1000} \sin(\frac{2\pi}{100}t)$. The tracking performance for parametric uncertainty case is depicted in Figure 10. The controller parameters are adjusted to overcome the uncertainty in system parameter as given in Figure 11.

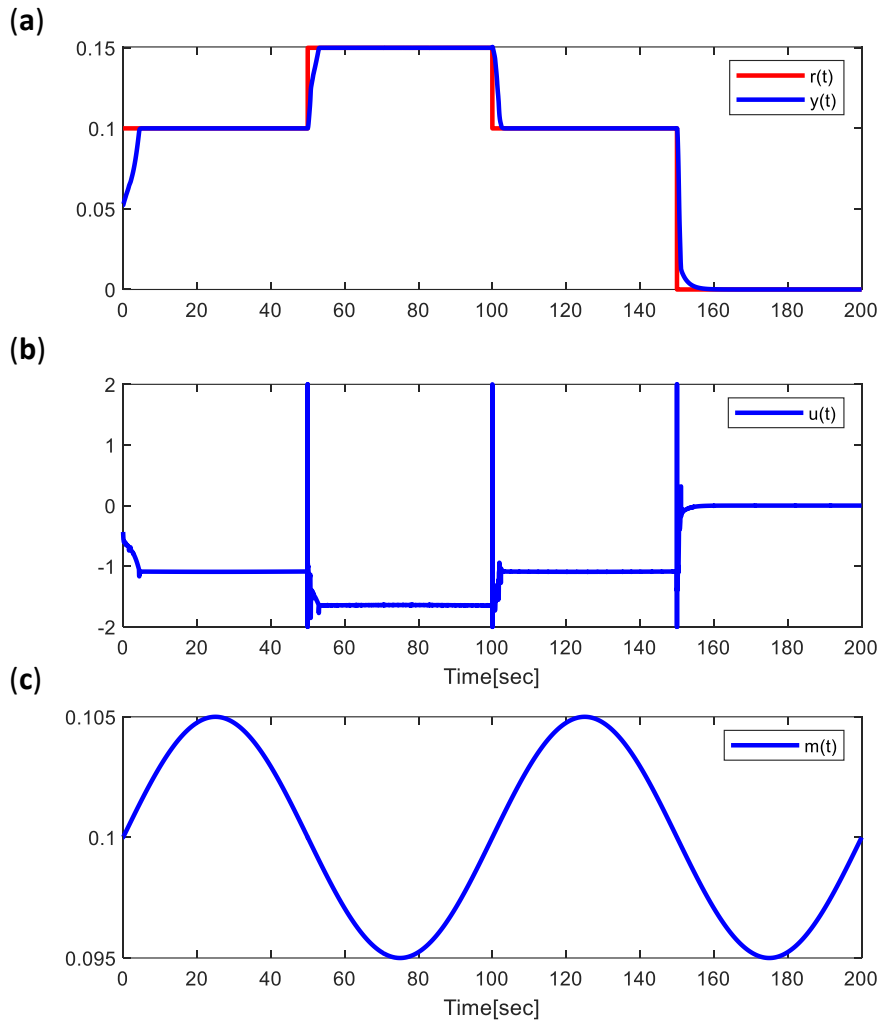


Figure 70. System Output (a) , control signal (b) and uncertain parameter (c).

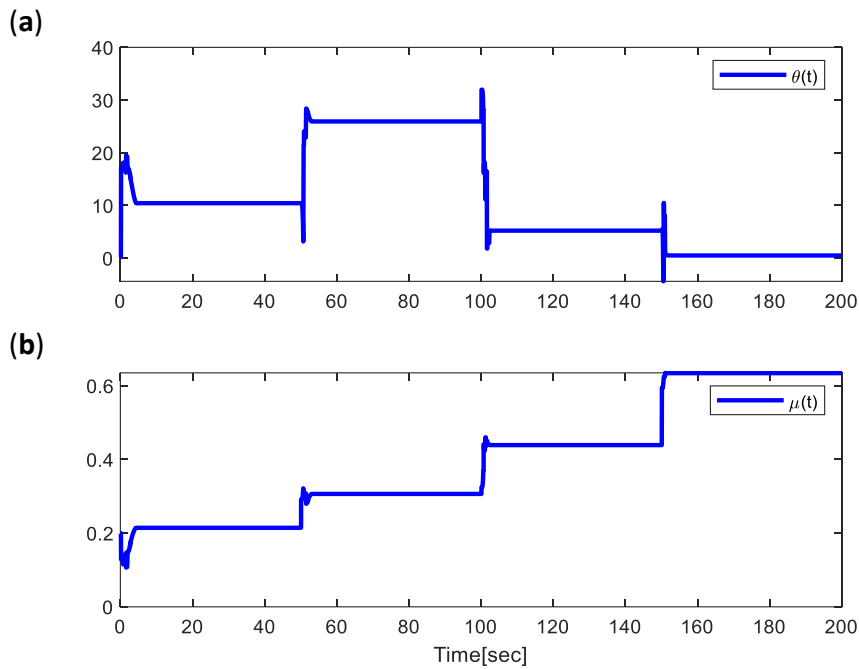


Figure 11. Evaluation of SMC parameters for parametric uncertainty case.

4.4. Input Disturbance Case

An sinusoidal type input disturbance ($u_d(t) = 0.05 \sin(\frac{2\pi}{50}t)$) has been applied to the control input to examine the disturbance rejection skills of SMC.

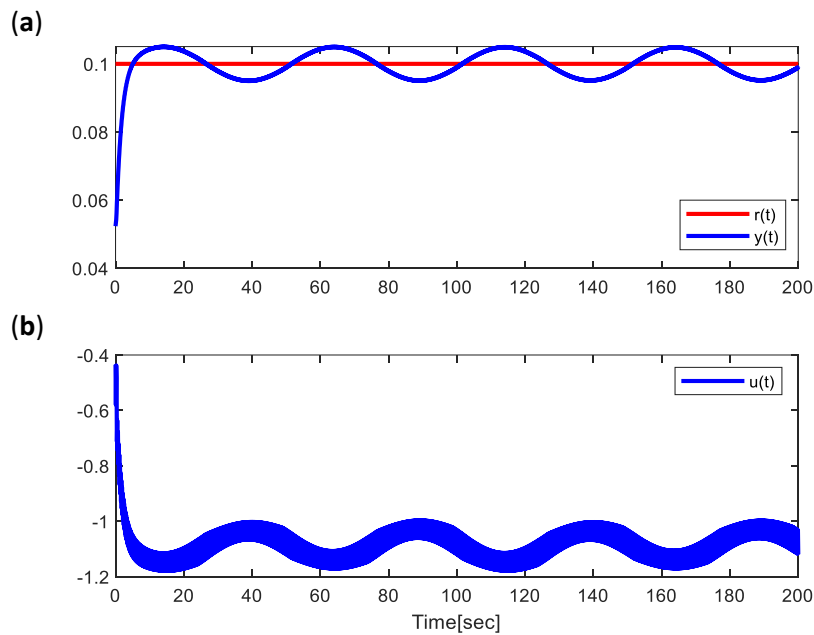


Figure 12. System Output (a) , and control signal (b) for input disturbance case.

The SMC performance for input disturbance case is shown in Figure 12. The alternation of the controller parameters are depicted in Figure 13.

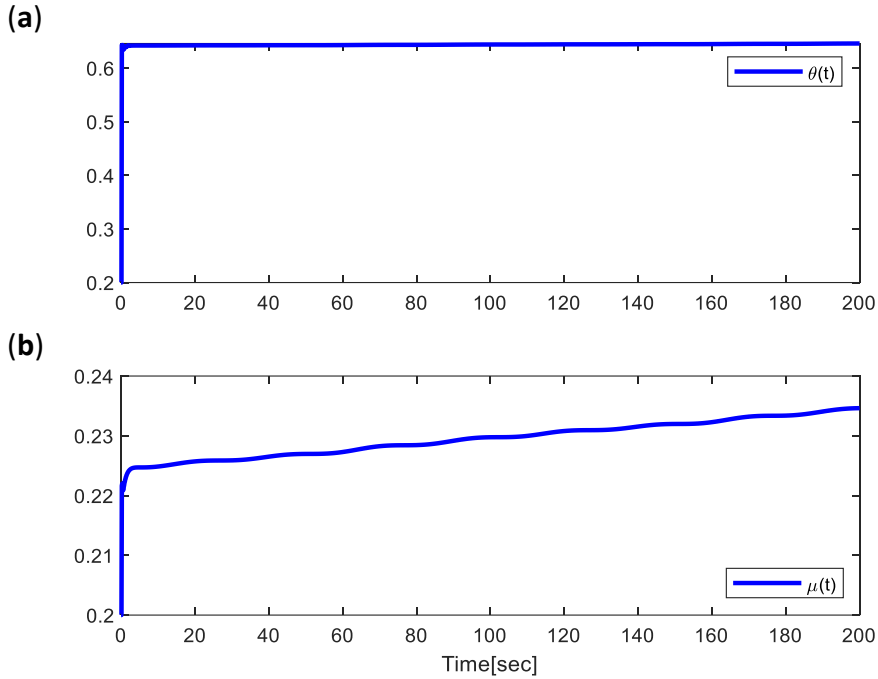


Figure 13. Evaluation of SMC parameters for input disturbance case.

The performance of the steepest descent and Levenberg marquardt methods are compared in

Table 1 for all cases using $J_c = \frac{1}{2} \int_{t=0}^{t_f} e^2(t) dt$ performance index function.

Table I. Comparison of Steepest Descent and Levenberg-marguardt

Cases\Learning Algorithm	Steepest Descent	Levenberg Marguardt
Nominal	1.248	0.5205
Measurement Noise	1.528	2.08
Parametric Uncertainty	4.247e+04	0.3957
Input Disturbance	0.6915	0.1313

Levenberg-Marquardt based adaptation mechanism has better control performance for all situations except measurement noise case as given in Table 1.

5. CONCLUSION AND FUTURE WORKS

In this paper, an adaptive SMC for nonlinear dynamic system has been introduced. The slope function of sliding surface and gain of switching function are optimized via model free adjustment mechanism. The robustness and stability performance of the introduced adaptive SMC has been examined on nonlinear inverted pendulum system for nominal, measurement noise, parametric uncertainty, and input disturbance situations. The controller parameters are optimized via steepest descent and levenberg-marquardt learning rules. The attained result indicates the effectiveness of adaptive SMC on nonlinear control systems.

As a future work, it is planned to identify the dynamics of the controlled system via a machine learning methods in order to attain more accurate model for estimation of system jacobian.

REFERENCES

- [1] S. Tokat, I. Eksin, and M. Güzelkaya, "A new design method for sliding mode controllers using a linear time-varying sliding surface," *Proc. Inst. Mech. Eng. Part I J. Syst. Control Eng.*, vol. 216, no. 6, pp. 455–466, 2002.
- [2] A. Levant, "Quasi-continuous high-order sliding-mode controllers," *IEEE Trans. Automat. Contr.*, vol. 50, no. 11, pp. 1812–1816, 2005.
- [3] S. Tokat, I. Eksin, and M. Guzelkaya, "Linear time-varying sliding surface design based on co-ordinate transformation for high-order systems," *Trans. Inst. Meas. Control*, vol. 31, no. 1, pp. 51–70, 2009.
- [4] S. Tokat, I. Eksin, and M. Guzelkaya, "Sliding mode control of high order systems using a constant nonlinear sliding surface on a transformed coordinate axis," *JVC/Journal Vib. Control*, vol. 14, no. 6, pp. 909–927, 2008.
- [5] S. Tokat, "Başlangıç koşuluna göre parametreleri ayarlanan zamanla değişen kayma yüzeyi tasarımı," in *EMO III. Otomasyon Sempozyumu*, 2002, pp. 1–5.
- [6] S. Tokat, I. Eksin, and M. Guzelkaya, "Sliding Mode Control Using a Nonlinear Time-Varying Sliding Surface," in *Mediterranean Conference on Control and Automation*, 2002, pp. 1–6.
- [7] S. Tokat, I. Eksin, M. Güzelkaya, and M. T. Söylemez, "Design of a sliding mode controller with a nonlinear time-varying sliding surface," *Trans. Inst. Meas. Control*, vol. 25, no. 2, pp. 145–162, 2003.
- [8] R. Kaya, "PID ve Kayma Kipli Kontrol Parametrelerinin Geliştirilmiş Yapay Arı Kolonisi Algoritması ile Optimizasyonu," İskenderun Teknik Üniversitesi, 2020.
- [9] S. Tokat, I. Eksin, and M. Güzelkaya, "New approaches for on-line tuning of the linear sliding surface slope in sliding mode controllers," *Turkish J. Electr. Eng. Comput. Sci.*, vol. 11, no. 1, pp. 45–54, 2003.

- [10] O. Eray and S. Tokat, "Interval type-2 sliding mode fuzzy controller with a time-varying Sliding surface," in *2nd International Conference on Computer Science and Engineering, UBMK 2017*, 2017, pp. 866–871.
- [11] S. Aydin and S. Tokat, "Sliding mode control of a coupled tank system with a state varying sliding surface parameter," in *IEEE 10th International Workshop on Variable Structure Systems, VSS'08*, 2008, pp. 355–360.
- [12] J. Liu and X. Wang, *Advanced Sliding Mode Control for Mechanical Systems*. 2011.
- [13] J.-J. E. Slotine and W. Li, *Applied Nonlinear Control*. Prentice Hall, 1991.
- [14] K. Uçak and G. Öke Günel, "An adaptive sliding mode controller based on online support vector regression for nonlinear systems," *Soft Comput.*, vol. 24, no. 6, pp. 4623–4643, 2020.
- [15] C. H. Tsai, H. Y. Chung, and F. M. Yu, "Neuro-sliding mode control with its applications to seesaw systems," *IEEE Trans. Neural Networks*, vol. 15, no. 1, pp. 124–134, 2004.
- [16] J. Hua, L. X. An, and Y. M. Li, "Bionic fuzzy sliding mode control and robustness analysis," *Appl. Math. Model.*, vol. 39, no. 15, pp. 4482–4493, 2015.
- [17] M. Ertugrul, O. Kaynak, and A. Şabanovic, "A comparison of various VSS techniques on the control of automated guided vehicles," in *1995 IEEE International Symposium on Industrial Electronics (ISIE 95)*, 1995, pp. 837–842.
- [18] M. Zribi and A. Oteafy, "Control of a Bioreactor Using Static and Dynamic Sliding Mode Controllers," in *2006 IEEE GCC Conference, GCC 2006*, 2006, pp. 1–6.
- [19] A. Derdiyok and M. Levent, "Sliding Mode Control of a Bioreactor," *Korean J. Chem. Eng.*, vol. 17, no. 6, pp. 619–624, 2000.
- [20] A. Bartoszewicz, "Time-varying sliding modes for second-order systems," *IEE Proc. - Control Theory Appl.*, vol. 143, no. 5, pp. 455–462, 1996.

**SWARM INTELLIGENCE BASED OPTIMAL CONTROL DESIGN METHOD FOR
ACTIVE SUSPENSION SYSTEM**

Hande DÖNMEZ

Undergraduate Student, Muğla Sıtkı Koçman University, Faculty of Engineering, Department of Electrical and
Electronics Engineering, Muğla, Turkey
ORCID: 0000-0002-3340-3151

Kemal UÇAK

Assis. Prof. Dr. Muğla Sıtkı Koçman University, Faculty of Engineering, Department of Electrical and Electronics
Engineering, Muğla, Turkey
ORCID: 0000-0001-7005-7940

ABSTRACT

The vehicle suspension system has a vital role in ensuring the stability of the vehicle while driving. For this reason, active suspension systems(ASS) have been proposed to eliminate the effects of external factors on the vehicle. Since the purpose of this system is to eliminate vibrations, optimal control design methods provide a more robust controller architecture than traditional control strategies. In this study, a Particle Swarm Optimization(PSO) based optimal controller design method has been proposed for ASS system. PSO has been deployed to optimize the diagonal elements of the matrices utilized to constitute the optimal control problem for algebraic riccati equation(ARE). The performance of the proposed control strategy has been evaluated for nominal, measurement noise and parametric uncertainty situations. When the attained results are compared with the passive suspension system, it has been observed that the driving comfort has been significantly enhanced in ASS.

Keywords: Active Suspension System, Linear Quadratic Regulator, Optimal Control, Particle Swarm Optimization, Swarm Intelligence.

1. INTRODUCTION

The driving comfort and safety systems used in road vehicles are increasing its importance day by day and are of great importance in reducing the loss of life and benefits in traffic accidents with technological developments[1]. Driving safety systems are of great importance for the driver, passengers and pedestrians. In the theoretical studies, very good results are obtained in practice by combining the advances in electronic technology[1]. Driving safety is directly related to the stable behavior of the vehicle during its movement. For this reason, the main purpose of driving safety systems is to maintain the stability of the vehicle, to dampen the vibration as soon as possible and to increase the driving comfort. For driving comfort,

various active suspension systems are available. These control problems are basically solved by designing an LQR from state space models.

In order to enhance the robustness of the LQR architectures, Swarm Intelligence based design methods can be deployed to constitute the optimal control problem. Thus, the robustness of LQR and optimization ability of Swarm Intelligence can be combined. There are various controller architectures based on PSO for ASS. Qazi et al proposed to tune the fuzzy controller parameters for semi suspension system via PSO algorithm[2][3]. Obaid et al utilized PSO to tune PI controller in inner loop and LQR parameters deployed in outer loop for ASS[4]. Emad et al introduced a decentralized PID controller optimized via PSO for ASS[5]. Peng et al introduced to use PSO in order to enhance the performance of a GA to solve multiobjective optimization problem vehicle suspension parameter[6]. Yamin et al deployed PSO to optimize the PID and skyhook controller for ASS[7]. Yan et al introduce to use improved PSO for semi-active suspension system[8]. Soliman et al proposed robust controller design methods based on PSO for ASS[9]. Hurel et al optimizes the Fuzzy PD controller parameters via PSO for ASS[10]. Li et al employed PSO and gradient descent algorithm to optimized the parameters of a fuzzy neural network PID parameters estimator for ASS[11]. Zhao et al obtained the optimal PID controller parameters for ASS via PSO[12].

In this paper, in order to attain the parameters of the optimal control problem, swarm intelligence based LQR has been introduced for active suspension control system where PSO is deployed to obtain \mathbf{Q} and \mathbf{R} matrices for ARE. The control performance has been evaluated for nominal, measurement noise and uncertainty situations to examine the fragility of designed controller. The obtained results indicates that PSO based optimal control strategy provides a robust optimal controller for measurement noise and parametric uncertainty cases.

The structure of this paper is as follows: active suspension system is given in section 2. PSO based LQR has been presented in section 3. Simulations results are given in section 4. The paper ends with a brief conclusion and future works part in section 5.

2. ACTIVE SUSPENSION SYSTEM

The schematic representation of the active suspension system for quarter-car model is illustrated in Figure 1 where x_2 indicates the vehicle body displacement (sprung mass in the quarter car model), x_1 denotes the tire displacement (unsprung mass in quarter car model), z_r is the road surface position[5][13]. In Figure 1, while the sprung mass is denoted via M_s , the mass of the vehicle body is given as M_{us} , and the unsprung mass stands for the tire in the quarter-car model. F_c indicates the control command. The spring K_s and the damper B_s

support the body weight over the tire. The stiffness of the tire in contact with the road is modeled by the spring K_{us} and the damper B_s [13].

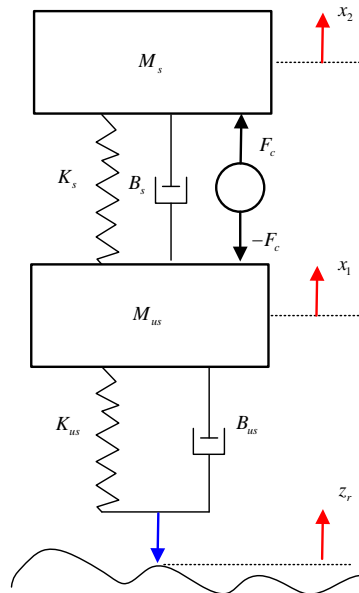


Figure 1. Active Suspension System for Quarter Car Model[13][14][15][16][17].

In order to derive the dynamics of the system, the quarter car model in Figure 1, can be decomposed to main parts. The free body diagrams indicating the applied forces to the bodies of whole system in Figure 1 are given in Figure 2. The forces impacting on M_s are resulting from spring force, damping force, active suspension force, and gravity[13][18].

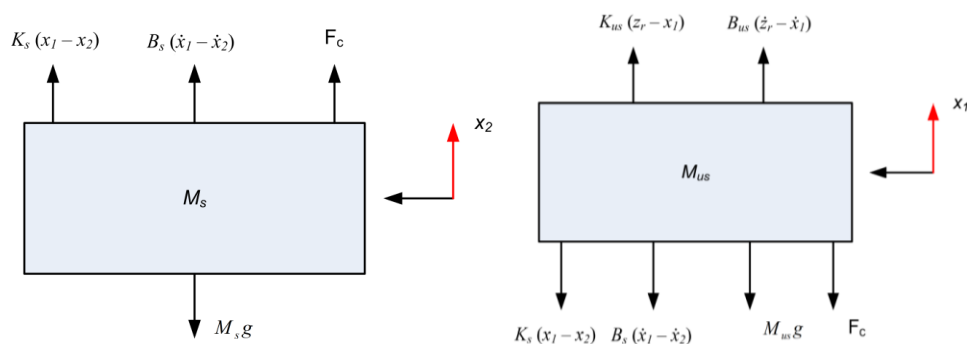


Figure 2. Free Body Diagram for M_s and M_{us}

By considering the forces given in Figure 2, the equations of motion (EOM) for M_s can be expressed as follows[13][18]:

$$\frac{d^2 x_2}{dt^2} = -g + \frac{F_c}{M_s} + \frac{B_s}{M_s} \frac{dx_1}{dt} - \frac{B_s}{M_s} \frac{dx_2}{dt} + \frac{K_s x_1}{M_s} - \frac{K_s x_2}{M_s} \quad (1)$$

Similarly, the dynamics of the M_{us} can be derived as follows[13][18]:

$$\frac{d^2 x_1}{dt^2} = -g - \frac{F_c}{M_{us}} - \frac{(B_s + B_{us})}{M_{us}} \frac{dx_1}{dt} + \frac{B_s}{M_{us}} \frac{dx_2}{dt} + \frac{B_{us}}{M_{us}} \frac{dz_r}{dt} - \frac{(K_{us} + K_s)x_1}{M_{us}} + \frac{K_s x_2}{M_{us}} + \frac{z_r K_{us}}{M_{us}} \quad (2)$$

In order to attain the equilibrium points for system in (1) and (2), the derivatives of the internal states and system input should be zero (derivatives of x_1 and x_2 , the road surface z_r and all its derivatives and the control force F_c are zero). Thus, the equations for equilibrium points can be obtained from (1) and (2) as follows:

$$\begin{aligned} K_s x_{eq1} - K_s x_{eq2} + M_{us} g + x_{eq1} K_{us} &= 0 \\ M_s g + K_s x_{eq2} - K_s x_{eq1} &= 0 \end{aligned} \quad (3)$$

Using (3), x_{eq1} and x_{eq2} can be acquired as

$$\begin{aligned} x_{eq1} &= -\frac{g(M_s + M_{us})}{K_{us}} \\ x_{eq2} &= -\frac{g(M_s K_{us} + K_s M_s + K_s M_{us})}{K_{us} K_s} \end{aligned} \quad (4)$$

New variables, z_{us} and z_s are defined through the dynamics of the system and equilibrium points as follows:

$$\begin{aligned} x_1 &= z_{us} - \frac{g(M_s + M_{us})}{K_{us}}, & x_2 &= z_s - \frac{M_s g}{K_s} - \frac{g(M_s + M_{us})}{K_{us}} \\ \frac{dx_1}{dt} &= \frac{dz_{us}}{dt}, & \frac{dx_2}{dt} &= \frac{dz_s}{dt} \\ \frac{d^2 x_1}{dt^2} &= \frac{d^2 z_{us}}{dt^2}, & \frac{d^2 x_2}{dt^2} &= \frac{d^2 z_s}{dt^2} \end{aligned} \quad (5)$$

Thus, the system dynamics given in (1)-(5) can be rewritten as in (6)

$$\begin{aligned} M_{us} \frac{d^2 z_{us}}{dt^2} &= -B_s \frac{dz_{us}}{dt} - B_{us} \frac{dz_{us}}{dt} - F_c + B_s \frac{dz_s}{dt} + B_{us} \frac{dz_r}{dt} - (z_{us} - z_s) K_s - (z_{us} - z_r) K_{us} \\ M_s \frac{d^2 z_s}{dt^2} &= B_s \frac{dz_{us}}{dt} + F_c - B_s \frac{dz_s}{dt} + B_{us} \frac{dz_r}{dt} - (z_s - z_{us}) K_s \end{aligned} \quad (6)$$

3. PSO BASED LQR DESIGN

Particle Swarm Optimization(PSO), proposed by Kennedy and Eberhart[19][20], is one of the most effective stochastic global optimization method used in controller design. PSO, which is a population-based optimization technique mimics the bird and fish flocks behaviours[3][21]. PSO starts with randomly initialized populations and each iteration the particles move towards the best solution at different speeds to optimize an objective function so as to obtain optimal values of the corresponding particles[22][23]. The update terms for velocity and positions of swarms are given below:

$$V_i^{(k+1)} = wV_i^{(k)} + c_1r_1(x_{i,best}^{(k)} - x_i^{(k)}) + c_2r_2(x_{g,best}^{(k)} - x_i^{(k)}) \quad (7)$$

$$x_i^{(k+1)} = x_i^{(k)} + V_i^{(k+1)} \quad (8)$$

where $V_i^{(k+1)}$ represents the next velocity of the particle, $V_i^{(k)}$ indicates the instantaneous velocity of the particle, $x_i^{(k)}$ is the instantaneous position of the particle, $x_i^{(k+1)}$ is the next position of the particle, W is an inertia weight used to improve the speed of convergence, C_1 , r_1 , C_2 , and r_2 indicates random numbers, C_1 and C_2 denotes the coefficients of acceleration, t represents the current time (iteration)[22].

$$Pbest_i^{(k)} = x_{i,best}^{(k)} = \begin{cases} x_{i,best}^{(k-1)} & f(x_i^{(k)}) \geq f(x_{i,best}^{(k-1)}) \\ x_i^{(k)} & f(x_i^{(k)}) < f(x_{i,best}^{(k-1)}) \end{cases} \quad (9)$$

$$Gbest^{(k)} = x_{gbest}^{(k)} = \min \{ f(x_{1,best}^{(k)}), f(x_{2,best}^{(k)}), \dots, f(x_{n,best}^{(k)}) \} \quad (10)$$

$Pbest_i^{(k)} = x_{i,best}^{(k)}$ and they denotes the best position of the particle. $Gbest^{(k)} = x_{gbest}^{(k)}$ and they represent the best position of all particles. $V_i^{(Pbest)}$ is the velocity of the $Pbest$ particle, $V_i^{(Gbest)}$ is the velocity of the $Gbest$ particle. The graphical interpretation of PSO is illustrated in Figure 3.

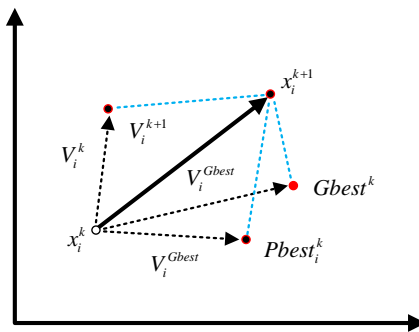


Figure 3. The graphical interpretation of PSO[22][24].

PSO can be deployed to design to obtain optimal control law. In this study, PSO is utilized to attain the optimal values of **Q** and **R** matrices entries required for optimal control problem given below:

$$J_{LQR} = \int_0^t (\mathbf{x}^T \mathbf{Q} \mathbf{x} + \mathbf{u}^T \mathbf{R} \mathbf{u}) dt \quad (11)$$

where

$$\mathbf{Q} = \begin{bmatrix} Q_1 & 0 & \dots & 0 \\ 0 & Q_2 & \dots & 0 \\ \vdots & & \ddots & \vdots \\ 0 & 0 & \dots & Q_n \end{bmatrix}, \quad \mathbf{R} = \begin{bmatrix} R_1 & 0 & \dots & 0 \\ 0 & R_2 & \dots & 0 \\ \vdots & & \ddots & \vdots \\ 0 & 0 & \dots & R_m \end{bmatrix} \quad (12)$$

For a given values of **Q** and **R** matrices, the solution of Algebraic Ricatti Equation(ARE) is straightforward as given in [25][26][27]. The PSO based optimal controller architecture is illustrated in Figure 4 where **x** is state vector of the system, **r** is desired reference signal, **y** denotes the controlled output vector, **Q** and **R** which are state and control matrices given in (11) can be optimized via PSO.

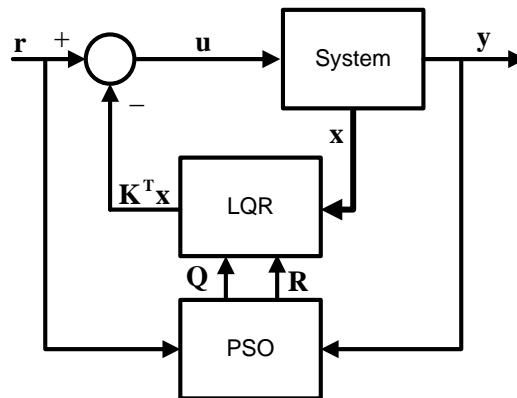


Figure 4. PSO based LQR Design.

4. SIMULATION RESULTS

The performance of the PSO based optimal control strategy has been tested on active suspension system. The dynamics of the ASS are derived in Section 2. The control performance of the introduced methodology has been assessed for nominal, measurement and parametric uncertainty cases to examine the robustness of the controller architecture. In section 4.1, the control performance for nominal case is given. The robustness of the

introduced design methodology with respect to measurement noise and parametric uncertainty cases are given in Section 4.2 and 4.3 respectively. The following objective function is utilized in PSO to acquire the optimal diagonal elements of \mathbf{Q} and \mathbf{R} matrices:

$$J = \int_{t=0}^{t_f} \left(\lambda_1 |z_s(t) - z_{us}(t)| + \lambda_2 \left| \frac{d^2 z_s(t)}{dt^2} \right| + \lambda_3 |z_r(t) - z_s(t)| + \lambda_4 |z_r(t) - z_{us}(t)| \right) dt \quad (13)$$

where $\lambda = [100 \ 0.1 \ 0.05 \ 0.05]$.

4.1. Nominal Case

The evaluation of the controller parameters and the diagonal elements of \mathbf{Q} and \mathbf{R} matrices are given in Figure 5.

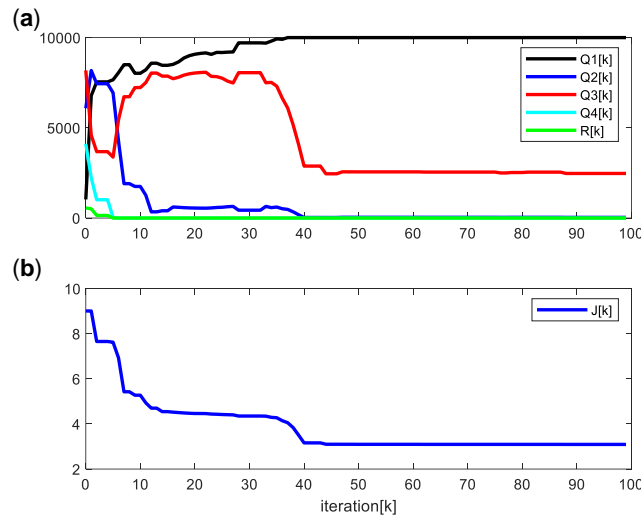


Figure 5 . Convergence of \mathbf{Q} and \mathbf{R} matrices elements(a), corresponding objective function value(b).

As a conclusion, the controller parameters are attained via ARE for nominal case as follows:

$$K = [2387.9 \ 207.1 \ 126.2 \ -16.3] \quad (14)$$

where performance function of PSO is $J = 3.0923$. The performance of the controller for nominal case is given in Figure 6 where z_r is road surface position, z_s denotes the vehicle body vertical position, z_{us} stands for tire vertical position. In Figure 6, the suppression of the vibrations due to road surface position(z_r) given in Figure 6 (a) are illustrated in Figure 6(c,d).

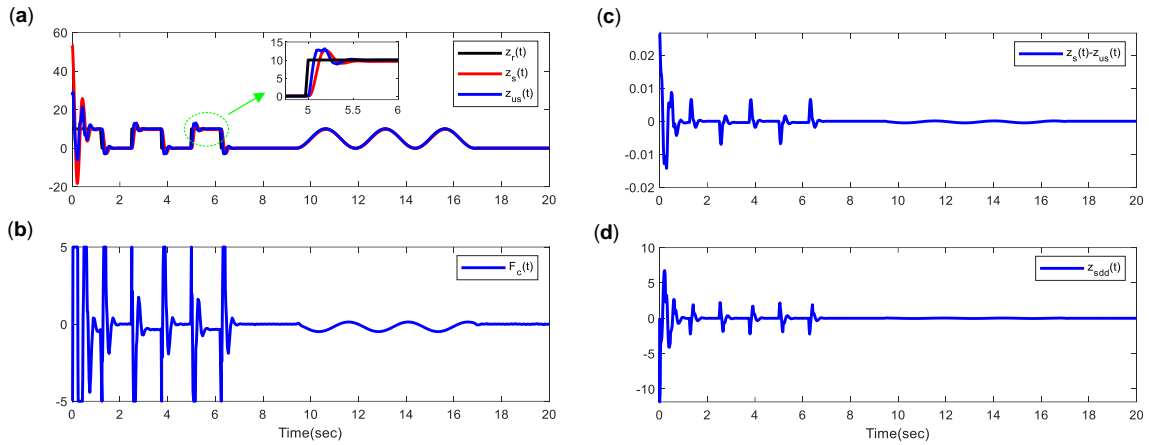


Figure 6. Positions(z_r, z_s, z_{us})(a), control signal(b), suspension deflection/travel(c), vehicle body vertical acceleration(d) for active suspension case.

As can be clearly seen from Figure 6, the vibrations resulting from the staircase and sinusoidal type surface position(z_r) can be successfully rejected. The performance of the passive suspension system($F_c(t) = 0$) is given in Figure 7 with $J = 10.02$.

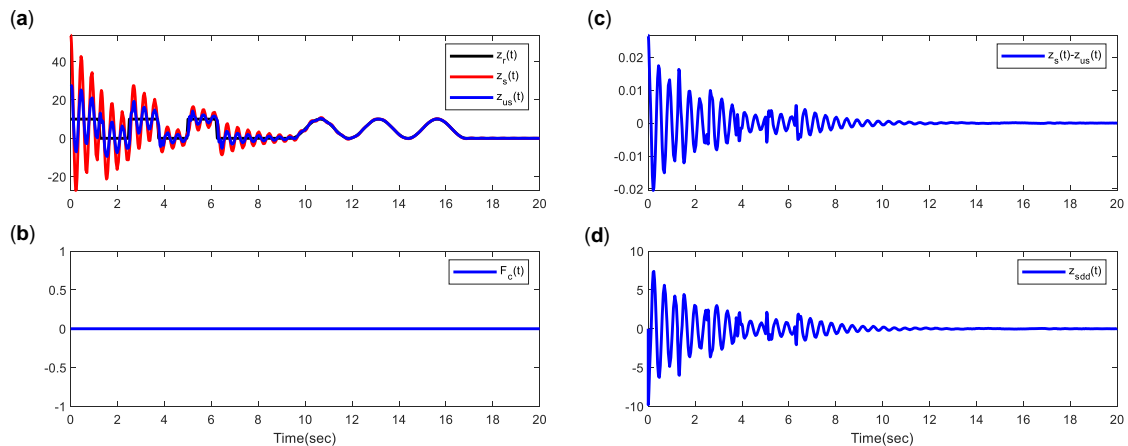


Figure 7. Positions(z_r, z_s, z_{us})(a), control signal(b), suspension deflection/travel(c), vehicle body vertical acceleration(d) for passive suspension case.

4.2. Measurement Noise Case

The robustness of the PSO based LQR is examined for measurement noise case. For this purpose, all measured states of the system is exposed to gaussian measurement noise. The control performance for measurement noise case is depicted in Figure 8.

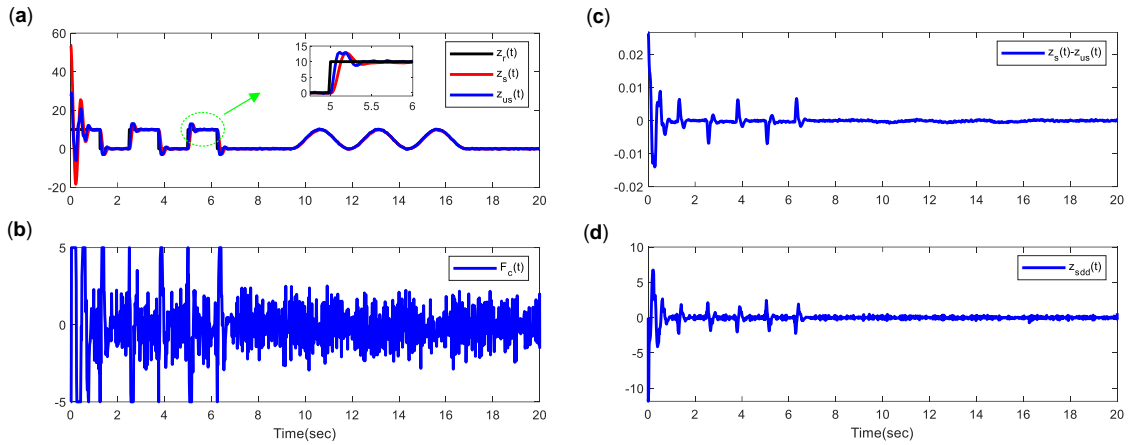


Figure 8. Positions (z_r, z_s, z_{us})(a), control signal(b), suspension deflection/travel(c), vehicle body vertical acceleration(d) for measurement noise case.

It is clearly seen from Figure 8(b) that the LQR controller rejects the measurement noises. The position errors are given in Figure 8 (a), and the outputs of the system are depicted in Figure 8 (c,d). The performance value is $J = 3.723$.

4.3. Parametric Uncertainty Case

By considering the M_{us} and M_s parameters as uncertain parameter, the PSO based LQR performance is examined for $M_{us}(t) = 1 + \sin\left(\frac{2\pi}{10}t\right)$, $M_s(t) = 2.45 + 0.45\sin\left(\frac{2\pi}{20}t\right)$. The rejection performance of the controller is shown in Figure 9 (a,b). As given in Figure 9 (a,b), the controller successfully suppress the uncertainty in controlled system. The performance value is computed as $J = 10.3$.

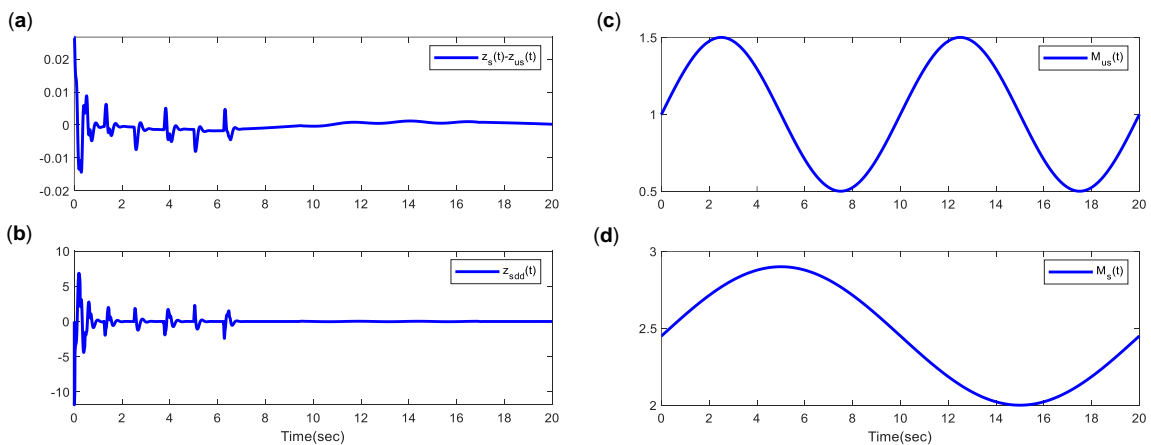


Figure 9. Suspension deflection/travel(a), vehicle body vertical acceleration(b), uncertain parameters(c,d) for parametric uncertainty case.

5. CONCLUSION AND FUTURE WORKS

In this paper, PSO based LQR mechanism has been introduced for Active Suspension System(ASS). It is aimed to obtain the optimal values of the diagonal elements of Q, and R matrices via PSO. The performance of the introduced mechanism has been assessed for various cases(nominal, measurement noise, parametric uncertainty) that are vital to test the applicability of designed control systems. It has been observed that the introduced controller design method provides robust controller architecture for measurement noises and parametric uncertainties.

As a future work, it is planned to introduce adaptive control methodologies for ASS system.

REFERENCES

- [1] M. T. Emirler, "Taşıt Savrulma Açısıl Hızının Sanal Sensör Kullanılarak Tahmin Edilmesi ve Taşıt Yanal Dinamiğinin Kontrolü," 2010.
- [2] A. J. Qazi, U. A. Farooqui, A. Khan, M. T. Khan, F. Mazhar, and A. Fiaz, "Optimization of Semi-active Suspension System Using Particle Swarm Optimization Algorithm," *AASRI Procedia*, vol. 4, pp. 160–166, 2013.
- [3] A. J. Qazi, A. Khan, M. T. Khan, M. A. Kamran, and K. Azam, "A Novel Applications of Particle Swarm Optimization Technique in Semi-Active Suspension System Control Semi-Active Suspension System Control," *J. Eng. Appl. Sci.*, vol. 31, no. 2, pp. 91–97, 2012.
- [4] M. A. M. Obaid, A. R. Husain, and Y. A. Alamri, "Intelligent optimal controller of active suspension system based on particle swarm optimization," *Int. J. Adv. Soft Comput. its Appl.*, vol. 6, no. 3, pp. 78–93, 2014.
- [5] H. Emad, A. Mary, and M. M. Ali, "Control of active car suspension system based on 2PID and PSO Optimization," *Eurasian J. Eng. Technol.*, vol. 5, pp. 155–170, 2022.
- [6] D. Peng, G. Tan, K. Fang, L. Chen, P. K. Agyeman, and Y. Zhang, "Multiobjective Optimization of an Off-Road Vehicle Suspension Parameter through a Genetic Algorithm Based on the Particle Swarm Optimization," *Math. Probl. Eng.*, vol. 2021, 2021.
- [7] A. Hafizal *et al.*, "Semi-active suspension system using MR damper with PSO-skyhook and sensitivity analysis of PID controller," *J. Adv. reseach*, vol. 1, no. 1, pp. 1–8, 2017.
- [8] H. Yan, J. Qiao, S. Zhang, T. Zhao, and Z. Wang, "The optimal control of semi-active suspension based on improved particle swarm optimization," *Math. Model. Eng.*, vol. 4, no. 3, pp. 157–163, 2018.
- [9] H. M. Soliman, M. A. Awadallah, and M. N. Emira, "Robust controller design for active suspensions using particle swarm optimisation," *Int. J. Model. Identif. Control*, vol. 5, no. 1, pp. 66–76, 2008.

- [10] J. Hurel, A. Mandow, and A. Garcia-Cerezo, "Tuning a fuzzy controller by particle swarm optimization for an active suspension system," in *IECON Proceedings (Industrial Electronics Conference)*, 2012, pp. 2524–2529.
- [11] M. Li, J. Li, G. Li, and J. Xu, "Analysis of Active Suspension Control Based on Fuzzy Neural Network PID," *World Electr. Veh. J.*, vol. 13, no. 226, pp. 1–15, 2022.
- [12] L. Zhao, Z. Zeng, Z. Wang, and C. Ji, "PID Control of Vehicle Active Suspension Based on Particle Swarm Optimization," *J. Phys. Conf. Ser.*, vol. 1748, no. 3, 2021.
- [13] J. Apkarian and Amin Abdossalami, "Laboratory Guide Active Suspension Experiment for Matlab /Simulink Users." 2013.
- [14] R. Darus and N. I. Enzai, "Modeling and control active suspension system for a quarter car model," in *CSSR 2010 - 2010 International Conference on Science and Social Research*, 2010, vol. 4, no. 7, pp. 1203–1206.
- [15] O. Demir, I. Keskin, and S. Cetin, "Modeling and control of a nonlinear half-vehicle suspension system: A hybrid fuzzy logic approach," *Nonlinear Dyn.*, vol. 67, no. 3, pp. 2139–2151, 2012.
- [16] S. Kashem, R. Nagarajah, and M. Ektesabi, "Vehicle suspension system," *Springer Tracts Mech. Eng.*, no. 9789811054778, pp. 23–37, 2018.
- [17] J. Ahmed *et al.*, "Active Suspension System Modeling for a Passenger Car Subjected to Random Profile Inputs," in *Recent Advances in Mechanical Engineering*, M. Muzammil, A. Chandra, P. P. Kankar, and K. Harish, Eds. 2021, pp. 427–434.
- [18] R. K. Pekgökgöz, M. A. Gurel, M. Bilgehan, and M. Kisa, "Active Suspension of Cars Using Fuzzy Logic Controller Optimized by Genetic Algorithm," *Int. J. Eng. Appl. Sci.*, vol. 2, no. 4, pp. 27–37, 2010.
- [19] R. S. A. AlWaily, "Design of Robust Mixed H₂/H_{inf} PID Controller Using Particle Swarm Optimization," *Int. J. Adv. Comput. Technol.*, vol. 2, no. 5, pp. 53–60, 2010.
- [20] Abolfazl Jalilvand, MeisamMahdavi, Ahmad Ashouri, and Ali Kimiyaghalam, "Advanced Particle Swarm Optimization-Based PID Controller Parameters Tuning," pp. 429–435, 2008.
- [21] D. Wang, D. Tan, and L. Liu, "Particle swarm optimization algorithm: an overview," *Soft Comput.*, vol. 22, no. 2, pp. 387–408, 2018.
- [22] H. A. Alhasan, "Parçacık Sürü Optimizasyonu(PSO) Kullanarak Öz Ayarlamalı PID Kontrolör Tasarımı," Kahramanmaraş Sütçü İmam University, 2018.
- [23] L. Xu-zhou, Y. Fei, and W. You-bo, "PSO Algorithm based Online Self-Tuning of PID Controller," in *Proceedings - 2007 International Conference on Computational Intelligence and Security, CIS 2007*, 2007, pp. 128–132.
- [24] H. Hosseini, M. Shahbazian, and M. A. Takassi, "The Design of Robust Soft Sensor Using ANFIS Network," *J. Instrum. Technol.*, vol. 2, no. 1, pp. 9–16, 2014.

- [25] V. Kumare and J. Jerome, “Algebraic Riccati equation based Q and R matrices selection algorithm for optimal LQR applied to tracking control of 3rd order magnetic levitation system,” *Arch. Electr. Eng.*, vol. 65, no. 1, pp. 151–168, 2016.
- [26] P. Benner, “Theory and Numerical Solution of Differential and Algebraic Riccati Equations,” in *Numerical Algebra, Matrix Theory, Differential-Algebraic Equations and Control Theory*, 2015, pp. 67–105.
- [27] C. Navasca and K. Morris, “Solution of Algebraic Riccati Equations Arising in Control of Partial Differential Equations,” no. 3, pp. 258–280, 2005.

**HEAVY METALS IN DISSOLVED AND PARTICULATE WATER OF THE TIGRIS
AND EUPHRATES AND SHATT AL-ARAB RIVERS**

Hamid T. Al-Saad

College of Marine Science, University. of Basrah, Iraq.

Shahinaz R.A Al-Shawi

Department of Geology, College. of Science, University. of Basrah, Iraq.

Hamzah A. Kadhim

Department of Geology, College. of Science, University. of Basrah, Iraq.

ABSTRACT

Six stations were selected in Tigris and Euphrates and Shatt Al-Arab River to measure the concentration of six Heavy Metals which were (Cd , Cu ,Fe , pb , Mn , Ni , Zn) the samples were taken from subsurface River during Autumn 2021 to Summer 2022 , The results of analyzes showed by using an inductively coupled plasma atomic emission spectrometer (ICP-OES) where The samples were taken as dissolved and particulate in water and The seasonal average of heavy metal concentrations ranges between the lowest value (8.75 mg\l) for cadmium in summer and the highest value (981.65 mg\l) for Iron in winter in dissolved as for particulate were the lowest value (15.46 µg/g) for manganese in summer and the highest value (773.76 µg/g) for iron in winter. These findings suggested that atmospheric sediments, gas emissions from oil production, power plants, and runoff from agricultural regions after rains were the primary causes of heavy metal contamination in rivers. If our findings are compared to those of previous study, this will be lies within previous data

**ACKNOWLEDGEMENTS MODEL FOR DETECTION OF COLLISION USING
CRYPTOGRAPHY FOR MANET**

K. Thamizhmaran

Department of ECE, Government College of Engineering, Bodinayakanue, Theni
Tamil Nadu, India (Deputed from Annamalai University)

ABSTRACT

MANET is the significant technologies used to more flowing more application conference, meeting, short time connection, natural issues like (flooding, forest fire, agriculture and military) ect., among various un-wired communication technologies where all the mobile nodes are mobile and which can be connected to random dynamically using wireless link in the random manner. But it stream including critical issue and challenges such as security, energy, delay, packet drop quality of service ect., In this research paper proposed Secure Two Acknowledgement method with MARS4 (STACK) that implement for new intrusion detection system for on-demand wireless networks. MARS4 can improve a best performance of trusted quality output to reduce transmission delay, transmission time and also increase network communication throughput help of Network Simulator-2.34 (NS2) to implement it.

Keywords: Ad hoc, MANET, Security, Routing, STACK, MAJRS4.

1. INTRODUCTION

The need for wireless temporary communication facilities is rapidly increasing, because the mobile ad-hoc communication service is synonymous with an ideal communication style realizing communication anytime, anywhere in the world with anyone. The accessibility of a route depends on the number of connections and the reliability of each link forming the route. Many routing metrics in terms of number of links have been proposed, such as the SPA. SPA finds a path having minimum weights to forward the packets to the destination node. SPA selection depends on direct traffic form source to destination, maximizing the network performance and minimizing the cost. Performance of the network can be enhanced through shortest path routing but it also depends upon the functionality of the routing protocol and the parameters that are selected for the shortest path routing. MANET is the one of emerging need part of natural issues in this type of network is non-fixed connect all the mobile nodes dynamically to communicate from source to destination using different types of routing protocols show in figure 1 Mobile Ad hoc Network.



Fig 1 Mobile Ad-hoc Networks

2. ROUTING

The routing protocols are vital role and it has to adapt quickly to the repeated changes in the ad-hoc network topology. MANET routing protocols Figure 2 are categorized into following three types. Table driven routing protocols: these kind of routing protocols are retains the network topology information in routing tables contains a updated list of destinations and their routes by time to time swapping their routing information with nearby nodes. Routing information is usually flooded in the entire network. At any time a node wants a route to the destination it runs a suitable path finding algorithm on the topology information it retains. On-demand routing protocols: These kinds of protocols are not maintaining topology information of the network, with the help of connection establishment process nodes can obtain necessary route when it is required, and therefore this type of protocols is not exchanging the routing information time to time. Hybrid routing protocols: In this protocols both table driven, on-demand routing advantages are combined. The routing is in the beginning established with certain proactively prospected routes then it serves the demand from additionally activated nodes through reactive flooding.

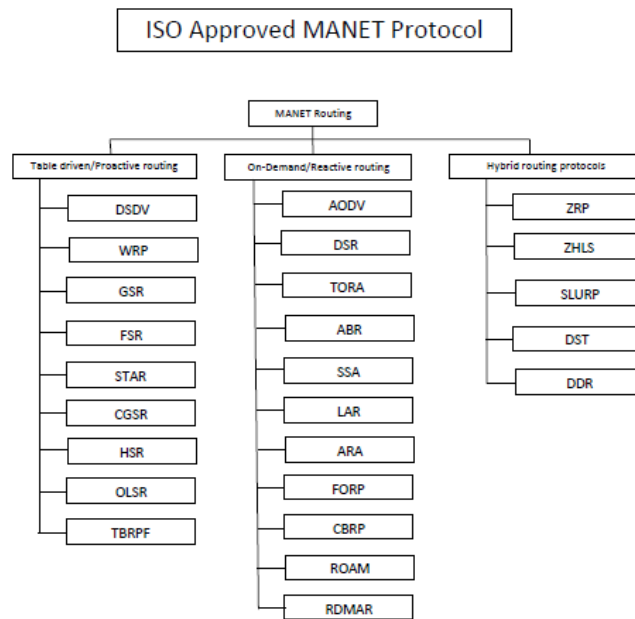


Figure 2 MANET routing protocols

3. BACKGROUND

Secure routing and intrusion detection in ad-hoc networks was taken up by Anand Patwardhan et al (2005). Malicious nodes detection in AODV-based mobile ad-hoc networks was addressed by Jongoh Choi et al (2005). An acknowledgment-based approach for the detection of routing misbehaviour in MANETs was discussed by Liu et al (2007). The detection of packet dropping attack using improved acknowledgement based scheme in MANETs was done by Aishwarya Sagar et al (2010). The impact of security attacks on a new protocol for mobile adhoc networks was analysed by Sahadevaiah et al (2010). Adaptive acknowledgment intrusion detection for MANETs with node detection enhancement was analyzed by Al-Roubaiey et al (2010). Secure routing for wireless mesh network was discussed by Celia li et al (2011). Performance analysis of secure routing protocols in MANET dicussed by K.Thamizhmaran et al (2012). Secure routing protocol in MANET – A survey taken by K.Thamizhmaran et al (2012). Secure intrusion detection system for MANETs was found by Shakshuki et al (2013). Implementation of A3ACK’s intrusion detection system under various mobility speeds was highlighted by Abdulsalam Basabaaa et al (2014). Energy efficient routing in MANETs through edge node selection using ESPR algorithm was discussed by Prabu and subramani (2014). Performance evaluation of EA3ACK in different topology’s using EAACK for MANET highlighted by K.Thamizhmaran (2016). Performance analysis of energy efficient enhanced adaptive 3-acknowledgement (EE-EA3ACK) using ECC in MANET analyzed by K.Thamizhmaran et al (2017). Comparison and parameter adjustment of topology based (S-EA3ACK) for MANETs done by K.Thamizhmaran et al (2017). Performance analysis of on-demand routing protocol

for MANET using EA3ACK algorithm addressed by K.Thamizhmaran et al (2017). Reduced end-to-end delay for MANETs using SHSP-EA3ACK algorithm proposed by K.Thamizhmaran et al (2017). However, all these algorithms address only the security problem because misbehavior attacks due to topology changes rapidly in MANETs due to the characteristics of wireless networks. The proposed approach scheme STACK with help of MARS4 hybrid cryptography is also based on this assumption to provide secure transmission with minimum delay.

4. PROBLEM IDENTIFICATION

The dynamic nature of MANETs requires the routing protocols to refresh the routing tables frequently and suffer from transmission contention time delay and congestion with packet dropping that are the results of the broadcasting nature of radio transmission since a node in MANETs cannot directly communicate with the nodes outside its communication range, a packet may have to be routed through intermediate nodes to reach the destination. Hence it becomes essential to monitor the constraints in intermediate nodes. Consequently, an efficient routing approach may generate route delay, packet dropping and route failures. The simplest scheme routing in MANETs is the one in finding a route without malicious nodes in the shortest path. This paper aims to provide unbreakable route for secure transmission with the shortest path. So a new routing algorithm named STACK using ACK with hybrid cryptography is proposed. This STACK provides better performance compared to the existing ACK and also reduces routing delay and packet dropping without any misbehavior at intermediate nodes.

5. PROPOSED WORK

In STACK mode, the three consecutive nodes (i.e., A, B, C) work in a group to overcome the drawbacks of watchdog scheme in the network. Node A first sends out STACK data packet P1(S) to node B. Then, node B forwards this packet to node C. When node C receives P1(S), as it is the third node in this three-node group, node C is required to send back a STACK acknowledgement packet P1(A) to node B. Node B forwards this P1(A) back to node A. If node A does not receive this acknowledgement packet within a predefined time period, both nodes B and C are reported as malicious. This process is shown in Figure 3.

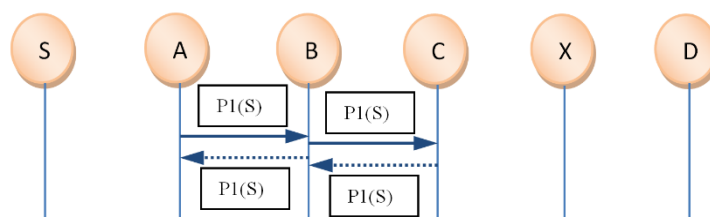


Fig. 3 STACK

Procedural Steps of STACK Algorithm

- STACK processing starts with hybrid cryptography.
- Hello packet transmission from source to destination through intermediate nodes.
- Destination node sends ACK message to source node in same route through intermediate nodes.
- If source node receives this acknowledgement packet within a predefined time period, then data transmission will be start.
- If node A does not receive this acknowledgement packet within a predefined time period, then the intermediate nodes are marked as malicious nodes.
- Switch to TACK. Send acknowledgement packet through intermediate node, this model to detect if there are any receiver collision, false misbehaviour nodes and limited transmission power in the route.
- Out of the three consecutive nodes in the TACK, the third node is required to send an ACK packet to the temporary source node same rout with opposite direction.
- If node A receives this acknowledgement packet within a predefined time period, then data transmission will be start, otherwise both nodes B and C are reported as malicious. when malicious report is received to the source node than, source node switch to MRA.
- MRA checks authentication (secure value) to all nodes and if MAR receives this acknowledgement packet within a predefined time period, then the data transmission will be start, otherwise marked as misbehaviour node.
- Transmit the data in the alternate path to the destination, and go to step1.

Procedural Steps of Hybrid Cryptography (MARS4 Algorithm)

- Now MAJE4 and RSA can be combined to have MARS4 as a very efficient security solution. It is assu
- med that A is the sender of a message and B is the receiver. MARS4 is designed to work as follows.
- A encrypts the original message (PT) with the help of MAJE4 and the symmetric key (K1) and forms the cipher text (CT).
- Again encrypt symmetric key K1 to (K2) of B using RSA.
- B now uses the RSA algorithm and its private key (K3) to decrypt symmetric key K1.

Then B uses K1 and the MAJE4 algorithm to decrypt the CT for the original plain text (PT).

STACK consists of three major parts, namely, ACK, 2-ACK, Misbehaviour Report Authentication (MRA). With the introduction of hybrid cryptography algorithm MARS4 prevents the attacker from forging acknowledgement packets and also simulate help of following simulator called NS 2.34 is used to test the Intrusion Detection System's (IDSs)

performance when the attackers are smart enough to forge acknowledgement packets claiming positive result while, in fact, it is negative. As watchdog is not an acknowledgement-based scheme, and as shown in Table 1, the following are the simulation parameters used for the analysis of routing protocol with hybrid shortest path algorithm.

Table 1 Simulation parameters

Parameter	Values
Examined protocol	STACK-MARS4
Application traffic	CBR
Transmission range	1000m
Packet size	512 bytes
Maximum speed	25m/s
Simulation time	900s
Number of nodes	60
Area	1000x1000m
Maximum number of malicious nodes	18

6. RESULT

Malicious nodes simply drop all the packets that they receive and send back forged positive acknowledgment packets to their previous nodes whenever necessary. This is a common method for attackers to degrade network performance while still maintaining their reputation. The proposed approach STACK is designed to tackle four of the six weaknesses of watchdog scheme, namely, receiver collision, limited transmission power, false misbehaviour, and partial dropping.

Table 2 Results of Parameter Values

End-to-End Delay						
Delay NN	10	20	30	40	50	60
TACK	0.57	0.52	0.47	0.41	0.33	0.24
STACK-MARS4	0.48	0.44	0.39	0.31	0.24	0.17
Malicious Node						
Delay MN	3	6	9	12	15	18
TACK	0.33	0.36	0.40	0.44	0.45	0.47
STACK-MARS4	0.23	0.27	0.32	0.34	0.35	0.37
Transmission Range						

Delay TR	0	250	400	600	800	1000
TACK	0	0.69	0.63	0.57	0.54	0.52
STACK-MARS4	0	0.46	0.42	0.37	0.30	0.28
Packet Drop						
Delay PD	5%	10%	15%	20%	25%	30%
TACK	0.12	0.18	0.24	0.28	0.33	0.38
STACK-MARS4	0.05	0.07	0.14	0.19	0.21	0.23
Routing Overhead						
RO NN	10	20	30	40	50	60
TACK	0.06	0.20	0.33	0.39	0.48	0.57
STACK-MARS4	0.05	0.16	0.27	0.35	0.41	0.43

End-to-end delay when the number of nodes is increased from 10 to 60. According to table 2, it is clear that in all acknowledgement-based IDSs, the proposed scheme STACK-MARS4 surpassed the performance of TACK in minimizing end-to-end delay by 8.5% when there are 10 to 60 nodes in the network. As the proposed algorithm finds different short routes frequently, it is possible to minimize the delay. It is observed from Table 2 that when compared with TACK algorithm, STACK-MARS4 decreases the delay by 9.5% with increase in the number of malicious nodes from 3 to 18 out of 60 nodes. If malicious node is detected, immediately the STACK-MARS4 algorithm finds alternate shortest route in between the sender and receiver. Transmission range is varied from 250 to 1000 meters and simulation is carried out to calculate the end-to-end delay using TACK & STACK-MARS4 methods. The obtained results are given in table 2. It is clear from the simulation results that the DSR scheme achieves the best performance, as it does not require acknowledgment scheme to detect misbehaviours. In case of the IDSs, STACK-MARS4 has the lowest delay in comparison with TACK, when there are 250 to 1000 meters of transmission ranges. When transmission range increases, connectivity among the nodes also increases, which enables the proposed method to identify more number of alternate paths which in turn reduces the delay. Finally routing overhead is analyzed using the two algorithms when the total number of nodes is varied from 10 to 60 and the simulation results are shown in table 3. Simulation results reveal that the proposed algorithm reduces the routing overhead by 6% than TACK algorithm. If any of the intermediate nodes is found to be busy, then the proposed algorithm is able to find alternate hybrid shortest path from the previous node itself which reduces the delay. From the entire above table 2, it is clear that the comparison of the STACK-MARS4 illustrate that the proposed algorithm outperforms the TACK by providing lowest end-to-end delay, packet drop and routing overhead with increase in the number of nodes.

7. CONCLUSION & FUTURE WORK

In this paper, the new routing protocol named STACK-MARS4 using TACK is proposed to address the problem. Acknowledgement based transmission is highly secure with the lowest delay and packet dropping. This STACK-MARS4 provides better performance compared to the existing TACK routing protocol by decreasing end-to-end delay by 8.5% lowering routing overhead by 6% and reducing packet drop by 10.7% compared to the existing TACK routing protocol. To enhance the merits of this research work, there is a plan to investigate the following issues in the future. However, the same concept can be applied in satellite to reduce end-to-end delay in the route and reduce packet loss, Possibilities of adopting secure quality oriented techniques to further improve the network performance of quality.

Reference

1. Anand Patwardhan and Iorga, Secure routing and Intrusion Detection in Ad-hoc networks, in Proc. 3rd Int. Conf. Pervasive Computer Communication, pp.191–199 (2005).
2. Jongoh Choi, et al, Malicious Nodes Detection in AODV- Based Mobile Ad Hoc Networks, GESTS Trans. Comp. Science and Engg, vol.18, no.1, pp.49-55 (2005).
3. Prabu, K. and Subramani, A. Performance comparison of routing protocol in MANET, Int. J. of Adv. Research in Com. Sci. and Soft Engg., Vol. 2, No. 9, pp.388–392 (2012).
4. K. Thamizhmaran, R. Santosh Kumar Mahto, and V. Sanjesh Kumar Tripathi, “Performance Analysis of Secure Routing Protocols in MANET”, International Journal of Advanced Research in Computer and Communication Engineering, Vol. 1, No. 9, pp. 651-654 (2012).
5. D. Raj Vikram Singh¹, S. Subhash Kumar Kesarwani and K.Thamizhmaran “Secure Routing Protocol in MANET – A Survey”, International Journal of Engineering Journals and Tech, Vol. 3, No. 3, pp. 22-29, (2012).
6. Prabu, K. and Subramani, A. Energy efficient routing in MANET through edge node selection using ESPR algorithm, Int. J. Mobile Network Design and Innovation, vol. 5, no. 3, pp.166–175 (2014).
7. K. Thamizhmaran “Performance Evaluation of EA3ACK in different topology’s Using EAACK for MANET, I - Manager Journal of information technology , Vol. 5, No. 4, pp. 5-10 (2016).
8. K.Thamizhmaran, M.Anitha and Alamelunachippan “Performance Analysis of energy-Efficient Enhanced Adaptive 3- Acknowledgement (EE-EA3ACK) Using ECC in MANET” ARPN, Vol. 12, No. 9, pp. 2901-2912 (2017).

9. K.Thamizhmaran, M.Anitha and Alamelunachippan “Comparison and Parameter Adjustment of Topology Based (S-EA3ACK) for MANETs”, International Journal of Control Theory and Application, Vol. 10, No. 30, pp. 423-436 (2017).
10. K.Thamizhmaran, M.Anitha and Alamelunachippan “Performance Analysis of On-demand Routing Protocol for MANET Using EA3ACK Algorithm”, International Journal of Mobile Network Design and Innovation (Inderscience), Vol. 7, No. 2, pp. 88-100 (2017).
11. K.Thamizhmaran, M.Anitha and Alamelunachippan “Reduced End-to-End Delay for MANETs using SHSP-EA3ACK algorithm”, Journal on Communication Engineering and System, Vol. 7, No. 3, pp. 8-15 (2018).

EFFICIENT MOBILE AD HOC NETWORK USING DYNAMIC SOURCE ROUTING PROTOCOL

K. Thamizhmaran

Department of ECE, Government College of Engineering, Bodinayakanue, Theni
Tamil Nadu, India (Deputed from Annamalai University)

ABSTRACT

The frequent discoveries result in a lot of network congestion. To avoid this multipath routing protocols are planned to seek out multiple routes to destination and put on to alternate secondary path just in case of route broken and its offer higher routing performance and security. In this developed research paper attempt to compare the performance of two reactive routing protocols for MANETs that is Secure Dynamic Source Routing (SDSR) and Dynamic Source Routing (DSR), on-demand gateway discovery protocol where a mobile device of MANET gets connected to gateway. SDRS using the Intrusion Detection system (IDS) and trust based routing, the performance results are analysed by varying simulation time. Furthermore, all the above mentioned protocols are compared based on several important performance metrics which are packet delivery ratio, end-to-end delay and average energy.

Keywords: MANET, IDS, TS-DSR, NS2.

INTRODUCTION

Wireless technologies such as Bluetooth or the 802.11 standards enable mobile devices to establish a MANET by connecting dynamically through the wireless medium without any centralised structure. MANET is a network having dynamic topology that consists of mobile nodes without base Station or centralized control. All mobile nodes perform functioning of routers that search and maintain routes to other nodes in the network. Difficulty in ad-hoc network is that for communication with other nodes, a node must be in the transmission range of base station but sometimes a node moves and network fails. MANET has solved this problem as in MANET nodes follow multi-hop pattern for communicating with other nodes. Routing is the process of moving information across internet work from source to destination by selecting best outgoing path that a packet has to take in internetnetwork. To perform this, a set of routing protocols needed that uses metrics to find optimal path for a packet to travel. Routing protocols designing goals are optimality, simplicity, low overhead, robustness, reliability and flexibility. Route request and Route reply messages are used to discover and store the paths found from the source to destination. After finding the paths, shortest path is selected by the source node. Paths discovered by shortest path algorithm cause problems like congestion problems as the centre of network carry more traffic, this results in poor

performance. The main goals of multipath routing protocols are to maintain reliable communication, to reduce routing overhead by use of secondary paths, to ensure load balancing, to improve quality of service, to avoid the additional route discovery overhead. The major focus of the routing is the performance and the efficiency of the protocol in the presence of a dynamic network environment.

1. LITRACHER SURVEY

Improvement and analysis of multipath routing protocol AOMDV based on CMMBCR was done by Yin-jun Yang (2011). A node disjoint multipath routing method based on AODV protocol for MANET was done by Lal, et al (2012). Increased throughput for load based channel aware routing in MANETs with reusable paths was done by Ayyasamy (2012). Specification based intrusion detection for unmanned aircraft systems was done by Mitchell (2012). A survey of attacks on MANET routing protocols was done by Tayal (2013). Review on MANET routing protocols and challenges was done by Habib (2013). A survey of intrusion detection in wireless network applications was done by Mitchell (2014). Behavior rule specification-based intrusion detection for safety critical medical cyber physical systems was done by Mitchell (2015). Trusted secure ad-hoc on-demand multipath distance vector routing in MANET was analysis by Abrar Omar Alkhamisi (2016).

2. PROPOSED METHOD

Secure Dynamic Source Routing: In this proposed work TS-DSR, when a route is needed from source to destination, then source starts a route discovery process by flooding a RREQ for destination. With the help of sequence numbers, RREQs are uniquely identified so that duplicate RREQs can be identified and discarded. When a non-duplicate RREQ is received then intermediate node records previous hop and search for a fresh route entry to the destination in routing table. If fresh route is present then the node sends a RREP to the source but if fresh route is not present, it rebroadcasts the RREQ. The routing information is updated by a node only if a RREP contains either a larger destination sequence number than previous one or a route with less hop count found. SDSR routing process with the help of IDS and trust-based routing, the attack identification and isolation in SDSR are carried out in two phases of routing such as route discovery phase and data forwarding phase. Trust Based Route Discovery Process Initially, each node assigns the trust value as 'one' to its neighboring nodes. Prior to rebroadcasting the received RREQ packet to the neighbors, every node checks for the trust value of the source that has broadcasted the RREQ packet. If the trust value is lesser than the threshold, then the RREQ packet from the corresponding source is dropped to block the flooding activity of the attacker. For instance, in the trust value of the source node is maintained by its neighboring nodes such as A, B, and C. The trust value of the source node is different in various neighboring nodes due to the network collisions. The trust value of the source node is very less, so these nodes do not forward the RREQ packet of the source node

into the network. For instance, the trust value of the node B is higher than node A, and so the source node selects router B for further data forwarding. Thus, the IDS and the trust based MTS-DSR protocol improve the routing performance and security in MANET.

3. EXPERIMENTAL SETUP

The NS-2 which is a discrete event driven simulator developed at UC Berkeley is used in this simulation process. Network Simulator NS-2 is useful in designing new protocols, comparison of different protocols and for evaluating the traffic. A scenario file is taken as input in the NS-2 simulation process that shows the motion of each node and the originating packets by each node. The simulation models are built using the NS-2 version 2.34 and it is run under bandwidth of 40 MHZ.

Table 1 Simulation parameters

Parameter	Values
Simulation area	680*680
Number of nodes	50
Number of packets	25
Constant bit rate	4 (packets/second)
Packet size	512 bytes
Initial energy/node	100 joules
Antenna model	Omni directional
Simulation time	500 sec

4. RESULTS AND DISCUSSION

The results for the above mentioned simulation experiment is shown with the help of graphs. In this section the comparison of DSR and SDSR is made and the metrics used for the analysis of results are packet delivery ratio and end to end delay, energy.

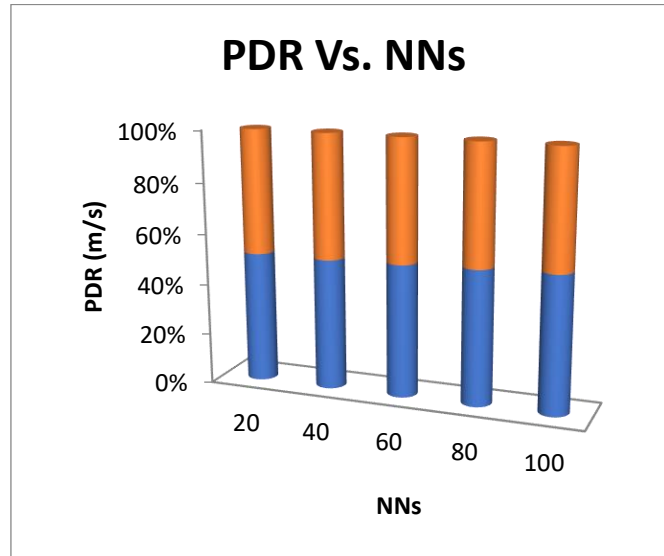


Fig 1 packet delivery ratio Vs. number of nodes

It is observed from Fig 1 that when compared with DSR algorithm, SDSR increases the delivery ratio above 85% with the increase in the number of nodes from 20 to 100. As the proposed algorithm finds maximum secure and lowest link failed route with minimum retransmit packets frequently, it is possible to increase the delivery ratio.

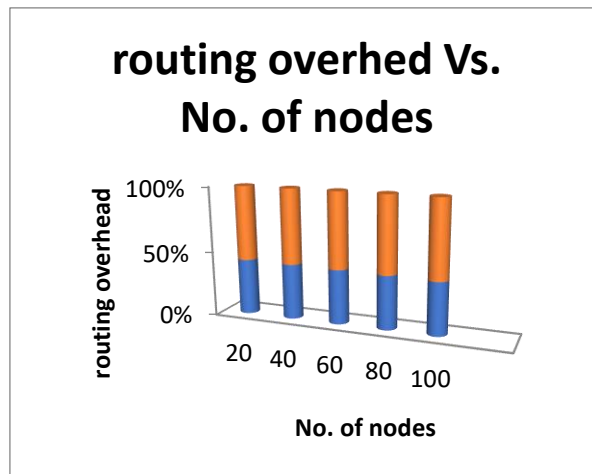


Fig 2 Routing overhead Vs. number of nodes

SDSR has the lowest overhead in comparison with DSR, when there are 680 of transmission ranges. When the transmission range increases, the connectivity among the nodes also increases, which enables the proposed method to identify more number of alternate secondary paths which in turn reduces the congestion. Fig 2 describes the decrease in overhead obtained by the proposed SDSR when there are 20 to 100 nodes.

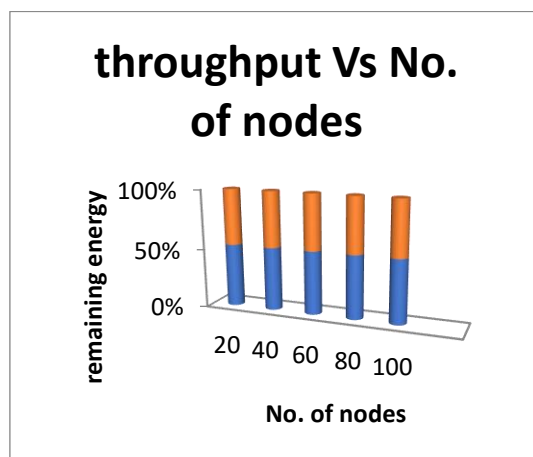


Fig 3 Throughput Vs. number of nodes

Fig 3 shows the graph of the throughput when the topology is size 680m, the number of nodes increased from 20 to 100. The proposed SDSR increases the throughput with the increasing topology size compared to DSR and SDSR.

5. SUMMARY

On the basis of simulation results it is concluded that SDSR is better than DSR. SDSR outperforms DSR due its ability to discover alternate routes when a current link fails. Although DSR incurs more routing overheads because of flooding the network and packet delays due its alternate route discovery process, it is very much efficient in case of packet delivery for the same reason. SDSR proves to be more efficient than DSR as it provides better throughput. Finally the conclusion is that when network load increases SDSR is a better on-demand routing protocol than DSR as it gives better statistics for packet delivery and throughput were implementing via network simulator 2. To increase the merits of this research work, there is a plan to investigate the following issues in our future research. The same concept can be applied in satellite to increase delivery ratio and reduce delay in the route and also to save more energy. The performance of SDSR can be tested in real time network environment.

REFERENCES

1. Das, et al (2000) "An implementation study of AODV routing protocol", Wireless Communication and Networking Conference, Vol. 3, pp. 1003-1008.
2. 4. Lal, et al (2012) "A node disjoint multipath routing method based on AODV protocol for MANET" IEEE 26th international Conference on Data Object Identifier, pp. 309-405.

3. Ayyasamy, Venkatachalapathy (2012) "Increased Throughput for Load based Channel Aware Routing in MANETs with Reusable Paths", International Journal of Computer Applications, Vol. 40, No. 2, pp. 20-23.
4. Mitchell, Chen (2012) "Specification based intrusion detection for unmanned aircraft systems", Proceedings of the first ACM MANET workshop on Airborne Networks and Communications, pp. 31-36.
5. Tayal, Gupta (2013) "A Survey of Attacks on MANET Routing Protocols", International Journal of Innovative Research in Science, Engineering and Technology, Vol. 2, No. 6, pp. 2280-2285.
6. Habib, et al (2013) "Review on MANET routing protocols and challenges", IEEE Student Conference on Research and Development SCORED, pp. 529-533.
7. Mitchell, Chen, (2014) "A survey of intrusion detection in wireless network applications", Computer Communications, Vol. 42, pp. 1-23.
8. Mitchell, Chen (2015) "Behavior Rule Specification-Based Intrusion Detection for Safety Critical Medical Cyber Physical Systems," in Dependable and Secure Computing, IEEE Transactions, Vol. 12, No. 1, pp. 16-30.
9. Abrar Omar Alkhamisi, Seyed M Buhari (2016) "Trusted Secure Ad hoc On-Demand Multipath Distance Vector Routing in MANET", IEEE 30th International Conference on Advanced Information Networking and Applications.

**PERFORMANCE ASSESSMENT OF NATURAL GAS DEHYDRATION
TECHNOLOGIES**

Hooman Fatoorehchi

Assistant Professor, School of Chemical Engineering, College of Engineering, University of Tehran, P.O. Box
11365-4563, Tehran, Iran

Seyed Amirreza Babaei

Bachelor student, School of Chemical Engineering, College of Engineering, University of Tehran,
Tehran, Iran

Niloofar Arabi

Bachelor student, School of Chemical Engineering, College of Engineering, University of Tehran,
Tehran, Iran

ABSTRACT

Natural gas dehydration is basically a process where we remove water vapor from the gas stream. This process helps us lower the temperature at which water will condense from the stream. This temperature is called the dew point temperature. Basically, the amount of water in natural gas is 5 times the allowed limit, and this requires us to reduce the amount of water vapor by dehydration so that we can use it for industries. Water vapor, like many other species, can be separated by physical or chemical methods or by using both. Gas dehydration is a fundamental step in gas treatment and is included in nearly all gas processing units. In the industry, we use three technologies for natural gas dehydration: 1) absorption with glycol solution 2) adsorption with molecular sieve 3) Joule-Thomson condensation. The dehydration process has many benefits, which has made it widely used in the industry. Dehydration allows us to continuously use downstream process equipment by reducing the risk of freezing hydrates. This freezing causes the formation of different crystals on the pipelines, which over time causes the general wear and tear of the pipes. In this paper, some dehydration methods will be explained and the advantages and disadvantages of each will be discussed.

Keywords: natural gas, dehydration, temperature, natural gas refinery

**ESTIMATION OF GLOBAL SOLAR RADIATION USING FIVE SUNSHINE BASED
MODELS FOR ILORIN, NORTH-CENTRAL, NIGERIA**

IBRAHIB B. B· USMAN A.

Department of Science Laboratory Technology, Physics/ Electronic, Institute of Applied Sciences, Kwara State
Polytechnic, Ilorin.

ABSTRACT

Estimation of global solar radiation using five sunshine hour models in Ilorin, north-central, Nigeria (8.54°N, 4.54°E) was developed using the Angstrom type regression equation. The solar radiation (W/m^2), hours of bright sunshine were collected from achieve of Nigeria Metrological Centre, Oshodi, Lagos, for a period from (1992-2022). The constants of the Angstrom-type regression equation (Models) were determined by plotting the clearness index (H/H_0) against the fraction of sunshine hours (n/N) to obtain the line of best fit. The result of the correlation were also tested for error using statistic test methods of the mean biased error, MBE, root mean square error, RMSE, and mean percentage error, MPE to assess the performance of the models. It was observed that out of all models used, modes III and IV gave the best prediction for global solar radiation using sunshine.

**BENTHIC FORAMINIFERA AS BIOSTRATIGRAPHICAL AND
PALEOECOLOGICAL INDICATORS: AN EXAMPLE FROM THE MIOCENE
DEPOSITS IN GEBEL ABU SHAAR EL QIBLI, GULF OF SUEZ REGION, EGYPT**

Mostafa M. Hamad

Cairo University, Faculty of science, Geology Department, Egypt.

ABSTRACT

The foraminiferal contents of the Miocene deposits exposed in two sections in Wadi Bali and Wadi Kharaza, Gebel Abu Shaar El Qibli plateau, Western side of the Gulf of Suez, Egypt were carefully studied for their benthic and planktonic foraminiferal content. Based on their lithofacies variations and microfaunal content, three rock units were studied, from base to top as follows: Abu Gerfan Formation, polymictic conglomerates (Early Miocene, Aquitanian), the overlying Gharamul Formation (carbonate and mixed siliciclastic-carbonate) (Middle Miocene, Burdigalian to Langhian), and evaporites of Gemsa Formation (Middle Miocene, Serravallian age) are reported. Detailed smaller, larger and planktonic foraminiferal investigations led to the recognition of three foraminiferal zones from base to top: 1) *Miogypsina complanata* / *Nonion granosus* Zone (Zone SBZ 24), comprising the Abu Gerfan Formation that ascribed to Early Miocene Aquitanian age, 2) *Miogypsina globulina* zone (SBZ 25) reposing the lower unit of Gharamul Formation, and correlated with the Early Miocene, Burdigalian age and lastly 3) *Borelis melo melo* Zone (SBZ 26) of Middle Miocene, Langhian age covering the upper part of Gharamul Formation. The Middle Miocene interval of Gharamul Formation is ascribed to the Langhian for first time where *Operculina complanata* (Defrance) and *Borelis melo melo* (Fichtel and Moll) are the main time-specific diagnostic taxa recognized in this interval. For the first time, planktonic foraminifera are documented from the Gharamul Formation in Gebel Abu Shaar El Qibli plateau being characterized by the occurrence of planktonic foraminifera such as *Globigerina praebuloides*, *Globigerina ciperoensis*, *Globigerinoides altiapertura*, *Globigerinoides trilobus* and *Globigerinoides subquadratus*. This association characterises the *Borelis melo melo* interval Zone. The variation in lithology and foraminiferal assemblages will be discussed here and reflects the variety of environmental settings characterizing the studied Miocene sequence, indicating an overall shallowing-upward trend, from continental to subaqueous fan delta facies of Abu Gerfan Formation to platform reefal facies and restricted lagoon-salina conditions represented by evaporites of Gemsa Formation.

Keywords: Early Miocene, biostratigraphy, Gharamul Formation, Gebel Abu Shaar El Qibli, Gulf of Suez, Egypt.

**STUDIES ON ENGINEERING APPLICATION DOMAINS OF INDUSTRY 5.0 IN
INDIA**

Shivam Priyadarshi

B.Tech. Mechanical Engineering students, North Eastern Regional Institute of Science and Technology (Deemed to be University), Itanagar, Arunachal Pradesh, INDIA-791 109

Mainak Pal

B.Tech. Mechanical Engineering students, North Eastern Regional Institute of Science and Technology (Deemed to be University), Itanagar, Arunachal Pradesh, INDIA-791 109

Lalawmpuia

B.Tech. Mechanical Engineering students, North Eastern Regional Institute of Science and Technology (Deemed to be University), Itanagar, Arunachal Pradesh, INDIA-791 109

Manapuram Muralidhar

Professor of Mechanical Engineering, North Eastern Regional Institute of Science and Technology (Deemed to be University), Itanagar, Arunachal Pradesh, INDIA-791 109

ABSTRACT

Global population has reached 8 billion with a baby girl Vinis Mabansag born in Tondo, Manila on 15th November 2022, Tuesday as per the United Nations. As the population increases the material requirements will also be increased. Manufacturing has to cater the needs of the people on Earth with the available resources including technology. With the advent of technologies in the yester- centuries like Steam engine, Electricity, Computers, the Internet & Robotics various industrial revolutions have been evolved. These include Industrial Revolution 1.0 (1760-1840), Industrial Revolution 2.0 (1871-1914), Industrial Revolution 3.0 (1970-2012), Industrial Revolution 4.0 (2011 and beyond) and Industrial Revolution 5.0 (2020 and beyond). After the initialization of digital India, AI and Internet, the manufacturing industry has undergone significant changes on the technology front. Most of the industries are embedding emerging technologies into various manufacturing machines/ processes to improve productivity, quality, reducing cycle time and quantities down to 1 with flexibility. Industry 5.0 emphasis on the integration of human hands and brains back into the industrial framework which focuses on transforming factories into the Internet of Things (IoT), smart facilities that use cognitive computing, collaboration with robots (cobot) and link via cloud servers. Man and machine coming together to improve the means and effectiveness of production are known as the Fifth Industrial Revolution 5.0. In India there are large number of micro small medium enterprises which produces 40 percent of national Industrial production. It seems not much work has been done in industry 5.0 application domains and hence in the

present work, an attempt has to be made to identify specific engineering application domains for Industry 5.0 considering its sub-systems for global society.

Keywords: Industry 5.0, Cobot, Digital Twins, Small to Medium Enterprise

FACTORS AFFECTING PEDESTRIANS' FREE-MOBILITY AND SOCIAL DISTANCING TO COMBAT COVID-19: EVALUATION OF PEDESTRIANS' MOBILITY AND URBAN SPACE IN DOWNTOWN OF NEKEMTE CITY, ETHIOPIA

Adane Obsie Bifa

Department of Urban and Regional Planning, College of Engineering and Technology, Wollega University;
P.O.Box 395, Nekemte, Ethiopia

Mulugeta Soruma Guta

Department of Urban and Regional Planning, College of Engineering and Technology, Wollega University;
P.O.Box 395, Nekemte, Ethiopia

ABSTRACT

Peoples' free mobility and social distancing in urban centers are among the methods to combat the pandemic of COVID-19. Proper implementation of social distancing needs adequate roads infrastructures to support basic human movement within the urban areas. However, socio-economics, transportation and urban space facilities of developing countries like Ethiopia are the challenging factors for free mobility and to implement social distancing. Thus, this study is used downtown of Nekemte city as case study to identify the factors affecting the pedestrians' free mobility and implementation of social distancing to fight against corona virus. A survey questionnaire containing 11 parameters explaining factors affecting pedestrians mobilities were distributed for pedestrians' and factor analysis was used to identify the most influencing parameter for the free mobility and social distance in the city. The result showed that *in adequate walkways* (i.e. narrow, deteriorated and overcrowded walkways and streets), *using pedestrians' ways for other function* and *in adequate urban public service spaces* such as at banks, shops, taxi and hospitals, are the major factors affecting the free mobility and implementation of social distancing against COVID-19. To achieve appropriate implementation of social distancing in down town areas, it needs a programs and policy to restrict on streets parking, streets vendors and using pedestrians' ways for others rather than for pedestrians' mobility hence enable to achieve healthy social and environment.

Keywords: Social distancing, COVID-19, Pedestrians' ways, Vendors, downtown of Nekemte, Factors analysis

**РАЗРАБОТКА СИСТЕМЫ ПРЕВЕНТИВНОЙ ДИАГНОСТИКИ
ТЕХНИЧЕСКОГО ОБЪЕКТА С ИСПОЛЬЗОВАНИЕМ ИСКУССТВЕННОГО
ИНТЕЛЛЕКТА**

DEVELOPMENT OF A SYSTEM FOR PREVENTIVE DIAGNOSTICS OF A
TECHNICAL OBJECT USING ARTIFICIAL INTELLIGENCE

К.т.н. Янкевич Н.С.,

Национальная академия наук Беларуси, ГНУ «Центр системного анализа и стратегических исследований
НАН Беларуси»

ORCID: 0000-0001-9642-9212

АННОТАЦИЯ

Внедрение информационных и коммуникационных технологий создало предпосылки для широкого использования искусственного интеллекта в различные области деятельности человека, включая машиностроение. В связи с этим актуализируется задача развития соответствующего математического аппарата в применении к различным техническим системам и агрегатам, в том числе, разработки «интеллектуальных» диагностических систем превентивной диагностики, позволяющих расширить возможности получения информации не только о текущем состоянии объекта, но и прогнозировать возможные отказы в будущем. При этом, несмотря на то, что уровень надежности технических средств непрерывно повышается, вопросы, связанные с учетом внешних условий эксплуатации (включая человеческий фактор), не решены полностью до сих пор.

В работе основное внимание уделено разработке математических моделей для анализа ситуаций отказа технического объекта, представленного как сложная техническая система, и их последствий.

В качестве методологической основы для построения вычислительных алгоритмов системы превентивной диагностики выбран системный подход. Вместе с тем, излишняя детализация и конкретизация может не только значительно затруднить, но и сделать подобный анализ практически невозможным. Поэтому при прогнозе надежности функционирования технического объекта в целом целесообразно получить комплекс вероятностных моделей, описывающих каждую из этих подсистем, а также модель, определяющую их взаимодействие.

Расчет вероятности отказа, связанного с технической системой в целом, осуществляется в соответствии с обычными правилами расчета ориентированных вероятностных графов. Разработан алгоритм и математический аппарат, отражающий

последовательность действий при реализации разработанных принципов для системы превентивной диагностики сложного технического объекта.

Ключевые слова: техническая система, превентивная диагностика

ABSTRACT

Introduction of information and communication technologies has created the prerequisites for the widespread use of artificial intelligence in various fields of human activity, including mechanical engineering. In this regard, the task of development of an appropriate mathematical apparatus as applied to various technical systems and units, including the development of "intelligent" diagnostic systems for preventive diagnostics, which make it possible to expand the possibilities of obtaining information not only about the current state of an object, but also to predict possible failures in the future. At the same time, despite the fact that the level of reliability of technical means is constantly increasing, issues related to taking into account external operating conditions (including the human factor) have not been fully resolved so far.

The paper focuses on the development of mathematical models for the analysis of failure situations of a technical object, presented as a complex technical system, and their consequences. A systematic approach has been chosen as a methodological basis for constructing computational algorithms for the preventive diagnostics system. At the same time, excessive detailing and concretization can not only significantly complicate, but also make such an analysis practically impossible. Therefore, when predicting the reliability of the operation of a technical object as a whole, it is advisable to obtain a set of probabilistic models that describe each of these subsystems, as well as a model that determines their interaction.

The calculation of the probability of a failure of the technical system as a whole is carried out in accordance with the usual rules for calculating directed probability graphs. An algorithm and a mathematical apparatus have been developed that reflect the sequence of actions in the implementation of the developed principles for a system of preventive diagnostics of a complex technical object.

Keywords: a technical system, preventive diagnostics

ENERGY STORAGE CHARACTERISTICS OF $0.5 \text{ BaTiO}_3 - \text{Bi}_x\text{Na}_x(\text{Mg}_{0.67}\text{Nb}_{0.33})_{1-x}\text{Nb}_x$

Asif Ali

Mr., Abdul Wali Khan University Mardan, Pakistan,

ORCID: 0000-0001-7329-9910

ABSTRACT

The role of oxide perovskites is very fascinating and technologically very important in electronic circuits in the form of capacitors, ferro-electric random-access memories (FeRam), sensors, actuators and energy storage applications. Dielectric materials with perovskite structure are widely used for above discussed practical applications. Capacitors are most widely used component in electronic devices. However the Multilayer ceramic capacitors are dominated over a single layer due to their volumetric efficiency. Barium titanate (BaTiO_3) based ceramics are of special interest for MLCCs applications. In the present research project, $0.5 \text{ BaTiO}_3 - \text{Bi}_x\text{Na}_x(\text{Mg}_{0.67}\text{Nb}_{0.33})_{1-x}\text{Nb}_x$ ($x = 0.10, 0.20, \text{ and } 0.30$) ceramics solid solid solution were synthesized by conventional solid state sintering route. While the obtained properties of samples were characterized by using different characterization tools. X-ray diffraction, Scanning Electron Microscopy for microstructural analysis, LCR meter and Ferroelectric tester were used for the study of energy storage characteristics of the sample. Phase identification of the samples showed the formation of a single phase cubic perovskite-structure (space group Pm-3 m) which was further confirmed using Raman spectroscopy. The Raman spectroscopy result are in agreement with the XRD. Microstructural analysis of the samples revealed some voids in the samples while grain size was observed to decrease with increasing NaNbO_3 concentration. The addition of NaNbO_3 shifted maximum temperature T_m , to below room temperature and the stability range of $0.5\text{BaTiO}_3-0.5\text{Bi}(\text{Mg}_{2/3}\text{Nb}_{1/3})\text{O}_3$ previously reported ceramics sample was enhanced. The sample with $x=0.20$ exhibited $\epsilon_r(\text{mid})$ with minimum variation of $\pm 15\%$ stable over a wide temperature range from - 85 to 500 °C and most importantly a low dielectric loss of < 0.05 stable across a wide temperature range - 100 to 426 °C was maintained. The thermally stable dielectric properties of sample $x = 0.2$ suggests that it could be useful candidate material for capacitor applications in both low (X9R) as well as harsh environment applications.

Keywords: BaTiO_3 , Capacitors, Ceramics, High Temperature dielectrics, Harsh Environment, X9R

**REGRESSION ANALYSIS ON SEPARATION PERFORMANCE OF LINEAR
VIBRATING SCREEN**

Bharath Kumar Shanmugam

Department of Mining Engineering, National Institute of Technology, Karnataka, Surathkal, Mangalore, 575025,
India.

Harsha Vardhan

Department of Mining Engineering, National Institute of Technology, Karnataka, Surathkal, Mangalore, 575025,
India.

Govinda Raj. M

Department of Mining Engineering, National Institute of Technology, Karnataka, Surathkal, Mangalore, 575025,
India.

Marutiram Kaza

R &D and SS, JSW Steel Limited, Vijayanagar Works, P.O Vijayanagar, Ballari , Karnataka, 583275, India.

Rameshwar Sah

R &D and SS, JSW Steel Limited, Vijayanagar Works, P.O Vijayanagar, Ballari , Karnataka, 583275, India.

Harish Hanumanthappa

Department of Mining Engineering, National Institute of Technology, Karnataka, Surathkal, Mangalore, 575025,
India

ABSTRACT

Separation is a method of classifying the material depending on the particle size. Blast Furnace Slag (BFS) was obtained from the blast furnace during iron making. The separation of -4+1mm size BFS will lead to the preparation of the material which can suitably replace limestone in cement manufacturing. Therefore, the usage of BFS conserves nonrenewable energy. The present study is on the investigation of the separation performance of linear vibrating screen. The dry separation of BFS was performed in linear vibrating screen. The separation efficiency was varied from 20 experimental trails from 2minutes to 40 minutes with an interval of 2 minutes for each trial. The highest separation efficiency of vibrating screen of 65.92% was obtained at 16 minutes. Screen clogging caused the reduction in efficiency with respect to separation time. Prediction using regression analysis was performed on the experimental results. The results show that the developed regression model was correlating with experimental results.

**PEDESTRIANS MOVEMENT PATTERNS IN THE SELF-MADE HABITATS WITH
EMPHASIZING ON SECURITY IMPROVEMENT BY COMBINING TWO UAVs
AND SPACE SYNTAX**

Mehrdad Karimimoshaver

Bu-Ali Sina University, Faculty of Art and Architecture, Department of Architecture, Hamedan, Iran
ORCID: 0000-0001-5536-2138

Attiyeh Khorshidi

Bu-Ali Sina University, Faculty of Art and Architecture, Department of Architecture, Hamedan, Iran

Alireza Gerami

Bu-Ali Sina University, Faculty of Art and Architecture, Department of Architecture, Hamedan, Iran
ORCID: 0000-0003-1317-6534

ABSTRACT

In recent years self – made habitats defined as an informal and marginalized or uncommon residential areas are increasing quickly which results in highly severe problems such as unauthorized and unmanageable growth which results in environmental, physical, social, cultural and similar hazards for all the cities and with the lack of suitable attentions will turn into more complex problems. Settlement and concentration of people with low income in these places that have no communication with the other social classes such as middle class causes not only decreasing the government control upon them but also results in creating and forming so many dangerous social abnormalities in these districts. The main goal of this research is investigating the best methodology for investigating the moving width and the number of floors in these buildings in a short time and with a low cost people movement pattern in all these habitats so it would be possible to predict the citizens behavioral patterns in these districts easily and improve their security factors. In this research after field and library studies, shots from Khezr district were taken by aerial survey and Unmanned Aerial Vehicle (UAV) methods. Then using the data of the outboard of UAVs and using two parameters- number of floors and the moving width- in the space syntax method analyzed informations and tried to extract the pedestrians movements patterns in this context. Using the results, solutions for improving the security in these districts will be proposed.

Keywords: Informal Inhabitants, Pedestrian, Security, UAV, Space Syntax

**BAYESIAN NETWORKS EFFECTIVENESS FOR ELECTRICAL SYSTEMS
MAINTENANCE PLANNING**

Mourad Nahal

Faculty of Sciences and Technologies, University of Souk Ahras, BP 1553, Souk Ahras 41000, Algeria

Yacine Saharoui

Faculty of Sciences and Technologies, University of Souk Ahras, BP 1553, Souk Ahras 41000, Algeria

Omar Reffas

Laboratoire des Systèmes Electromécaniques Badji-Mokhtar University, BP 12, Annaba 23000, Alegria.

Chaouki Moumeni

Faculty of Sciences and Technologies, University of Souk Ahras, BP 1553, Souk Ahras 41000, Algeria

Naziha Zerari

Faculty of Sciences and Technologies, University of Souk Ahras, BP 1553, Souk Ahras 41000, Algeria

ABSTRACT

Due to its financial benefits, the static synchronous compensator is now utilized more and more in electrical networks. This paper intends to propose a method for reactive energy compensation by optimizing a complex electrical system maintenance based on a reliability procedure. The intricacy of electrical system architecture is simply one facet of its complexity; the electrical network and interactions with reactive energy compensators (STATCOM) are equally important. In order to address this complexity constraint and evaluate the time-variant dependability of an electrical system, Bayesian networks are used. In order to optimize the electrical system's preventive control interval, a global cost that takes into account additional expenses associated with system operational uncertainty is included into the probabilistic technique. The found results can be applied to enhance the performance of the electrical system reliability.

Keywords: Reliability, Maintenance, Electrical system, BNs

BIODEGRADATION OF AZO DYES BY HALOPHILIC BACTERIA

Shagufta Noreen

Department of Biotechnology, Faculty of Science, Jinnah University for Women, Karachi, Pakistan

Suad Naheed

Department of Biotechnology, Faculty of Science, Jinnah University for Women, Karachi, Pakistan

ABSTRACT

The trend of urbanization and industrialization has granted the world with a lot of applicable and remarkable benefits. Along with the various advantages it also brings some issues and the revolution of industry comes with environmental problems. Like other industries, development in textile industry has brought the contamination of soil and water with effluent dyes, Therefore treatment of dye-contaminated wastewater discharged from the textile and other dye-stuff industries is necessary to prevent contamination of soil surface and ground water. The cost effective biological strategy is the need of the time to complete mineralization of organic pollutants. The current study is design to treat the toxic synthetic dyes that is present in textile waste effluent by using different microorganism in an environmental friendly manner.

Total forty bacterial strains were isolated from effluent and dye contaminated soil samples using MSM (Minimal Salt) medium. After wards, the isolates were exploited for their dye degradation activity by employing agar well diffusion and calorimetric methods.

Six out of forty bacterial cultures presented maximum dye degradation efficiency against five different azoic dyes. This suggests that these bacteria release extracellular enzymes which showed dye degradation ability. However, this research is beneficial to explore biodegradation potential of bacteria so that they can be used in the treatment of different waste effluents release from textile dyeing sector.

Keywords: Dye Degradation, Halophiles, Azoic Dyes